THE UNIVERSITY *of* EDINBURGH

The First Law of Thermodynamics and 2d CFT Descriptions for Near-Extremal and Near-EVH Black Holes

Maria Johnstone

Doctor of Philosophy
University of Edinburgh
2013

Declaration

I declare that this thesis was composed by myself and that the work contained therein is my own, except where explicitly stated otherwise in the text.

(*Maria Johnstone*)

For Frank

Abstract

In this thesis we investigate the quantum aspects of black holes near extremality. In particular we seek evidence that a near-extremal black hole has a microscopic description in terms of a two dimensional conformal field theory (CFT).

We first demonstrate how the low temperature expansion of the first law of thermodynamics leads to an expression for the entropy of extremal black holes which can be recast as the Cardy formula for the entropy of a chiral two dimensional CFT, in agreement with the Extremal Black Hole/CFT correspondence. We apply Sen's entropy function formalism to fortify this result by reproducing it in a gravitational setup.

We extend our first law analysis to a class of near-Extremal Vanishing Horizon (near-EVH) black holes. These black holes have low entropy and temperature, and their geometries contain locally asymptotically AdS_3 throats in the near horizon region. The low temperature expansion of the first law is compatible with the first law for a three dimensional BTZ black hole. As the BTZ black hole has an AdS/CFT description in terms of a non-chiral two dimensional CFT, our result can be viewed as thermodynamic evidence for the EVH/CFT correspondence, which states that gravity on the near horizon EVH geometry is described by a 2d CFT. A near-EVH black hole, or low energy excitation around an EVH black hole, is described by excitations of the dual 2d CFT.

As case studies of our first law analysis and the EVH/CFT correspondence, we focus on two asymptotically $AdS_5 \times S^5$ classes of near-EVH black holes. The two cases have interesting individual properties and, by the AdS/CFT correspondence, dual descriptions as states in $\mathcal{N} = 4$ super Yang-Mills theory . We can compare these (UV) pictures to the two dimensional descriptions that emerge from the near horizon, or low energy, dynamics. All EVH near horizon geometries have local AdS_3 factors which become BTZ black holes when the configurations are excited from EVH to near-EVH.

In the study of static black holes with three R-charges, we examine the non-BPS and near-BPS regimes separately. While the non-BPS near horizon limit is locally regular, in the near-BPS case the near horizon procedure requires focussing geometrically on a strip of the horizon, and the degrees of freedom of the dual CFT_2 can be associated with stretched strings between giant gravitons in the transverse five-sphere.

The near-EVH limit of non-BPS stationary charged black holes is obtained by taking the vanishing limit of one or both of the angular momenta. When one of the momenta is small, the AdS_3 angle is a combination of azimuthal angles in the AdS_5 and S^5 regions of the geometry. Taking the vanishing limit of both of the angular momenta leads to a near horizon limit which contains a BTZ black hole that is non-trivially fibred by a three-sphere.

For each of the case studies we use the AdS_3/CFT_2 dictionary to specify dual IR CFT_2 descriptions of the black holes. We outline a map between the UV and IR near-EVH excitations and demonstrate how the first law reduces in the near-EVH limit to the first law of a BTZ black hole. As a consistency check we compare our results with those of the Kerr/CFT correspondence.

Acknowledgements

I am indebted to my supervisor Joan Simón for the guidance he has given me and for all he has taught me. He has been a truly inspirational advisor with the patience of a saint, and has been incredibly motivational and generous with his time.

I am also deeply grateful to my other collaborators Jan deBoer, Shahin Sheikh-Jabbari and Hossein Yavartanoo for sharing their ideas with me. I have learned so much from working with them. I would also like to thank my hosts at KIAS in Seoul and KITP in Santa Barbara for hospitality during my research.

I owe thanks to my second supervisor, José Figueroa-O'Farrill, for his constant support throughout my graduate studies. I am grateful to Patricia Ritter, Paul Reynolds, Paul deMedieros and Arjun Bagchi for support during my PhD years. I would also like to express my appreciation of the friendly administration and I.T. staff of the maths department. And, of course, thanks to Rollo Jenkins - housemate, officemate, friend - for always being good craic.

I would like to thank my friends at home, in Edinburgh, and all over the world for always lifting my spirits. A special thanks to Jenny, Mike and Purdie for making life that bit easier when I've been burning the midnight oil. I am thankful every day to have the love and support of my fantastic boyfriend Malky MacLeod.

Finally, the encouragement and love of my four wonderful parents, Jessica and Peter, Keith and Maggie, and my immediate and extended family have always been hugely important to me, and I thank them from the bottom of my heart.

My research was supported by the Engineering and Physical Sciences Research Council (EPSRC).

Contents

Abstract **4**

1 Introduction **8**
1.1 Brown and Henneaux . . . 9
1.2 Two Dimensional Conformal Field Theories . . . 12
1.3 AdS/CFT . . . 14
1.4 BTZ Black Holes and 2d CFTs . . . 16
1.5 The Kerr/CFT Correspondence . . . 20
1.5.1 Generators of the ASG . . . 21
1.5.2 Explicit realisation of the Virasoro algebra . . . 22
1.5.3 Extremal black Hole/CFT correspondence in d> 4 . . . 24
1.6 Black Hole Extremality and CFT_2 Chirality . . . 25
1.7 Pinching AdS_3 Orbifolds . . . 29
1.8 The EVH/CFT Correspondence . . . 32
1.9 Outline of the Thesis . . . 34

2 The Low Temperature Limit of Black Holes **36**
2.1 Introduction . . . 36
2.1.1 Black hole potentials and charges . . . 36
2.1.2 Laws of black hole thermodynamics . . . 38
2.2 The Low Temperature Limit of the First Law: Finite Horizon Black Holes . . . 40
2.2.1 Extremal black holes in four and five dimensions . . . 40
2.2.2 Low temperature first law analysis . . . 41
2.2.3 Sen's entropy function . . . 42
2.2.4 Scalar probe analysis . . . 43
2.3 The Low Temperature Limit of the First Law: Vanishing Horizon Black Holes . . . 44
2.4 Discussion . . . 47

3 Case Study I: Static Charged Black Holes **48**
3.1 Static Three Charged Solutions to Type IIB Supergravity . . . 48
3.2 The Set of EVH and Near-EVH Black Holes . . . 50
3.2.1 The set of EVH black holes . . . 51
3.2.2 The set of near-EVH black holes . . . 51
3.3 Near Horizon Geometry Analyis: Static Charged Black Holes . . . 52
3.3.1 The non-BPS EVH near horizon geometry . . . 53
3.3.2 The non-BPS near-EVH near horizon geometry . . . 53
3.3.3 The near-BPS VH near horizon geometry . . . 55
3.3.4 The near-BPS near-VH near horizon geometry . . . 56
3.4 IR 2d Description . . . 58
3.4.1 Non-BPS near-EVH . . . 58
3.4.2 Near-BPS near-EVH . . . 59
3.5 First Law of Thermodynamics: Static Charged near-EVH Black Holes . . . 60
3.5.1 Non-BPS first law . . . 61
3.5.2 Near-BPS first law . . . 61
3.6 EVH/CFT_2 vs. AdS_5/CFT_4 . . . 63

3.6.1 EVH/CFT$_2$ vs. AdS$_5$/CFT$_4$: non-BPS . . . 63
3.6.2 EVH/CFT$_2$ vs. AdS$_5$/CFT$_4$: near-BPS . . . 65
3.7 A Check: Comparison with Kerr/CFT . . . 65
3.7.1 Non-BPS near-EVH regime . . . 67
3.7.2 Near-BPS near-VH regime . . . 67
3.8 Discussion . . . 68

4 Case Study II: Rotating Two Charged Black Holes **70**
4.1 Rotating Two Charged Solutions to Type IIB Supergravity . . . 70
4.2 The Set of EVH and Near-EVH Black Holes . . . 74
4.2.1 EVH black holes . . . 74
4.2.2 Near-EVH black holes . . . 74
4.3 Near Horizon Geometry Analysis: Rotating Two Charged Black Holes . . . 76
4.3.1 The static EVH near horizon geometry . . . 77
4.3.2 The nearly-static near-EVH near horizon geometry . . . 77
4.3.3 The rotating EVH near horizon geometry . . . 79
4.3.4 The rotating near-EVH near horizon geometry . . . 81
4.4 IR 2d Description . . . 82
4.4.1 Nearly-static near-EVH . . . 82
4.4.2 Rotating near-EVH . . . 83
4.5 First Law of Thermodynamics: Rotating Charged near-EVH Black Holes . . . 83
4.5.1 Nearly-static first law . . . 83
4.5.2 Rotating first law . . . 84
4.6 EVH/CFT$_2$ vs. AdS$_5$/CFT$_4$ . . . 85
4.6.1 EVH/CFT$_2$ vs AdS$_5$/CFT$_4$: nearly-static . . . 85
4.6.2 EVH/CFT$_2$ vs AdS$_5$/CFT$_4$: rotating . . . 86
4.7 A Check: Comparison with Kerr/CFT . . . 87
4.7.1 Nearly-static near-EVH regime . . . 90
4.7.2 Rotating near-EVH regime . . . 90
4.8 Discussion . . . 91
4.A Horizon Structure . . . 92
4.B Calculation of Q$_1$ and Q$_3$ . . . 93
4.C Null self dual orbifold: static (near-)EVH . . . 94
4.D Choice of U(1) . . . 95
4.E Near Horizon Geometries as 5 Dimensional Geometries . . . 96

5 Summary and Outlook **98**

A Frolov-Thorne Temperatures **102**

Chapter 1

Introduction

Black holes are some of the most mysterious objects in physics. Classically, they are solutions of Einstein's equations, surrounded by an event horizon such that no object inside this event horizon, not even light, can escape the black hole. In the quantum theory, however, they radiate with a finite Hawking temperature [1], and have assigned to them an entropy defined by Bekenstein [2] and Hawking [3]

$$S_{\rm BH} = \frac{A_{\rm H}}{4G_N}, \tag{1.1}$$

where $A_{\rm H}$ is the area of the black hole horizon, and G_N is the gravitational Newton's constant.

The existence of a macroscopic black hole entropy calls for a microscopic understanding. Indeed, Boltzmann's equation

$$S = k_B \log n, \tag{1.2}$$

where k_B is Boltzmann's constant, states that $n = \exp\left(\frac{A_{\rm H}}{4G_N k_B}\right)$ microstates are responsible for this entropy. The statistical nature of (1.1) by definition prompts one to ask what are the underlying quantum states that give rise to it, and it is an ongoing quest to understand this entropy as the logarithm of the number of microstates associated with the black hole.

This counting has been achieved in e.g. [4] (see [5] for a review) when we embed certain four and five dimensional black holes in a string theory setting. In ten dimensional spacetime, strings end on surfaces called D branes [6], which can wrap around compact dimensions. The D branes provide the degrees of freedom that give rise to the black hole charges, and the number of ways, or degeneracy, of wrapping around the compact dimensions results in a microscopic entropy that produces the macroscopic black hole entropy. Although this is an encouraging result, this microstate counting is limited to supersymmetric [4] and (near-)extremal non-BPS [7, 8, 9], black holes[1]. While extremal black holes, which have a minimal mass for given angular momentum and electric charge, are theoretical, near-extremal black holes have been observed in nature [11]. It is yet to be fully understood, and the motivation for this thesis, how the entropy of near- and non-extremal black holes arises from statistical mechanics based on a quantum field theory.

The holographic principle is a conceptual framework that can be used to understand the microscopic description of experimentally observed black holes. It states that the information contained in some region of space can be represented by a theory on the boundary of that space. In particular, 't Hooft and Susskind [12] suggested that our observed universe (three spatial dimensions and one time dimension) can be described by degrees of freedom living on the boundary of the universe. This principle suggests that gravity in d+1 dimensions is equivalent to a local field theory in d dimensions; then by this principle the entropy associated to a black hole with horizon of area $A_{\rm H}$ could be attributed to quantum states residing on the horizon [13, 14, 15].

[1] There are results in e.g. [10] for non-extremal microscopic countings, but they are generically not understood.

1.1 Brown and Henneaux

Brown and Henneaux [16] first introduced a quantitive approach to identifying gravity with a quantum field theory. They computed the conserved charges associated to the asymptotic symmetry (ASG) group of three dimensional Anti de Sitter (AdS) space, where the ASG of a spacetime is the group of symmetry transformations ξ that preserve its chosen boundary conditions at spatial infinity (allowed diffeomorphisms) but are not associated with trivial conserved charges (trivial diffeomorphisms). It was then demonstrated that the Dirac bracket algebra of these charges gives the algebra of a two dimensional conformally invariant quantum field theory.

Pure gravity in three dimensions with a negative cosmological constant Λ is described by an Einstein-Hilbert action and some boundary terms

$$I = I_{EH} + I_{bdy} = \frac{1}{16\pi G_3}\int d^3x\sqrt{g}\left(\mathcal{R} - \frac{2}{\ell_3^2}\right) + I_{bdy}\ . \tag{1.3}$$

In three dimensions the gravitational field has no dynamical degrees of freedom, so the spacetime away from sources is locally equivalent to the empty space solution of the Einstein equations. Three dimensional anti de Sitter space

$$ds^2 = -\frac{r^2}{\ell_3^2}dt^2 + \ell_3^2\frac{dr^2}{r^2} + r^2 d\phi^2 \tag{1.4}$$

with radius of curvature given by $\ell_3 = \sqrt{-\frac{1}{\Lambda}}$ is the empty space solution to the equations of motion.

Three dimensional anti de Sitter space: Anti de Sitter space of dimension $2+1$ is a negatively curved Lorentzian manifold, defined as a hyperboloid in $\mathbb{R}^{2,2}$

$$x_1^2 + x_2^2 - x_3^2 - x_4^2 = -\ell_3^2 \tag{1.5}$$

with metric

$$ds^2 = dx_1^2 + dx_2^2 - dx_3^2 - dx_4^2. \tag{1.6}$$

In global coordinates the metric is

$$ds^2 = \ell_3^2\left(-\left(1+\frac{r^2}{\ell_3^2}\right)dt^2 + \frac{dr^2}{\left(1+\frac{r^2}{\ell_3^2}\right)} + \frac{r^2}{\ell_3^2}d\phi^2\right) \tag{1.7}$$

where the coordinates

$$x_1 = \ell_3\sinh\mu\cos\phi, \qquad x_2 = \ell_3\sinh\mu\sin\phi \tag{1.8}$$

$$x_3 = \ell_3\cosh\mu\sin t, x_4 = \ell_3\cosh\mu\cos t; \tag{1.9}$$

$$\sinh\mu = \frac{r}{\ell_3} \tag{1.10}$$

have ranges

$$\phi \in [0, 2\pi], \qquad r \in (0,\infty), \qquad t \in [0, 2\pi]. \tag{1.11}$$

Three dimensional anti de Sitter space has $\mathrm{SO}(2,2)$ symmetry and its conformal boundary is the cylinder $\mathbb{R}\times\mathrm{S}^1$.

Another form of AdS_3 that will be familiar in this thesis is the metric (1.4). This is achieved by first transforming to the Poincaré patch, with the coordinate definitions

$$x_1 = \ell_3\phi r, \qquad x_2 = \frac{1 - r^2(\ell_3^2 - \phi^2 + t^2)}{2r}, \qquad x_3 = \ell_3 tr, \qquad x_4 = \frac{1 + r^2(\ell_3^2 - \phi^2 + t^2)}{2r}$$

to get

$$ds^2 = \ell_3^2 \left(\frac{dr^2}{r^2} + r^2 \left(-dt^2 + d\phi^2 \right) \right) \tag{1.12}$$

with the ranges

$$t \in \mathbb{R}, \qquad u \in (0, \infty), \qquad \phi \in \mathbb{R}. \tag{1.13}$$

Notice that if $\phi \in [0, 2\pi]$ in these Poincaré-like coordinates, the AdS_3 boundary is also a cylinder.

Asymptotically AdS_3 solutions

$$ds^2 = -\left(\frac{r^2}{\ell_3^2} + \alpha^2 \right) dt^2 + \left(\frac{r^2}{\ell_3^2} + \alpha^2 - \frac{A^2}{\ell_3^2} \right)^{-1} dr^2 + 2\alpha A dt d\phi + (r^2 - A^2) d\phi^2 \tag{1.14}$$

approach AdS_3 space at spatial infinity $r \to \infty$, and are considered to be excitations of the ground state (1.4).

The gauge symmetry of a theory with action (1.3) is diffeomorphism invariance, and the gauge parameter is the field dependent vector field $\xi^\mu(x)$. The Lagrangian is invariant, $\delta L = 0$, for a transformation of the metric

$$\xi : \bar{g} \mapsto \bar{g} + \delta_\xi \bar{g}, \tag{1.15}$$

where the infinitesimal symmetry transformation of the metric under the action of the diffeomorphism ξ is given by the Lie derivative:

$$\delta_\xi \bar{g} = \mathcal{L}_\xi \bar{g}. \tag{1.16}$$

Asymptotic symmetries are necessary for the definition of the global charges of the theory, which in the Hamiltonian formalism are the canonical generators of the asymptotic symmetries of the theory. The boundary conditions determine the structure of the ASG, but are not completely fixed by the theory. The behaviour of a perturbation at spatial infinity, i.e. the boundary conditions of the perturbed metric, determine the form of the symmetry transformations of the asymptotic symmetry group. The diffeomorphisms that preserve the boundary conditions obey

$$\mathcal{L}_\xi (\bar{g} + h)_{\mu\nu} \overset{r\to\infty}{\longrightarrow} h_{\mu\nu}, \tag{1.17}$$

where $\bar{g}$ is the background spacetime and h describes a perturbation.

One choice of boundary conditions satisfied by both (1.4) and (1.14) is

$$h_{\mu\nu} = h_{\nu\mu} = \mathcal{O} \begin{pmatrix} 1 & 0 & 1 \\ 0 & \frac{1}{r^4} & 0 \\ 1 & 0 & 1 \end{pmatrix} \tag{1.18}$$

in the basis (t, r, ϕ), and the ASG is generated by ∂_t and ∂_ϕ. If we relax the boundary conditions from $g_{tr} = g_{\phi r} = 0$ to $g_{tr} = g_{\phi r} = O\left(\frac{1}{r^3}\right)$ at infinity, then there is an infinite number of diffeomorphisms ξ that preserve the asymptotic structure of the spacetime,

$$\begin{aligned} \xi = &\left(\xi_0^t(t,\phi) + \frac{1}{r^2}\xi_{-2}^t(t,\phi) + \mathcal{O}(r^{-4}) \right) \partial_t + \left(\xi_1^r r(t,\phi) + \mathcal{O}(r^{-1}) \right) \partial_r \\ &+ \left(\xi_0^\phi(t,\phi) + \frac{1}{r^2}\xi_{-2}^\phi(t,\phi) + \mathcal{O}(r^{-4}) \right) \partial_\phi, \end{aligned} \tag{1.19}$$

where the transformation coefficients satisfy

$$\frac{1}{\ell_3^2}\partial_\phi \xi_0^t(t,\phi) = \partial_t \xi_0^\phi(t,\phi), \qquad \partial_t \xi_0^t(t,\phi) = \partial_\phi \xi_0^\phi(t,\phi) = -\xi_1^r r(t,\phi), \tag{1.20}$$

$$\xi_{-2}^t(t,\phi) = -\frac{\ell_3^2}{2}\partial_t \xi_1^r r(t,\phi), \qquad \xi_{-2}^\phi(t,\phi) = \frac{1}{2}\partial_\phi \xi_1^r r(t,\phi). \tag{1.21}$$

The Hamiltonian H of the system is the sum of a linear combination of constraints [17]

$$H_v = \int d^n x \xi^\mu(x) \mathcal{H}_\mu(x) \tag{1.22}$$

plus an appropriate surface term $J[\xi]$ that cancels the unwanted surface terms in the variation of the "volume piece" H_v. The surface term $J[\xi]$, which is a functional of the vector fields, is used to calculate the charges associated to the symmetry generators. The surface term associated to the generator of time translations is the mass of the configuration, and the surface term associated to the generator of rotations is its angular momentum:

$$J\left[\frac{\partial}{\partial t}\right] = 2\pi\left(1 - \alpha^2 - \frac{A^2}{\ell_3^2}\right), \qquad J\left[\frac{\partial}{\partial \phi}\right] = 4\pi A\alpha. \tag{1.23}$$

The algebra of the asymptotic symmetry generators yields a representation of the Lie algebra of the corresponding vector fields,

$$\{H[\xi_1], H[\xi_2]\} = H[[\xi_1, \xi_2]] + K[\xi_1, \xi_2], \tag{1.24}$$

where the functional K is called the central charge. For the solutions of the equations of motion, the Lie algebra is

$$\{J[\xi_1], J[\xi_2]\} = J[[\xi_1, \xi_2]] + K[\xi_1, \xi_2]. \tag{1.25}$$

We also know that the Dirac bracket of two transformation vectors is

$$\{J[\xi_1], J[\xi_2]\} = \delta_{\xi_2} J[\xi_1], \tag{1.26}$$

which is the variation of the charge associated to ξ_1, on the surface deformed by ξ_2. So we write

$$\delta_{\xi_2} J[\xi_1] = J[[\xi_1, \xi_2]] + K[\xi_1, \xi_2]. \tag{1.27}$$

We can evaluate this variation on the ground state, where $J[\xi_1] = J[\xi_2] = 0$, to get

$$\delta_{\xi_2} J[\xi_1] = K[\xi_1, \xi_2], \tag{1.28}$$

and we see that the charges $J[\xi]$ are the central charges of the representation of the ASG. We note this is in any dimension. Due to the periodicity of ϕ, the generators (1.19) can be expanded in a Fourier series with a countable basis $\{M_n, N_n\}$ given in [16]. Then the algebra obeyed by the canonical asymptotic symmetry generators is

$$\{J[M_m], J[M_n]\} = (m-n)J[M_{m+n}] + \frac{c}{12}(m^3 - m)\delta_{m+n,0} \tag{1.29}$$

$$\{J[N_m], J[N_n]\} = (m-n)J[N_{m+n}] + \frac{c}{12}(m^3 - m)\delta_{m+n,0} \tag{1.30}$$

$$\{J[M_m], J[N_n]\} = 0, \tag{1.31}$$

where

$$c = \frac{3\ell_3}{2G_3}. \tag{1.32}$$

This algebra, generated by $L_m \equiv J[M_m]$, $\bar{L}_m \equiv J[N_m]$, is the direct sum of two Virasoro algebras

$$[L_m, L_n] = (m-n)L_{m+n} + \frac{c}{12}(m^3 - m)\delta_{m+n}, \qquad [L_m, \bar{L}_n] = 0, \tag{1.33}$$

and similarly for $[\bar{L}_m, \bar{L}_n]$ with $c = \bar{c}$. We will see in the following section that this is the algebra obeyed by the symmetry generators of a two dimensional conformal field theory with central charge (1.32). We emphasise that the central charge (1.32), which is a property of a quantum field theory, is a function of the gravitational parameters. This classical result suggests the existence of a duality between gravity on AdS_3 space and a two dimensional conformal field theory.

1.2 Two Dimensional Conformal Field Theories

The algebra (1.33) that emerges from the Poisson bracket of the canonical symmetry generators of three dimensional asymptotically anti de Sitter space is the algebra associated with two dimensional conformal field theories (CFTs). Here we give some basic facts about 2d CFTs.

Conformal field theories [19, 20] are quantum field theories that obey a conformal symmetry generated by conformal transformations $\sigma^\alpha \to \tilde{\sigma}^\alpha(\sigma)$ preserving the angles, but not the distance, between vectors. These theories have no dimensionful parameters, i.e. no mass or dimensionful coupling constant, as the β function

$$\beta(g') = \frac{dg'}{d\log E}, \tag{1.34}$$

which measures the change in the coupling g' as a function of the energy E, vanishes exactly: $\beta(g') = 0$.

Euclidean coordinates (σ^1, σ^2) can be mapped into the analogue of lightcone coordinates

$$(z, \bar{z}) \equiv (\sigma^1 + i\sigma^2, \sigma^1 - i\sigma^2) \tag{1.35}$$

where the flat Euclidean metric is given by

$$ds^2 = (d\sigma^1)^2 + (d\sigma^2)^2 = dzd\bar{z}. \tag{1.36}$$

Examples of conformal transformations are translations, $z \to z + a$, rotations $z \to wz : |w| = 1$, and scaling transformations $z \to wz : Re(w) \neq 1$.

The lightcone coordinates (1.35) allow us to split 2d fields, also called operators, into left and right-moving pieces associated with holomorphic and anti-holomorphic functions. A field or operator is labelled as primary if it transforms in a "natural" way under conformal transformations $(z, \bar{z}) \to (f(z), \bar{f}(\bar{z}))$ as

$$\mathcal{O}(z, \bar{z}) \to \bar{\mathcal{O}}(z, \bar{z}) = f'(z)^{-\tilde{h}} \bar{f}'(\bar{z})^{-\bar{\tilde{h}}} \mathcal{O}(z, \bar{z}), \tag{1.37}$$

and the operator product expansion (OPE) of two operators

$$\mathcal{O}_i(z, \bar{z})\mathcal{O}_j(z, \bar{z}) = \sum_k C_{ij}^k (z - w, \bar{z} - \bar{w})\mathcal{O}_k(w, \bar{w}) \tag{1.38}$$

provides information of the outcome of two operators approaching each other.

The numbers $(\tilde{h}, \bar{\tilde{h}})$ of a CFT operator $\mathcal{O}$ are called conformal weights, and describe how it transforms under rotations and scalings. The spin $\mathcal{J}_{2\mathrm{d}} = \tilde{h} - \bar{\tilde{h}}$ of an operator is its eigenvalue under rotations generated by the operator

$$L = z\partial - \bar{z}\bar{\partial} = -i(\sigma^1\partial_2 - \sigma^2\partial_1), \tag{1.39}$$

and its scaling dimension $\Delta_{2\mathrm{d}} = \tilde{h} + \bar{\tilde{h}}$ is its eigenvalue under dilatations generated by the operator

$$D = z\partial + \bar{z}\bar{\partial} = \sigma^\alpha \partial_\alpha. \tag{1.40}$$

Translational invariance gives rise to conserved currents encoded in the stress energy tensor

$$T_{\alpha\beta} = -\frac{4\pi}{\sqrt{g}} \frac{\delta S}{\delta g^{\alpha\beta}}, \tag{1.41}$$

where $g_{\alpha\beta}$ are the metric components on the two dimensional background, which can be described in terms of holomorphic ($T_{zz}(z)$) and anti-holomorphic ($T_{\bar{z}\bar{z}}(\bar{z})$) components. While in the classical theory the stress tensor is traceless, $T_\alpha^\alpha = 0$, in the quantum theory the stress tensor is not trace free,

$$\langle T_\alpha^\alpha \rangle = -\frac{c}{12}\mathcal{R}_2 = -\frac{\bar{c}}{12}\mathcal{R}_2, \tag{1.42}$$

where $\mathcal{R}_2$ is the Ricci scalar of the background. c and $\bar{c}$ are the left-moving and right-moving central charges of the CFT, computed from the operator product expansion (OPE) of the stress tensor,

$$T(z)T(w) = \frac{c/2}{(z-w)^4} + \frac{2T(w)}{(z-w)^2} + \frac{\partial T(w)}{z-w} + \text{non-singular terms}, \tag{1.43}$$

$$\bar{T}(\bar{z})\bar{T}(\bar{w}) = \frac{\bar{c}/2}{(\bar{z}-\bar{w})^4} + \frac{2\bar{T}(\bar{w})}{(\bar{z}-\bar{w})^2} + \frac{\partial \bar{T}(\bar{w})}{\bar{z}-\bar{w}} + \text{non-singular terms}. \tag{1.44}$$

We can see from (1.42) that curved backgrounds require $c = \bar{c}$ [2].

We can express the stress tensor on the plane as a Laurent expansion of its left and right-moving pieces

$$T(z) = \sum_{m=-\infty}^{\infty} \frac{L_m}{z^{m+2}}, \qquad \bar{T}(\bar{z}) = \sum_{m=-\infty}^{\infty} \frac{\bar{L}_m}{z^{m+2}}, \tag{1.45}$$

which we can invert to obtain the Virasoro modes

$$L_n = \frac{1}{2\pi i}\oint dz z^{n+1} T(z), \qquad \bar{L}_n = \frac{1}{2\pi i}\oint dz \bar{z}^{n+1} \bar{T}(\bar{z}). \tag{1.46}$$

In radial quantisation $L_n, \bar{L}_n$ are the conserved charges associated to the conformal transformations $\delta z = z^{n+1}$ generated by the vector fields [3] $l_n = z^{n+1}\partial_z$.

The algebra of these conserved charges is the Virasoro algebra (1.33). Representations of this algebra classify the states of the CFT .

In the quantum theory these conserved charges $L_n, \bar{L}_n$ are generators of the transformations. An eigenstate $|\Psi\rangle$ of L_0 and $\bar{L}_0$ has eigenvalues $\tilde{h}$ and $\bar{\tilde{h}}$:

$$L_0|\Psi\rangle = \tilde{h}|\Psi\rangle, \qquad \bar{L}_0|\Psi\rangle = \bar{\tilde{h}}|\Psi\rangle. \tag{1.47}$$

Primary states, also called highest weight states, are states $|\Psi\rangle$ of lowest energy such that

$$L_n|\Psi\rangle = \bar{L}_n|\Psi\rangle = 0, \qquad n > 0. \tag{1.48}$$

The vacuum state $|0\rangle$ has conformal weight $\tilde{h} = \bar{\tilde{h}} = 0$ so that $L_n|0\rangle = \bar{L}_n|0\rangle = 0$, $n \geq 0$. L_0 and $\bar{L}_0$ generate scaling and rotations while L_{-1} and $\bar{L}_{-1}$ generate translations in the plane.

Representations of the Virasoro algebra can be built by acting on the primary states with raising operators $L_{-n}, \bar{L}_{-n},\ n > 0$, giving an infinite tower of descendant states. Then knowledge of the spectrum of primary states allows us to work out the spectrum of the whole theory.

While this section has mainly discussed two dimensional conformal field theory on a plane, the states of the CFT associated with the Virasoro algebra (1.33) arising in section (1.1) are widely thought to reside on the cylindrical boundary of AdS_3. States on the cylinder with coordinates $\tau, \sigma \sim \sigma + 2\pi$ live on spatial slices of constant τ and evolve by the Hamiltonian ∂_τ, while the Hamiltonian on the plane is given by the dilatation operator (1.40), where the map between coordinates on a cylinder $w = \sigma + i\tau$ with metric $ds^2 = dwd\bar{w} = -d\tau^2 + d\sigma^2$ to the complex plane is $z = e^{-iw}$. The Hamiltonian of a two dimensional conformal field theory, which measures the energy of states on a cylinder, is mapped to the dilatation operator $D = L_0 + \bar{L}_0$ on the plane. A state $|\Psi\rangle$ on the plane given by (1.47) corresponds to some state on a cylinder of radius R with energy given by $E = \tilde{h} + \bar{\tilde{h}} - 2\pi\frac{c+\bar{c}}{24R}$, where the Casimir energy is [20]

$$E = -2\pi\frac{c+\bar{c}}{24R}. \tag{1.49}$$

[2] This is called the gravitational anomaly.

[3] The algebra satisfied by these vector fields is the Witt algebra.

1.3 AdS/CFT

The connection between gravity and a conformal field theory described in section 1.1 was extended in [21] to an equivalence between string theory or M theory on asymptotically $\mathrm{AdS}_{\mathrm{d}+1} \times \mathcal{M}$ spaces, where $\mathcal{M}$ is a compact manifold, and a conformal field theory on its conformal d-dimensional boundary. d+1 dimensional anti de Sitter space is the higher dimensional analogue of AdS_3 space introduced in section 1.1, with conformal $\mathbb{R} \times \mathrm{S}^{\mathrm{d}-1}$ boundary.

The defining example [21] of the AdS/CFT correspondence is type IIB string theory on $\mathrm{AdS}_5 \times \mathrm{S}^5$ and its dual description of $\mathcal{N} = 4$ Super Yang-Mills theory. The identification between the two theories was made upon examination of D branes, the hypersurfaces on which open strings end. A stack of N coincident type IIB D3 branes in flat 10d string theory can be described in terms of closed strings or open strings.

In the open string picture, we take the low energy limit of a system of open strings stretched between N D3 branes separated by a distance r. This involves sending the string length l_s to zero[4] so that the inverse tension of the string $\alpha' = l_s^2 \to 0$[5], and sending $r \to 0$ also, so that the string mass

$$m_{string}^2 = \frac{r^2}{\alpha'^2} \tag{1.50}$$

remains finite. The 10d gravitational coupling

$$\kappa_{10} \sim (\alpha')^4 g_s^2, \tag{1.51}$$

with the string coupling g_s kept finite, also vanishes in this limit, so that there are no interactions between closed and open strings. In this limit, the theory decouples into the action of free gravity in 10d and $\mathcal{N} = 4$ Super Yang-Mills Theory with gauge group $SU(N)$ and coupling parameter $\lambda_{tHooft} = g_{YM}^2 N$.

The equivalent closed string picture is obtained by taking the $\alpha' \to 0$ limit of type IIB string theory. As the spectrum of excitations of closed strings contains gravitons, the low energy limit of the closed string sector of string theory describes a supergravity theory. The gravitational background created by the stack of D3 branes has asymptotically flat metric[6]

$$ds^2 = H^{-\frac{1}{2}}(-dt^2 + d\mathbf{x}_3^2) + H^{\frac{1}{2}}(dr^2 + r^2 d\Omega^2), \tag{1.52}$$

and an RR 5-form field strength

$$F_5 = (1 + *)dt \wedge d\mathbf{x} \wedge dH^{-1}, \tag{1.53}$$

where

$$H = 1 + \frac{R^4}{r^4}, \quad R^4 = 4\pi(g_s N)(\alpha')^2. \tag{1.54}$$

An observer at infinity measures the energy of an excitation of proper energy $E_{(r)}$ localised at r as

$$E_\infty = E_{(r)} \left(1 + \frac{R^4}{r^4}\right)^{-\frac{1}{4}}. \tag{1.55}$$

An excitation approaching $r = 0$ will appear to an asymptotic observer to suffer a large redshift as its energy at $r \simeq 0$ appears as:

$$E_\infty \simeq E_{(r)} \frac{r}{R} \simeq E_{(r)} \frac{r}{(g_s N \alpha'^2)^{\frac{1}{4}}}. \tag{1.56}$$

Thus the $\alpha' \to 0$ limit admits any excited string modes localised in the $r \to 0$ region, as any modes of large energy are infinitely redshifted so that they appear to have low energy. The

[4] In this limit the strings act like components of a gauge field living on the worldvolume of the branes.

[5] By taking just the string length scale to zero, we decouple all massive string modes as they become infinitely heavy.

[6] Placing D-branes in flat space breaks the Poincaré symmetry from ISO(9,1) to ISO(3,1)×SO(6).

metric (1.52) in this region is of the form

$$ds^2 = \alpha' \left[\frac{U^2 (dx_\mu dx^\mu)}{\sqrt{4\pi g_s N}} + \sqrt{4\pi g_s N} \frac{dU^2}{U^2} + \sqrt{4\pi g_s N} d\Omega_5^2 \right], \tag{1.57}$$

with $U = \frac{r}{\alpha'}$, describing $AdS_5 \times S^5$ space with AdS radius and 5-sphere radius

$$R \equiv R_{AdS_5} = R_{S^5} = (4\pi g_s N)^{\frac{1}{4}} l_s. \tag{1.58}$$

The units of RR 5-form flux through the 5-sphere measures the number of D3-branes $N = \int_{S^5} F_5$.

The closed string picture then describes string theory on $AdS_5 \times S^5$ near the horizon of the D brane geometry, while the asyptotically flat region admits free fields corresponding to the massless closed string modes. In the low energy limit, these two types of excitations decouple from each other. Thus the closed string picture of the low energy limit of a stack of N coincident D3 branes describes full IIB string theory on $AdS_5 \times S^5$ decoupled from free gravity in 10d.

Maldacena identified that the dynamics of open strings and closed strings describe the same system, and conjectured that the IIB string theory on $AdS_5 \times S^5$ is an equivalent theory to the four dimensional $\mathcal{N} = 4$ super Yang-Mills theory .

We can see from the relation between gravity parameters R, l_s, g_s and field theory parameters $\lambda_{\prime tHooft}, N$

$$\frac{R}{l_s} = \lambda_{\prime tHooft}^{\frac{1}{4}}, \qquad \lambda_{\prime tHooft} = 4\pi g_s N = g_{YM}^2 N \tag{1.59}$$

that perturbative field theory is valid for $\lambda_{\prime tHooft} << 1$, classical gravity is valid for $\lambda_{\prime tHooft} >> 1$, and quantum string corrections are suppressed for $N >> 1$ as $N \sim \frac{R^4}{l_P^4}$ from $g_s^2 l_s^8 = l_P^8$. The central charge N^2 of the $\mathcal{N} = 4$ Super Yang–Mills theory is related to the effective 5d Newton's constant by $\frac{1}{16\pi G_5} = \frac{N^2}{8\pi^2}$ [7].

If we define $\varepsilon \equiv \frac{1}{r}$, then the region close to the conformal boundary of the near horizon geometry is reached by sending $\varepsilon \to 0$. Translations along ε are related to scaling, or energy, transformations in the dual field theory, so we can interpret $\varepsilon = \frac{1}{r}$ as an energy scale in the dual strongly coupled CFT [22, 23]. Then movement away from the boundary corresponds to a renormalisation group flow in the CFT.

The duality is expected to apply to anti de Sitter space of d+1 dimensions and d dimensional conformal field theories. The isometries of spacetime manifest themselves as global symmetries of the dual field theory, which is defined to reside on the boundary manifold of AdS [24], and physical states are organised as representations of the isometry group. A map between field theory and string theory quantities was given in [24], which states that the AdS/CFT correspondence requires an equivalence between the CFT partition function and the string theory partition function,

$$\langle \exp \left[i \int_{boundary} \psi_0(x) \mathcal{O}(x) \right] \rangle_{CFT} = Z_{IIB} \left[\psi(x, \varepsilon)|_{\varepsilon=0} = \psi_0(x) \right], \tag{1.60}$$

where ψ are (bulk) fields in string theory with boundary values ψ_0, and $\mathcal{O}(x)$ are (boundary) operators of the dual CFT.

Black hole solutions arise as the low energy limit[8] of string theory. While the near horizon geometry of an extremal D3-brane describes the product of AdS_5 space, the geometry near the horizon of a non-extremal D3-brane is that of a black hole sitting in the AdS part of the spacetime. The temperature and entropy of this black hole are mapped by the AdS/CFT correspondence to the temperature and entropy of a thermal ensemble in the dual CFT [25]. Black holes in this spacetime are thermal mixed states in the dual $\mathcal{N} = 4$ super Yang-Mills theory , and the thermodynamic charges of a black hole correspond to the quantum charges carried by the states in the dual CFT.

[7] As the 5d Newton's constant scales like N^{-2}, only objects with mass $\mathcal{O}(N^2)$ will have significant gravitational backreaction on the geometry.

[8] The low energy limit of string theory is supergravity coupled to other fields.

1.4 BTZ Black Holes and 2d CFTs

In the majority of successful cases of precisely matching the degeneracy of CFT states with black hole entropy, the near horizon region contains an AdS_3 factor, and the microscopic entropy is accounted for by counting the states of the dual 2d CFT. In this section we follow [26], [27] in outlining the AdS_3/CFT_2 dictionary between the 3d gravitational and 2d CFT stress tensors, the Virasoro generators and gravity conserved charges, and the Cardy formula.

Stationary axisymmetric solutions to 3d gravity with a negative cosmological constant (1.3) are spacetimes of the form

$$ds^2 = -N^2(r)dt^2 + \frac{dr^2}{N^2(r)} + r^2\left(N_\phi(r)dt + d\phi\right)^2 \tag{1.61}$$

where

$$N^2(r) = \frac{r^2}{\ell_3^2} - 8G_3M + \left(\frac{4G_3J}{r}\right)^2, \qquad N_\phi(r) = \frac{J}{2r^2}, \qquad t \in (-\infty, \infty), \qquad r \in (0, \infty), \qquad \phi \in [0, 2\pi].$$

The inner and outer horizons $r_\pm$ are situated at the zeros of $N^2(r)$:

$$r_\pm^2 = \frac{4G_3\ell_3^2M \pm 4G_3\ell_3\sqrt{\ell_3^2M^2 - J^2}}{2}. \tag{1.62}$$

The values of the horizons decide the nature of the spacetime [5, 28]:

1. $\ell_3 M < J$: this is a space with a conical singularity.
2. $-1 < \ell_3 M - J < 0$: this is a conic space that can be resolved in string theory if $J \in \mathbb{Z}$ and $\sqrt{J - M\ell_3} \in \mathbb{Q}$.
3. $M = -\frac{1}{8G_3}, J = 0$: this is global AdS_3 (1.7).
4. $\ell_3 M + J \geq 0$ and $\ell_3 M - J \geq 0$: this is a rotating BTZ black hole with mass M and angular momentum J.

We are interested in this section - and thesis - in scenarios 3 and 4. We may write the BTZ black hole metric (1.61) as

$$ds^2 = -\frac{(r^2 - r_+^2)(r^2 - r_-^2)}{r^2\ell_3^2}dt^2 + \frac{\ell_3^2r^2}{(r^2 - r_+^2)(r^2 - r_-^2)}dr^2 + r^2\left(d\phi - \frac{r_+r_-}{\ell_3 r^2}dt\right)^2 \tag{1.63}$$

with inner and outer event horizons at $r = r_\pm$. The ADM mass and angular momentum are given by

$$M = \frac{r_+^2 + r_-^2}{8G_3\ell_3}, \quad J = \frac{r_+r_-}{4G_3\ell_3}, \tag{1.64}$$

and the angular momentum, Hawking temperature and Bekenstein-Hawking entropy are [26]

$$\Omega = \frac{r_-}{\ell_3 r_+}, \qquad T_H = \frac{\kappa}{2\pi} = \frac{r_+^2 - r_-^2}{2\pi\ell_3^2 r_+}, \qquad S_{BH} = \frac{A_H}{4G_3} = \frac{\pi r_+}{2G_3}. \tag{1.65}$$

In order to have a well-defined action and variational principle[9] for asymptotically AdS_3 spacetimes, we take an ansatz for the metric in Gaussian normal coordinates

$$ds^2 = d\eta^2 + g_{ij}dx^i dx^j. \tag{1.66}$$

Inserting this ansatz into the variation of I_{EH} (1.3) gives a boundary term that is inconsistent

[9] This is the principle of least action. We vary the path, keeping the end points fixed and require $\delta S = 0$, where $S = \int dL$ is the integral of the Lagrangian between two instants of time. The variational principle keeps this area fixed.

with the variational principle, and we thus require the Gibbons-Hawking term

$$I_{GH} = \frac{1}{8\pi G_3}\int_{\partial\mathcal{M}} d^2x\sqrt{g}\mathrm{Tr}\tilde{K}, \qquad \tilde{K}_{ij} = \frac{1}{2}\partial_\eta g_{ij} \tag{1.67}$$

in the action. Varying the total action $I_{EH} + I_{GH}$ gives bulk pieces that vanish when the equations of motion are satisfied, and a boundary piece defining the stress tensor $\tilde{T}^{ij}$:

$$\delta(I_{EH} + I_{GH}) = \frac{1}{2}\int_{\partial\mathcal{M}} d^2x\sqrt{g}\,\tilde{T}^{ij}\delta g_{ij}, \qquad \tilde{T}^{ij} = -\frac{1}{8\pi G_3}(\tilde{K}^{ij} - \mathrm{Tr}\tilde{K}g^{ij}). \tag{1.68}$$

If we write the ansatz so that it grows as r^2 at infinity, in line with (1.4) and (1.63),

$$g_{ij} = e^{2\frac{\eta}{\ell}}g^{(0)}_{ij} + g^{(2)}_{ij} + \ldots, \tag{1.69}$$

where $g^{(0)}_{ij}$ is its conformal boundary metric - which we identify with the metric of the boundary CFT - , then the action requires another term to avoid divergences in the variation: $I_{tot} = I_{EH} + I_{GH} + I_{ct}$, where

$$I_{ct} = -\frac{1}{8\pi G_3\ell_3}\int_{\partial\mathcal{M}} d^2x\sqrt{g}. \tag{1.70}$$

Then the variation of the action is

$$\delta I = \frac{1}{2}\int d^2x\sqrt{g^{(0)}}\,T^{ij}\delta g^{(0)}_{ij}, \qquad T_{ij} = \frac{1}{8\pi G\ell}\left(g^{(2)}_{ij} - \mathrm{Tr}(g^{(2)})g^{(0)}_{ij}\right), \tag{1.71}$$

where T_{ij} is the AdS_3 stress tensor. It has nonzero trace[10]:

$$\mathrm{Tr}(T) = -\frac{1}{8\pi G_3\ell_3}\mathrm{Tr}(g^{(2)}) = -\frac{\ell_3}{16\pi G_3}\mathcal{R}^{(0)} \tag{1.73}$$

and obeys all the properties of a stress tensor in a two dimensional CFT. This nonzero trace is the Weyl anomaly [20], $\mathrm{Tr}(T) = -\frac{c}{24\pi}\mathcal{R}^{(0)}$, and reproduces Brown and Henneaux's central charge (1.32).

Now, we write the boundary metric as a flat metric on the cylinder: $g^{(0)}_{ij}dx^idx^j = dzd\bar{z}$ with $z, \bar{z}$ given in (1.35). From the stress tensor

$$T_{zz} = \frac{1}{8\pi G_3\ell_3}g^{(2)}_{zz}\ , \quad T_{\bar{z}\bar{z}} = \frac{1}{8\pi G_3\ell_3}g^{(2)}_{\bar{z}\bar{z}} \tag{1.74}$$

we can define the Virasoro generators

$$L_n - \frac{c}{24}\delta_{n,0} = \oint dz\ e^{-inz}T_{zz} \tag{1.75}$$

$$\bar{L}_n - \frac{c}{24}\delta_{n,0} = \oint d\bar{z}\ e^{in\bar{z}}T_{\bar{z}\bar{z}} \tag{1.76}$$

which obey the Virasoro algebra (1.33). Then the conserved charges in asymptotically AdS_3 space are given by the $n = 0$ Virasoro generators:

$$L_0 - \frac{c}{24} = \frac{1}{2}(M\ell_3 - J)\ , \quad \bar{L}_0 - \frac{c}{24} = \frac{1}{2}(M\ell_3 + J). \tag{1.77}$$

[10] using

$$\mathrm{Tr}(g^{(2)}) = \frac{1}{2}\ell_3^2\mathcal{R}^{(0)}. \tag{1.72}$$

For a non-rotating BTZ black hole[11]

$$ds^2 = -\frac{(r^2 - r_+^2)}{\ell_3^2}dt^2 + \frac{\ell_3^2}{(r^2 - r_+^2)}dr^2 + r^2 d\phi^2, \tag{1.78}$$

we have $g^{(2)}_{zz} = g^{(2)}_{\bar{z}\bar{z}} = r_+^2/4$, and hence

$$L_0 = \bar{L}_0 = \frac{\ell_3}{16G}\left(1 + \frac{r_+^2}{\ell_3^2}\right) \qquad \Rightarrow \qquad M = \frac{r_+^2}{8G_3\ell_3^2}\ , \quad J = 0. \tag{1.79}$$

Note that the pure AdS_3 metric has $L_0 = \bar{L}_0 = 0$, so $M\ell_3 = -\frac{c}{12} = -\frac{\ell_3}{8G_3}$. As AdS_3 has the lowest mass of any solution, it plays the role of the vacuum.

Cardy formula for BTZ black holes: We give a brief outline of the Cardy formula for a BTZ black hole as per [26]. Let $\tilde{h}_0$ be the smallest eigenvalue of a state under L_0, and let us define an effective central charge

$$c_{\text{eff}} = c - 24\tilde{h}_0. \tag{1.80}$$

For large $\tilde{h}$ or c, the density of states with eigenvalue, or conformal weight, $\tilde{h}$ of L_0 is then [29]

$$\rho(\tilde{h}) \approx \exp\left(2\pi\sqrt{\frac{c_{\text{eff}}\tilde{h}}{6}}\right)\rho(\tilde{h}_0). \tag{1.81}$$

For a BTZ black hole, we assume that $\tilde{h}_0 = 0$ and we will analyse the density of states with eigenvalue under $L_0 - \frac{c}{24}$ and $\bar{L}_0 - \frac{c}{24}$:

$$S = \ln\rho\left(\tilde{h} - \frac{c}{24}\right) + \ln\rho\left(\bar{\tilde{h}} - \frac{c}{24}\right) = 2\pi\sqrt{\frac{c}{6}\left(L_0 - \frac{c}{24}\right)} + 2\pi\sqrt{\frac{c}{6}(\bar{L}_0 - \frac{c}{24})}, \tag{1.82}$$

which exactly reproduces the three dimensional Bekenstein-Hawking entropy S_{BH} in (1.65) when (1.77) are used in (1.82). This result demonstrates that the entropy associated with counting the states in a two dimensional quantum field theory exactly matches the entropy of a three dimensional classical black hole.

AdS_3/CFT_2 partition functions and higher derivatives: We now investigate the equality of string theory and CFT partition functions (1.60) in a low energy three(two) dimensional setting:

$$Z_{AdS}(g^{(0)}) = Z_{CFT}(g^{(0)}) \tag{1.83}$$

where $g^{(0)}$ labels a conformal class of boundary metrics, taken here to be the flat metric on a torus of modular parameter $\tilde{\tau}$. The partition function for the 2d CFT is [27]

$$Z_{CFT} = Tr\left[e^{2\pi i\tilde{\tau}(L_0 - \frac{c}{24})}e^{-2\pi i\bar{\tilde{\tau}}(\bar{L}_0 - \frac{c}{24})}\right]. \tag{1.84}$$

and for asymptotically AdS space it is

$$Z_{grav} = \sum e^{-I}. \tag{1.85}$$

In the case of the saddle point AdS_3, the variation of the action (1.71) may be written as

$$\delta I = 4\pi^2 i(-T_{zz}\delta\tilde{\tau} + T_{\bar{z}\bar{z}}\delta\bar{\tilde{\tau}}), \qquad \text{with} \qquad T_{zz} = -\frac{c}{48\pi}, \qquad T_{\bar{z}\bar{z}} = -\frac{c}{48\pi}, \tag{1.86}$$

where we have used (1.75) and $L_0 = \bar{L}_0 = 0$, giving the AdS_3 action to be

$$I_{AdS_3} = \frac{i\pi}{12}(c\tilde{\tau} - c\bar{\tilde{\tau}}). \tag{1.87}$$

[11] Note that if we set $r_+^2 = -\ell_3^2$ we recover AdS_3.

In the limit of low temperature, $Im(\tilde{\tau}) \to \infty$, we get

$$\ln Z_{AdS_3} = -\frac{i\pi}{12}(c\tilde{\tau} - c\bar{\tilde{\tau}}) + \text{exponentially suppressed terms.} \tag{1.88}$$

As the stationary BTZ metric (1.78) is related to the AdS_3 metric (1.7) by a change of coordinates

$$z' = -\frac{z}{\tilde{\tau}}, \qquad r' = \frac{\ell_3}{r_+}\sqrt{r^2 - r_+^2}, \tag{1.89}$$

BTZ with $\tilde{\tau}'$ is equivalent to AdS_3 $\tilde{\tau}$ when the identification $\tilde{\tau}' = -\frac{1}{\tilde{\tau}}$ is made. Then the BTZ action and partition function are, for high temperature, $Im(\tilde{\tau}) \to 0^+$,

$$I_{BTZ} = -\frac{i\pi}{12}\left(\frac{c}{\tilde{\tau}} - \frac{c}{\bar{\tilde{\tau}}}\right), \qquad \ln Z_{BTZ} = \frac{i\pi}{12}\left(\frac{c}{\tilde{\tau}} - \frac{c}{\bar{\tilde{\tau}}}\right) + \text{exponentially suppressed terms.} \tag{1.90}$$

We note that

$$\ln Z_{CFT} = 2\pi i\tilde{\tau}\left(L_0 - \frac{c}{24}\right) - 2\pi i\bar{\tilde{\tau}}\left(\bar{L}_0 - \frac{c}{24}\right) \tag{1.91}$$

to get

$$L_0 - \frac{c}{24} = \frac{1}{2\pi i}\frac{\partial \ln Z_{CFT}}{\partial\tilde{\tau}} = -\frac{c}{24\tilde{\tau}^2} \quad \Rightarrow \quad \sqrt{c\left(L_0 - \frac{c}{24}\right)} = \frac{ic}{12\tilde{\tau}}, \tag{1.92}$$

and similarly for $\bar{L}_0$, $\bar{\tilde{\tau}}$, c. Then we read the Cardy formula for the black hole entropy:

$$S_{BTZ} = \ln Z_{BTZ} = 2\pi\sqrt{\frac{c}{6}\left(L_0 - \frac{c}{24}\right)} + 2\pi\sqrt{\frac{c}{6}\left(\bar{L}_0 - \frac{c}{6}\right)} = S_{CFT}. \tag{1.93}$$

This result can be generalised to rotating BTZ black holes (1.63), by describing them as quotients of AdS_3 space [27], whence the action may be written as

$$I(\tilde{\tau}, \bar{\tilde{\tau}}) = \frac{i\pi}{12}\left[c\left(\frac{A\tilde{\tau} + B}{C\tilde{\tau} + D}\right) - c\left(\frac{A\bar{\tilde{\tau}} + B}{C\bar{\tilde{\tau}} + D}\right)\right]. \tag{1.94}$$

We note that in theories with actions containing higher derivative terms the analogue of the Brown Henneaux central charge may be written as

$$c = \frac{\ell_3}{2G_3}g_{\mu\nu}\frac{\partial L}{\partial R_{\mu\nu}}, \tag{1.95}$$

and the BTZ black hole entropy is generalised by Wald's entropy formula [30] to

$$S = -\frac{1}{8G_3}\int_H dx\sqrt{h}\frac{\delta L}{\delta R_{\mu\nu\alpha\beta}}\epsilon^{\mu\nu}\epsilon^{\alpha\beta}. \tag{1.96}$$

Left and right moving temperatures: Associated to the left and right moving operators in the dual CFT are left and right moving temperatures. Here we derive these quantities using the relationships between the thermodynamic expressions of the dual black holes (1.64-1.65). While in Chapter 2 we will discuss the first law of thermodynamics in detail, we will simply state it here for the BTZ black hole;

$$T_{\rm H} dS_{\rm BH} = dM - \Omega dJ, \tag{1.97}$$

from which the following relations immediately follow:

$$\beta_T \equiv \frac{1}{T_{\rm H}} = \frac{\partial S_{\rm BH}}{\partial M}, \qquad \Omega = \frac{\partial M}{\partial J}. \tag{1.98}$$

We define the quantities

$$h_\pm \equiv \frac{M\ell_3 \pm J}{2}, \qquad \beta_+ = \frac{\partial S_{\rm BH}}{\partial h_+} \equiv \frac{1}{T_L}, \qquad \beta_- = \frac{\partial S_{\rm BH}}{\partial h_-} \equiv \frac{1}{T_R}. \tag{1.99}$$

It is then straightforward to check, using the chain rule and the expressions for $T_{\rm H}$ and Ω (1.65), that the left and right moving temperatures are given by

$$T_L = \frac{r_+ + r_-}{4\pi\ell_3}, \qquad T_R = \frac{r_+ - r_-}{4\pi\ell_3}. \tag{1.100}$$

1.5 The Kerr/CFT Correspondence

So far, we have encountered possible dual descriptions of black holes in anti de Sitter space with holographic field theory duals. The degeneracy of states in these quantum field theories explain the black hole entropy (1.1).

The black holes in asymptotically AdS space do not, however, describe those that are observed in the real world. Strominger et al [31] employed the asymptotic symmetries technique of Brown and Henneaux described in section 1.1 and utilised the results of Brandt et al [32] to suggest a microscopic description for the extremal limit of the experimentally observed asymptotically flat Kerr black hole [33].

The authors used certain boundary conditions for extremal Kerr black holes in the near horizon limit to show that the generators of the ASG, defined in section 1.1, form an algebra that can be quantised to give one copy of a Virasoro algebra (1.33) with non–vanishing central charge. This algebra is compatible with the existence of a dual 2d CFT description of the black holes.

The vacuum Einstein equations in four dimensions are solved by the Kerr metric (in Boyer-Lindquist coordinates):

$$ds^2 = g_{\mu\nu}dx^\mu dx^\nu = -\frac{\hat{\Delta}}{\hat{\rho}^2}\left(d\hat{t} - a\sin^2\theta d\hat{\phi}\right)^2 \tag{1.101}$$

$$+ \frac{\sin^2\theta}{\hat{\rho}^2}\left((\hat{r}^2+a^2)d\hat{\phi} - ad\hat{t}\right)^2 + \frac{\hat{\rho}^2}{\hat{\Delta}}d\hat{r}^2 + \hat{\rho}^2 d\theta^2 \tag{1.102}$$

$$\hat{\Delta} = r^2 - 2mr + a^2, \qquad \hat{\rho} = r^2 + a^2\cos^2\theta. \tag{1.103}$$

As this metric is invariant under time $\hat{t}$ and angular $\hat{\phi}$ translations, $\mathcal{L}_{\partial_{\hat{t}}} g_{\mu\nu} = \mathcal{L}_{\partial_{\hat{\phi}}} g_{\mu\nu} = 0$, its corresponding conserved charges are its mass M and angular momentum J_ϕ. The inner and outer horizons are located at the roots of $\hat{\Delta} = 0$,

$$r_\pm = m \pm \sqrt{m^2 - a^2}, \tag{1.104}$$

where the parameters a and m respectively parameterise the angular momentum and mass of the black hole. The Hawking temperature, Bekenstein-Hawking entropy and angular velocity of the horizon[12] are

$$T_{\rm BH} = \frac{r_+ - m}{4\pi m r_+}, \qquad S_{\rm BH} = \frac{2\pi m r_+}{G_4} \qquad \Omega_\phi = \frac{a}{2mr_+}. \tag{1.105}$$

A black hole is *extremal* when its inner and outer horizons coincide, $r_+ = r_- = r_0$ so that its temperature $T_{\rm BH}$ vanishes. For the Kerr black hole, we can see from (1.104) that this is achieved for $m = a = r_0$. Taking a near horizon limit of the extremal geometry enhances the isometry group to $\mathrm{SL}(2,\mathbb{R}) \times \mathrm{U}(1)$ so that the metric

$$ds^2 = 2G_4 J\Omega^2(\theta)\left(-r^2dt^2 + \frac{dr^2}{r^2}\right) + 2G_4 J\Omega^2(\theta)d\theta^2 + \Lambda^2(\theta)(d\phi + rdt)^2 \tag{1.106}$$

contains a circle bundle over an AdS_2 base. The U(1) is generated by ∂_ϕ, while the $\mathrm{SL}(2,\mathbb{R})$,

[12] These quantities will be discussed in more detail in Chapter 2.

generated by

$$\xi_0 = 2\partial_t, \tag{1.107}$$

$$\xi_1 = 2\sin t\frac{r}{\sqrt{r^2+1}}\partial_t - 2\cos t\sqrt{r^2+1}\partial_r + \frac{2\sin t}{\sqrt{r^2+1}}\partial_\phi, \tag{1.108}$$

$$\xi_2 = -2\cos t\frac{r}{\sqrt{r^2+1}}\partial_t - 2\sin t\sqrt{r^2+1}\partial_r - \frac{2\cos t}{\sqrt{r^2+1}}\partial_\phi, \tag{1.109}$$

acts both on the AdS_2 subspace and along the fiber to preserve the form of $(d\phi + rdt)$ [31]. This metric at a fixed θ has the form of a warped circle fibration over AdS_2 in which the fiber radius depends on the angle θ[13]. This observation is in fact universal for extremal black holes in 4 and 5 dimensions [37], as extremality of the black holes induces this structure on the near horizon regions.

The isometry group of the near horizon extremal Kerr (1.106) is shared by the near horizon geometry of an extremal ($r_+ = r_-$) asymptotically AdS_3 BTZ black hole (1.63)

$$ds^2 = \Gamma\left(-r^2dt^2 + \frac{dr^2}{r^2}\right) + \gamma\left(d\phi + krdt\right)^2, \tag{1.110}$$

with $\Gamma = \frac{\ell_3^2}{4}$, $\gamma = \ell_3^2$, $k = -\frac{1}{2}$. The authors took this isometry matching as a clue to some dual CFT description, and followed the steps of Brown and Henneaux, sketched in section 1.1, to search for a symmetry algebra associated to a two dimensional CFT.

1.5.1 Generators of the ASG

We discussed in section 1.1 how the Lagrangian is invariant under a transformation (1.15) of the metric, where the gauge symmetries ξ are generated by conserved charges. Brandt et al [32] have developed a framework to evaluate the conserved charges that generate these gauge symmetries. Their method utilises linearised theory around solutions to the equations of motion obtained by perturbing the background metric $\bar{g}$ to $g = \bar{g} + h$. Strominger et al chose the boundary conditions

$$h_{\mu\nu} = h_{\nu\mu} = \mathcal{O}\begin{pmatrix} r^2 & 1 & \frac{1}{r} & \frac{1}{r^2} \\ & 1 & \frac{1}{r} & \frac{1}{r} \\ & & \frac{1}{r} & \frac{1}{r^2} \\ & & & \frac{1}{r^3} \end{pmatrix} \tag{1.111}$$

in the basis (t, ϕ, θ, r). The transformations

$$\xi = \left(-r\epsilon'(\phi) + \mathcal{O}(1)\right)\partial_r + \left(C + \mathcal{O}(\frac{1}{r^3})\right)\partial_t + \left(\epsilon(\phi) + \mathcal{O}(\frac{1}{r^2})\right)\partial_\phi + \mathcal{O}\left(\frac{1}{r}\right)\partial_\theta \tag{1.112}$$

are solutions to (1.17) and generate the allowed symmetry transformations of the ASG. The subleading terms correspond to trivial diffeomorphisms, i.e. the generators of the transformations due to these diffeomorphisms vanish and so the asymptotic symmetry group of these spacetimes is generated by the asymptotic Killing vectors:

$$\zeta_\epsilon = \epsilon(\phi)\partial_\phi - r\epsilon'(\phi)\partial_r. \tag{1.113}$$

As ϕ is a periodic coordinate, the functions $\epsilon(\phi)$ can be written as

$$\epsilon_n(\phi) = -e^{-in\phi}, \tag{1.114}$$

so that the generators of the ASG can be written

$$\zeta_n = \zeta(\epsilon_n) = rine^{-in\phi}\partial_r - e^{-in\phi}\partial_\phi \tag{1.115}$$

[13] One sees similar squashed geometries with AdS_2 and AdS_3 factors in decoupling limits of near-extremal black holes in anti-de Sitter space [28, 34, 35]. (Also see [36].)

and form one copy of a Witt algebra:

$$i[\zeta_m, \zeta_n] = (m-n)\zeta_{m+n}. \tag{1.116}$$

Conserved charges associated with gauge symmetries: According to [32], the conserved charge $Q_\zeta[g(x)]$ associated with diffeomorphism invariance is given by the flux of an antisymmetric superpotential $\mathrm{d}-2$ form $k_f^{[\nu\mu]}$ through the boundary of a spacelike surface Σ of the 4d spacetime

$$Q_\zeta[g(x)] = \int_{\partial\Sigma} k_\zeta\Big|_{g(x)} \tag{1.117}$$

where $g(x) = \bar{g} + h$ describes the background metric $\bar{g}$ (1.106) and the fluctuations (1.111). This superpotential is given by

$$k_\zeta[h,g] = \frac{1}{4}\epsilon_{\alpha\beta\mu\nu}(\zeta^\nu D^\mu h - \zeta^\nu D_\sigma h^{\mu\sigma} + \zeta_\sigma D^\nu h^{\mu\sigma} + \frac{1}{2}hD^\nu\zeta^\mu - h^{\nu\sigma}D_\sigma\zeta^\mu + \frac{1}{2}h^{\sigma\nu}(D^\mu\zeta_\sigma + D_\sigma\zeta^\mu))dx^\alpha \wedge dx^\beta, \tag{1.118}$$

where $\zeta^\mu(x)$ are the generators of the ASG, and the covariant derivative D_μ is calculated with respect to the background metric $\bar{g}$. Indices are lowered and raised by applying the background metric $\bar{g}_{\mu\nu}$ and its inverse $\bar{g}^{\mu\nu}$.

Algebra of the conserved charges: A theorem by Brandt et al [32] gives the Dirac bracket algebra of the generators of the gauge symmetries of spacetime,

$$\{Q_{\zeta_m}, Q_{\zeta_n}\}_{DB} = Q_{[\zeta_m,\zeta_n]} + \frac{1}{8\pi G}\int_{\partial\Sigma} k_{\zeta_m}[\mathcal{L}_{\zeta_n}\bar{g}, \bar{g}], \tag{1.119}$$

with the central charge

$$K_{\zeta_m,\zeta_n} = \frac{1}{8\pi G}\int_{\partial\Sigma} k_{\zeta_m}[\mathcal{L}_{\zeta_n}\bar{g}, \bar{g}] \tag{1.120}$$

arising as a central extension of the algebra from the conserved charge Q_ζ by substitution of $\mathcal{L}_\zeta(\bar{g})$ for h.

From (1.120) we can see that when exact Killing vectors of the background metric are considered, there is no central charge in the algebra:

$$\mathcal{L}_\zeta(\bar{g}) = 0 \quad \Rightarrow \quad K_{\zeta_m,\zeta_n} = 0. \tag{1.121}$$

For an appropriate definition of the quantum version of the charges, the Dirac bracket algebra defines a Virasoro algebra. This is calculated explicitly for the Kerr black hole below.

1.5.2 Explicit realisation of the Virasoro algebra

The superpotential of the Kerr black hole (1.101) is given in [31] to be

$$k_{\zeta_\epsilon} = \frac{1}{4\Lambda}\left(2\Lambda^2\epsilon' r h_{r\phi} - \epsilon\Lambda^2\left(\Lambda^2\frac{h_{tt}}{r^2} + (\Lambda^2+1)h_{\phi\phi} + 2r\partial_\phi h_{r\phi}\right)\right)d\theta\wedge d\phi. \tag{1.122}$$

The symmetry transformations of the background metric under the action of the ASG is given by its Lie derivative with respect to the generators (1.113) of the ASG with $\epsilon_n(\phi) = -e^{-in\phi}$:

$$\mathcal{L}_{\phi_n}\bar{g}_{tt} = 4GJ\Omega^2(1-\Lambda^2)r^2 ine^{-in\phi} \tag{1.123}$$

$$\mathcal{L}_{\phi_n}\bar{g}_{r\phi} = \frac{-2GJ\Omega^2 r}{1+r^2}n^2 e^{-in\phi} \tag{1.124}$$

$$\mathcal{L}_{\phi_n}\bar{g}_{\phi\phi} = 4GJ\Omega^2\Lambda^2 ine^{-in\phi} \tag{1.125}$$

$$\mathcal{L}_{\phi_n}\bar{g}_{rr} = \frac{-4GJ\Omega^2}{(1+r^2)^2}ine^{-in\phi}. \tag{1.126}$$

For the Kerr metric, the functions $\Omega(\theta)$ and $\Lambda(\theta)$ are given by

$$\Omega^2 \equiv \frac{1+\cos^2\theta}{2}, \quad \Lambda \equiv \frac{2\sin\theta}{1+\cos^2\theta}. \tag{1.127}$$

Substitution into (1.122) yields

$$K_{\zeta_m,\zeta_n} = \frac{1}{8\pi G}\int e^{-i(m+n)\phi}\Lambda GJ\Omega^2\left(\frac{-rimn^2}{1+r^2} + 2\Lambda^2(1-\Lambda^2)in + \frac{ir^2n^3}{1+r^2}\right)d\theta d\phi \tag{1.128}$$

$$\overset{r\to\infty}{=} \frac{1}{8\pi}\int e^{-i(m+n)\phi}\Lambda J\Omega^2 i\left(n^2(n-m)+2n\Lambda^2\right) \tag{1.129}$$

$$= \frac{Ji}{8\pi}\int e^{-i(m+n)\phi}\sin\theta\left(n^2(n-m) + 2n\frac{\sin^2\theta}{(1+\cos^2\theta)^2}\right) \tag{1.130}$$

$$= \delta_{m+n,0}\frac{Ji}{2}\left(n^2(n-m)+4n\right) \tag{1.131}$$

$$= -i(m^3+2m)\delta_{m+n,0}J, \tag{1.132}$$

where we have used the identity

$$\int_0^{2\pi} e^{-i(m+n)\phi} = 2\pi\delta_{m+n,0}. \tag{1.133}$$

To obtain the quantum charge algebra, Strominger et al defined the quantum generators

$$\hbar\bar{L}_n \equiv Q_{\zeta_n} + \frac{3J_\phi}{2}\delta_{n,0} \tag{1.134}$$

and applied the standard rule for moving from a classical to a quantum theory by quantising the Dirac brackets, $\{.,.\}_{DB} \to -\frac{i}{\hbar}[.,.]$, so that (1.119) gives

$$\{Q_{\zeta_m}, Q_{\zeta_n}\}_{DB} \to -\frac{i}{\hbar}\left[Q_{\zeta_m}, Q_{\zeta_n}\right] = -i(m-n)Q_{\zeta_{m+n}} - im(m^2+2)\delta_{m+n,0}J_\phi. \tag{1.135}$$

Substitution of the quantum expression for the charges (1.134) into the Lie bracket gives

$$\frac{-i}{\hbar}\left[\hbar\bar{L}_m - \frac{3J}{2}\delta_m, \hbar\bar{L}_n - \frac{3J}{2}\delta_n\right] = -i\bar{L}_{m+n} + i(m-n)\frac{3J_\phi}{2}\delta_{m+n,0} - im(m^2+2)\delta_{m+n,0}J_\phi$$

$$\Rightarrow \qquad -i\hbar[\bar{L}_m, \bar{L}_n] = (m-n)\bar{L}_{m+n} + \frac{J_\phi}{\hbar}(m^3-m)\delta_{m+n,0}, \tag{1.136}$$

where the Witt algebra (1.116) obeyed by the generators ζ of the ASG has been used. This quantum charge algebra is a Virasoro algebra (1.33) with central charge

$$c_\phi = 12J_\phi, \tag{1.137}$$

with J_ϕ the angular momentum of the extremal Kerr black hole.

We now have an expression for a central charge that could be attributed to a two dimensional conformal field theory, and look towards calculating the associated temperature.

A quantum field in the extremal Kerr black hole background can be expanded in eigenmodes of energy ω and angular momentum $\tilde{m}$. The Frolov-Thorne vacuum is a diagonal density matrix in the energy-angular momentum eigenbasis with a Boltzmann weighting factor

$$\hat{\rho} \propto e^{-\frac{\omega-\Omega_\phi \tilde{m}}{T_{\rm H}}}. \tag{1.138}$$

Near the horizon [31], this may be written as

$$e^{-\frac{2\pi\tilde{m}}{T_\phi}}, \tag{1.139}$$

where the dimensionless quantity $T_\phi = \frac{1}{2\pi}$ is the Frolov-Thorne temperature associated to the near horizon extremal black hole. A detailed calculation of Frolov-Thorne temperatures in arbitrary dimension can be found in Appendix A.

The entropy of the left-moving sector of a two dimensional CFT is [38]

$$S = 2\pi\sqrt{\frac{\bar{c}}{6}\left(\bar{L}_0 - \frac{\bar{c}}{24}\right)}, \tag{1.140}$$

where the energy $\bar{L}_0 - \frac{\bar{c}}{24}$ is related to the temperature T and entropy S by the first law of thermodynamics:

$$d\left(\bar{L}_0 - \frac{\bar{c}}{24}\right) = TdS. \tag{1.141}$$

Using $\sqrt{\bar{L}_0 - \frac{\bar{c}}{24}} = \frac{S}{2\pi}\frac{6}{\bar{c}}$, we can write

$$dS = \pi\sqrt{\frac{\bar{c}}{6\left(\bar{L}_0 - \frac{\bar{c}}{24}\right)}} \quad \Rightarrow \quad \sqrt{\bar{L}_0 - \frac{\bar{c}}{24}} = \pi\sqrt{\frac{\bar{c}}{6}}T \tag{1.142}$$

allowing us to express the entropy in terms of the central charge $\bar{c}$ and temperature T:

$$S = \frac{\pi^2}{3}\bar{c}T. \tag{1.143}$$

Identifying $(\bar{c}, T)$ with (c_ϕ, T_ϕ), we find that the Cardy formula for the left moving sector of a 2d CFT then reproduces the Bekenstein-Hawking entropy for the Kerr black hole:

$$S_{\rm Cardy} = \frac{\pi^2}{3}c_\phi T_\phi = 2\pi J_\phi = S_{\rm BH}. \tag{1.144}$$

The geometry near the horizon of the extremal Kerr geometry can then be associated with a thermal state of the 2d CFT at temperature $T_{NHEK} = 1/2\pi$.

1.5.3 Extremal black Hole/CFT correspondence in d>4

Originally formulated for black holes in 4 dimensions, the Kerr/CFT correspondence has been generalised in e.g. [36, 38, 39] to higher dimensions and curved spacetimes. The near horizon geometry of extremal black holes in dimension d$= 2n + D$, where $D = 0, 1$, can be written in Poincaré coordinates as

$$ds^2 = \tilde{A}\left(-\rho^2 dt^2 + \frac{d\rho^2}{\rho^2}\right) + \sum_{\alpha=1}^{n-1} F_\alpha dy_\alpha^2 + \sum_{i,j=1}^{n-1+D} \widetilde{g}_{ij}\widetilde{e}_i\widetilde{e}_j, \tag{1.145}$$

with

$$\widetilde{e}_i = d\phi_i + k_i\rho dt, \qquad k_i = \frac{1}{2\pi T_i}. \tag{1.146}$$

A near horizon geometry in the class (1.145) contains an AdS_2 base and, for constant $\widetilde{g}_{ij}$, a circle fibration for each azimuthal angle. Each ϕ_i has associated to it an ASG generated by

$$\zeta_n^{(i)} = -e^{(-in\phi_i)}\partial_{\phi_i} - inre^{(-in\phi_i)}\partial_r, \tag{1.147}$$

as in (1.115). Each diffeomorphism generates a Virasoro algebra , with central charge

$$c_i = \frac{6k_i S_{\rm BH}}{\pi} \tag{1.148}$$

computed as in subsection 1.5.1 from the central extension of the Dirac bracket algebra (1.119) of the conserved charges (1.117). The entropy of a two dimensional CFT with central charge c_i reproduces the black hole entropy,

$$S_{\rm BH} = \frac{\pi^2}{3} c_i T_i, \tag{1.149}$$

where each Frolov-Thorne temperature is given by

$$T_i = -\frac{T'_{\rm BH}(r_0)}{\Omega'_i(r_0)}, \qquad T'_{\rm BH}(r_0) \equiv \left.\frac{\partial T_{\rm BH}}{\partial r_+}\right|_{r_+=r_0}, \qquad \Omega'_i(r_0) \equiv \left.\frac{\partial \Omega_i}{\partial r_+}\right|_{r_+=r_0}. \tag{1.150}$$

Pope et al [38] suggested that, as the relation $S_{\rm BH} = S_{\rm CFT}(c_i)$ has no features that depend on the dimension of these black holes (1.145), it is likely to hold in any dimension.

In Chapter 2, we will investigate the first law of thermodynamics for generic extremal black holes and give a *thermodynamic* argument for the existence of the Frolov-Thorne temperature and central charge.

However, apart from these quantities, we know little else of this proposed holographic dual to an extremal black hole. We will see in the following sections that a special class of nearly extremal black holes with vanishing horizon size (EVH black holes) may also have 2d dual descriptions. The near horizon geometry of these black holes contain locally AdS_3 geometries, allowing us to use the AdS_3/CFT_2 correspondence outlined in section 1.4 to glean information on the CFT duals.

1.6 Black Hole Extremality and CFT_2 Chirality

We may ask whether the AdS_2 base of the extremal black holes in section 1.5 has a a one dimensional CFT dual that would satisfy the Cardy formula producing the extremal black hole entropy (1.149). However, it was shown in [40] that a consistent quantum theory of gravity in this background should not have any states charged under the isometry group $SL(2,\mathbb{R})$. All degrees of freedom transform trivially under $SL(2,\mathbb{R})$, as excitations in AdS_2 back-react and can modify the *asymptotic* structure of the spacetime [41].

The fibred AdS_2 component (1.110) appears in the near horizon geometry (1.145) of many extremal, asymptotically flat or AdS black holes. In particular, it shows up in the near horizon geometry of extremal BTZ black holes. In this section, following [40] we outline how the near horizon geometry of an extremal BTZ black hole can be identified with the Discrete Lightcone Quantisation (DLCQ) of a 2d CFT.

The extremal limit of a BTZ black hole (1.63) is obtained by setting $r_+ = r_- \equiv r_0$ so that the geometry is given by

$$ds^2 = -\frac{(r^2-r_0^2)^2}{r^2\,\ell_3^2}\,dt^2 + \frac{\ell_3^2\,r^2}{(r^2-r_0^2)^2}\,dr^2 + r^2\left(d\phi - \frac{r_0^2}{r^2}\,\frac{dt}{\ell_3}\right)^2. \tag{1.151}$$

We note that the boundary of this spacetime is conformal to a cylinder of radius ℓ_3:

$$ds^2 \to \frac{r^2}{\ell_3^2}(-dt^2 + \ell_3^2 d\phi^2), \tag{1.152}$$

and its near horizon geometry[14] can be written as an S^1 fibration over AdS_2:

$$\begin{aligned} ds^2 &= \frac{\ell_3^2}{4}\frac{d\rho^2}{\rho^2} - \frac{\rho^2}{r_0^2}\frac{d\tau^2}{\ell_3^2} + r_0^2\left(d\varphi + \frac{\rho}{r_0^2}\frac{d\tau}{\ell_3}\right)^2 \\ &= \frac{\ell_3^2}{4}\frac{d\rho^2}{\rho^2} + 2\frac{\rho}{\ell_3}d\tau d\varphi + r_0^2 d\varphi^2\,. \end{aligned} \tag{1.154}$$

The geometry (1.154) is called the spacelike self-dual orbifold of AdS_3. The $SL(2,\mathbb{R})$ component of the isometry group $SL(2,\mathbb{R})\times U(1)$ corresponds to isometries of the AdS_2 base. A change of coordinates

$$\hat{u} = t/\ell_3 - \phi\,, \qquad \hat{v} = t/\ell_3 + \phi, \qquad r^2 - r_0^2 = \ell_3^2 e^{2\rho}\,, \qquad \{\hat{u},\hat{v}\}\sim\{\hat{u}-2\pi,\hat{v}+2\pi\} \tag{1.155}$$

will make the boundary cylinder more apparent, and the extremal BTZ metric in these coordinates is then

$$ds^2 = r_+^2 d\hat{u}^2 + \ell_3^2 d\rho^2 - \ell_3^2 e^{2\rho} d\hat{u}d\hat{v}. \tag{1.156}$$

We take the near horizon limit by focussing on the region close to the horizon, $r\to r_0 \Leftrightarrow \rho\to -\infty$:

$$\rho = \rho_0 + r, \quad u = \hat{u}\,\frac{r_+}{\ell_3}, \quad v = \frac{e^{2\rho_0}\ell_3}{r_+}\,\hat{v}, \quad \{u,v\}\sim\{u-2\pi\frac{r_+}{\ell_3}, v+2\pi\frac{\ell_3}{r_+}e^{2\rho_0}\} \quad (\rho_0\to-\infty)$$

to get a metric

$$ds^2 = \ell_3^2(du^2 + dr^2 - e^{2r}\,du\,dv), \qquad \{u,v\}\sim\{u-2\pi\frac{r_0}{\ell_3}, v\}. \tag{1.157}$$

The $r\to\infty$ boundary of this near horizon metric is a null cylinder

$$ds^2 \sim dudv, \qquad \{u,v\}\sim\{u-2\pi\frac{r_0}{\ell_3}, v\}. \tag{1.158}$$

This null cylinder has a metric conformal to the standard lightcone metric on a cylinder, but has a compact *null* direction (u); the spacelike circle at the causal boundary of the extremal BTZ geometry has become a light-like circle at the horizon. Thus moving from the boundary to the horizon is like boosting the spacelike circle so that it becomes approximately null.

At any fixed r, the metric is one of a boosted cylinder:

$$ds^2 = du^2 - e^{2r}\,du\,dv. \tag{1.159}$$

To see this, we take a cylinder of radius R:

$$ds^2 = -dt^2 + R^2 d\phi^2, \qquad \{t,\phi\}\sim\{t,\phi+2\pi\}. \tag{1.160}$$

We can define the coordinates

$$T = 2Rt, \qquad U = t - R\phi, \qquad \{T,U\}\sim\{T,U-2R\pi\} \tag{1.161}$$

and write the metric as

$$ds^2 = dU^2 - dUdT. \tag{1.162}$$

Now, we may boost the cylinder with rapidity 2γ by scaling $T = e^{2\gamma}\hat{T}$ so that the boosted metric is given by

$$ds^2 = dU^2 - e^{2\gamma}dUd\hat{T}, \qquad \{\hat{T},U\}\sim\{\hat{T},U-2R\pi\}, \tag{1.163}$$

[14]The near horizon limit is

$$r^2 = r_0^2 + \epsilon\rho, \qquad t = \frac{\tau}{\epsilon}, \qquad \varphi = \phi - \frac{\tau}{\epsilon\ell_3}, \qquad \epsilon\to 0. \tag{1.153}$$

and can be identified for $R = \frac{r_0}{\ell_3}$ with fixed radial surfaces of the near horizon extremal BTZ metric (1.159).

The right-moving Hamiltonian of a CFT on the boundary of the asymptotically AdS_3 geometry is given by

$$\partial_{\hat{v}} = L_0 - \frac{c}{24}. \tag{1.164}$$

The Hamiltonian defined in the near horizon geometry is given by

$$\partial_v \sim e^{-2\rho_0}\, \partial_{\hat{v}}\,, \tag{1.165}$$

so that near the horizon, as $\rho_0 \to -\infty$, all finite energy states $|s\rangle$ are annihilated by the right-moving zero mode of the Virasoro generator:

$$\partial_{\hat{v}}|s\rangle = e^{2\rho_0}\partial_v|s\rangle = (L_0 - c/24)|s\rangle = 0 \tag{1.166}$$

so that the right-moving sector is frozen to its vacuum state. That is, one chiral set of Virasoro generators of the CFT is frozen in this limit, in the sense that there are no physical states charged under them. As the left-moving Hamiltonian does not scale with ρ_0, the left-moving states are not affected by the near-horizon limit.

Thus the near horizon limit of the extremal BTZ black hole focuses in on energies so low that they lie below the black hole mass gap, thus eliminating all non-extremal dynamics [42].

The $SL(2,\mathbb{R})$ isometries are associated to reparameterisations of the non-compact coordinate v on the boundary, while the physical states only carry momentum along the compact null direction u on which only the U(1) part of the isometry group acts. Thus, AdS/CFT is telling us that physical states cannot be charged under the $SL(2,\mathbb{R})$ isometry group associated to the AdS_2 base in (1.154). The AdS_2 factor cannot be excited: it is the geometric manifestation of the frozen $\bar{L}_0$ sector, and the excitations in the dynamical L_0 sector involve the remaining third space-time coordinate. Because the right-movers are frozen very little dynamics is left in this case.

We note from (1.154) that the φ direction at generic ρ is a spacelike circle, becoming null at the boundary, while τ is always null. The chiral CFT resides on the null cylinder causal boundary of the self-dual orbifold. Once the periodicity of the φ direction is fixed to 2π, the only parameter of the self-dual orbifold metric, r_0, is then related to the value of the light-cone momentum $p^+ = \bar{L}_0 - \frac{c}{24}$ defining the DLCQ sector.

DLCQ of 2d CFT = chiral CFT: We now demonstrate how a CFT with one sector frozen is in fact the DLCQ of a 2d CFT. The DLCQ prescription emerges when approaching the horizon:

$$\text{Near Horizon of Extremal BTZ} \xrightarrow{\text{boundary}} \text{Boosted Cylinder} = \text{DLCQ of CFT} \tag{1.167}$$

Let us consider a 2d CFT on a cylinder of radius R with metric (1.160) and write it in terms of left-moving coordinate u and right-moving coordinate v:

$$ds^2 = -dudv, \tag{1.168}$$

$$u = t - R\phi \sim u - 2\pi R; \qquad v = t + R\phi \sim v + 2\pi R. \tag{1.169}$$

The operator conjugate to u, measuring the energy in the left-moving sector, is

$$P^v = \left(\tilde{h} + n - \frac{c}{24}\right)\frac{1}{R} \equiv \left(\bar{L}_0 - \frac{c}{24}\right)\frac{1}{R}, \tag{1.170}$$

where n is quantised, and the momentum operator conjugate to v, measuring the energy in the right-moving sector, is

$$P^u = \left(\tilde{h} - \frac{c}{24}\right)\frac{1}{R} \equiv \left(L_0 - \frac{c}{24}\right)\frac{1}{R}. \tag{1.171}$$

We perform a boost with rapidity γ which leaves the metric (1.168) invariant while scaling the coordinate periodicities

$$U = e^{\gamma} u \sim U - 2\pi R e^{\gamma}, \qquad V = e^{-\gamma} v \sim V - 2\pi R e^{-\gamma}. \tag{1.172}$$

If we send $\gamma \to \infty$ and keep $\hat{R} \equiv R e^{\gamma}$ fixed, the periodicities $\{U, V\} \sim \{U - 2\pi\hat{R}, V\}$ can be identified with those of the near horizon extremal BTZ boundary and the DLCQ of 2d CFT on a cylinder is the same configuration as (1.158), with $\hat{R}$ identified with $\frac{r_0}{\ell_3}$.

We can see from the energies in the boosted sectors[15]

$$P^V = \left(\tilde{h} + n - \frac{c}{24}\right)\frac{e^{-\gamma}}{R}, \qquad P^U = \left(\tilde{h} - \frac{c}{24}\right)\frac{e^{\gamma}}{R} \tag{1.173}$$

that there will be an infinite energy gap in the right-moving sector unless we set $\tilde{h} = \frac{c}{24}$. Then the energy of the left-moving sector is given by

$$P^V = \frac{n}{\hat{R}}. \tag{1.174}$$

Thus the right-moving sector is frozen to $\tilde{h} = c/24$, and all physical finite energy states only carry momentum along the finite direction u.

We can see from the expressions for the left and right-moving temperatures (1.100)

$$T_L = \frac{r_+ + r_-}{4\pi\ell_3}, \qquad T_R = \frac{r_+ - r_-}{4\pi\ell_3} \tag{1.175}$$

that the identification of the DLCQ sector with the extremal BTZ black hole allows us to assign the temperatures $(T_L, T_R) = (\hat{R}/2\pi, 0)$ to the the CFT.

So we see that the DLCQ limit defines a Hilbert space

$$\mathcal{H} = \{|\text{anything}\rangle_L \otimes |c/24\rangle_R\} \tag{1.176}$$

and the surviving chiral sector is in the state in which it was placed to realize the dual to an extremal black hole, namely a thermal state at a temperature $T_L = T_{\text{DLCQ}} = \hat{R}/(2\pi)$, corresponding to the left-moving thermal state $|\, T = \hat{R}/2\pi\rangle \otimes |\, c/24\rangle$ in the Hilbert space of the CFT dual to AdS_3.

It was shown in [43] that globally the self-dual orbifold geometry has two causal boundaries, each of which is a null cylinder carrying a DLCQ of a CFT. Both the near horizon geometry of extremal BTZ and the 3d uplift of the AdS_2 background with constant electric flux can thus be regarded globally as duals of two DLCQ CFTs, each giving rise to one chiral theory [43]. We can then view the self-dual orbifold as a thermal state in a single CFT emerging from tracing over the Hilbert space living in one of the boundaries.

The authors of [40] concluded that gravity on the near horizon geometry of an extremal BTZ black hole is described by the chiral sector of a two dimensional conformal field theory, which is equivalent to the DLCQ of the 2d CFT. This conclusion is sketched in Figure (1.1).

[15] using $\partial_V = e^{-\gamma}\partial_v$ and $\partial_U = e^{\gamma}\partial_u$.

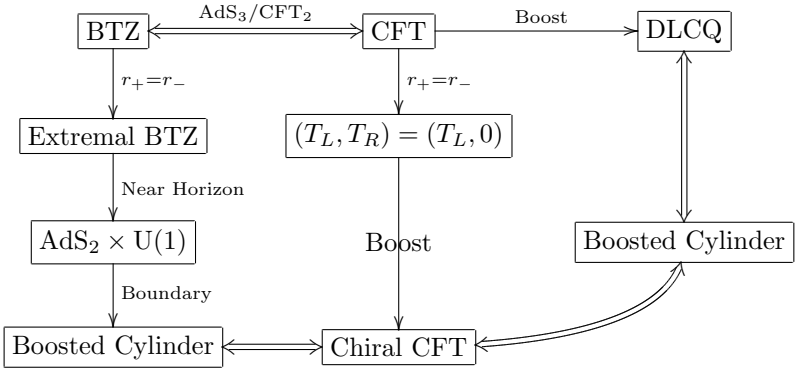

Figure 1.1: Relating the extremal BTZ geometry to the chiral sector of a 2d CFT.

To connect with the Kerr/CFT correspondence, we note that we can embed the extremal BTZ near horizon geometry into $\mathrm{d} = 2n + D$ dimensions where $D = 0, 1$ to obtain a geometry with isometry group $\mathrm{SL}(2,\mathbb{R}) \times \mathrm{U}(1)^{n-1+D}$. This is done by setting

$$\tilde{A} \equiv \frac{\ell_3^2}{4}, \qquad \widetilde{g}_{ij} = \begin{cases} \frac{4r_0^2}{\ell_3^2} & i = j\,, \\ 0 & i \neq j \end{cases}, \qquad k_i = \frac{\ell_3}{4r_0} \tag{1.177}$$

in (1.145). We could apply the Kerr/CFT machinery in subsection 1.5.3 to suggest that a higher dimensional extremal black hole with near horizon geometry of the form

$$ds^2 = \frac{\ell_3^2}{4}\left(-\rho^2 dt^2 + \frac{d\rho^2}{\rho^2}\right) + \sum_{i=1}^{n-1+D} \frac{4r_0^2}{\ell_3^2}\left(d\phi_i + \frac{\ell_3}{4r_0}\rho dt\right)^2 + \sum_{\alpha=1}^{n-1} F_\alpha dy_\alpha^2 \tag{1.178}$$

has $n - 1 + D$ chiral dual CFT descriptions, each with a central charge c_i and Frolov-Thorne temperature $T_i = \frac{2r_0}{\pi\ell_3}$. The DLCQ picture suggests that each chiral CFT has geometric dual

$$ds^2 = \frac{\ell_3^2}{4}\left(-\rho^2 dt^2 + \frac{d\rho^2}{\rho^2}\right) + \frac{4r_0^2}{\ell_3^2}\left(d\phi_i + \frac{\ell_3}{4r_0}\rho dt\right)^2 \tag{1.179}$$

which can be identified with (1.154) by replacing τ by $\frac{1}{2}\ell_3 r_0 t$. Although such a geometry (1.178) would contain the same isometry group as the general form of the extremal near horizon geometry (1.145), the latter contains the non-trivial warping factors $\tilde{A}, \tilde{g}_{ij}$, and the relationship between the extremal black hole/CFT correspondence and the DLCQ picture is yet to be fully understood.

1.7 Pinching AdS_3 Orbifolds

We saw in section 1.4 that BTZ black holes have dual descriptions in terms of thermal ensembles in a 1+1 dimensional CFT. In section 1.6 we considered thermal ensembles in a single chiral sector of this CFT, which are dual to the near horizon region of extremal BTZ black holes and explain their statistical degeneracy.

Null self-dual orbifold: In [44], and also [45], the authors examined the ground state, or $p^+ = 0$ sector, of this DLCQ chiral CFT, where the lightcone momenta are related to the

gravity conserved charges according to

$$\begin{aligned} p^- &= L_0 - \frac{c}{24} = \frac{M_{\rm BTZ}\ell_3 - J_{\rm BTZ}}{2} = \frac{c}{24}\left(\frac{r_+ - r_-}{\ell_3}\right)^2, \\ p^+ &= \bar{L}_0 - \frac{c}{24} = \frac{M_{\rm BTZ}\ell_3 + J_{\rm BTZ}}{2} = \frac{c}{24}\left(\frac{r_+ + r_-}{\ell_3}\right)^2. \end{aligned} \tag{1.180}$$

Then for an extremal BTZ black hole, where $r_+ = r_- \equiv r_0$, we have

$$p^- = 0, \qquad p^+ = \frac{c}{6}\frac{r_0^2}{\ell_3^2} \tag{1.181}$$

and we can see that the ground state $p^+ = 0$ of the CFT corresponds to the $r_0 = 0$ limit of (1.154), which is the massless ($M = 0$ (1.64)) BTZ black hole [16]. The extremal black hole has zero Hawking temperature by definition (1.65), and its dual CFT state has a vanishing left-moving temperature for $r_0 = 0$ (1.175). On the gravity side, under a change of coordinates

$$\rho = r^2, \qquad \varphi = x^-, \qquad \tau = 2\ell_3 x^+, \tag{1.182}$$

the $r_0 = 0$ limit of the spacelike self-dual orbifold gives the *null self-dual orbifold*

$$ds^2 = r^2 dx^+ dx^- + \ell_3^2 \frac{dr^2}{r^2}, \qquad x^- \sim x^- + 2\pi, \tag{1.183}$$

which can be viewed as a state, ie the $p^+ = 0$ sector of the Discrete Light-Cone Quantization (DLCQ) of the 2d CFT where a chiral sector of the CFT is decoupled.

This geometry can also be achieved by first taking the horizon size of (1.151) to zero to give the massless BTZ black hole

$$ds^2 = r^2 d\tilde{x}^+ d\tilde{x}^- + \ell_3^2 \frac{dr^2}{r^2}, \qquad \tilde{x}^\pm = \phi \pm t, \qquad \phi \sim \phi + 2\pi \tag{1.184}$$

and then taking the near horizon limit

$$r = \epsilon\rho, \qquad \tilde{x}^- = x^-, \qquad \tilde{x}^+ = \frac{x^+}{\epsilon^2}, \qquad \epsilon \to 0 \tag{1.185}$$

to give the null self-dual orbifold (1.183).

This geometry was found in [46] as the near horizon limit of an extremal vanishing horizon black hole. As it has the same boundary as the spacelike self-dual orbifold, it can be viewed as belonging to the same semiclassical Hilbert space.

We can excite the null orbifold to the spacelike self-dual orbifold by adding a wave to the metric

$$ds^2 = \frac{\ell_3^2}{r^2}\left[dx^+ dx^- + kr^2 (dx^-)^2 + dr^2\right], \tag{1.186}$$

where (1.186) is isometric to (1.154) for $r_0^2 = k\ell_3^2$. This injects some chiral momentum while keeping its causal null boundary. On the CFT side, this corresponds to a chiral excitation of the left-moving sector from $p^+ = 0$ to $p^+ = \frac{ck}{6}$.[17] So the null orbifold *allows* finite excitations.

Pinching orbifolds: The near horizon geometry of the massless BTZ black hole (1.184) can also be obtained by taking the *pinching* near horizon limit

$$r = \epsilon\rho, \qquad \tilde{x}^\pm = \frac{x^\pm}{\epsilon}, \qquad \epsilon \to 0 \tag{1.187}$$

[16] Note that the $M_{\rm BTZ} = 0$ BTZ black hole does not describe the true ground state of the system, which is global AdS_3.

[17] We note that adding a wave to the massless BTZ gives extremal BTZ.

of the massless BTZ black hole (1.184) gives the *pinching AdS_3 orbifold*

$$ds^2 = \rho^2 dx^+ dx^- + \ell_3^2 \frac{d\rho^2}{\rho^2} \qquad x^\pm \sim x^\pm + 2\pi\epsilon\,, \tag{1.188}$$

so called due to the vanishing periodicity of the compact directions $x^\pm$. It has the same geometry of a massless BTZ black hole, but with vanishing periodicity.

The pinching AdS_3 orbifolds appearing in the near horizon geometry of some black holes [28, 47, 48, 49, 50] prompted the authors of [44] to investigate the effect of this "pinching" on the dual CFT.

The CFT dual to the pinching orbifold (1.188) is defined on a cylinder (1.160) of radius R_p. The vanishing periodicity sends this radius to zero, $R_p = \epsilon R$. As the momentum operators scale like $P^u \sim P^v \sim \frac{1}{R_p} \sim \frac{1}{\epsilon}$ from (1.170-1.171), there is an infinite mass gap in both sectors. In the pinching orbifold, there are no dynamics when you probe energies below this mass gap. So the pinching limit freezes out (decouples) both sectors for fixed c_p, where c_p is the central charge of the CFT defined on the pinching cylinder:

$$\mathcal{H} = \{|c_p/24\rangle_L \otimes |c_p/24\rangle_R\}\,. \tag{1.189}$$

Since the difference between energy levels is proportional to $\frac{1}{c_p R_p}$, keeping this fixed will allow dynamics in the CFT; that is, there may not be energy to excite states, but if the system is "heated up", the states can be excited. This requires taking a large limit of the "pinching" central charge c_p so that $c_p = \frac{c}{\epsilon}$. As CFTs with an AdS_3 dual have a mass gap of the order of $1/c$, a pinching CFT with a large central charge will have a mass gap like $\frac{1}{c_p} \sim \epsilon$, and some nontrivial dynamics may survive the limit.

The question now is whether a CFT defined on a pinching cylinder can have a finite entropy. We can see from studying the Cardy formula of a CFT defined on a pinching cylinder

$$S_{\text{pinching}} = 2\pi\sqrt{\frac{c_p}{6}\left(l_0 - \frac{c_p}{24}\right)} + 2\pi\sqrt{\frac{c_p}{6}\left(\bar{l}_0 - \frac{c_p}{24}\right)}\,, \tag{1.190}$$

that the CFT entropy will be kept finite for $c_p \sim \frac{1}{\epsilon}$ and $l_0 - \frac{c_p}{24} \sim \epsilon$. This can be achieved by defining generators

$$l_n \equiv \frac{1}{\tilde{K}} L_{n\tilde{K}}\,, \quad n \neq 0\,, \qquad l_0 \equiv \frac{1}{\tilde{K}}(L_0 - \frac{c}{24}) + \frac{c}{24}\tilde{K}\,, \tag{1.191}$$

for $\tilde{K} = \frac{1}{\epsilon}$, which obey a Virasoro algebra with central charge $c_p = c\tilde{K}$. The spectrum of l_0 has a spacing of $1/\tilde{K}$ compared to that of L_0, and the relation between a CFT on a regular cylinder of radius R specified by $\{L_n, \bar{L}_n, c\}$ and a CFT defined on a pinching cylinder of radius R_p specified by $\{l_n, \bar{l}_n, c_p\}$ is summarised in Table 1.1.

Parameter	Finite CFT	Pinching CFT
Radius	R	$R_p = \epsilon R$
Central Charge	c	$c_p = \frac{c}{\epsilon}$
Generators	L_0	$l_0 \sim \epsilon$
Mass Gap	$\frac{1}{cR}$	$\frac{1}{c_p R_p} \sim 1$

Table 1.1: Relation between quantities defining a CFT on a regular cylinder and those on a pinching cylinder.

On the 3d bulk side, the BTZ entropy

$$S_{\rm BTZ} = \frac{2\pi r_+}{4G_3} \tag{1.192}$$

is kept finite for $r_+ \sim \epsilon$, as $G_3 \sim \epsilon$ from (1.32) for fixed AdS_3 radius ℓ_3.

The pinching AdS_3 orbifolds emerging in the near horizon limit of massless BTZ black holes thus allow us to explore the possibility of *non-chiral* dual descriptions of extremal BTZ black holes. These non-chiral CFT_2s are defined on pinching cylinders and allow dynamics in the large central charge limit, that is, when (1.32) is modified to $\frac{c}{\epsilon}$.

1.8 The EVH/CFT Correspondence

We have seen that an extremal black hole, whose near horizon geometry contains a warped $\mathrm{AdS}_2\times\mathrm{S}^1$ factor, has a microscopic description in terms of a chiral two dimensional conformal field theory. The AdS_2 factor corresponds to the frozen sector of the dual CFT, and physical states are charged under the the $\mathrm{U}(1)$ component of the $\mathrm{SL}(2,\mathbb{R}) \times \mathrm{U}(1)$ isometry group, as excitations in the dynamical sector involve the third spacetime coordinate.

We have also seen that the $r_0 \to 0$ limit of an extremal BTZ black hole has two inequivalent near horizon geometries, capturing different physics of the same system. While one near horizon limit of a massless BTZ black hole corresponds to the ground state of a chiral CFT, an inequivalent locally AdS_3 near horizon geometry may allow non-trivial dynamics in both sectors in a large central charge limit. This latter near horizon limit involves an angle of vanishing periodicity, so that the boundary of the near horizon geometry is a pinching cylinder. It also results in a vanishing Hawking temperature and a horizon area of zero size, and the large central charge limit is equivalent to a vanishing limit of the three dimensional Newton's constant $G_3 \sim c^{-1}$:

$$T_{\rm H} \sim A_{\rm H} \sim G_3 \to 0. \tag{1.193}$$

The limit (1.193) of an extremal BTZ black hole is the simplest example of an extremal vanishing horizon (EVH) black hole. This three dimensional geometry may be embedded into higher dimensions to give a generic EVH black hole[18], with a microscopic two dimensional description defined on the pinching cylinder at the boundary of the near horizon local AdS_3. In a generic EVH black hole, vanishing of the horizon area appears because a one dimensional cycle[19] on the horizon manifold becomes of zero size, so that its near horizon geometry includes a 3d metric of the form

$$ds^2 \propto -\epsilon^2\rho^2\frac{d\tau^2}{\ell_3^3} + \ell_3^3\frac{d\rho^2}{\rho^2} + \epsilon^2\rho^2 d\varphi^2 + \dots. \tag{1.194}$$

The appearance of this local AdS_3 throat combined with the scaling limit (1.193) inspired the authors of [51] to propose the EVH/CFT correspondence,

EVH/CFT Correspondence: Gravity on the near horizon of an EVH geometry is described by a 2d CFT

(1.195)

in the scaling limit

$$T_{\rm H} \sim A_{\rm H} \sim G_d \to 0, \tag{1.196}$$

which is an extension of (1.193) for $G_d \sim G_3$. Near-EVH black holes are excitations of EVH black holes that have arbitrarily small temperature and area. Examples of near-EVH black holes are [34, 28, 48, 46, 49, 50].

In four dimensions, the most general form of a black hole solution to four dimensional gauged Einstein-Maxwell dilaton theory with vanishing temperature and horizon was found, and it was subsequently demonstrated that the near horizon region of *any* 4d EVH black hole contains

[18] The earliest known example is in [47].

[19] Of course, this can also occur for higher dimensional cycles, for which $A_{\rm H} \sim \epsilon^p$ as $T_{\rm H} \sim \epsilon \to 0$. This possibility will not be considered in this work.

a pinching AdS_3 factor, suggesting that the degeneracy of their microstates can be captured by a two-dimensional CFT in accord with the AdS_3/CFT_2 duality. It was also demonstrated that when the horizon size is increased from zero to some small parameter, the near horizon geometry of a near-EVH black hole contains a locally BTZ black hole, the entropy of which captures the entropy of the 4d near-EVH black hole. This result will be fortified in Chapter 2, where we will demonstrate that the first law of thermodynamics for near-EVH black holes in generic dimension agrees gives the first law of thermodynamics for the near horizon BTZ black hole. While an EVH black hole is dual to the ground state of the dual CFT_2, a near-EVH black hole describes its excitations. These are thermal states in the dual CFT, and we may use the AdS_3/CFT_2 dictionary to compute the quantum numbers of these states.

By examining the equation of motion of a massless scalar field in the background of a four dimensional EVH black hole, the authors determined that in the near horizon geometry an infinite potential barrier develops so that the low energy physics in the EVH near horizon geometry is decoupled from the rest of the space. The pinching issue was addressed by taking large $G_3 \sim G_4$ and c_p so that the BTZ and 4d near-EVH entropy remain finite.

It is a natural question to ask if the statement of the EVH/CFT correspondence is consistent with the picture depicted by the Kerr/CFT correspondence (section 1.5). In order to make a comparison between the two proposals, we focus on the chiral sector of the CFT dual to the near horizon near-EVH black hole, and take the near-EVH limit of the central charges (1.148) computed via the Kerr/CFT prescription. We anticipate that only one of the Kerr/CFT central charges c_i, appearing in the Virasoro algebra associated with the azimuthal angle φ, will survive the near-EVH limit, and that it will parametrically agree with the central charge of the DLCQ of the EVH CFT. Our expectation, following the discussion of section 1.6, is that the CFT_2 associated to the finite (in the near-EVH limit) Kerr/CFT central charge is the DLCQ of the dual CFT description that arises in the EVH/CFT correspondence.

EVH/CFT correspondence in 5d: The five dimensional extension of the EVH/CFT correspondence is more complicated and we have yet to prove that any 5d EVH black hole has a near horizon pinching AdS_3 factor, or that the near horizon limit is a decoupling limit in this dimension. However, while for the original Kerr/CFT correspondence there's no dual AdS/CFT description, asymptotically AdS_5 black holes have the virtue of four dimensional CFT descriptions in terms of thermal mixed states in the dual $\mathcal{N} = 4$ super Yang-Mills theory . For this reason, we will investigate two AdS_5 case studies of the EVH/CFT correspondence in Chapters 3 and 4. States in the (UV) CFT_4 carry charges $\Delta_{\rm UV}, \mathcal{J}_i$, and the bulk limit (1.196) corresponds to taking a large N limit, $N\epsilon^\alpha \sim 1$, in the dual theory. For specific choices of α, non trivial dynamics are permitted in the bulk, boundary and CFT_2 descriptions. The near-EVH near horizon limit of these black holes probes, on the field theory side, a sector of the UV theory describing low-lying (IR) excitations. The question is whether there exists an alternative description for the physics of low-lying excitations, and whether this alternative description is in terms of a 2d CFT with quantum numbers $\Delta_{\rm 2d}$, $\mathcal{J}_{\rm 2d}$.

Geometrically, near-extremal near horizon limits typically involve non-trivial (singular) large gauge transformations defining the near horizon geometry (IR description) in terms of the isometry coordinates of the boundary geometry (UV CFT theory)

$$r = r_0 + \epsilon\,\rho, \qquad \varphi_i^{\rm IR} = \varphi_i^{\rm IR}\left(\varphi_i^{\rm UV}, t^{\rm UV}, \epsilon\right), \qquad t^{\rm IR} = t^{\rm IR}\left(\varphi_i^{\rm UV}, t^{\rm UV}, \epsilon\right) \quad \epsilon \to 0. \tag{1.197}$$

This suggests, as also expected from a purely field theoretical perspective, the existence of a non-trivial relation between the UV and IR Hamiltonians. If the IR theory is conformal, there will therefore be an interesting relation between quantum numbers of the form[20]

$$(\Delta_{\rm IR}, \mathcal{J}_{\rm IR}) = (\Delta_{\rm IR}(\Delta_{\rm UV}, \mathcal{J}_i), \mathcal{J}_{\rm IR}). \tag{1.198}$$

The relationship between these quantities and $\Delta_{\rm 2d}$, $\mathcal{J}_{\rm 2d}$ will be examined in Chapters 3 and 4.

Figure 1.2 is a pictorial representation of the EVH/CFT mechanism.

[20]The importance of these singular large gauge transformations for extremal black holes has been emphasised in [52, 53].

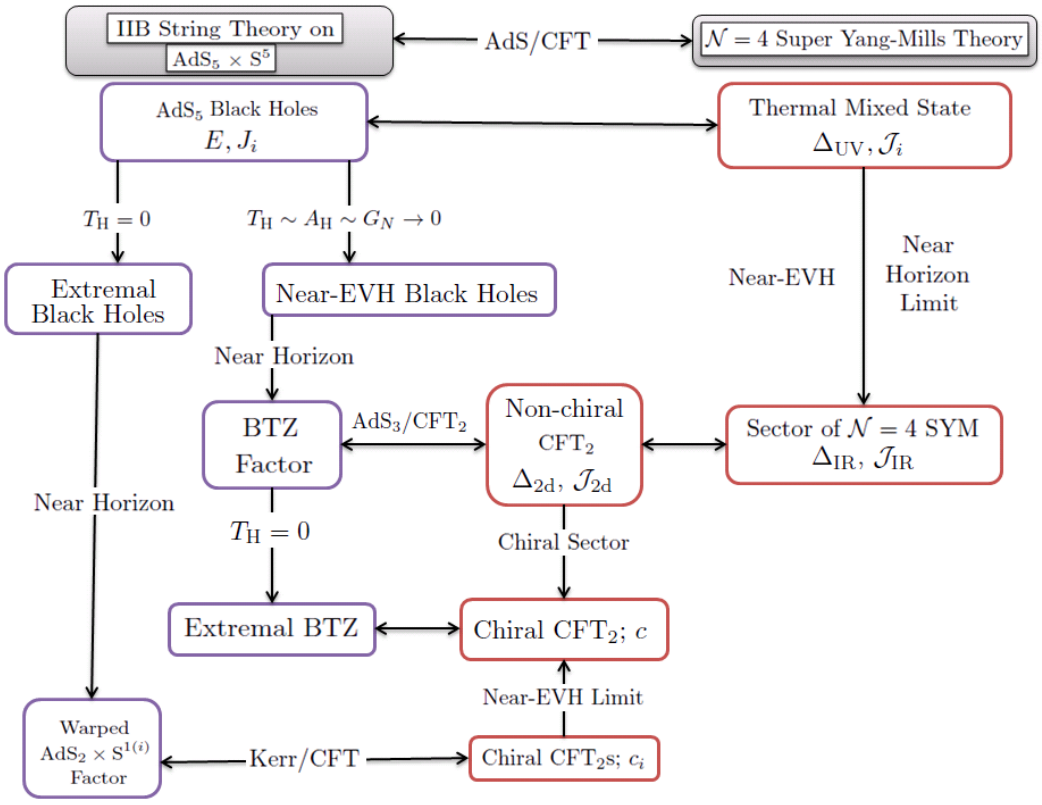

Figure 1.2: *The EVH/CFT setup for AdS_5 black holes.* Near-extremal asymptotically AdS black holes have dual descriptions in terms of thermal mixed states in the dual $\mathcal{N} = 4$ super Yang-Mills theory . We study the low energy excitations through the near-EVH near horizon geometry and identify potential IR 2d CFTs describing them. Bulk descriptions are outlined in purple and dual field theory quantities have red borders.

1.9 Outline of the Thesis

This thesis is organised as follows. In Chapter 2, we will start by discussing the thermodynamics of generic black holes in general relativity and the laws of thermodynamics they satisfy, particularly the first law. The rest of the Chapter will comprise an analysis of the first law applied to extremal and near-EVH black holes respectively. The first correction to the first law for extremal black holes with finite entropy gives a Cardy-like expression for the entropy compatible with the Kerr/CFT correspondence in section 1.5. The expression is in exact agreement with Sen's entropy function formalism and a scalar probe analysis. This expansion in thermodynamic quantities also reproduces the Frolov-Thorne temperatures associated with the chiral CFTs in section 1.5.

We also analyse the first law of thermodynamics in the near-EVH regime introduced in section 1.8. For a near-EVH black hole in generic dimension and background with one vanishing U(1), the first law of thermodynamics is compatible with the first law of thermodynamics of a BTZ black hole. This thermodynamic argument suggests that the physics of *any* near-EVH black hole is captured by a BTZ black hole, and consequently by its AdS_3/CFT_2 dual. One may then speculate that the near horizon near-EVH limit of a black hole is a decoupling limit. This idea is backed up by a scalar probe analysis.

Chapters 3 and 4 are case studies of the first law analysis and the EVH/CFT correspondence

in five dimensional anti de Sitter space. Chapter 3 will analyse static three charged black holes in AdS_5 supergravity. These will be embedded into 10d supergravity and the near horizon limit of the near-EVH cases will be taken. The near-BPS and non-BPS regimes have different near horizon limits and properties. In the non-BPS case, the scaling limit (1.196) applies and the near horizon geometry contains a pinching AdS_3 factor. For near-BPS black holes, however, T_H is kept finite in the near-EVH limit and the local AdS_3 factor is not pinching. Its dual CFT_2 description can be interpreted in terms of strings stretched between giants. The first law analysis of Chapter 2 will be applied to the near-BPS and non-BPS black holes. We then explore the idea that these emergent local AdS_3 geometries describe the low energy excitations of the original ultravoilet (UV) CFT in terms of an infrared (IR) 2d CFT. As a consistency check of the EVH/CFT correspondence, the limit in which the Kerr/CFT predictions agree with those of the EVH/CFT correspondence will be discussed.

The near-EVH limit of stationary asymptotically AdS_5 black holes will be presented in Chapter 4. These black holes rotate in two planes, and the near-EVH limit can be taken by sending one or both momenta to zero. Although these cases have very different near horizon geometries and will be analysed separately, it will be made manifest that the first law of thermodynamics will universally reduce to the first law for a BTZ black hole in the near-EVH limit. The connection between the UV and IR CFTs will be investigated, as will the connection between the EVH CFTs and the Kerr CFTs.

We will conclude the thesis with a discussion of results and open questions.

Chapter 2

The Low Temperature Limit of Black Holes

This Chapter contains the results of [54], which was done in collaboration with M. M. Sheikh-Jabbari, J. Simón, and H. Yavartanoo. It is a lightly edited version of the arxiv preprint.

We study the low temperature expansion of the first law of thermodynamics for near-extremal black holes. We show that for extremal black holes with non-vanishing entropy, the leading order contribution yields an expression for their extremal entropy in agreement with the entropy function result and the Cardy formula for the entropy of a two dimensional chiral conformal field theory (CFT). When their area vanishes due to the vanishing of a one-cycle on the horizon, such leading contribution is always compatible with the first law satisfied by a BTZ black hole. These results are universal and consistent both with the presence of local AdS_2 and AdS_3 near horizon throats for extremal black holes and with the suggested quantum microscopic descriptions (AdS_2/CFT_1, Kerr/CFT and EVH/CFT).

2.1 Introduction

We discussed in Chapter 1 how the near horizon limit of extremal and near-EVH black holes leads to the identification of certain CFT_2-like quantities. Geometrically, for finite horizon black holes an AdS_2 throat appears, while in the near-EVH case this is promoted to a local AdS_3. We now ask what happens to the thermodynamics of these black holes in the extremal and near-EVH limits. Our analysis will focus on the first law of thermodynamics for these black holes. In this section, we set the stage by first introducing the conserved charges and chemical potentials associated to black holes in four dimensional asymptotically flat spacetime, and the physical laws they satisfy. Following this, we discuss how Beckenstein and Hawking, among others, drew an equivalence between the laws of black hole mechanics and the laws obeyed by thermodynamic systems. For spacetimes in which we can define conserved charges, our expression of the first law of thermodynamics can be extended to generic dimension and background.

2.1.1 Black hole potentials and charges

Black holes are solutions to classical theories of gravity, possibly coupled to matter, characterised by the existence of an event horizon. Physically, a black hole is defined as a region where gravity is so strong that nothing can escape. When a sufficiently large quantity of matter is compactified into a small region, a spacetime singularity occurs; black holes describe the endpoints of gravitational collapse.

The black hole event horizon $\Gamma_{\rm H}$ is a null hypersurface that satisfies

$$\xi \cdot \xi|_{\Gamma_{\rm H}} = 0, \tag{2.1}$$

where a null hypersurface is one whose normal $\hat{n}$ is null, $\hat{n}^2 = \hat{n}^\mu \hat{n}_\mu = 0$, and ξ is a Killing

vector field defined by a one parameter group of isometries. For regular black holes, spatial sections of $\Gamma_{\rm H}$ are smooth and compact. If $\hat{n}$ is normal to $\Gamma_{\rm H}$, then $\hat{n}\cdot\nabla\hat{n}^\mu = 0$ on $\Gamma_{\rm H}$[1], so for $\xi = \upsilon\hat{n}$ for some υ, we have

$$\xi\cdot\nabla\,\xi^\mu|_{\Gamma_{\rm H}} = \kappa\xi^\mu \tag{2.4}$$

where

$$\kappa = \xi\cdot\partial\log|\upsilon| \tag{2.5}$$

is the surface gravity of the Killing horizon. It is so called because in a static asymptotically flat spacetime κ is the force required at infinity to hold a unit mass particle at rest near the Killing horizon [55].

If $\kappa \neq 0$, then the event horizon comprises a branch of a bifurcate Kiling horizon, which is a pair of null surfaces that intersect on a spacelike 2-surface such that they are each Killing horizons with the same normal Killing field ξ^μ. If $\kappa = 0$ then the black holes are extremal and the event horizon is a single Killing horizon.

In a four dimensional theory with vanishing cosmological constant, the black hole solution includes a metric which asymptotes to Minkowski spacetime. A stationary, axisymmetric black hole has event horizon $\Gamma_{\rm H}$ that is a Killing horizon of $\xi = \partial_t + \Omega\partial_\phi$. As ϕ is constant on orbits of ∂_t, particles moving on orbits of ξ rotate with angular velocity Ω relative to an inertial observer at infinity. We say that the black hole has angular velocity Ω, which can be computed by solving (2.1).

In a theory including electromagnetism, e.g. Einstein-Maxwell theory, the solution will include a gauge field $\mathcal{A} = \mathcal{A}_\mu dx^\mu$. The chemical potential Φ is the electric potential difference between the event horizon $\Gamma_{\rm H}$ and spacelike infinity $\imath^0$ given by evaluating $\xi^\mu\cdot A_\mu$ on the horizon.

The associated electric charge is

$$Q = \frac{1}{4\pi}\int_{S^2_\infty}\star\mathcal{F} \tag{2.6}$$

where $\mathcal{F}$ is the gauge field strength and S^2_∞ is a two-sphere that approaches $\imath^0$. If the black hole is stationary there exists a conserved energy momentum current $J_\mu = -T_{\mu\nu}\hat{\omega}^\nu$ so that the *total energy* of matter on a spacelike hypersurface Σ is

$$E(\Sigma) = -\int_\Sigma\star J. \tag{2.7}$$

The Komar mass, which is the conserved charge associated to time translation symmetry, is generated by a timelike Killing one form $\hat{\omega} = \hat{\omega}_\mu dx^\mu$, where $\hat{\omega}^\mu\partial_\mu = \partial_t$. In asymptotically flat spacetime the Komar mass is given by

$$M_{Komar} = -\frac{1}{8\pi}\int_{S^2_\infty}\star d\hat{\omega}. \tag{2.8}$$

The conserved charge associated to rotational symmetry is the Komar angular momentum, generated by the Killing one form $\hat{k} = \hat{k}_\mu dx^\mu$, where $\hat{k}^\mu\partial_\mu = \partial_\phi$. In asymptotically flat spacetime this is

$$J_{Komar} = \frac{1}{16\pi}\int_{S^2_\infty}\star d\hat{k}. \tag{2.9}$$

[1]We can see this by noting that $\Gamma_{\rm H}$ belongs to a family $H(x) =$ constant so that $\hat{n} = \upsilon dH$ for some function υ. Then

$$\hat{n}\cdot\nabla\hat{n}^\mu = \hat{n}^\mu\hat{n}\cdot\partial\log|\upsilon| - \hat{n}^2\partial^\mu\log|\upsilon| + \frac{1}{2}\partial^\mu(\hat{n}^2) \tag{2.2}$$

$$\Rightarrow\ \hat{n}\cdot\nabla\hat{n}^\mu|_{\Gamma_{\rm H}} = \hat{n}^\mu\hat{n}\cdot\partial\log|\upsilon||_{\Gamma_{\rm H}} + \frac{1}{2}\partial^\mu(\hat{n}^2)\Big|_{\Gamma_{\rm H}} \propto \hat{n}^\mu|_{\Gamma_{\rm H}}\,, \tag{2.3}$$

as $\hat{n}^2 = 0$ on $\Gamma_{\rm H}$. We can then choose υ so that $\hat{n}\cdot\nabla\hat{n}^\mu|_{\Gamma_{\rm H}} = 0$.

2.1.2 Laws of black hole thermodynamics

In 1973 Bardeen et al [3] demonstrated that the mass of a black hole behaves like the energy of a thermodynamic system, its surface gravity acts like temperature, and the horizon area plays the role of entropy of a thermodynamic system. It was then natural to draw an analogy between black hole mechanics and the laws of thermodynamics.

Mathematical analogues of the zeroth and first laws of thermodynamics for stationary black holes were formulated by Bardeen, Carter and Hawking in [3].

The zeroth law states that the surface gravity κ is constant over the horizon of a stationary black hole:

Theorem 2.1.1. *(Zeroth Law of Black Hole Mechanics) κ is constant on each connected component of the future event horizon of a stationary black hole spacetime satisfying the dominant energy condition ($-T^{\mu}_{\nu}V^{\nu}$ is a future-directed timelike or null vector, for energy-momentum tensor $T_{\mu\nu}$ and future-directed timelike or null vectors V_{μ}).*

The second law of black hole mechanics states that the horizon area must be non-decreasing in any (classical) process.

Theorem 2.1.2. *(Second Law of Black Hole Mechanics, Hawking Area Theorem)[56] Let $(\mathcal{M}, g)$ be a strongly asymptotically predictable spacetime[2] which obeys the null energy condition stating that $T_{\mu\nu}V^{\mu}V^{\nu} \geq 0$, where V_{μ} are future-directed timelike or null vectors. Let Σ_1, Σ_2 be spacelike Cauchy surfaces for U, where $\Sigma_2 \subset J^{+}(\Sigma_1)$. Then for $H_i = \Sigma_i \cap \Gamma_H$,*

$$area(H_2) \geq area(H_1). \tag{2.11}$$

Although Hawking showed [56] that the second law of black hole mechanics can be compared to the second law of thermodynamics, the former is a theorem in differential geometry while the latter has a statistical origin.

For a perturbation of a stationary black hole, the first law relates the changes undergone by the mass and angular momentum with the horizon area of the black hole.

Theorem 2.1.3. *(First Law of Black Hole Mechanics [57]) Consider a stationary, asymptotically flat black hole solution of the vacuum Einstein equations, with bifurcate Killing horizon. Assume a small amount of matter, carrying energy δM and angular momentum δJ crosses Γ_H and the black hole eventually becomes stationary. Then the area of $H_i = \Gamma_H \cap \Sigma_i$ increases by δA_H given by*

$$\frac{\kappa \delta A_H}{8\pi} = \delta M - \Omega \delta J. \tag{2.12}$$

Additional terms may appear on the right hand side of (2.12) when matter fields are present [58].

Another way of looking at this [55] is by considering a stationary, asymptotically flat black hole solution of the vacuum Einstein equations, with bifurcate Killing horizon, mass M, angular momentum J, electric charge Q, horizon surface A_{H}, surface gravity κ and angular velocity Ω_{H}.

Let δg be a non-singular (on and outside Γ_{H}) asymptotically flat metric perturbation, satisfying the linearised Einstein equations. Then the perturbed spacetime has (ADM) mass $M + \delta M$, angular momentum $J + \delta J$, electric charge $Q + \delta Q$ and horizon area (measured at the bifucation two sphere) $A_{\mathrm{H}} + \delta A_{\mathrm{H}}$ satisfying

$$\frac{\kappa \delta A_{\mathrm{H}}}{8\pi} = \delta M - \Omega \delta J - \Phi \delta Q. \tag{2.13}$$

[2] An asymptotically flat spacetime $(\mathcal{M}, g)$ is strongly asymptotically predictable if $\exists$ some globally hyperbolic open set $U \subset \mathcal{M}$ such that

$$J^{-}(\mathcal{I}^{+}) \cup \Gamma_{\mathrm{H}} \subset U, \tag{2.10}$$

where $J^{-}(\mathcal{I}^{+})$ is the causal past of $\mathcal{I}^{+}$; that is, physics is predictable from a Cauchy surface for U outside the black hole and on Γ_{H}.

Hawking radiation: Although the laws of black hole mechanics closely resemble the laws of thermodynamics, the connection was superficial until 1975, when Hawking discovered [1] that particle creation occurs in the vicinity of black holes. Consider a massless scalar Ψ in the spacetime of spherically symmetric gravitational collapse

$$\Psi = \sum_i \left(a_i f_i(x) + a_i^+ \bar{f}_i(x) \right) \tag{2.14}$$

in a basis $\{f_i, \bar{f}_i\}$ with $f_i \sim e^{-i\omega v}$ and $i = \omega, l, \tilde{m}$. Here a_i and a_i^+ are creation and annihilation operators, and v is a positive frequency eigenfunction. While the quantum field is initially in its vacuum state, the expected number of outgoing particles in the ith mode at light-like infinity I^+ is

$$\left(e^{\frac{2\pi\omega_i}{\kappa}} - 1 \right)^{-1}, \tag{2.15}$$

which is a thermal spectrum at Hawking temperature

$$T_{\rm H} = \frac{\kappa}{2\pi}. \tag{2.16}$$

The radiation emitted from the black hole is in a thermal mixed state and is in exact agreement with the radiation emitted from a perfectly thermal black body.

The Hawking effect allowed for the surface gravity to be viewed as the physical temperature of the black hole, just as the mass can be viewed as its energy. Although as a perfect absorber a black hole will not emit anything and classically has a temperature of absolute zero, in the quantum theory the creation of particle pairs results in a radiation with a thermal spectrum.

Hawking's semiclassical calculation of the black hole temperature led to a correlation between the laws of black hole physics and thermodynamics. The Hawking effect and its implications are clues to the fundamental features that a quantum theory of gravity will have.

Laws of black hole thermodynamics: As black holes radiate with a temperature, the zeroth law of black hole mechanics is the same as the zeroth law of thermodynamics, that the temperature is constant throughout a body in thermal equilibrium. The first law (2.13) can be rewritten as

$$dE = T_{\rm H} dS_{\rm BH} + \Omega dJ + \Phi dQ \tag{2.17}$$

where

$$S_{\rm BH} = \frac{A_{\rm H}}{4}. \tag{2.18}$$

This is the same as the first law of thermodynamics if we interpret $S_{\rm BH}$ as the Beckenstein-Hawking entropy of a black hole. Restoring units, this is

$$S_{BH} = \frac{c^3 A_{\rm H}}{4\hbar G_N}. \tag{2.19}$$

The first law of thermodynamics was first formulated for asymptotically flat spacetimes in four dimensions, and was generalised to higher dimensions and curved spacetimes in e.g. [59].

Although $S_{\rm BH}$ cannot *classically* decrease by the second law of black hole mechanics (2.11), the thermal radiation (2.16) allows the black hole entropy to quantum mechanically decrease. Beckenstein proposed [2, 60] that the area is proportional to the black hole entropy obeying a generalised second law where the sum of this entropy and matter outside the black hole

$$S_{tot} = S_{matter} + S_{\rm BH} \tag{2.20}$$

should never decrease.

First law in higher dimensions: There is no physically reasonable objection to the expectation that Hawking radiation is essentially unmodified in higher dimensions [61]: a black hole emits radiation that, up to greybody factors, has a Planckian spectrum of temperature $T = \frac{\kappa}{2\pi}$ and chemical potentials Ω, Φ etc. The laws of black hole mechanics described above are valid

in any number of dimensions. In particular, although the evaluation of conserved charges may vary with the backgroud, the first law

$$T_{\rm H} dS = dM - \sum_{a=1}^{m} \Omega^a dJ_a - \sum_{q=m+1}^{n} \Omega^q dJ_q \tag{2.21}$$

will always hold. In the above, we take Ω^a to be angular velocities for $i = 1, \cdots m$ evaluated by demanding that the Killing vector

$$\xi = \partial_t + \sum_{a=1}^{m} \Omega^a \partial_{\phi^a} \tag{2.22}$$

becomes null on the horizon,

$$\xi \cdot \xi|_{\Gamma_{\rm H}} = 0. \tag{2.23}$$

We take Ω^q to be chemical potentials associated to gauge fields $\mathcal{A}^{(q)}$ for $q = m+1, \cdots n$ given by

$$\Omega^q = \xi \cdot \mathcal{A}^{(q)}\big|_{\Gamma_{\rm H}}. \tag{2.24}$$

The black holes we will take as case studies in Chapters 3 and 4 are solutions to $\mathrm{U}(1)^3$ 5d gauged supergravity, where the angular momenta and charges are modified to [62]

$$J^{(a)} = \frac{1}{16\pi} \int_{S^3} \star d\hat{k}^{(a)}, \qquad Q^{(q)} = \frac{1}{16\pi} \int_{S^3} \left(X_q^{-2} \star \mathcal{F}^{(q)} + \frac{1}{2} |\epsilon_{qrs}| \mathcal{A}^{(r)} \wedge \mathcal{F}^{(s)} \right) \tag{2.25}$$

where X^q are functions of the scalar fields and $\mathcal{F}^{(q)}$ are the gauge field strengths. Evaluation over the sphere is performed at infinity and

$$\hat{k}^{(a)} = \hat{k}^{(a)}_\mu dx^\mu, \qquad \hat{k}^{\mu(a)} \partial_\mu = \partial_{\phi^{(a)}}, \tag{2.26}$$

and the mass is evaluated by integrating the first law of thermodynamics (2.21).

2.2 The Low Temperature Limit of the First Law: Finite Horizon Black Holes

We now turn to examining the first law of thermodynamics (2.21) for nearly-extremal black holes in four and five dimensions.

2.2.1 Extremal black holes in four and five dimensions

We consider the first law satisfied by a set of four and five dimensional black holes charged under gauge fields $\mathcal{A}^{(i)}$ with $\mathbb{R} \times \mathrm{U}(1)^{d-3}$ invariant metrics which in adapted coordinates look like

$$ds^2_{\rm bh} = -N_l^2 dt^2 + \frac{dr^2}{g^{rr}} + g_{\theta\theta} d\theta^2 + \gamma_{ab} (d\phi^a - B^a dt)(d\phi^b - B^b dt)\,, \tag{2.27}$$

where all components are functions of r, θ. The Killing vector field

$$\xi = \partial_t + \sum_{a=1}^{d-3} \Omega^a \partial_{\phi^a} \tag{2.28}$$

is null on the event horizon which is located ar $r = r_+$, the largest root of $g^{rr}(r_+) = 0$. The horizon angular velocities Ω^a and chemical potentials Ω^q, collectively labelled by Ω^i, are determined by solving (2.23) and (2.24) to get

$$\Omega^a = B^a(r_+), \qquad \Omega^q = \left(\xi^t \mathcal{A}^{(q)}_t + \sum \xi^a \mathcal{A}^{(q)}_{\phi^a} \right)\Big|_{r_+}. \tag{2.29}$$

There are n conserved charges J_i where $i = 1, \ldots, n$. The angular momenta J_a are associated to the angular velocities Ω^a, where $a = 1, ..d-3$, and the electric charges J_q are associated to the chemical potentials Ω^q, where $q = d-3+1, ..n$.

As explained in Chapter 1, extremal black holes have coincident inner and outer horizons, $r_+ = r_-$, and vanishing Hawking temperature, $T_{\rm H} = 0$. It was proved in [37] that any regular extremal black hole with $\mathbb{R} \times {\rm U}(1)^{d-3}$ isometry group has an *on-shell near horizon* geometry of the form

$$ds^2 = \Gamma(\theta) g_{AdS_2} + g_{\theta\theta}(\theta) d\theta^2 + \gamma_{ab}(\theta)(d\varphi^a + e^a \rho dt)(d\varphi^b + e^b \rho dt) \tag{2.30}$$

where

$$g_{AdS_2} = -\rho^2 d\tau^2 + d\rho^2/\rho^2 \tag{2.31}$$

is the metric on AdS_2 spacetime. While (2.30) is proved to hold for any 4d or 5d classical theory of Einstein gravity coupled to an arbitrary number of Abelian Maxwell-type gauge fields and neutral scalar fields with lagrangian density $\mathcal{L}$, it is known to hold for more general extremal black holes.

This solution is invariant under ${\rm SO}(2,1) \times {\rm U}(1)^n$. While ${\rm SO}(2,1)$ is geometrically realised as the isometries of the AdS_2 g_{AdS_2}, $n-d+3$ of the ${\rm U}(1)$ symmetries are associated with non-geometrical Abelian gauge fields.

2.2.2 Low temperature first law analysis

Given a thermodynamical system with $n+1$ charges, the limit of vanishing temperature defines an n-dimensional extremal surface (ES) characterised by the relation $M_e = M_e(J_i)$[3], compatible with (2.21):

$$dM_e = \sum_{i=1}^{n} \Omega_e^i dJ_i \,, \quad \Omega_e^i = \left.\frac{\partial M}{\partial J_i}\right|_{\rm ES} . \tag{2.32}$$

We study the first non-trivial correction due to a small but non-zero temperature for a near-extremal black hole with non-vanishing extremal entropy $S_e \neq 0$. If r_e is the extremal black hole horizon radius, turning on temperature corresponds to a deformation in black hole parameter space satisfying $r_\pm = r_e \pm \Delta\epsilon$, where $\Delta \sim \epsilon^0$ is defined on the extremal surface, so that $T_{\rm H} \sim r_+ - r_- \sim \epsilon$ for near-extremal black holes. As an extremal black hole is represented by a point on the extremal surface in parameter space, a near-extremal black hole is represented by a point in parameter space $(M_e + \delta M,\, J_i)$ that has been orthogonally displaced from the extremal point (M_e, J_i). Assuming *analyticity* of all thermodynamical quantities, we define this deformation as

$$T_{\rm H} = T'_{\rm H} \,|_{\rm ES}\, \epsilon, \quad \Omega^i = \Omega^i_e + \Omega^{i\prime} \,|_{\rm ES}\, \epsilon \,, \tag{2.33}$$

where *prime* denotes differentiation w.r.t the deviation from extremality, i.e. orthogonal motion away from the extremal surface. The question we explore is which physical excitations are relevant at first order in ϵ for regular black holes. To this end we first show that δM is second order in ϵ

$$dM - \sum_i \Omega_e^i dJ_i \equiv d\,(\delta M) \propto \epsilon^2 \,. \tag{2.34}$$

To prove this, let $g^{rr}(r; M, J_i) = 0$ be the equation specifying the location of the horizon(s). At an extremal point this has a double root, $g_{rr}(r, M_e, J_i) = C(r - r_e)^2$. Turning on δM, and relying on analyticity, we have

$$g^{rr}(r; M_e + \delta M, J_i) = \delta A + \delta B (r - r_e) + (C + \delta C)(r - r_e)^2 + \ldots , \tag{2.35}$$

with δA, δB and δC proportional to δM. We require g^{rr} to have roots at $r_\pm = r_e \pm \Delta\epsilon$, that is,

$$g^{rr}(r_\pm; M_e + \delta M, J_i) = 0 = \delta A \pm \delta B (\Delta\epsilon) + (C + \delta C)(\Delta\epsilon)^2 + \ldots ,$$

[3] We assume that the black hole mass is uniquely specified by J_i in the extremal limit.

giving $\delta A = -C\epsilon^2\Delta^2, \quad \delta B = \mathcal{O}(\epsilon^2)$ and hence (2.34) follows. We note that condition (2.34) determines the absence of physical excitations above extremality at first order in ϵ for our (finite horizon) black holes.

The first law (2.21) at first order in ϵ then reduces to [63]

$$\epsilon T'_{\rm H}\Big|_{\rm ES} dS_e = dM_e - \sum_{i=1}^{n} \Omega^i_e dJ_i - \epsilon \sum_{i=1}^{n} \Omega^{i'}\Big|_{\rm ES} dJ_i + d(\delta M), \tag{2.36}$$

yielding

$$dS_e = \sum_{i=1}^{n} k^i dJ_i\,, \quad k^i = k^i(J_k) = -\frac{\Omega^{i'}}{T'_{\rm H}}\Big|_{\rm ES}\,, \tag{2.37}$$

where d is the derivative tangential to the extremal surface, and we have used (2.34). Note that, despite considering the near-extremal limit (2.33), all quantities in (2.37), including the entropy, are evaluated on the extremal surface and are independent of the deformation ϵ. Thus, (2.34) implies that the low temperature expansion of the first law for regular black holes in the leading order yields information on the entropy of the extremal black holes and not on excitations above them. This information may arise at second or higher orders in the expansion of the first law [64].

In the above we merely used thermodynamic considerations and the only crucial input from black holes is (2.34). Below, we will interpret this condition, but now we want to prove that regular black holes *do* satisfy (2.37). We show this using Sen's entropy function formalism [65], which relies on the near horizon geometry of regular extremal black holes.

2.2.3 Sen's entropy function

The presence of SO(2, 1) in the near horizon geometry (2.30) allows us to employ the entropy function formalism. We define the function

$$f\left(\Gamma, \gamma_{ab}, e^a, e^q, \vec{u}(\theta)\right) = \int_{\Gamma_{\rm H}} \sqrt{-\det\, g}\, \mathcal{L} \tag{2.38}$$

where e^a are the constants in (2.30), e^q are constants appearing in the expression for the field strengths $\mathcal{F}^i_{\mu\nu} = \mathcal{F}^i_{\mu\nu}(e^a, e^q)$, and $\vec{u}$ are scalar fields.

By Sen's analysis, the equations of motion for backgrounds (2.30) correspond to

$$\frac{\partial f}{\partial e^a} = J_a, \quad \frac{\partial f}{\partial \Gamma} = 0, \quad \frac{\partial f}{\partial e^q} = J_q, \quad \frac{\partial f}{\partial \gamma_{ab}} = 0, \quad \frac{\partial f}{\partial u_s} = 0. \tag{2.39}$$

Solving the equations of motion is equivalent to extremising the entropy function $\mathcal{E}$

$$\mathcal{E} = 2\pi \left(\sum_{i=1}^{n} e^q J_q - f\left(\Gamma(\theta), \gamma_{ab}(\theta), e^a, e^q, \vec{u}(\theta)\right) \right). \tag{2.40}$$

The on-shell evaluation of $\mathcal{E}$ equals the entropy of the extremal black hole, i.e. $\mathcal{E}_{\rm eom} = S_e$. Computing the on-shell variation of (2.40) yields

$$dS_e = 2\pi \sum_{i=1}^{n} e^i\, dJ_i \tag{2.41}$$

which matches (2.37) if

$$k^i = 2\pi e^i. \tag{2.42}$$

This identification is manifest when studying the near horizon limit $r = r_0 + \epsilon\rho$ in metrics (2.27) in a near-extremal regime [38, 63, 65]

$$t = \lambda \frac{\tau}{\epsilon}, \quad \varphi^a = \phi^a - \Omega^a_e \lambda \frac{\tau}{\epsilon}, \quad \epsilon \to 0. \tag{2.43}$$

For an extremal solution we have $g^{rr}(r_0) = g^{rr\prime}(r_0) = 0$. Expansion in ϵ gives

$$-N_l^2 dt^2 + \frac{dr^2}{g^{rr}} = -\frac{\rho^2}{2}(N_l^2)''(r_0)\lambda^2 d\tau^2 + \frac{2}{g^{rr\prime\prime}(r_0)}\frac{d\rho^2}{\rho^2} \tag{2.44}$$

$$= \frac{2}{g^{rr\prime\prime}(r_0)}\left[-\lambda^2\frac{g^{rr\prime\prime}(r_0)(N_l^2)''(r_0)}{4}\rho^2 d\tau^2 + \frac{d\rho^2}{\rho^2}\right], \tag{2.45}$$

where regularity required $N_l(r_0) = N_l'(r_0) = 0$. We find that that the near horizon geometry of an extremal black hole contains an AdS_2 factor,

$$\begin{aligned} ds^2_{\rm bh} = &\frac{2}{g^{rr\prime\prime}(r_0)} g_{AdS_2} + g_{\theta\theta}d\theta^2 + \\ &\gamma_{ab}(r_0)\left(d\phi^a - (B^a(r_0) + (\epsilon\rho)B^{a'}(r_0))\frac{\lambda\tau}{\epsilon}\right)\left(d\phi^b - (B^b(r_0) + (\epsilon\rho)B^{b'}(r_0))\frac{\lambda\tau}{\epsilon}\right), \end{aligned} \tag{2.46}$$

where g_{AdS_2} is the AdS_2 metric (2.31) and

$$\lambda = \frac{2}{\sqrt{g^{rr\prime\prime}(r_0)(N_l^2)''(r_0)}} = \frac{1}{2\pi T_{\rm H}'}. \tag{2.47}$$

Then, using (2.43), the near horizon geometry is given by (2.30) where (2.42) is satisfied:

$$\Gamma(\theta) = \frac{2}{g^{rr\prime\prime}(r_0)}, \qquad e^a = B'(r_0)\lambda = \frac{\Omega^{a\prime}(r_0)}{2\pi T_{\rm H}'} = \frac{k^a}{2\pi}. \tag{2.48}$$

In the near horizon region the gauge potentials take the form

$$\mathcal{A}^{(q)} = \mathcal{A}_t^{(q)}dt + \sum \mathcal{A}_{\phi^a}^{(q)}d\phi^a \tag{2.49}$$

$$= \left(\mathcal{A}_t^{(q)}(r_0) + \mathcal{A}_{\phi^a}^{(q)}(r_0)\Omega_e^a\right)\lambda\frac{d\tau}{\epsilon} + \mathcal{A}_{\phi^a}^{(q)}(r_0)d\varphi + \rho\left(\mathcal{A}_t^{(q)\prime}(r_0) + \mathcal{A}_{\phi^a}^{(q)\prime}(r_0)\Omega_e^a\right)\lambda d\tau. \tag{2.50}$$

Then the $\rho\tau$ component of the field strength in the near horizon limit

$$\mathcal{F}_{\rho\tau}^{(q)} = e^q = \left(\mathcal{A}_t^{(q)\prime}(r_0) + \mathcal{A}_{\phi^a}^{(q)\prime}(r_0)\Omega_e^a\right)\lambda = \Omega^{q\prime}\lambda = \frac{k^q}{2\pi} \tag{2.51}$$

gives our desired result (2.42)[4].

This generic agreement between (2.37) and (2.41) establishes that *on-shell* near horizon geometries of extremal black holes *always* satisfy (2.37).

2.2.4 Scalar probe analysis

A similar conclusion can be reached by probing the extremal black hole background by a quantum field Ψ. A quantum field in a black hole background at *finite* temperature has a mixed quantum state described by a density matrix whose eigenvalues equal the standard Boltzmann factors

$$\hat{\varrho} \equiv \exp\left[-\beta\left(\omega - \sum_{i=1}^{n}\tilde{m}_i\Omega^i\right)\right]. \tag{2.52}$$

Notice the "chemical" potentials are fully determined by the black hole geometry, while the quantum numbers $\{\omega, \tilde{m}_i\}$ label the quantum state.

[4]The last equalities of (2.48) and (2.51) are valid for the following reason: we have functions $D_i(r)$ evaluated at r_0 to give chemical potentials $D_i(r_0)$. Taking the derivative with respect to r and evaluating at r_0 gives $\frac{\partial D_i(r)}{\partial r}\Big|_{r=r_0}$. The same is true for r_0: The chemical potentials $D_i(r_0)$ can be differentiated and evaluated on the extremal horizon to give $\frac{\partial D_i(r_0)}{\partial r_0}\Big|_{r_0=r_0}$. Then $\frac{\partial D_i(r)}{\partial r}\Big|_{r=r_0} = \frac{\partial D_i(r_0)}{\partial r_0}\Big|_{r_0=r_0}$ to leading order in ϵ.

In the near-extremal limit, this becomes

$$\exp\left[-\frac{1}{T'_H(r_0)\epsilon}\left(\omega-\sum_{i=1}^{n}\tilde{m}_i\Omega_e^i\right)+\frac{1}{T'_H(r_0)}\sum_{i=1}^{n}\tilde{m}_i\Omega^{i\prime}(r_0)\right]. \tag{2.53}$$

The near-extremal limit (2.33) thus requires $\omega=\sum_i\Omega_e^i\tilde{m}_i+\mathcal{O}(\epsilon^\alpha)$, $\alpha\geq 1$ to prevent the vanishing or blow up of the probability density $\hat{\varrho}$, constraining the energy quantum of the scalar fields in terms of the remaining modes. This is the analogue of the black hole extremality condition (2.32) and spectrum of excitations (2.34) for the scalar probe.

It is clear that in the regime $\alpha>1$ and in the limit $\epsilon\to 0$,

$$\hat{\varrho}=\exp\left(-\sum_i k^i(J_k)\tilde{m}_i\right) \tag{2.54}$$

reproduces the chemical potentials in (2.37).

A different take on the procedure described above consists in interpreting the near horizon limit (2.43) as a large gauge transformation to reproduce the same constraint on the quantum numbers. Consider a quantum scalar field and decompose it into Fourier modes

$$\Psi=\sum_{\omega,\tilde{m},l}\varphi_{\omega\tilde{m}l}\exp\left[-i\omega t+i\sum_{i=1}^{n}\tilde{m}_i\phi^i\right]f_l(r,\theta). \tag{2.55}$$

The near horizon limit involves the time scaling and angular shifts in (2.43). Writing the Fourier modes in terms of the new coordinates gives

$$\exp\left[i\left(-\omega+\sum_{i=1}^{n}\tilde{m}_i\Omega_e^i\right)\frac{\tau}{2\pi T'_{\rm H}\epsilon}+i\sum_{i=1}^{n}\tilde{m}_i\varphi^i\right]. \tag{2.56}$$

In the limit $\epsilon\to 0$, it is natural to require $\omega=\sum_i\Omega_e^i\tilde{m}_i+\mathcal{O}(\epsilon^\alpha)$, as before.

2.3 The Low Temperature Limit of the First Law: Vanishing Horizon Black Holes

We now apply the first law analysis of the previous section to the near-EVH black holes of the EVH/CFT correspondence (1.195) discussed in section 1.8. Systems satisfying $S_e\sim\epsilon^p$, $p>0$ as $T_{\rm H}\sim\epsilon\to 0$ do not obey the analysis of the previous section. Here we consider black holes with $S_e/T_{\rm H}$ *finite*, i.e. $p=1$. Since black holes in this category have vanishing horizon area, we refer to them as extremal vanishing horizon (EVH) ones. In parameter space, they exist at the co-dimension k ($k\geq 2$) *EVH surface* defined by the intersection of the $T_{\rm H}=S_e=0$ surfaces. In all known examples, the EVH surface corresponds to $r_+=r_-=\tilde{c}=0$, where $\tilde{c}$ is a function of the remaining parameters.

Inspired by the finiteness of $S_e/T_{\rm H}$ and the Cardy-like growth in the density of states of a 2d CFT, we want to identify a set of sufficient conditions under which $p=1$ EVH black holes allow a first law of thermodynamics compatible with a 2d CFT microscopic description. For this purpose, we *assume* that vanishing of the entropy is due to the vanishing of a single *one-cycle*. This requires the existence of a vanishing eigenvalue in the near horizon metric γ_{ab} in (2.30). Let this eigenvalue be along the ∂_φ direction. Then, close to the horizon $r\to\epsilon r$, $\epsilon\to 0$, the length of this one-cycle must scale like $\gamma_{\varphi\varphi}\sim\gamma(\theta)\,r^2$. The geometry is smooth for $\gamma(\theta)=\Gamma(\theta)$, as in (2.30), giving rise to

$$ds^2=\Gamma(\theta)\left(\epsilon^2r^2(-dt^2+d\varphi^2)+\frac{dr^2}{r^2}\right)+ds_\perp^2 \tag{2.57}$$

as the *near horizon* geometry of an EVH black hole. Notice the isometry of the first factor is locally enhanced to $\mathrm{SO}(2,2)$. The geometry is smooth at $r=0$ and $ds_\perp^2$ is $\mathrm{SO}(2,2)$ invariant

when $ds^2_\perp$ is r independent. These statements were proved in 4d Einstein-Maxwell-dilaton theories [51] and have been verified in several 4d and 5d studies [44, 51, 66]. We expect them to hold for any EVH black hole and we will assume them hereafter.

As discussed in Chapter 1, there exist two inequivalent near-horizon geometries: the null self-dual orbifold of AdS_3 [44] after redefining $t+\varphi \to (t+\varphi)/\epsilon^2$ keeping $t-\varphi$ fixed and the *pinching* AdS_3 orbifold [44] after $t, \varphi \to t/\epsilon, \varphi/\epsilon$. The former reduces the isometry to $SO(2,1)\times U(1)$ and does not allow for dynamical excitations [44]. Searching for non-trivial excitations, responsible for $d\delta M \sim T dS_e \sim \epsilon^2$ in (2.34) when we turn on the temperature, we will focus on the second option.

Note that the 3d metric in (2.57) can be obtained by taking the near horizon limit ($r \to \epsilon r$) of metrics (2.27)

$$t = \frac{\tau}{\epsilon}, \quad \varphi_i = \phi_i - \Omega_i^{(0)} \frac{\tau}{\epsilon}, \quad \chi = \epsilon\, \varphi\,, \quad \epsilon \to 0\,, \tag{2.58}$$

where ϕ_i, $i = 1, \cdots, n-1$ parameterize the non-singular U(1) symmetries of the original EVH black hole solution. These include both the isometries of $ds^2_\perp$ and the Abelian U(1) symmetries due to the gauge fields of the solution. The resulting geometry includes the *pinching* AdS_3 orbifold [44], due to $\chi \sim \chi + 2\pi\epsilon$, and it is written in a co-rotating frame since $\Omega_i^{(0)}$ are the horizon angular velocities or electric potentials at the EVH point.

Having identified the relevant EVH geometry, we now turn to thermodynamics and switch on temperature and entropy

$$T_H = \epsilon T_{\rm H}^{(1)}\,, \ S_{\rm BH} = \epsilon S^{(1)}\,, \tag{2.59}$$

along the k orthogonal directions in parameter space that infinitesimally move away from the EVH surface. By construction, $dS_{\rm BH}$ is a one-form belonging to the space of EVH orthogonal deformations. In gravity, these deformations will correspond to the near-EVH black holes. By analyticity, any thermodynamical quantity Z will allow an expansion $Z = Z^{\rm EVH} + \sum_{n>0} \epsilon^n Z^{(n)}$, with $dZ^{\rm EVH} = 0$. Besides (2.59), we have

$$\begin{aligned} dM &= \epsilon dM^{(1)} + \epsilon^2 dM^{(2)} + \cdots\,, \\ dJ_i &= \epsilon dJ_i^{(1)} + \epsilon^2 dJ_i^{(2)} + \cdots\,, \\ \Omega_i &= \Omega_i^{(0)} + \epsilon \Omega_i^{(1)} + \cdots\,. \end{aligned} \tag{2.60}$$

Since $T_{\rm H} dS_{\rm BH} \sim \epsilon^2$, the Ω_i in the near-EVH regime relevant to our leading order analysis are of the form

$$\Omega_i^{\text{near-EVH}} = \begin{cases} \Omega_a^{(0)} & a = k-1, \cdots, n\,, \\ \epsilon \Omega_\alpha^{(1)} & \alpha = 1, \cdots, k-2\,, \\ \Omega_\varphi & \text{for pinching direction } \varphi\,. \end{cases} \tag{2.61}$$

We singled out the angular velocity along the pinching direction, because even though it vanishes at the EVH point, its value in the near-EVH regime can be non-vanishing. This is because $\Omega_\varphi \sim d\varphi/dt$ and as discussed previously, both coordinates scale in the same way. Noting the coordinate scalings (2.58), a similar argument leads to the scaling of Ω_a and Ω_α given in (2.61). There is no second order contribution, because at this order the only non-trivial contribution would come from $dJ_i^{(0)}$ which vanishes, by construction.

Using (2.34), i.e. $d\delta M \equiv \epsilon^2 \left(dM^{(2)} - \sum_a \Omega_a^{(0)} dJ_a^{(2)} \right)$, and plugging (2.59), (2.60) and (2.61) into the first law, one obtains

$$T_{\rm H}^{(1)} dS^{(1)} = dM^{(2)} - \sum_a \Omega_a^{(0)} dJ_a^{(2)} - \Omega_\varphi dJ_\varphi^{(2)} - \sum_\alpha \Omega_\alpha^{(1)} dJ_\alpha^{(1)}\,. \tag{2.62}$$

As we will show below, (2.62) is indeed the first law for a BTZ black hole [67].

Consider the subset of $\Omega_\alpha^{(1)}$ that are geometrically realised. One can always work in a co-rotating frame by performing the coordinate transformation

$$\varphi_\alpha = \phi_\alpha - A_\alpha \frac{\tau}{\epsilon} - B_\alpha \frac{\chi}{\epsilon}\,, \tag{2.63}$$

where A_α and B_α are first order in ϵ, extending the transformation (2.58) to the near-EVH regime. Equivalently, these angular velocities must satisfy the identity

$$\Omega_\alpha^{(1)} = A_\alpha^{(1)} + B_\alpha^{(1)}\Omega_\varphi \,. \tag{2.64}$$

For those Ω_α that are not geometrical, the corresponding transformation is a U(1) gauge transformation. Either way, recalling the symmetries of the near-EVH solution, (2.63) is just a large gauge or coordinate transformation by an element in the $\mathrm{SO}(2,2)\times\mathrm{U}(1)^{k-1}$ symmetry group.

We can parameterise excitations in the α directions, i.e. first order deformations belonging to a $k-2$ dimensional space, by $z_\alpha = \epsilon z_\alpha^{(1)} + \cdots$. Then, as $\Omega_\alpha = \epsilon\Omega_\alpha^{(1)} + \cdots$, $J_\alpha = \epsilon J_\alpha^{(1)} + \cdots$, $\Omega_\alpha^{(1)}$ and $J_\alpha^{(1)}$ are linear in $z_\alpha^{(1)}$, and must therefore be linearly related as $\Omega_\alpha^{(1)} = M_{\alpha\beta}J_\beta^{(1)}$, where only the symmetric part of the matrix $M_{\alpha\beta}$ is relevant for the first law (2.21). Then $A_\alpha^{(1)} = C_{\alpha\beta}^{(0)}J_\beta^{(1)}$, $B_\alpha^{(1)} = D_{\alpha\beta}^{(0)}J_\beta^{(1)}$, where $C_{\alpha\beta}^{(0)}$ and $D_{\alpha\beta}^{(0)}$ are symmetric matrices of the EVH parameters. It follows that

$$\begin{aligned} d\left(\sum_\alpha A_\alpha^{(1)}J_\alpha^{(1)}\right) &= 2\sum_\alpha A_\alpha^{(1)}dJ_\alpha^{(1)}\,, \\ d\left(\sum_\alpha B_\alpha^{(1)}J_\alpha^{(1)}\right) &= 2\sum_\alpha B_\alpha^{(1)}dJ_\alpha^{(1)}\,. \end{aligned} \tag{2.65}$$

We plug (2.64) and (2.65) into (2.62), which then simplifies to

$$T_{\mathrm{BTZ}}\; dS_{\mathrm{BTZ}} = dM_{\mathrm{BTZ}} - \Omega_{\mathrm{BTZ}}dJ_{\mathrm{BTZ}}\,, \tag{2.66}$$

where we defined

$$\begin{aligned} T_{\mathrm{H}}^{(1)} = T_{\mathrm{BTZ}}\,, \quad \epsilon S^{(1)} = S_{\mathrm{BTZ}}\,, \quad \Omega_\varphi = \Omega_{\mathrm{BTZ}}\,, \\ M_{\mathrm{BTZ}} = \epsilon\left(M^{(2)} - \sum_a \Omega_a^{(0)}J_a^{(2)} - \frac{1}{2}\sum_\alpha A_\alpha^{(1)}J_\alpha^{(1)}\right)\,, \\ J_{\mathrm{BTZ}} = \epsilon\left(J_\varphi^{(2)} + \frac{1}{2}\sum_\alpha B_\alpha^{(1)}J_\alpha^{(1)}\right)\,. \end{aligned} \tag{2.67}$$

The BTZ subscript is to stress the fact that (2.66) has the same form as the first law for a BTZ black hole [67] introduced in section 1.4. This reinforces the expectation that near-EVH black holes have a universal near horizon geometry given by a pinching BTZ, as explicitly checked for several near-EVH black holes, e.g. [51], and as will be demonstrated in Chapters 3 and 4. This is consistent with the idea that near-EVH deformations in parameter space correspond to large gauge transformations in gravity.

Notice that the entropy and conserved charges of the pinching BTZ black hole have an explicit ϵ multiplying them. We have included this factor when taking into consideration the pinching of the AdS_3 angle, which induces an ϵ-dependent periodicity. As S_{BTZ}, M_{BTZ} and J_{BTZ} are calculated by evaluating the Komar integral over the angular direction at infinity, we expect this extra ϵ factor in their expressions. We will see in Chapters 3 and 4 that this is indeed the case. As we discussed in sections 1.7 and 1.8, this factor is cancelled by scaling the three dimensional Newton's constant appropriately, $G_3 \sim \epsilon$. When our black holes are solutions to supergravity in AdS with dual CFTs, this is achieved by taking a large N limit.

Scalar probe analysis for near-EVH black holes This thermodynamic evidence for the existence of a BTZ black hole in the near horizon geometry of a near-EVH black hole is enhanced by probing a near-EVH black hole with a scalar field Ψ. Consider the Fourier decomposition of the probe

$$\Psi = \sum_{\omega,\tilde{m},l} \varphi_{\omega\tilde{m}l}\exp\left[-i\omega t + i\sum_{i=1}^{n}\tilde{m}_i\phi_i\right] f_l(r,\theta). \tag{2.68}$$

Expanding in the near-EVH limit, we get

$$\Psi = \sum_{\omega,m,l} \varphi_{\omega ml} \exp\left[-i\omega\frac{\tau}{\epsilon} + i\sum_{a=k-1}^{n} \tilde{m}_a \left(\varphi_a + \Omega_a^0 \frac{\tau}{\epsilon}\right)\right. \tag{2.69}$$

$$\left. + i\tilde{m}_\chi \frac{\chi}{\epsilon} + i\sum_{\alpha=1}^{k-2} \tilde{m}_\alpha \left(\varphi_\alpha + A_\alpha \frac{\tau}{\epsilon} + B_\alpha \frac{\chi}{\epsilon}\right)\right] f_l(r,\theta). \tag{2.70}$$

Collecting coefficients of the near horizon isometry coordinates τ and χ, we identify the probe quantum numbers in the IR near horizon geometry as

$$\omega_{NH} = \frac{1}{\epsilon}\left(\omega - \sum_{a=k-1}^{n} \tilde{m}_a \Omega_a^0 - \sum_\alpha \tilde{m}_\alpha A_\alpha\right), \qquad \tilde{m}_{NH} = \frac{1}{\epsilon}\left(\tilde{m}_\chi + \sum_\alpha \tilde{m}_\alpha B_\alpha\right). \tag{2.71}$$

When we expand the density matrix (2.52) in the near-EVH limit, we find, using $T_{\rm H} = \epsilon T_{\rm BTZ}$, that[5]

$$\hat{\varrho} \propto \exp\left[-\frac{1}{T_{\rm BTZ}}\left(\omega_{NH} - \tilde{m}_{NH}\Omega_{\rm BTZ}\right)\right]. \tag{2.72}$$

Thus the Ψ quantum state is the same as one outside of a BTZ black hole, in agreement with (2.66).

2.4 Discussion

We conclude this Chapter by relating the main physical inputs leading to (2.37) and (2.66) to the proposed microscopic descriptions in the literature. It is worth stressing that (2.37) is always compatible with a Cardy-like density of states growth at temperature $T = k(J)^{-1}$ whenever $n = 1$, where the Frolov-Thorne temperature was calculated in Appendix A. This does not uniquely select the existence of a 2d chiral CFT microscopic interpretation, but it is certainly consistent with it. Indeed, the central charge of such a CFT would equal $c = 3S_e/(\pi^2 k)$. This is in agreement with the Kerr/CFT proposal [31] outlined in section 1.5, which identifies a chiral Virasoro algebra with this central charge as the asymptotic symmetry group of the *same* near horizon geometries (2.30) with some prescribed boundary conditions.

It is known, via the $\mathrm{AdS}_3/\mathrm{CFT}_2$ duality [68] summarised in section 1.4, that a generic BTZ black hole corresponds to a thermal mixed state in the dual 2d non-chiral CFT, and an extremal BTZ to a mixed state at zero temperature. It was shown that the near horizon limit of extremal BTZ corresponds to the Discrete Light-Cone Quantisation (DLCQ) of the dual CFT_2 which has only one dynamical chiral sector, leading to a 2d chiral CFT [40]. This explains why the chiral sector associated with AdS_2 excitations is frozen (if suitable boundary conditions are used) and identifies the chiral Kerr/CFT sector with the second chiral sector of the original 2d CFT.

This also ties nicely with our result (2.66) for EVH black holes. Our thermodynamic analysis indicates that excitations above an EVH black hole correspond to a configuration compatible with a BTZ black hole, i.e. that *the physics of near-EVH black holes are captured by BTZ black holes*. The generic form of our result can be viewed as strong evidence that the same structure exists for any EVH black hole where the vanishing of the horizon area is due to a vanishing one-cycle, as conjectured in [51]. As these black holes have dual descriptions in terms of non-chiral CFTs, (2.66) is *thermodynamic* evidence in favour of the EVH/CFT correspondence (1.195). The specific case studies of Chapters 3 and 4 will demonstrate how this thermodynamic statement agrees with the existence of the geometric structure in the near horizon region.

[5] We note that, as we are working in a co-rotating frame, there is no rotation in the φ_a, φ_α directions, so that the quantum numbers associated to these coordinates do not appear in the expression for the density matrix.

Chapter 3

Case Study I: Static Charged Black Holes

This Chapter contains results of [69] which was done in collaboration with J. de Boer, M. M. Sheikh-Jabbari and J. Simón. It is an edited version of the published paper, with more recent results added in light of [66] and [54].

We consider families of static charged asymptotically AdS_5 Extremal black holes with Vanishing Horizon (EVH black holes) whose near horizon geometries develop locally AdS_3 throats. Using the AdS_3/CFT_2 duality decribed in section 1.4, we propose an EVH/CFT_2 correspondence to describe the near horizon low energy IR dynamics of near-EVH black holes involving a specific large N limit of the 4d $\mathcal{N}=4$ super Yang-Mills theory . We consider both non-BPS and near-BPS regimes and their near horizon limits, emphasise the differences between the local AdS_3 throats emerging in either case, and discuss potential dual IR 2d CFTs for each case. We obtain a natural quantisation for the central charge of the near-BPS emergent IR CFT which we interpret in terms of the open strings stretched between giant gravitons. These black holes are concrete examples of the "UV first law" of thermodynamics reducing to the "IR first law" satisfied by the near horizon BTZ black holes in this near-EVH limit as outlined in Chapter 2. As evidence of the EVH/CFT correspondence introduced in section 1.8, we give a map between the UV and IR near-EVH excitations. We also discuss the connection between the Kerr/CFT correspondence outlined in section 1.5 and our EVH/CFT proposal in the cases where the two overlap.

3.1 Static Three Charged Solutions to Type IIB Supergravity

In this section, we review the characterisation of extremal vanishing horizons among R-charged AdS_5 black holes. These are solutions of type IIB supergravity with constant dilaton, and metric and RR 4-form potential given by [70]

$$\begin{aligned} ds_{10}^2 &= \sqrt{\Delta}\left(-\frac{X}{H_1H_2H_3}\frac{dt^2}{r^2}+r^2\frac{dr^2}{X}+r^2\,d\Omega_3^2\right)+\frac{L^2}{\sqrt{\Delta}}\left(\sum_{i=1}^{3}H_i\left(d\mu_i^2+\mu_i^2\left[d\psi_i+\mathcal{A}_i\,dt\right]^2\right)\right)\\ C_4 &= -\frac{r^4}{L}\Delta\,dt\wedge d^3\Omega-L\sum_{i=1}^{3}\tilde{q}_i\,\mu_i^2\left(L\,d\psi_i-\frac{q_i}{\tilde{q}_i}dt\right)\wedge d^3\Omega\,. \end{aligned} \tag{3.1}$$

The configuration is determined by a set of scalar functions $\{H_i,\,X,\,\Delta\}$ and gauge fields $\{\mathcal{A}_i\}$

$$H_i=1+\frac{q_i}{r^2},\qquad \mathcal{A}_i=-\frac{\sqrt{q_i(\mu+q_i)}}{L^2(r^2+q_i)},\qquad \tilde{q}_i=\sqrt{q_i(\mu+q_i)},\;\; i=1,2,3 \tag{3.2}$$

$$X(r) = r^2 - \mu + \frac{r^4}{L^2} H_1\, H_2\, H_3, \qquad \Delta = H_1\, H_2\, H_3 \left[\frac{\mu_1^2}{H_1} + \frac{\mu_2^2}{H_2} + \frac{\mu_3^2}{H_3} \right], \tag{3.3}$$

AdS radius L, the unit radius 3-sphere metric $d\Omega_3^2$ and a further 2-sphere $\mu_1^2 + \mu_2^2 + \mu_3^2 = 1$ parameterised by

$$\mu_1 = \cos\alpha\,, \qquad \mu_2 = \sin\alpha \sin\beta\,, \qquad \mu_3 = \sin\alpha\cos\beta\,, \quad \alpha, \beta \in [0, \frac{\pi}{2}]. \tag{3.4}$$

Charges and Thermodynamics These solutions have four independent parameters $\{\mu,\, q_i\}$ determining the mass and R-charges of the black hole

$$E = \frac{\pi}{4G_N^{(5)}} \left(\frac{3}{2}\mu + q_1 + q_2 + q_3 \right), \qquad J_i = \frac{\pi L}{4G_N^{(5)}} \tilde{q}_i = \frac{\pi L}{4G_N^{(5)}} \sqrt{q_i(\mu + q_i)} \tag{3.5}$$

in terms of the five dimensional Newton's constant

$$G_N^{(5)} = \frac{G_N^{(10)}}{(\pi^3 L^5)} = \frac{\pi}{2}\, \frac{L^3}{N^2}. \tag{3.6}$$

The temperature and entropy for these black holes are [70]

$$\begin{aligned} T_{\rm H} &= \frac{r_+^6 + \mu L^2 r_+^2 - (q_1q_2 + q_1q_3 + q_2q_3) r_+^2 - 2q_1q_2q_3}{2\pi r_+^2 L^2 \sqrt{(r_+^2 + q_1)(r_+^2 + q_2)(r_+^2 + q_3)}}\,, \\ S_{\rm BH} &= \frac{\pi N^2}{L^3} \sqrt{(r_+^2 + q_1)(r_+^2 + q_2)(r_+^2 + q_3)}\,, \end{aligned} \tag{3.7}$$

where r_+^2 is the (outer) horizon radius, defined as the largest root of $X(r)$ in (3.2).

Angular velocities in the azimuthal directions on the S^5 are given by the gauge fields (3.2) evaluated at the horizon r_+,

$$\Omega_i = -\mathcal{A}_i(r_+), \tag{3.8}$$

and the black holes satisfy the first law of thermodynamics

$$T_{\rm H} dS_{\rm BH} = dE - \sum_{i=1}^{3} \Omega_i dJ_i. \tag{3.9}$$

A subset of the family (3.1) of black holes are BPS black holes with energy E a linear combination of the electric charges. This subset is defined by $\mu = 0$ so that $\tilde{q}_i = q_i$, giving $\ell E = J_1 + J_2 + J_3$, i.e. the system is BPS. Thus μ measures the deviation from BPSness. The generic BPS solutions in this class preserve 1/4 of the supersymmetries of the original 5d theory, i.e. two (out of eight) real supercharges in 5d [38, 71]. We also note that BPS AdS_5 black holes can only happen if we have electric charges turned on, i.e. neutral rotating AdS_5 black holes cannot be BPS; moreover, all the static BPS AdS_5 black holes have naked singularities, which can be removed by the addition of rotation [71].

Four dimensional $\mathcal{N} = 4$ super Yang-Mills theory description Using the AdS/CFT correspondence sketched in section 1.3, the black holes (3.1) correspond to thermal states in the dual $\mathcal{N} = 4$ super Yang-Mills theory defined on $\mathbb{R}\times S^3$ carrying charges :

$$\Delta_{\rm UV} = \ell E\,, \qquad \mathcal{J}_i = J_i\,. \tag{3.10}$$

Gravitational energy E becomes conformal dimension $\Delta_{\rm UV}$, and the electric charges J_i, R-charges $\mathcal{J}_i$ of the dual 4d gauge theory. By construction, these are functions of the the four parameters (q_1, q_2, q_3, μ) and scale like N^2.

Intersecting giant description: These singular configurations were interpreted as distributions of smeared giant gravitons in [72], where the flux quantisation conditions

$$\frac{N_i}{N} = \frac{2J_i}{N^2} = \frac{\tilde{q}_i}{L^2}, \qquad i = 1, 2, 3 \tag{3.11}$$

were derived for each of the three types of giants supporting these black holes. Here N_i is the number of giant gravitons in each stack. Since each giant type involves a different 3-cycle in the transverse 5-sphere [73], pairs of giants belonging to different types intersect on circles. This observation was used in [28, 34, 74] to argue that two R-charged AdS_5 black holes should allow a dual 2d CFT description defined on the S^1 where giants intersect and with central charge proportional to the total number of such intersections, i.e. $c \sim N_i N_j$ $(i \neq j)$. This interpretation will play an important role when we discuss the near-BPS regime.

3.2 The Set of EVH and Near-EVH Black Holes

In this section we describe the criteria for the family of black holes (3.1) to be (near-)EVH. To this end we examine the parameter space.

Extremality vs charges: For completeness, we review the conditions under which *finite* horizon extremal R-charged black holes appear [70]:

a) For *single* R-charge configurations characterised by $\{\mu, q_1\}$, the condition for extremality coincides with the condition for the black hole to be BPS, *i.e.* $\mu \to 0$. However, as one may easily check, no local AdS_3 geometry appears as one takes the near horizon limit.

b) For *two* R-charge configurations characterised by $\{\mu, q_2, q_3\}$, horizons exist when μ has values above a lower bound μ_c. As extremality is preserved when

$$\mu = \mu_c = \frac{q_2 q_3}{L^2}, \tag{3.12}$$

the scale $\mu - \mu_c$ measures the amount of non-extremality.

c) For *three* R-charge black holes, with three generic charges of the *same* order of magnitude, horizons exist for μ above a certain quantity and below which we have a naked singularity [70]. As soon as the extremal limit is achieved for black holes in this class, the horizon size is necessarily *finite*. Thus, in this regime, EVH black holes can not appear.[1]

We can solve the horizon equation to express q_1 and μ in terms of the other parameters

$$\begin{aligned} q_1 &= r_+^2 r_-^2 C(r_\pm, q_2, q_3)\,, \\ \mu - \mu_c &= (r_+^2 + r_-^2)\mu_c\, C(r_\pm, q_2, q_3) + r_+^2 r_-^2\, ((q_2+q_3)C(r_\pm, q_2, q_3) - 1) \end{aligned} \tag{3.13}$$

where the scalar function $C(r_\pm, q_2, q_3)$ is

$$C(r_\pm, q_2, q_3) \equiv \frac{L^2 + q_2 + q_3 + r_+^2 + r_-^2}{\mu_c\, L^2 - r_+^2 r_-^2} \tag{3.14}$$

and μ_c is given by (3.12) The function $X(r)$ characterising the existence of horizons becomes[2]

$$X(r) = \frac{(r^2 - r_+^2)(r^2 - r_-^2)}{L^2 r^2}(r^2 + \mu_c\, L^2\, C(r_\pm, q_2, q_3)). \tag{3.15}$$

[1] If one of the charges is parametrically smaller than the other two, the three-charge system can under favorable circumstances be viewed as a perturbation of the EVH configuration identified in b), as we will describe in detail in the following.

[2] We note that q_1 blows up for $\mu_c L^2 = r_+^2 r_-^2$. We will not, however, be probing this regime of parameters as (near-)EVH black holes only occur for $q_1 < q_i$, $i = 2, 3$.

3.2.1 The set of EVH black holes

Consider the four dimensional parameter space, either in terms of $(q_1, q_2, q_3; \mu)$ or $(q_1, q_2, q_3; r_+)$. We define the subset of EVH black holes as a limit of near-extremal black holes in which $A_{\rm H}, T_{\rm H} \sim \epsilon \to 0$. From inspection of (3.7), we find

$$A_{\rm H}, T_{\rm H} \sim \epsilon \to 0, \quad \Rightarrow r_+ \sim \epsilon, \quad q_1 q_2 q_3 \sim \epsilon^n, \ n \geq 4, \mu L^2 - (q_1 q_2 + q_1 q_3 + q_2 q_3) \sim \epsilon^m, \ m \geq 2. \tag{3.16}$$

It is straightforward to check that this is the most general configuration that arises from choosing the horizon r_+ to be $\mathcal{O}(\epsilon)$. From (3.13) we can see that $r_+ = 0$ gives $q_1 = 0$, and so EVH black holes require

$$\boxed{r_+ = 0, \qquad q_1 q_2 q_3 = 0, \qquad \text{and} \qquad \mu = \mu_c = \frac{q_2 q_3}{L^2}.} \tag{3.17}$$

We can distinguish between two types of EVH configurations:

$$\begin{aligned} \textbf{non-BPS}: &\qquad r_+ = q_1 = 0; \ \mu_c \text{ finite} \\ \textbf{near-BPS}: &\qquad r_+ = q_1 = 0; \ \mu_c \sim \epsilon^2. \end{aligned} \tag{3.18}$$

q_1 - and, as will be apparent, all quantities corresponding to it - is clearly distinct from q_2 and q_3, so we will take $i = 2, 3$ for the rest of the Chapter.

3.2.2 The set of near-EVH black holes

To explore the physics of near-EVH black holes, we describe regions in parameter space close to the EVH surface. Given a generic $q_1 = 0$ EVH point parameterised by (3.17), one can decompose the space of deformations into *tangential* and *orthogonal*. Tangential movement along the EVH surface corresponds to parametric change in an EVH black hole: a change in parameters $(q_2, q_3) \to (q_2 + \delta q_2, q_3 + \delta q_3)$ will return a different value on the EVH surface:

$$\mu + \delta\mu = \frac{(q_2 + \delta q_2)(q_3 + \delta q_3)}{L^2}. \tag{3.19}$$

Orthogonal deformations correspond to excitations of EVH black holes to near-EVH black holes; we discuss the non-BPS and near-BPS situations separately below.

Near-EVH non-BPS black holes: Non-BPS EVH black holes are described by $(q_1, q_2, q_3; \mu) = (0, q_2, q_3; \frac{q_2 q_3}{L^2})$, so the most general orthogonal deformation is obtained by computing the normal at a point on the surface, given by the gradient:

$$\left(0, q_2, q_3; \frac{q_2 q_3}{L^2}\right) \qquad \longrightarrow \qquad \left(\delta q_1, q_2 - \frac{q_3}{L^2}\delta\mu, q_3 - \frac{q_2}{L^2}\delta\mu; \frac{q_2 q_3}{L^2} + \delta\mu\right). \tag{3.20}$$

We can see from (3.16) that we can choose

$$\delta\mu = M\epsilon^2, \qquad \delta q_1 = \epsilon^4 \hat{q}_1, \tag{3.21}$$

and so the most general physical excitations of non-BPS EVH black holes are parameterised by $M, \hat{q}_1$.

Once these deformations are turned on, the equation determining the horizon location $X(r_\pm) = 0$ becomes

$$\mathbf{V}\left(\frac{r_\pm}{\epsilon}\right)^4 - M\left(\frac{r_\pm}{\epsilon}\right)^2 + \frac{\hat{q}_1 q_2 q_3}{L^2} = 0, \qquad \mathbf{V} = \frac{L^2 + q_2 + q_3}{L^2}. \tag{3.22}$$

This is solved by

$$r_\pm^2 = \epsilon^2 \left(\frac{M \pm \sqrt{M^2 - 4\mathbf{V}\frac{\hat{q}_1 q_2 q_3}{L^2}}}{2\mathbf{V}}\right), \tag{3.23}$$

so we can see that extremality is preserved for $M = 2\sqrt{\mathbf{V}\hat{q}_1 q_2 q_3}/L$. The temperature and entropy in the near-EVH limit are

$$S_{\rm BH} = \frac{\pi N^2 \sqrt{q_2 q_3}}{L^3} r_+, \qquad T_{\rm H} = \frac{ML^2 \left(\frac{r_+}{\epsilon}\right)^2 - 2\hat{q}_1 q_2 q_3}{2\pi \left(\frac{r_+}{\epsilon}\right)^3 L^2 \sqrt{q_2 q_3}} \epsilon. \tag{3.24}$$

By construction, as in Chapter 2, $S_{\rm BH} \sim T_{\rm H} \sim \epsilon$, due to the scaling of r_+ (3.16).

Near-BPS black holes: Near-BPS EVH black holes are described by $(q_1, q_2, q_3; \mu) = (0, \epsilon\hat{q}_2, \epsilon\hat{q}_3; \epsilon^2 \frac{\hat{q}_2\hat{q}_3}{L^2})$, so the most general orthogonal deformation is

$$\left(0, \epsilon\hat{q}_2, \epsilon\hat{q}_3; \epsilon^2\hat{\mu}_c\right) \qquad \longrightarrow \qquad \left(\delta q_1, \epsilon\hat{q}_2 - \frac{q_3}{L^2}\delta\mu, \epsilon\hat{q}_3 - \frac{q_2}{L^2}\delta\mu; \epsilon^2\hat{\mu}_c + \delta\mu\right). \tag{3.25}$$

We can see from (3.16) that we can choose

$$\delta q_1 = \epsilon^2 \hat{q}_1, \qquad \delta\mu = M\epsilon^2, \tag{3.26}$$

where $\mu_c = \epsilon^2 \frac{\hat{q}_2\hat{q}_3}{L^2} = \epsilon^2\hat{\mu}_c$; and so the most general physical excitations of near-BPS VH black holes are parameterised by $M, \hat{q}_1$.

Once these deformations are turned on, the equation determining the horizon location $X(r_\pm) = 0$ becomes

$$\left(\frac{r_\pm}{\epsilon}\right)^4 - \left(\frac{r_\pm}{\epsilon}\right)^2 M + \frac{\hat{q}_1\hat{q}_2\hat{q}_3}{L^2} = 0, \tag{3.27}$$

which is solved by

$$r_\pm^2 = \epsilon^2 \left(\frac{M \pm \sqrt{M^2 - 4\frac{\hat{q}_1\hat{q}_2\hat{q}_3}{L^2}}}{2}\right); \tag{3.28}$$

so extremality is preserved for $M = 2\sqrt{\hat{q}_1\hat{q}_2\hat{q}_3}/L$. The temperature and entropy in the near-EVH limit are

$$S_{\rm BH} = \frac{\pi\sqrt{\left(\left(\frac{r_+}{\epsilon}\right)^2 + \hat{q}_1\right)\hat{q}_2\hat{q}_3}}{L^3} N^2\epsilon^2, \qquad T_{\rm H} = \frac{\left(\frac{r_+}{\epsilon}\right)^2 ML^2 - 2\hat{q}_1\hat{q}_2\hat{q}_3}{2\pi\sqrt{\left(\left(\frac{r_+}{\epsilon}\right)^2 + \hat{q}_1\right)\hat{q}_2\hat{q}_3} L^2 \left(\frac{r_+}{\epsilon}\right)^2}. \tag{3.29}$$

We note here that $A_{\rm H} \sim N^2\epsilon^2$ and $T_{\rm H} \sim 1$ have different scalings, and their ratio is not finite. Thus the special cases of near-BPS black holes have different criteria to their non-BPS counterparts (1.196). In fact, as $T_{\rm H} \sim 1$, it is not fully correct to define them as extremal, and we shall call them (near-)VH black holes. As we will see, the scaling of $A_{\rm H}$ and $T_{\rm H}$ will impact on the near horizon geometry analysis.

3.3 Near Horizon Geometry Analyis: Static Charged Black Holes

In this section we study the near horizon geometries corresponding to the non-BPS and near-BPS VH black holes identified in (3.17) together with their near-extremal versions (3.20),(3.25) .

3.3.1 The non-BPS EVH near horizon geometry

Let us consider a static EVH black hole $\mu = \mu_c$ and study its deep interior geometry by expanding in small ϵ for $r = \epsilon\rho$. The metric expansion is

$$\begin{aligned} ds^2 = \mu_1 \Big[-\frac{\mathbf{V}\epsilon^2}{\sqrt{q_2q_3}}\rho^2 dt^2 + \frac{\sqrt{q_2q_3}}{\mathbf{V}}\frac{d\rho^2}{\rho^2} + \frac{L^2\epsilon^2}{\sqrt{q_2q_3}}\rho^2 d\psi_1^2 \Big] \\ + \mu_1\sqrt{q_2q_3}d\Omega_3^2 + \frac{L^2}{\mu_1\sqrt{q_2q_3}}\sum_{i=2}^{3} q_i \left(d\mu_i^2 + \mu_i^2 \left(\psi_i - \Omega_i^{(0)} t \right)^2 \right), \end{aligned} \tag{3.30}$$

where $\mathbf{V}$ is defined in (3.22) and

$$\Omega_i^{(0)} = -\frac{\sqrt{q_i + L^2}}{L^2} \tag{3.31}$$

is the angular velocity at the EVH point, obtained by expanding $\mathcal{A}_i = \mathcal{A}_i^{(0)} + \epsilon^2 \mathcal{A}_i^{(2)}$ in ϵ.

As we discussed in sections 1.8 and 2.3, extremality determines the scaling $-\epsilon^2\rho^2\, dt^2$ together with $d\rho^2/\rho^2$ giving rise to an AdS_2 throat responsible for the $\mathrm{SO}(2,1)$ isometry enhancement of the near horizon geometry [37]. The new feature here is the *vanishing* size of the one-cycle along ψ_1 as $\epsilon^2\rho^2$. Notice this is the isometry direction in the 5-sphere with vanishing R-charge ($\mathcal{J}_1 = 0$). This is responsible for the vanishing of the entropy and transforms the standard AdS_2 throat into a local AdS_3 throat.

The near horizon geometry is obtained by considering the $\epsilon \to 0$ limit of

$$r = \epsilon\frac{(q_2q_3)^{\frac{1}{4}}}{L}x, \quad t = \frac{L}{(q_2q_3)^{\frac{1}{4}}}\frac{\tau}{\epsilon}, \quad \psi_1 = \frac{\hat{\chi}}{\epsilon}, \quad \psi_i = \hat{\psi}_i + \Omega_i^{(0)} t, \tag{3.32}$$

The resulting metric is

$$ds^2 = \mu_1 \Big[-\frac{x^2 d\tau^2}{\ell_3^2} + \frac{\ell_3^2 dx^2}{x^2} + x^2 d\hat{\chi}^2 \Big] + \mu_1\sqrt{q_2q_3}d\Omega_3^2 + \frac{L^2}{\mu_1\sqrt{q_2q_3}}\sum_{i=2}^{3} q_i \left(d\mu_i^2 + \mu_i^2 d\hat{\psi}_i^2 \right). \tag{3.33}$$

Due to the $2\pi\epsilon$ periodicity in $\hat{\chi}$, this geometry describes a warped locally $\mathrm{AdS}_3 \times \mathrm{S}^3$ geometry, with radii given by

$$R_{AdS_3}^2 = \ell_3^2 = \frac{\sqrt{q_2q_3}}{\mathbf{V}}, \qquad R_{S^3}^2 = \sqrt{q_2q_3}\,. \tag{3.34}$$

More precisely, the local AdS_3 throat is the *pinching* AdS_3 orbifold introduced in section 1.7, corresponding to the near horizon of a massless BTZ black hole. Once more, notice how the circle in AdS_3 comes from the direction in the 5-sphere where there is no R-charge at the EVH point. Besides the pinching, which does not introduce a curvature singularity, the geometry (3.33) is otherwise everywhere smooth except at $\mu_1 = 0$.

3.3.2 The non-BPS near-EVH near horizon geometry

Near-EVH non-BPS black holes are parametrically described by excitations (3.26) from the EVH vacua (3.18), and we will see that the excitations are encoded in the near horizon geometry as local BTZ black holes. The excitations are described by the BTZ mass and angular momentum. The near horizon limit is as in (3.32), and the near horizon geometry is

$$\begin{aligned} ds^2 =& \mu_1 \Big[-\frac{(x^2 - x_+^2)(x^2 - x_-^2)}{\ell_3^2 x^2} d\tau^2 + \frac{\ell_3^2 x^2 dx^2}{(x^2 - x_+^2)(x^2 - x_-^2)} + x^2 \left(d\hat{\chi} - \frac{x_+ x_-}{\ell_3 x^2} d\tau \right)^2 \Big] \\ &+ \mu_1\sqrt{q_2q_3}d\Omega_3^2 + \frac{L^2}{\mu_1\sqrt{q_2q_3}}\sum_{i=2}^{3} q_i \left(d\mu_i^2 + \mu_i^2 d\hat{\psi}_i^2 \right). \end{aligned} \tag{3.35}$$

The first line is conformal to a local BTZ black hole (1.63) built on the pinching AdS_3 orbifold. The inner and outer horizons of the near horizon BTZ black hole are given in terms of (3.22)

by

$$x_{\pm}^2 = \frac{L^2}{\sqrt{q_2 q_3}} \left(\frac{M \pm \sqrt{M^2 - 4\mathbf{V}\frac{\hat{q}_1 q_2 q_3}{L^2}}}{2\mathbf{V}} \right) . \tag{3.36}$$

We note that $\hat{q}_1 = 0$ corresponds to a vanishing inner horizon, while $M = 0$ forces $\hat{q}_1 = 0$[3]; so M controls the outer horizon size.

It was shown in [28] that there exists a non-trivial consistent truncation of type IIB with a constant dilaton, metric and self-dual 5-form to six dimensions of the form

$$ds^2 = \mu_1 ds_6^2 + \frac{L^2}{\mu_1} \left(\sqrt{q_2/q_3}\,(d\mu_2^2 + \mu_2^2\, d\psi_2^2) + \sqrt{q_3/q_2}\,(d\mu_3^2 + \mu_3^2\, d\psi_3^2) \right) . \tag{3.37}$$

Notice this is indeed of the form found above with $ds_6^2 = ds_{BTZ}^2 + \sqrt{q_2 q_3}/L^2 d\Omega_3^2$, where the 6d part is a space of negative constant scalar curvature $\mathcal{R}_6 = -\frac{6(q_2+q_3)}{L^2\sqrt{q_2 q_3}}$.

Temperature and entropy: To use the standard thermodynamic relations satisfied by BTZ black holes, we must compactify (3.35) to three dimensions. Consider the ansatz

$$ds^2 = \mu_1 g_{\mu\nu}^{(3)} dx^\mu dx^\nu + \mu_1 \sqrt{q_2 q_3} d\Omega_3^2 + \frac{L^2}{\mu_1 \sqrt{q_2 q_3}} \sum_{i=2}^{3} q_i \left(d\mu_i^2 + \mu_i^2 d\hat{\psi}_i^2 \right) , \tag{3.38}$$

and plug it into the 10d type IIB supergravity action. Focussing on its Einstein-Hilbert term

$$\frac{1}{16\pi G_{10}} \int \sqrt{-g_{(10)}}\, ({}^{10}\mathcal{R} + \cdots) = \frac{1}{16\pi G_3} \int \sqrt{-g_{(3)}}\, ({}^{3}\mathcal{R} + \cdots) , \tag{3.39}$$

we can identify the 3d Newton's constant to be

$$\frac{1}{G_3} = \frac{(q_2 q_3)^{3/4} L^4}{16 G_{10}} (2\pi)^4 = \frac{2(q_2 q_3)^{3/4} N^2}{L^4} . \tag{3.40}$$

We stress that although the metric (3.38) is singular in μ_i, the integral (3.39) produces a finite value for the 3d Newton's constant (3.40). We will see that this is the case in all calculations of G_3 in this thesis.

We can now compute the temperature and entropy of the pinching BTZ black holes (3.35), which equal

$$\begin{aligned} T_{\rm BTZ} &\equiv \frac{x_+^2 - x_-^2}{2\pi x_+ \ell_3^2} = \frac{L}{\epsilon (q_2 q_3)^{\frac{1}{4}}}\, T_{\rm H} , \\ S_{\rm BTZ} &\equiv \frac{2\pi\epsilon \cdot x_+}{4 G_3} = S_{\rm BH} , \end{aligned} \tag{3.41}$$

where for $T_{\rm H}$ and $S_{\rm BH}$ we have used (3.24) and (3.36). We can see that the BTZ temperature agrees with the near-EVH limit of the 10d temperature, up to the time scaling (3.32), while the 10d entropy in the limit is captured by the 3d BTZ entropy.

The null orbifold appearance: Following the discussion in section 1.7, there should exist a second inequivalent near horizon limit when we restrict ourselves to deformations preserving extremality

$$x_+ = x_- = x_0 \qquad \Longleftrightarrow \qquad M = 2\frac{\sqrt{\mathbf{V}}}{L^2} \sqrt{\hat{q}_1 q_2 q_3} . \tag{3.42}$$

[3] $M^2 \geq \sqrt{4\mathbf{V}\frac{\hat{q}_1 q_2 q_3}{L^2}}$, as discussed in section 1.4, and from section 3.2 we cannot have $q_1 > q_i$.

Indeed, for this subset of excitations, we can modify the singular large gauge transformations appearing in (3.32) to

$$\begin{aligned} t &= \frac{L}{(q_2 q_3)^{1/4}} \frac{\tau}{\epsilon^2}, \qquad \psi_1 = \hat{\chi} + \frac{\tau}{\ell_3\, \epsilon^2}, \\ \psi_i &= \hat{\psi}_i + \Omega_i^{(0)} \frac{L}{(q_2 q_3)^{1/4}} \frac{d\tau}{\epsilon^2}, \quad i = 2, 3\,. \end{aligned} \tag{3.43}$$

The resulting metric

$$\begin{aligned} ds^2 = \mu_1 \left(\ell_3^2 \frac{d\sigma^2}{4\sigma^2} + 2\sigma\, d\hat{\chi}\, \frac{d\tau}{\ell_3} \right) + \mu_1 \sqrt{q_2 q_3} d\Omega_3^2 \\ + \frac{L^2}{\mu_1 \sqrt{q_2 q_3}} \sum_{i=2}^{3} q_i \left(d\mu_i^2 + \mu_i^2 \left(d\hat{\psi}_i - \Omega_i^{(2)} \frac{L}{(q_2 q_3)^{1/4}} d\tau \right)^2 \right) \end{aligned} \tag{3.44}$$

contains the null self-dual orbifold described in section 1.7, where $\sigma = x^2 - x_0^2$, in lieu of the BTZ geometry. The null AdS_3 orbifold does not have a pinching angle and is non-trivially fibered over the 7d transverse space.

Near horizon and near-BPS order of limits: One could ask whether we could take the near-BPS limit after zooming in on the geometry close to the horizon. This would require taking $q_2 \sim q_3 \sim \epsilon$, resulting in an unreliable supergravity description since both AdS_3 and S^3 become Planck scale. We also note that the definition of $\hat{q}_1$ would need to be changed to comply with (3.13), ie $\hat{q}_1 = \frac{\tilde{q}_1}{\epsilon^2}$; then the horizon size (3.36) would become very large.

3.3.3 The near-BPS VH near horizon geometry

For near-BPS VH black holes (3.18), the near horizon geometry for $r = \epsilon \frac{R}{L} x$ and $t = \frac{L}{R}\tau$, is

$$ds_{10}^2 = \mu_1 \epsilon \left(-x^2 \frac{d\tau^2}{R^2} + R^2 \frac{dx^2}{x^2} + x^2 d\hat{\chi}^2 + R^2 d\Omega_3^2 + x^2 \frac{d\mu_1^2}{\mu_1^2} \right) \tag{3.45}$$

$$+ \frac{L^2}{\mu_1} \sum_{i=2}^{3} \frac{\hat{q}_i}{\sqrt{\hat{q}_2 \hat{q}_3}} \left(d\mu_i^2 + \mu_i^2 \left(d\psi_i - \Omega_i^{(0)} \frac{L}{R} d\tau \right)^2 \right), \tag{3.46}$$

where $R = (\hat{q}_2 \hat{q}_3)^{\frac{1}{4}}$ is the AdS_3 and S^3 radius and $\Omega_i^{(0)} = \frac{1}{L}$ is the angular velocity at the EVH point. We can see that the first line is locally $AdS_3 \times S^3$ for constant values of $\mu_1 = \cos\alpha$; we thus focus geometrically on a strip of the transverse S^5 by demanding

$$\alpha = \alpha^0 + \sqrt{\epsilon}\hat{\alpha}, \qquad \beta = \beta^0 + \sqrt{\epsilon}\hat{\beta}, \qquad d\mu_i = \sqrt{\epsilon} d\hat{\mu}_i. \tag{3.47}$$

and redefining

$$\psi_i - \Omega_i^{(0)} \frac{L}{R} \tau = \sqrt{\epsilon}\hat{\psi}_i. \tag{3.48}$$

In this "strip" picture, the near horizon geometry becomes

$$ds_{10}^2 = \mu_1^0 \epsilon \left[\left(-\frac{x^2 d\tau^2}{\ell_3^2} + \frac{\ell_3^2 dx^2}{x^2} + x^2 d\psi_1^2 \right) + R^2 d\Omega_3^2 + \frac{L^2}{(\mu_1^0)^2} \sum_{i=2}^{3} \frac{\hat{q}_i}{\sqrt{\hat{q}_2 \hat{q}_3}} \left(d\hat{\mu}_i^2 + (\mu_i^0)^2 d\hat{\psi}_i^2 \right) \right]. \tag{3.49}$$

Locally, this is $AdS_3 \times S^3 \times \mathbb{R}^4_+$. The AdS_3 and S^3 have equal radii $\ell_3 = R = (\hat{q}_2 \hat{q}_3)^{\frac{1}{4}}$ and the coordinates of the non-compact manifold $\mathcal{M}_4$ with metric

$$ds_{\mathcal{M}_4}^2 = d\hat{\mu}_i^2 + (\mu_i^0)^2 d\hat{\psi}_i^2 \tag{3.50}$$

have ranges

$$\hat{\mu}_i \in [0,\infty], \qquad \hat{\psi}_i \in [0,\infty]. \tag{3.51}$$

We can see that although this metric does not suffer the pinching as in section 3.3.1, it is multiplied by an overall ϵ factor[4]. The scaling limit (3.47) of the near-BPS VH black hole does not involve the pinching and vanishing temperature that is common in the EVH/CFT correspondence as described in section 1.8 and involved in the first law analysis in section 2.3. Nonetheless, the geometry does have a near horizon local AdS_3 geometry and potential CFT_2 dual description.

3.3.4 The near-BPS near-VH near horizon geometry

Near-VH near-BPS black holes are parametrically described by excitations (3.25) from the EVH vacua (3.18), and we will show that the excitations are encoded in the near horizon geometry as local BTZ black holes. The near horizon limit is as in (3.47), but with the radial and time variables scaled like

$$r^2 = \epsilon^2 \left(\frac{R^2}{L^2} x^2 - \hat{q}_1 \right), \qquad t = \frac{L}{R}\tau. \tag{3.53}$$

The near horizon geometry

$$\begin{aligned} ds^2_{10} = \mu_1^0 \epsilon \Bigg[& \left(-\frac{(x^2-x_+^2)(x^2-x_-^2)}{\ell_3^2 x^2} d\tau^2 + \frac{\ell_3^2 x^2 dx^2}{(x^2-x_+^2)(x^2-x_-^2)} + x^2 (d\psi_1 - \frac{x_+ x_-}{\ell_3 x^2} d\tau)^2 \right) \\ & + R^2 d\Omega_3^2 + \frac{L^2}{R^2 (\mu_1^0)^2} \sum_{i=2}^{3} \hat{q}_i \left(d\hat{\mu}_i^2 + (\mu_i^0)^2 d\hat{\psi}_i^2 \right) \Bigg] \end{aligned} \tag{3.54}$$

contains a BTZ factor, where the BTZ inner and outer horizons are given in terms of (3.27)

$$x_\pm^2 = \frac{L^2}{R^2} \left(\frac{M \pm \sqrt{M^2 - 4\frac{\hat{q}_1 \hat{q}_2 \hat{q}_3}{L^2}}}{2} + \hat{q}_1 \right), \tag{3.55}$$

the size of which are controlled by the near-EVH excitations M and $\hat{q}_1$ as in section 3.3.2. We see that the near horizon geometry of a near-BPS black hole is excited from an AdS_3 geometry to a BTZ black hole as in section 3.3.2. Although the geometry does not contain a pinching angle, it has an overall epsilon scaling.

Temperature and entropy: To use the standard thermodynamic relations satisfied by BTZ black holes, we must compactify (3.54) to three dimensions. Consider the ansatz

$$ds^2 = \epsilon \mu_1^0 g^{(3)}_{\mu\nu} dx^\mu dx^\nu + \epsilon \mu_1^0 R^2 d\Omega_3^2 + \epsilon \frac{L^2}{R^2 \mu_1^0} \sum_{i=2}^{3} \hat{q}_i \left(d\hat{\mu}_i^2 + (\mu_i^0)^2 d\hat{\psi}_i^2 \right), \tag{3.56}$$

and plug it into the 10d type IIB supergravity action. First we note that the volume of the non-compact 4d manifold (3.50) is very large for small ϵ,

$$\mathrm{Vol}(\mathcal{M}_4) = L^4 \frac{(2\pi)^2}{\epsilon} \mu_2^0 \mu_3^0 \int d\hat{\mu}_2 d\hat{\mu}_3. \tag{3.57}$$

[4] If ψ_i is *not* scaled with $\sqrt{\epsilon}$, the metric will look like (recalling that $d\mu_i$ remains *finite* and $\mu_i \in [0,1]$)

$$\begin{aligned} ds^2_{10} = \mu_1^0 \epsilon \Bigg[& \left(-\frac{x^2 d\tau^2}{\ell_3^2} + \frac{\ell_3^2 dx^2}{x^2} + x^2 d\psi_1^2 \right) + R^2 d\Omega_3^2 \Bigg] \\ & + \frac{L^2}{\mu_1^0} \sum_{i=2}^{3} \frac{\hat{q}_i}{\sqrt{\hat{q}_2 \hat{q}_3}} \left(d\mu_i^2 + (\mu_i^0)^2 \left(d\psi_i - \Omega_i^{(0)} \frac{L}{R} d\tau \right)^2 \right). \end{aligned} \tag{3.52}$$

Geroch's argument [75], which states that the first order contribution to an expansion of a solution to the equations of motion is itself also a solution, ensures that (3.49) is on-shell. As (3.52) is isometric to (3.49), it must also be a solution. Our subsequent analysis is unchanged for this alternative near horizon limit.

So at each strip of the S^5 there is a geometry that looks like an $AdS_3\times S^3$ transverse to an infinite flat space.

Focussing on its Einstein-Hilbert term

$$\frac{1}{16\pi G_{10}}\int\sqrt{-g_{(10)}}\left({}^{(10)}\mathcal{R}+\cdots\right)=\frac{1}{16\pi G_3}\int\sqrt{-g_{(3)}}\left({}^{(3)}\mathcal{R}+\cdots\right), \tag{3.58}$$

and recalling that ${}^{(10)}\mathcal{R}+\cdots=\left(\frac{1}{\epsilon\mu_1^0}\right){}^{(3)}\mathcal{R}+\cdots$, we can write the left hand side of (3.58) as

$$\frac{1}{16\pi G_{10}}\int\sqrt{-g_{(3)}}\sqrt{\epsilon^3(\mu_1^0)^3\times\epsilon^3(\mu_1^0)^3(R^2)^3d\Omega_3^2\times\epsilon^4\frac{L^8}{R^8(\mu_1^0)^4}}\times\mathrm{Vol}(\mathcal{M}_4)\left(\frac{1}{\epsilon\mu_1^0}\right){}^{(3)}\mathcal{R}$$

which gives[5]

$$\frac{2\pi^2}{16\pi G_{10}}\frac{\epsilon^4L^4}{R}\int\sqrt{-g_{(3)}}\times\mathrm{Vol}(\mathcal{M}_4){}^{(3)}\mathcal{R}. \tag{3.59}$$

This will yield, utilising the expression for the ten dimensional Newton's constant (3.6),

$$\frac{1}{G_3}=\frac{2\pi^2}{G_{10}}\frac{\epsilon^4L^4}{R}\mathrm{Vol}(\mathcal{M}_4)\quad=16N^2\epsilon^2\frac{R^3}{L^4}\mu_2^0\mu_3^0\int d\mu_2d\mu_3, \tag{3.60}$$

so we may calculate the BTZ entropy,

$$S_{\rm BTZ}=\frac{2\pi x_+}{4G_3}=S_{\rm BH}\left(8\mu_2^0\mu_3^0\int d\mu_2d\mu_3\right), \tag{3.61}$$

where the entropy $S_{\rm BH}$ in the near-EVH near-BPS regime of parameters is given in (3.29). It is interesting to emphasise that focusing on a "strip" of a black hole horizon, when taking the near horizon limit, is generic in non-extremal black holes. The difference is that the 2d geometry close to the generic non-extremal horizon is Rindler, whereas the (near-)BPS and (near-)EVH case studied here give rise to AdS_3 (BTZ). Technically, this occurs to guarantee analyticity in the ϵ expansion of the black hole metric components when taking its near horizon limit, ensuring that the limiting metric remains a solution to supergravity equations. Conceptually, if one thinks of the horizon as the location where the black hole degrees of freedom live (at least from the perspective of an observer at infinity), it is clear that such a near horizon description will never reproduce the correct entropy because it loses the information on the curvature of the original horizon by approximating it with a flat tangent plane.

Gravitationally, and for the reasons just mentioned, it is natural to interpret the so obtained near horizon Bekenstein-Hawking entropy (3.61) as an *entropy density*; that is, $S_{\rm BTZ}=S_{\text{per strip}}$. This is more even so in the particular example discussed in this subsection, given the microscopic interpretation of the BPS R-charged black holes as a distribution of smeared giant gravitons on the 5-sphere [72] and the arguments provided in [34] identifying the open strings stretched between these giants as responsible for the entropy of their near-BPS limits. The dependence on the point where the strip lies, i.e. $\mu_2^0\mu_3^0$, provides the natural measure where to integrate this density. Not surprisingly, one finds

$$\int_{\mu_2^2+\mu_3^2\leq1}\mu_2\mu_3d\mu_2d\mu_3=\frac{1}{8}. \tag{3.62}$$

That is, if we suitably sum over the entropies of each BTZ black hole located at different strips (different values of μ_2,μ_3), given in (3.61), we recover the entropy of the original 5d black hole. Unfortunately, it is not clear to us what the process of integrating over this entropy density means in the language of 2d CFTs that naturally would arise as the dual descriptions of the near horizon geometries (3.54)[6].

[5]The S^3 is written in Hopf coordinates $ds^2=d\theta^2+\sin^2\theta d\phi^2+\cos^2\theta d\psi^2$ and the volume element is $\int dV=\int\sin\theta\cos\theta d\theta d\phi d\psi=2\pi^2$.

[6]It is possible that requiring to have a consistent on-shell near horizon geometry is responsible for the focusing on a horizon "strip". Recently, there have been discussions trying to argue that the low energy physics in (non-

The Hawking temperature associated to each BTZ black hole geometry is given by

$$T_{\rm BTZ} \equiv \frac{x_+^2 - x_-^2}{2\pi x_+ \ell_3^2} = \frac{L^2}{2\pi x_+ R^4}\sqrt{M^2 - 4\frac{\hat{q}_1\hat{q}_2\hat{q}_3}{L^2}} = \frac{L}{R}T_H\,, \tag{3.63}$$

which agrees up to time scaling (3.47) with the Hawking temperature (3.29) in the near-EVH limit. We note the temperature of each BTZ black hole gives the exact Hawking temperature, independently of the strip picture, as it is by definition a constant value.

3.4 IR 2d Description

In this section we use the results of sections 1.1 and 1.4 to compute the central charges of the IR 2d CFT that is dual to the asymptotically AdS_3 structure emerging in the near horizon of non-BPS and near-BPS near-VH black holes. While the non-BPS quantities will adhere to the pinching arguments of section 1.7, the near-BPS near horizon AdS_3 is not a pinching geometry.

3.4.1 Non-BPS near-EVH

The central charge c of the IR 2d CFT and the quantum numbers $(L_0, \bar{L}_0)$ describing the gravitational black holes described in the previous section can be extracted from standard AdS_3/CFT_2 [5], where the effective central charge c is related to the pinching central charge c_p by $c = \epsilon c_p$ as per section 1.7, and the mass and angular momentum of the BTZ built on a pinching AdS_3 orbifold have an extra ϵ in their expressions, as they are evaluated by integrals over U(1)s with periodicity $2\pi\epsilon$:

$$c = \frac{3\ell_3}{2G_3}\epsilon = \frac{3q_2q_3}{L^4\mathbf{V}}\ N^2\epsilon \tag{3.64}$$

$$\ell_3 M_{\rm BTZ} = L_0 + \bar{L}_0 - \frac{c}{12} = \frac{x_+^2 + x_-^2}{8\ell_3 G_3}\epsilon\,, \sim N^2\epsilon \tag{3.65}$$

$$J_{\rm BTZ} = L_0 - \bar{L}_0 = \frac{x_+x_-}{4\ell_3 G_3}\epsilon\ \sim N^2\epsilon. \tag{3.66}$$

Requiring a *finite* central charge to have a *finite* gap in this IR 2d CFT is achieved by the *large* N limit:

$$\boxed{N^2\epsilon = \text{fixed.}} \tag{3.67}$$

It is manifest the entropy $S_{\rm BH}$ in (3.24) remains finite in this limit, as do the near-EVH excitations

$$\ell_3 M_{\rm BTZ} = \frac{M}{4L^2\sqrt{\mathbf{V}}}N^2\epsilon \qquad J_{\rm BTZ} = \frac{\sqrt{\hat{q}_1q_2q_2}}{2L^3}N^2\epsilon, \tag{3.68}$$

which will be related with precise combinations of the UV quantum numbers.

We note how the non-BPS EVH point $(0, q_2, q_3; \mu(q_2, q_3))$ determines the IR 2d CFT by fixing its central charge, whereas its orthogonal deformations (3.20) encode their *finite* excitations. Any tangential deformation would have simply changed the value of (q_2, q_3), which would correspond to a different CFT. This mechanism will be apparent throughout the analysis of near-EVH black holes in this thesis.

Using Cardy's formula (1.93) [5]

$$S_{\rm CFT} = 2\pi\sqrt{\frac{c}{6}\left(L_0 - \frac{c}{24}\right)} + 2\pi\sqrt{\frac{\bar{c}}{6}\left(\bar{L}_0 - \frac{\bar{c}}{24}\right)}\,, \tag{3.69}$$

one can immediately check the bulk entropy (3.24) is reproduced for the near-EVH black holes.

)extremal black holes is described by a 2d CFT, without appealing to its near horizon geometry, but to the wave equations satisfied by probe fields on the geometry [76, 77]. If one would take a similar attitude in these black holes, one can envision keeping the information about the full black hole geometry.

3.4.2 Near-BPS near-EVH

There is no pinching here, so the CFT central charge and BTZ conserved charges are calculated using the expressions 1.32 and 1.77 in Chapter 1:

$$c = \frac{3\ell_3}{2G_3} = \frac{3R^4}{L^4} N^2\epsilon^2 \left(8\mu_2^0\mu_3^0 \int d\mu_2 d\mu_3\right) \tag{3.70}$$

$$\ell_3 M_{\rm BTZ} = L_0 + \bar{L}_0 - \frac{c}{12} = \frac{x_+^2 + x_-^2}{8\ell_3 G_3}\,, \tag{3.71}$$

$$J_{\rm BTZ} = L_0 - \bar{L}_0 = \frac{x_+ x_-}{4\ell_3 G_3}\,. \tag{3.72}$$

The near-EVH excitations equal

$$\ell_3 M_{\rm BTZ} = \frac{M + 2\hat{q}_1}{4L^2} N^2\epsilon^2 \left(8\mu_2^0\mu_3^0 \int d\mu_2 d\mu_3\right) \tag{3.73}$$

$$J_{\rm BTZ} = \frac{\sqrt{\hat{q}_1(\hat{q}_1 + M + \frac{\hat{q}_2\hat{q}_3}{L^2})}}{2L^2} N^2\epsilon^2 \left(8\mu_2^0\mu_3^0 \int d\mu_2 d\mu_3\right)\,. \tag{3.74}$$

Again, notice how the static EVH point $(0, \epsilon\hat{q}_2, \epsilon\hat{q}_3; \epsilon^2\hat{\mu}(\hat{q}_2, \hat{q}_3))$ determines the IR 2d CFT by fixing its central charge, whereas its orthogonal deformations (3.25) encode their *finite* excitations. Any tangential deformation would have simply changed the value of $(\hat{q}_2, \hat{q}_3)$, which would correspond to a different CFT.

The "volume factor" $\left(8\mu_2^0\mu_3^0 \int d\mu_2 d\mu_3\right)$ multiplies the central charge and BTZ conserved quantities as it did for the BTZ entropy (3.61). If we were to suitably sum over the value of the central charge at each strip, this would agree up to the pinching factor ϵ with the near-BPS limit of the central charge in the non-BPS regime (3.64). However, the mass and angular momentum here are parametrically different to the non-BPS values (3.68), as the two types of excitation are different.

In the near-BPS case we may view the central charge in terms of giant gravitons: from (3.11) we see that in the limit (3.25)

$$N_i = \frac{\hat{q}_i}{L^2} N\epsilon \quad \Rightarrow \quad c = 3N_2N_3 \left(8\mu_2^0\mu_3^0 \int d\mu_2 d\mu_3\right), \tag{3.75}$$

so that the sum of the values of the central charge at each strip will give us the total number of giant intersections. This is evidence in favour of the view that the central charge counts the number of giant intersections in the focussed strip.

Again, we can use Cardy's formula (1.93) [5]

$$S_{\rm CFT} = 2\pi\sqrt{\frac{c}{6}\left(L_0 - \frac{c}{24}\right)} + 2\pi\sqrt{\frac{\bar{c}}{6}\left(\bar{L}_0 - \frac{\bar{c}}{24}\right)} \tag{3.76}$$

to check the three dimensional Beckenstein Hawking entropy (3.61) is reproduced for the near-EVH black holes.

Scaling of N: For non-BPS black holes, it was obvious that near-EVH excitations are finite in a specific large N limit (3.67). In the near-BPS regime, however, the choice of scaling is more subtle. We discuss here two possible large N limits one could take together with the near-EVH limit.

$N\epsilon^2 \sim 1$: The entropy of the original black hole (3.29) goes to zero, for finite N, as a consequence of the dilute giant graviton approximation. Given the overall ϵ scaling in the near horizon metric (3.54), it is natural to interpret the latter as a rescaling of the 10d Planck scale, i.e. $\ell_p^4 \to \epsilon^2\ell_p^4$, as we usually do in the decoupling limits leading to the AdS/CFT correspondence [68]. Keeping L finite requires N to scale as $N\epsilon^2 \sim 1$ if g_s remains fixed, i.e. $\alpha' \to \epsilon\alpha'$. This is the same scaling considered in [28]. Given the non-compactness of the transverse space in the

limit (3.26), it is the entropy density that one should require to keep finite

$$s = \frac{S}{\text{Vol}(\mathcal{M}_4)} \propto \left(N\epsilon^2\right)^2 \text{ finite but large} \quad \Longrightarrow \quad N\epsilon^2 \sim 1. \tag{3.77}$$

Thus, both considerations are consistent with the same scaling. We provide two further physical arguments for why $N\epsilon^2 \sim 1$ can be a meaningful limit to study:

1. One can estimate the *mass density* of open strings stretched between intersecting giants as

$$m_{\text{open}} = \frac{M_{\text{open}}}{\text{length}\,\mathcal{M}_4} \sim \epsilon^{1/2} \frac{L\delta\hat{\alpha}}{\ell_s^2} \frac{1}{L\epsilon^{-1/2}} \sim \frac{\sqrt{g_s}}{L^2}\delta\hat{\alpha}\sqrt{N\epsilon^2}\,. \tag{3.78}$$

   where we used $L^4 = 4\pi g_s \ell_s^4 N$ and kept g_s fixed. Thus, requiring energy density finiteness of these excitations also dictates the scaling $N\epsilon^2 \sim 1$.

2. The smallest distance computed in the near horizon metric (3.54) is of order $\ell \sim L\sqrt{\epsilon}$ and the curvature invariants of the near horizon metric (3.54) are of order ℓ^{-2}. In order to have a valid supergravity approximation in which stringy corrections are small we need to require $\ell \gtrsim \ell_s$. Since $\ell/\ell_s \sim \left(N\epsilon^2\right)^{1/4}$, for a fixed g_s, validity of supergravity leads to $N\epsilon^2 \sim 1$. The validity of the supergravity description also demands $sL^4 \gtrsim 1$ where s is the entropy density. This latter, as discussed above, is also satisfied with $N\epsilon^2 \sim 1$ scaling.

$N\epsilon \sim 1$: However, the number of giants (3.11) in the limit described above blows up and we do not have a notion of "giant density". In the truncated three dimensional theory, we do not have a concept of density either when discussing the thermodynamic quantities. We also note that in the limit $N\epsilon^2 \sim 1$, the three dimensional Newton's constant $G_3 \sim (N\epsilon)^{-2}$ vanishes. While this is desirable in the pinching case, we do not require $G_3 \to 0$ to keep a finite mass gap in the dual CFT_2. We will see that in the near-EVH near-BPS limit, specific combinations of the gauge theory charges (3.10) scale like $N\epsilon$. Although a definition of "charge density" would allow them to remain finite for $N\epsilon^2 \sim 1$, we do not know what this means in gauge theory language. We also note that taking a near-EVH limit of these charges is independent of the geometry.

One way to address these questions is to scale N like $N\epsilon \sim 1$. Keeping a finite AdS_5 radius requires then that $g_s\epsilon \sim 1$, resulting in a large 'tHooft coupling in the dual gauge theory, $\lambda_{tHooft} = g_{\text{YM}}^2 N = g_s N \sim \frac{1}{\epsilon^2}$. We may ask why the entropy in ten dimensions remains finite in this limit, when the near horizon area seems to be infinite. To understand this, we first note that taking the near-EVH limit of the entropy is independent of the near horizon geometry. This implies that the near-EVH limit should be accompanied by the $N\epsilon \sim 1$ scaling. Then, recalling (3.52), we can view the horizon manifold in the near horizon geometry as the product of a *small* manifold and a *finite*, *compact* piece:

$$ds^2_{r=r_+} \sim \epsilon \left[x_+^2 \left(d\psi_1 - \frac{d\tau}{\ell_3} \right)^2 + R^2 d\Omega_3^2 \right] + \frac{L^2}{R^2 (\mu_1^0)^2} \sum_{i=2}^{3} \hat{q}_i \left(d\mu_i^2 + (\mu_i^0)^2 d\psi_i^2 \right). \tag{3.79}$$

The volume of this spacetime does not blow up, and scales like $(N\epsilon)^2$.

For these reasons, we adopt the large N limit

$$\boxed{N\epsilon \sim 1.} \tag{3.80}$$

In this limit, the 10d bulk quantities are kept finite, as are the dual $\mathcal{N} = 4$ super Yang-Mills theory charges. The AdS_3 and CFT_2 expressions also remain finite for (3.80).

3.5 First Law of Thermodynamics: Static Charged near-EVH Black Holes

We now explicitly demonstrate how the BTZ first law of thermodynamics follows from the 10d one (3.9) as described in section 2.3, which we may view as further supporting evidence of

the EVH/CFT correspondence reviewed in section 1.8. We will give well-defined values to the abstract objects (2.67) introduced in section 2.3, and show that the generic proposal holds in both the non-BPS and near-BPS cases.

The 10d dimensional black holes (3.1) interpolate between asymptotically AdS_5 and locally AdS_3 geometries. As a near horizon limit of a system probes its low-energy sector, we call the near horizon sector the IR sector, and we label the asymptotically AdS_5 system by UV. Physical variations appearing in the first law are generically defined as one-forms on the black hole parameter space. In our examples, the UV $\{dE, dJ_1, dJ_i\}$ forms are defined on a four dimensional space spanned by (q_1, q_2, q_3, μ), while in the IR, physical variations belong to the subspace of orthogonal deformations to the EVH hyperplane, leaving the EVH point fixed.

3.5.1 Non-BPS first law

As advocated in section 2.3, we distinguish two categories of 10d black holes charges in the near-EVH non-BPS regime (3.21):

- $Y = \{E, J_2, J_3\}$ with an ϵ expansion of the form $Y = Y^{(0)} + \epsilon^2 Y^{(2)}$.
- J_1 with expansion $J_1 = \epsilon^2 J_1^{(2)}$.

$Y^{(0)}$ is the value of charges *at the EVH point*, whereas $Y^{(2)}$ are the *near-EVH excitations*. Ω_i have analogous expansions to J_2 and J_3, with finite $\Omega_i^{(0)}$ values at the EVH point (3.18), corresponding to $\Omega^{(0)}$ in section 2.3, and with ϵ^2 corrections.

Consider the UV first law (3.9). Using (3.41), its left hand side equals

$$T_{\rm H} dS_{\rm BH} = \frac{\epsilon (q_2 q_3)^{\frac{1}{4}}}{L} T_{\rm BTZ} dS_{\rm BTZ} \,. \tag{3.81}$$

To discuss its right hand side, we first note that there are no non-trivial fibrations in the near horizon geometry (3.35), so that $A_\alpha = B_\alpha = 0$ (2.63). In agreement with our analysis of the previous Chapter, we find

$$\epsilon^2 \left(E^{(2)} - \Omega_2^{(0)} J_2^{(2)} - \Omega_3^{(0)} J_3^{(2)} \right) = \frac{\epsilon (q_2 q_3)^{\frac{1}{4}}}{L} M_{\rm BTZ}. \tag{3.82}$$

We also have

$$\Omega_1^{(0)} = \frac{(q_2 q_3)^{\frac{1}{4}}}{L} \Omega_{\rm BTZ}, \qquad J_1 = \epsilon J_{\rm BTZ}. \tag{3.83}$$

Adding all contributions and dropping the overall $\frac{\epsilon (q_2 q_3)^{\frac{1}{4}}}{L}$ constant factor, the exact IR first law is derived

$$\boxed{\begin{array}{c} T_{\rm H} dS_{\rm BH} = dE - \Omega_1 dJ_1 - \sum_{i=2}^{3} \Omega_i dJ_i \\ \Downarrow \\ T_{\rm BTZ} dS_{\rm BTZ} = dM_{\rm BTZ} - \Omega_{\rm BTZ} dJ_{\rm BTZ}. \end{array}} \tag{3.84}$$

This reduction is our first example of the first law derivation in section 2.3. We will see in the following section and Chapter 4 that this result is universal for near-EVH black holes.

3.5.2 Near-BPS first law

As the near-BPS near-VH black hole does not have a vanishing temperature, and its near horizon geometry (3.54) does not contain a pinching AdS_3 orbifold, we do not necessarily expect the first law proposal of section 2.3 to hold. Nevertheless, we examine the first law (3.9) in the near-BPS near-VH regime (3.26). We first distinguish the categories of 10d black holes charges and chemical potentials in this regime:

- $Y = \{E, J_2, J_3\}$ with an ϵ expansion of the form $Y = \epsilon Y^{(1)} + \epsilon^2 Y^{(2)}$, where $Y^{(1)}$ are functions of the EVH parametes $\hat{q}_2, \hat{q}_3$ and $Y^{(2)}$ encode the near-EVH excitation parameters $\hat{q}_1, M$.

- J_1 with expansion $J_1 = \epsilon^2 J_1^{(2)}(\hat{q}_1, M)$.

The angular velocities scale like $\Omega_1 = \Omega_1^{(0)} + \mathcal{O}(\epsilon^2)$, $\Omega_i = \Omega_i^{(0)}(\hat{q}_2, \hat{q}_3) + \mathcal{O}(\epsilon)$. As described in section 2.3, $\Omega_1^{(0)}$ depends on the near-EVH parameters and gives the BTZ angular velocity, up to the temporal scaling:

$$\Omega_{\rm BTZ} = L^2 \frac{\sqrt{\hat{q}_1(\hat{q}_1 + M + \frac{\hat{q}_2\hat{q}_3}{L^2})}}{R^3 x_+^2} = \frac{L}{R}\Omega_1^{(0)}. \tag{3.85}$$

On the left hand side of the first law, we have from (3.63) and (3.61)

$$T_{\rm BTZ} dS_{\rm BTZ} = \frac{L}{R}\left(8\mu_2^0\mu_3^0 \int d\mu_2 d\mu_3\right) T_{\rm H} dS_{\rm BH}\,. \tag{3.86}$$

On the right hand side, the near-EVH expansion is[7]

$$E - \sum_{i=2}^{3} \Omega_i dJ_i = \epsilon\left(E^{(1)} - \sum_{i=2}^{3}\Omega_i^{(0)} J_i^{(1)}\right) + \epsilon^2\left(E^{(2)} - \sum_{i=2}^{3}\Omega_i^{(0)} J_i^{(2)}\right). \tag{3.87}$$

As the system is near-BPS, the first order contribution vanishes, $E^{(1)} - \sum_{i=2}^{3}\Omega_i^{(0)} J_i^{(1)} = 0$. In the near-BPS regime, we cannot define the BTZ mass as in (2.67). Instead, we define a notion of "First Law Mass"[8] as per section 2.3 as

$$M_{\text{1st Law}} = \epsilon^2\left(E^{(2)} - \sum_{i=2}^{3}\Omega_i^{(0)} J_i^{(2)}\right), \tag{3.89}$$

so that its variation is proportional to the variation of the BTZ mass (3.73)[9]

$$dM_{\rm BTZ} = \frac{L}{R}\left(8\mu_2^0\mu_3^0 \int d\mu_2 d\mu_3\right) dM_{\text{1st Law}}. \tag{3.92}$$

The BTZ angular momentum is given by

$$J_{\rm BTZ} = \left(8\mu_2^0\mu_3^0 \int d\mu_2 d\mu_3\right) \frac{\sqrt{\hat{q}_1(\hat{q}_1 + M + \frac{\hat{q}_2\hat{q}_3}{L^2})}}{2L^2} N^2\epsilon^2 = \left(8\mu_2^0\mu_3^0 \int d\mu_2 d\mu_3\right) J_1. \tag{3.93}$$

---

[7] There are $\mathcal{O}(\epsilon^2)$ terms like $\sum_{i=2}^{3}\Omega_i^{(1)} J_i^{(1)}$, but these do not contribute to the near horizon geometry; also $dJ_i^{(1)} = 0$.

[8] To connect with section 2.3, we note that the scaling (3.48) is a combination of a gauge shift and a pinching:

$$\psi_i \to \varphi_i = \psi_i - \mathcal{A}_i\tau, \qquad \varphi_i \to \hat{\psi}_i = \frac{\varphi_i}{\sqrt{\epsilon}}, \tag{3.88}$$

where $\mathcal{A}_i = \Omega_i^{(0)}$.

[9] We have

$$\left(E^{(2)} - \sum_{i=2}^{3}\Omega_i^{(0)} J_i^{(2)}\right)\epsilon^2 = \frac{\hat{q}_2\hat{q}_3 + 2\hat{q}_1 L^2 + ML^2}{4L^5} N^2\epsilon^2 = \frac{\hat{q}_2\hat{q}_3}{4L^5} N^2\epsilon^2 + \frac{2\hat{q}_1 + M^2}{4L^3} N^2\epsilon^2 \tag{3.90}$$

so that

$$d\left(E^{(2)} - \sum_{i=2}^{3}\Omega_i^{(0)} J_i^{(2)}\right)\epsilon^2 = d\left(\frac{2\hat{q}_1 + M^2}{4L^3}\right) N^2\epsilon^2 \sim dM_{\rm BTZ}, \tag{3.91}$$

as $\hat{q}_2, \hat{q}_3$ parameterise the EVH plane.

Adding all contributions and dropping the overall $\frac{L}{R}\left(8\mu_2^0\mu_3^0\int d\mu_2 d\mu_3\right)$ factor, the exact IR first law is derived

$$\boxed{\begin{aligned} T_{\rm H} dS_{\rm BH} &= dE - \Omega_1 dJ_1 - \sum_{i=2}^{3}\Omega_i dJ_i \\ &\Downarrow \\ T_{\rm BTZ} dS_{\rm BTZ} &= dM_{\rm BTZ} - \Omega_{\rm BTZ} dJ_{\rm BTZ}. \end{aligned}} \tag{3.94}$$

We can see that this relation is satisfied regardless of the transverse volume and of N scaling. The first law result (3.94) holds even though the EVH black hole has finite temperature and no pinching angle. This an indication that there may be a more general way than the one in section 2.3 of deriving the BTZ first law from the near-EVH one.

3.6 EVH/CFT$_2$ vs. AdS$_5$/CFT$_4$

Our black holes have a UV description as thermal states in $\mathcal{N}=4$ super Yang-Mills theory. Taking the low energy limit of the (UV) field theory corresponds to focussing on an IR sector of the theory. On the other hand, our AdS$_3$ near horizon geometry hints at the emergence of an IR 2d CFT dual description. Here we advocate a more direct connection between the two CFTs.

The analysis of the RG flow in field theory and gravity is beyond the scope of this thesis, but we can gain some insight by studying how the quantum numbers of a bulk scalar field probe transform along the flow. Given the isometries of the original black hole (3.1), the UV quantum numbers of this scalar field will be associated with the eigenvalues of the following operators

$$\Delta_{\rm UV} = \ell E = i\ell\partial_t, \qquad J_{2,3} = -i\partial_{\psi_2,\psi_3} \qquad J_1 = -i\partial_{\psi_1}. \tag{3.95}$$

Similarly, the IR quantum numbers are mapped to

$$\Delta_{\rm IR} = i\ell_3\partial_\tau, \qquad J_{\rm IR} = -i\partial_{\psi_{\rm IR}}, \tag{3.96}$$

where $\psi_{\rm IR}$ is the AdS$_3$ angle; in the non-BPS case, $\psi_{\rm IR}=\hat\chi$ and in the near-BPS case $\psi_{\rm IR}=\psi_1$. From now on, as the notation above suggests, we will identify these eigenvalues with the gravity conserved charges. Though this need not hold generically, it will turn out to provide us with the right intuition.

3.6.1 EVH/CFT$_2$ vs. AdS$_5$/CFT$_4$: non-BPS

The conformal dimension $\Delta_{\rm UV}$ of the non-BPS states dual to the non-BPS black holes is expected to "run" along the RG flow implemented by the near horizon limit $r=\epsilon\rho$, $\epsilon\to 0$. Hence, its relation to $\Delta_{\rm IR}$ is non-trivial. On the other hand, given the quantised nature of the remaining conserved U(1) charges, these will not run.

Given the large gauge transformations (3.32) implemented in the near-EVH non-BPS regime, we learn the angular momentum along the AdS$_3$ pinching circle equals

$$\mathcal{J}_{\rm IR} = -i\frac{\partial}{\partial\hat\chi} = -i\frac{\partial\psi_1}{\partial\hat\chi}\frac{\partial}{\partial\psi_1} = \frac{1}{\epsilon}\mathcal{J}_1 = J_{\rm BTZ}, \tag{3.97}$$

where we used (3.68).

The IR conformal dimension equals

$$\Delta_{\rm IR} = i\ell_3\partial_\tau = i\ell_3\left(\frac{\partial t}{\partial\tau}\frac{\partial}{\partial t}+\sum_{i=2}^{3}\frac{\partial\psi_i}{\partial\tau}\frac{\partial}{\partial\psi_i}\right) \tag{3.98}$$

$$= \frac{\ell_3}{\epsilon(q_2q_3)^{\frac{1}{4}}}\left(\Delta_{\rm UV}-L\sum_{i=2}^{3}\Omega_i^{(0)}\mathcal{J}_i\right) \tag{3.99}$$

$$= \frac{\ell_3}{\epsilon(q_2q_3)^{\frac{1}{4}}}\left(\Delta_{\rm UV}^{(0)}-L\sum_{i=2}^{3}\Omega_i^{(0)}\mathcal{J}_i^{(0)}\right)+\epsilon\frac{\ell_3}{(q_2q_3)^{\frac{1}{4}}}\left(\Delta_{\rm UV}^{(2)}-L\sum_{i=2}^{3}\Omega_i^{(0)}\mathcal{J}_i^{(2)}\right) \tag{3.100}$$

$$= \Delta_{\rm IR}^0+\ell_3 M_{\rm BTZ}, \tag{3.101}$$

where we have used (3.82) and where

$$\Delta_{\rm IR}^0 = \frac{\ell_3}{\epsilon(q_2q_3)^{\frac{1}{4}}}\left(\Delta_{\rm UV}^{(0)}-L\sum_{i=2}^{3}\Omega_i^{(0)}\mathcal{J}_i^{(0)}\right) = -\frac{\ell_3}{\epsilon(q_2q_3)^{\frac{1}{4}}}\frac{N^2q_2q_3}{4L^4}. \tag{3.102}$$

Notice $\Delta_{\rm IR}^0$ only depends on the EVH point (and not the excitations) and could consequently be interpreted as a "zero point energy" from the IR 2d CFT perspective. This contribution is generically divergent, but vanishes when supersymmetry is preserved, i.e. $q_2q_3=0$. This would reproduce the expected $\Delta_{\rm IR}=L_0+\bar{L}_0$ bound in this case, due to the protection of supersymmetry along the RG flow. Near the BPS point, i.e. $q_2q_3\sim\epsilon^2$, the "zero point energy" still remains finite in the large N limit (3.67).

We conclude that both $\Delta_{\rm IR}$ and $\mathcal{J}_{\rm IR}$ match the expected IR 2d CFT quantities. This is a good piece of evidence in favour of the EVH/CFT correspondence since despite lack of supersymmetry, the RG flow from the UV to the deep IR does not lead to contributions not captured by the 2d CFT. This fact supports the expectation that the near-EVH sector in the UV dual 4d CFT is a decoupled sector described by this IR 2d CFT where the UV quantum numbers were reshuffled (1.198).

Null orbifold discussion: We can repeat the procedure for the null orbifold case, where the near horizon limit is given in (3.43). Here, we have

$$\Delta_{\rm IR} = i\ell_3\partial_\tau = i\ell_3\left(\frac{\partial t}{\partial\tau}\frac{\partial}{\partial t}+\sum_{i=2}^{3}\frac{\partial\psi_i}{\partial\tau}\frac{\partial}{\partial\psi_i}\right)$$

$$= \frac{\ell_3}{\epsilon^2(q_2q_3)^{\frac{1}{4}}}\left(\Delta_{\rm UV}-L\sum_{i=2}^{3}\Omega_i^{(0)}\mathcal{J}_i-\sqrt{\mathbf{V}}\mathcal{J}_1\right)$$

$$= \frac{\ell_3}{\epsilon^2(q_2q_3)^{\frac{1}{4}}}\left(\Delta_{\rm UV}^{(0)}-L\sum_{i=2}^{3}\Omega_i^{(0)}\mathcal{J}_i^{(0)}\right)+\frac{\ell_3}{(q_2q_3)^{\frac{1}{4}}}\left(\Delta_{\rm UV}^{(2)}-L\sum_{i=2}^{3}\Omega_i^{(0)}\mathcal{J}_i^{(2)}-\sqrt{\mathbf{V}}\mathcal{J}_1^{(2)}\right)$$

$$= \frac{\Delta_{\rm IR}^0}{\epsilon}+\ell_3 M_{\rm BTZ}-\sqrt{\mathbf{V}}\mathcal{J}_1^{(2)}, \tag{3.103}$$

where we recall that the null orbifold limit does not include the pinching of an angle, so that $M_{\rm BTZ}\sim N^2$. As the conformal dimension, after subtracting the zero point energy, scales like N^2, one can deduce that the null orbifold limit does *not* require a large N scaling. We expect that the extra contribution $\sqrt{\mathbf{V}}\mathcal{J}_1^{(2)}$ to the conformal dimension is associated to some notion of spectral flow, which is geometrically realised as rotations in the manifold transverse to the orbifold. We will come across similar "extra terms" in the rotating case study of Chapter 4. Also

$$\mathcal{J}_{\rm IR} = \mathcal{J}_1 \sim N^2\epsilon^2 \to 0, \tag{3.104}$$

which is expected as there is no rotation in the null orbifold (3.44).

3.6.2 EVH/CFT$_2$ vs. AdS$_5$/CFT$_4$: near-BPS

In the near-EVH near-BPS limit, the charges (3.10) scale like

$$\Delta_{\rm UV} \sim N^2\epsilon, \qquad \mathcal{J}_1 \sim (N\epsilon)^2, \qquad \mathcal{J}_i \sim N^2\epsilon. \tag{3.105}$$

It is clear that in the large N limit (3.80), $\Delta_{\rm UV}$ and $\mathcal{J}_i$ diverge, while $\mathcal{J}_1$ is kept finite. However, we will see that the combination

$$\Delta_{\rm IR} \equiv \Delta_{\rm UV} - \sum_{i=2}^{3} \mathcal{J}_i \sim (N^2\epsilon^2) \tag{3.106}$$

remains finite. The near-EVH (3.26) near horizon (3.53) limit focusses the dynamics onto a sector of $\mathcal{N}=4$ super Yang-Mills theory. It was argued in [34] that $\mathcal{J}_1$ and $\Delta_{\rm IR}$ characterise a set of "almost-quarter-BPS" operators associated to open strings stretched between smeared giant gravitons [34]. In the following, we will provide evidence that the sector of $\mathcal{N}=4$ super Yang-Mills theory decoupled in the near-EVH near-BPS limit is described by a 2d CFT, in line with the open string picture.

The angular momentum along the AdS$_3$ circle is given by $J_1 = \mathcal{J}_{\rm IR}$, which is proportional to the BTZ angular momentum, so that

$$\mathcal{J}_{\rm IR} = -i\frac{\partial}{\partial\psi_1} = \frac{J_{\rm BTZ}}{\left(8\mu_2^0\mu_3^0\int d\mu_2 d\mu_3\right)}. \tag{3.107}$$

The conformal dimension

$$\Delta_{\rm IR} = i\ell_3\partial_\tau = i\ell_3\left(\frac{\partial t}{\partial\tau}\frac{\partial}{\partial t} + \sum_{i=2}^{3}\frac{\partial\psi_i}{\partial\tau}\frac{\partial}{\partial\psi_i}\right) \tag{3.108}$$

$$= \Delta_{\rm UV} - L\sum_{i=2}^{3}\Omega_i^{(0)}\mathcal{J}_i = \Delta - \sum_{i=2}^{3}\mathcal{J}_i \tag{3.109}$$

$$= \epsilon\left(\Delta_{\rm UV}^{(1)} - L\sum_{i=2}^{3}\Omega_i^{(0)}\mathcal{J}_i^{(1)}\right) + \epsilon^2\left(\Delta_{\rm UV}^{(2)} - L\sum_{i=2}^{3}\Omega_i^{(0)}\mathcal{J}_i^{(2)}\right) \tag{3.110}$$

$$= \frac{\hat{q}_2\hat{q}_3}{4L^5}N^2\epsilon^2 + \frac{\ell_3 M_{\rm BTZ}}{\left(8\mu_2^0\mu_3^0\int d\mu_2 d\mu_3\right)} \tag{3.111}$$

is the sum of some "zero point energy" $\Delta_{\rm IR}^0$, and a term proportional to the BTZ mass, where we have used (3.89). The "zero point energy"

$$\Delta_{\rm IR}^0 = \frac{\hat{q}_2\hat{q}_3}{4L^4}N^2\epsilon^2 = \frac{N_2N_3}{4} \tag{3.112}$$

is proportional to the number of giant intersections[10]. It is finite in the large N limit as expected, and agrees up to $-\epsilon$ with the near-BPS limit of the zero point energy (3.102) in the non-BPS case.

We conclude that $\Delta_{\rm IR}$ and $\mathcal{J}_{\rm IR}$ match the expected IR 2d CFT quantities (3.71 -3.72), up to the "volume factor" $\left(8\mu_2^0\mu_3^0\int d\mu_2 d\mu_3\right)$. This is further evidence for the argument that the 2d CFT dual to the near horizon AdS$_3$ geometry captures the dynamics of the sector of the $\mathcal{N}=4$ super Yang-Mills theory we have focussed on by taking a near-EVH near horizon limit.

3.7 A Check: Comparison with Kerr/CFT

In this section, we investigate the behaviour of the CFT data, i.e. central charges and Frolov-Thorne temperatures, provided by the Kerr/CFT correspondence described in section 1.5, and its extremal black hole extension [78], when the extremal horizon size vanishes. When the latter

[10] The number of giants corresponding to $\mathcal{J}_1$ is of order $N\epsilon^2$.

occurs, the AdS_2 near horizon responsible for the boundary conditions proposed in [79, 78] may disappear, giving rise to the local AdS_3 throats discussed in this note. We thus seek a connection between the 2d CFTs appearing in the EVH/CFT correspondence discussed in previous sections and the 2d chiral CFTs emerging in the Kerr/CFT correspondence described in section 1.5. As outlined in section 1.6, our perspective is that a 2d chiral CFT is the Discrete Light-Cone Quantization (DLCQ) of a standard 2d CFT [40]. To explore this perspective, we examine the Kerr/CFT Frolov-Thorne temperatures and central charges in the context of the family of embedded black holes (3.1). In the region of parameters where Kerr/CFT and EVH/CFT overlap, we can always derive one of the Kerr/CFT descriptions from the EVH/CFT.

We recall from 1.5 that the extremal black hole/CFT correspondence [78] applies to near horizon geometries of the form

$$\begin{aligned} ds^2 &= \tilde{A}\left(-\rho^2\,dt^2+\frac{d\rho^2}{\rho^2}\right)+\sum_{\alpha=1}^{n-1}F_\alpha\,dy_\alpha^2+\sum_{i,j=1}^{n-1+\epsilon}\tilde{g}_{ij}\,\tilde{e}_i\,\tilde{e}_j\,,\\ \tilde{e}_i &= d\phi_i+k_i\rho\,dt. \end{aligned} \tag{3.113}$$

When certain boundary conditions are applied to these near horizon geometries, one discovers that the asymptotic symmetry group includes a single Virasoro algebra extension for each of the compact U(1) isometries ∂_{ϕ_i} [38]. Their central charges equal [38]

$$c_i=\frac{6k_iS_{\rm BH}}{\pi}, \tag{3.114}$$

where $S_{\rm BH}$ stands for the entropy of the original *finite* extremal black hole. The application of Cardy's formula

$$S_{Cardy}=2\pi\sqrt{\frac{c_i}{6}\left(L_0^i-\frac{c_i}{24}\right)}=\frac{\pi^2}{3}c_iT_i=S_{\rm BH}, \tag{3.115}$$

always reproduces $S_{\rm BH}$ since the CFT temperature T_i equals

$$k_i=\frac{1}{2\pi T_i}\,,\qquad T_i=-\frac{T_H'^0}{\Omega_i'^0}\,,\quad\text{with}\quad T_H'^0\equiv\left.\frac{\partial T_{\rm H}}{\partial r_+}\right|_{r_+=r_0}\,,\qquad \Omega_i'^0\equiv\left.\frac{\partial\Omega_i}{\partial r_+}\right|_{r_+=r_0}\,, \tag{3.116}$$

where $T_H(r_+)$ and $\Omega_i(r_+)$ are the temperature and angular velocities on the outer horizon r_+ and r_0 stands for its extremal value.

Finite extremal R-charged AdS_5 black holes fit this discussion. Since these have three U(1) isometries describing independent rotations in S^5, there should exist three inequivalent chiral CFTs reproducing the black hole entropy. This system was analysed in [80], where the following Frolov-Thorne temperatures were computed

$$T_i=\frac{(r_0^2+q_i)^2(q_1q_2q_3+r_0^6)}{\pi\tilde{q}_i\,L\,r_0^7\,\sqrt{H_1H_2H_3(r_0)}}. \tag{3.117}$$

These fix the central charges through (3.114).

Given the emergence of local AdS_3 throats in these situations, we are interested in matching the AdS_3/CFT_2 dictionary to the limiting values of the Kerr/CFT predictions above and, whenever possible, interpret and justify the latter results in terms of the former. As we have seen, the large N scalings in the non-BPS (3.67) and near-BPS (3.80) scenarios render the respective AdS_3 and CFT_2 charges finite.

Taking the near-EVH limit: Since Kerr/CFT works for extremal finite size black holes, while EVH/CFT works for near-EVH black holes which can be extremal or non-extremal, we need to compare them in some region of parameter space where both apply. This can be achieved by restricting to the extremal excitations in the EVH/CFT side, i.e. when the BTZ geometry obtained in the near horizon limit of near-EVH black holes is an extremal BTZ, and considering the vanishing entropy limit in the Kerr/CFT side. The second step involves a singular limit. On the CFT side, this is because some of the Kerr/CFT central charges tend

to zero trying to reproduce the appearance of a vanishing geometric cycle to account for the vanishing entropy. On the bulk side, this is because of the non-commutativity between taking the near horizon limit of a near-EVH black hole and taking the near-EVH limit of the near horizon of an extremal finite horizon black hole. The two limit procedures lead to different geometries.

3.7.1 Non-BPS near-EVH regime

The Frolov-Thorne temperatures (3.117) in the near-EVH limit (3.21) with $x_+ = x_- = x_0$ are

$$T_1 = \frac{L\sqrt{\hat{q}_1}\epsilon}{x_0\pi(q_2q_3)^{\frac{1}{4}}}, \qquad T_2 = \frac{q_2^{\frac{1}{4}}\hat{q}_1L^5}{\pi\sqrt{q_3+L^2}q_3^{\frac{3}{4}}x_0^5\epsilon}, \qquad T_3 = \frac{q_3^{\frac{1}{4}}\hat{q}_1L^5}{\pi\sqrt{q_2+L^2}q_2^{\frac{3}{4}}x_0^5\epsilon}. \tag{3.118}$$

Extremality gives $M = 2\sqrt{\mathbf{V}\hat{q}_1q_2q_3}/L$, so $x_0^2 = L\sqrt{\frac{\hat{q}_1}{\mathbf{V}}}$ and we may compare T_1 to the left moving temperature in the extremal case

$$T_L = \frac{x_+ + x_-}{4\pi\ell_3} = \frac{x_0}{2\pi\ell_3} \tag{3.119}$$

to find that the two temperatures agree up to epsilon: $T_1 = \epsilon T_L$. Then we compute the leading terms in the Kerr/CFT central charges in the near-EVH limit

$$c_{\psi_1} = \frac{3q_2q_3N^2}{L^4\sqrt{\mathbf{V}}}, \qquad c_{\psi_2} = \frac{3\sqrt{\hat{q}_1q_2}q_3^{(3/2)}\sqrt{q_3+L^2}N^2\epsilon^2}{L^6\mathbf{V}^{(3/2)}}, \qquad c_{\psi_3} = \frac{3\sqrt{\hat{q}_1q_3}q_2^{(3/2)}\sqrt{q_2+L^2}N^2\epsilon^2}{L^6\mathbf{V}^{(3/2)}}. \tag{3.120}$$

In the large N scaling limit (3.67) we see that $c_i \sim \epsilon$ and $T_i \sim \epsilon^{-1}$. The corresponding CFTs thus have infinite mass gaps, and an infinitely high energy would be required to populate the levels.

Following [81], $\hat{\chi} = \epsilon\psi_1$ implies

$$c_{\hat{\chi}} = \epsilon c_{\psi_1}, \tag{3.121}$$

which is in exact agreement with the Brown Henneaux central charge (3.64). This is in accord with our proposal/vision for connecting Kerr/CFT and EVH/CFT: the chiral 2d CFT appearing in Kerr/CFT is the DLCQ of the one appearing in the EVH/CFT.

In the pinching CFT, the scaling of the quantities $c_{\psi_1} \sim N^2$, $T_1 \sim \epsilon$ can be interpreted as stating that the mass gap is being sent to zero and a very low energy would be required to populate the levels, in agreement with the discussions of section 1.7. We can translate these quantities to a CFT on a regular cylinder, where $c_{\hat{\chi}} \sim T_L \sim 1$, so that the mass gap and Frolov-Thorne temperature are finite.

Although it would be tempting to interpret the central charge $c_{\hat{\chi}}$ in terms of intersecting giant gravitons, the microscopic understanding of the non-BPS regime is not established.

Comment on the null self-dual orbifold: In (3.43), we identified a different near horizon limit giving rise to a different local AdS_3 throat, corresponding to the null self-dual orbifold. It is straightforward to see the central charge describing this throat is the same as in the previous discussion. The difference in scaling in the time coordinate and the absence of pinching are consistent with the chiral nature of the dual CFT description, which is identified with the one emerging in the limiting Kerr/CFT description. In this case, though, the absence of pinching suggests the surviving chiral sector is *not* decoupled. It is worth stressing the appearance of non-trivial gauge fields in the transverse dimensions. Note also the discussion in footnote 11. These are reminiscent of the deformations recently discussed in [82]. It would be interesting to understand the physics of these.

3.7.2 Near-BPS near-VH regime

The purpose of this section is to describe the limiting behaviour of the three CFTs that reproduce the entropy for extremal finite R-charged AdS_5 black holes in the near-BPS regime (3.26)

and to identify which one matches, if any, with the 2d CFT that one may associate with the near horizon AdS_3 geometry (3.54). Geometrically, it is expected the latter should correspond to the chiral CFT based on the Virasoro extension of the isometry direction along which giant gravitons intersect. Thus, one expects c_1 and T_1 to have different scaling behaviour from the two remaining Kerr/CFT descriptions.

Let us analyse the CFT temperatures first. The form for the inner and outer BTZ horizons (3.55) shows that at extremality $x_+ = x_- = x_0$ gives $\hat{\mu}_c = \frac{M^2}{4\hat{q}_1}$ and

$$x_0^2 = \frac{L^2}{R^2}\left(\frac{M}{2} + \hat{q}_1\right) \quad \Rightarrow \quad T_L = \frac{x_+ + x_-}{4\pi\ell_3} = \frac{1}{2\pi R}\frac{L}{R}\sqrt{\frac{M}{2} + \hat{q}_1}, \quad T_R = 0. \tag{3.122}$$

While the Frolov-Thorne temperatures scale like $T_i \sim \epsilon^{-1}$, when we compute the near-EVH expansion of the parameters in T_1 we find that it is in exact agreement with T_L,

$$T_1 = T_L. \tag{3.123}$$

The leading terms of the central charges in the near-BPS near-VH limit are

$$c_1 = \frac{3\hat{q}_2\hat{q}_3}{L^4}N^2\epsilon^2 = 3N_2N_3, \qquad c_i = \frac{3R^4(\frac{M}{2} + \hat{q}_1)}{L^4\hat{q}_i}N^2\epsilon^3. \tag{3.124}$$

where we used the quantisation conditions (3.11). c_1 agrees up to the "volume factor" with the Brown Henneaux central charge (3.70). It also agrees with the total number of giant intersections, independently of whether N is scaled, confirming our expectation that the surviving CFT is the one living on the intersection of giant gravitons.

Here, as in subsection 3.7.1, we see that the other two CFT descriptions break down as their central charges $c_i \sim \epsilon$ vanish and Frolov-Thorne temperatures $T_i \sim \epsilon^{-1}$ diverge.

We do not understand either in field theory or in gravitational terms, what the proper connection is between the description above and the one emerging in Kerr/CFT. We do want to emphasise that our approach insisted on taking a near horizon limit to study the IR properties of the *on-shell* system. In this near-BPS regime, this forced us to lose part of the degrees of freedom responsible for the full black hole entropy. Both the Kerr/CFT central charge c_1 and our near horizon analysis suggest the potential existence of a 2d CFT which is *not* intrinsically localised in the horizon. Similar observations have been made using low energy probes in (non-)extremal black holes [76, 77], without explicitly relying on the near horizon geometry.[11]

It would be very interesting to provide *any* technical evidence confirming the structures uncovered in gravity, along the lines of [83], by which the sector in $\mathcal{N} = 4$ super Yang-Mills theory may be equivalently described by a (non-)chiral CFT whose degrees of freedom should be the open strings stretched between giant gravitons.

3.8 Discussion

In this Chapter we studied aspects of Extremal Vanishing Horizon (EVH) black holes in the family of static R-charged AdS_5 black holes, envisioning that a generic black hole in this family can be understood as excitations above the EVH black hole. As discussed in section 1.8, generic non-BPS near-EVH black holes are defined as black holes with $A_{\rm H}, T_{\rm H}, G_N \to 0$ while the ratios $A_{\rm H}/T_{\rm H}$ and $A_{\rm H}/G_N$ remain finite, where $A_{\rm H}$ is the horizon area, $T_{\rm H}$ is the Hawking temperature and G_N is the Newton constant. We saw that near-BPS VH black holes have some other subtleties: the Hawking temperature is finite and as a result the near horizon limit required focussing on "strips" of the horizon. Despite these differences, we showed that in the near horizon limit of a generic EVH black hole one obtains an approximate AdS_3 throat, which is excited in the near-EVH limit to a BTZ black hole.

[11] If we start with a generic BPS or extremal black hole, take the near horizon limit first (as is done in [78, 38]) and then take the nearly vanishing horizon limit, as we have done in this section, we obtain a different geometry than when we first take the near-EVH black hole limit and then take the near horizon limit, as we did in sections 3.3.2 and 3.3.4. Nonetheless, despite having different geometries, as we have shown the entropies obtained in these two cases are equal.

We discussed that R-charged AdS_5 EVH black holes can be BPS or non-BPS and we have seen that the near horizon limit is only well-defined in the 10d uplift of the black hole, as the angular direction of the local AdS_3 geometry comes from the transverse S^5.

The appearance of the AdS_3 geometry in the near-BPS case required geometrically focussing on a strip of the S^5. In the non-BPS case this was not necessary, though the AdS_3 throat becomes a pinching orbifold of AdS_3, a feature seemingly generic to all non-BPS EVH black holes. We discussed the possibility to resolve the pinching orbifold using large N and large central charge limits.

As mentioned, in the near-BPS case the near-EVH sector of the dual four dimensional gauge theory has an interpretation in terms of stretched strings between giant gravitons. This interpretation compliments our results, which state that the excitations may be described by the CFT_2.

We applied our first law analysis of near-EVH black holes to these asymptotically AdS_5 black holes. The non-BPS case is compatible with the analysis of section 2.3 and the BTZ first law is extracted from the expansion of the 5d first law. Although near-BPS black holes do not undergo the near horizon limit (2.58) outlined in section 2.3, the first law reduces in the near-EVH limit to that of the BTZ black hole. It would be interesting to invesigate the derivation of a *generic* first law near-EVH expansion that reflects this result.

As we noted in section 1.8, the appearance of an approximate near horizon AdS_3 throat motivated the EVH/CFT proposal [51]: near-EVH black holes or low energy excitations around an EVH black hole is described by a subsector of a 2d CFT. Moreover, when dealing with asymptotic AdS_5 black holes, there is also a UV dual CFT ($\mathcal{N} = 4$ super Yang-Mills theory in this case). Based on the gravity picture we then proposed a relation between the IR and UV dual CFTs. Exploring and establishing this proposal further is an open interesting question.

We also discussed how the EVH/CFT and Kerr/CFT proposals are related to each other along the lines of discussions in [40, 44, 50, 84, 85]: The chiral CFT appearing in Kerr/CFT in the near-EVH locus in the parameter space corresponds to the DLCQ of the 2d CFT whose pinching orbifold limit appears in the EVH/CFT. This, together with our discussions here, can potentially be used to identify the microscopic degrees of freedom of the dual 2d CFT and it would be interesting to pursue this further.

The EVH black holes are not limited to static ones and can be stationary, e.g. the one considered in [51]. Within the class of asymptotic AdS_5 black holes we have a more general family of EVH black holes which involve rotation as well as R-charge. This class of charged-rotating AdS_5 EVH black holes will be studied in Chapter 4.

Chapter 4

Case Study II: Rotating Two Charged Black Holes

The following work was done in collaboration with M. M. Sheikh-Jabbari, J. Simón, and H. Yavartanoo, and is published in [66]. This Chapter is a lightly edited version of the published paper.

We extend the analysis of Chapter 3 to consider families of charged rotating asymptotically AdS_5 extremal black holes with vanishing horizon (EVH black holes) whose near horizon geometries develop locally AdS_3 throats. Using the AdS_3/CFT_2 duality, we propose an EVH/CFT_2 correspondence to describe the near-horizon low energy IR dynamics of near-EVH black holes involving a specific large N limit of the 4d $\mathcal{N}=4$ super Yang-Mills theory . We solidify our claims in Chapter 2 by demonstrating explicitly how the "UV first law" of thermodynamics reduces to the "IR first law" satisfied by the near horizon BTZ black holes in this near-EVH limit. We give a map between the UV and IR near-EVH excitations as further evidence of the EVH/CFT correspondence outlined in section 1.8. We also discuss the connection between our EVH/CFT proposal and the Kerr/CFT correspondence in the cases where the two overlap.

4.1 Rotating Two Charged Solutions to Type IIB Supergravity

The particular class of black holes considered here are solutions to the $U(1)^3$ 5d gauged supergravity whose bosonic action is [86]

$$S_{5d}=\frac{1}{16\pi G_5}\int d^5x\sqrt{-g}\ \Big(\mathcal{R}-\frac{1}{2}\partial\vec{\varphi}^2-\frac{1}{4}\sum_{i=1}^{3}X_i^{-2}\mathcal{F}_i^2+\frac{4}{\ell^2}\sum_{i=1}^{3}X_i^{-1}$$
$$+\frac{1}{4}\epsilon_{\mu\nu\rho\sigma\lambda}\mathcal{F}_1^{\mu\nu}\mathcal{F}_2^{\rho\sigma}\mathcal{A}_3^{\lambda}\Big), \tag{4.1}$$

where $\vec{u}=(u_1,u_2)$ and

$$X_1=e^{-\frac{1}{\sqrt{6}}u_1-\frac{1}{\sqrt{2}}u_2},\quad X_2=e^{-\frac{1}{\sqrt{6}}u_1+\frac{1}{\sqrt{2}}u_2},\quad X_3=e^{\frac{2}{\sqrt{6}}u_1}\,. \tag{4.2}$$

Its most general asymptotically AdS_5 black hole solutions include three electric charges, two angular momenta (spins) and mass. They form a six parameter family of solutions. The four parameter subclass of static black holes was constructed in [87]. The EVH black holes in this subclass, which are two-charge black holes, were studied in Chapter 3 and [34, 28].

In this work we consider black holes with two independent spins, mass and two equal R-charges, with the third R-charge a function of the remaining charges. These solutions were first

constructed in [88][1]. Their metrics are

$$\begin{aligned} ds^2 &= H^{-\frac{4}{3}}\Big[-\frac{X}{\rho^2}\,(dt - a\,\sin^2\theta\,\frac{d\phi}{\Xi_a} - b\,\cos^2\theta\,\frac{d\psi}{\Xi_b})^2 \\ &\quad + \frac{C}{\rho^2}(\,\frac{ab}{f_3}dt - \frac{b}{f_2}\sin^2\theta\frac{d\phi}{\Xi_a} - \frac{a}{f_1}\cos^2\theta\frac{d\psi}{\Xi_b})^2 \\ &+ \quad \frac{Z\sin^2\theta}{\rho^2}(\frac{a}{f_3}dt - \frac{1}{f_2}\frac{d\phi}{\Xi_a})^2 + \frac{W\cos^2\theta}{\rho^2}(\frac{b}{f_3}dt - \frac{1}{f_1}\frac{d\psi}{\Xi_b})^2\Big] + H^{\frac{2}{3}}\,(\frac{\rho^2}{X}dr^2 + \frac{\rho^2}{\Delta_\theta}d\theta^2\,)\,, \end{aligned} \tag{4.3}$$

gauge and scalar fields

$$\begin{aligned} \mathcal{A}^1 &= \mathcal{A}^2 = P_1(dt\,-\,a\,\sin^2\theta\,\frac{d\phi}{\Xi_a}\,-\,b\cos^2\,\theta\,\frac{d\psi}{\Xi_b}) \\ \mathcal{A}^3 &= P_3(b\,\sin^2\theta\,\frac{d\phi}{\Xi_a}\,+\,a\,\cos^2\theta\,\frac{d\psi}{\Xi_b}) \\ X_1 &= X_2 = H^{-\frac{1}{3}}, \quad X_3 = H^{\frac{2}{3}}\,, \end{aligned} \tag{4.4}$$

where

$$\begin{aligned} H &= \tilde{\rho}^2/\rho^2, \quad \rho^2 = r^2\,+\,a^2\,\cos^2\theta\,+\,b^2\,\sin^2\theta, \quad \tilde{\rho}^2 = \rho^2\,+\,q\,, \\ f_1 &= a^2\,+\,r^2, \quad f_2 = b^2\,+\,r^2, \quad f_3 = (a^2+r^2)(b^2+r^2)\,+qr^2; \\ \Delta_\theta &= 1 - \frac{a^2}{\ell^2}\,\cos^2\theta - \frac{b^2}{\ell^2}\,\sin^2\theta, \\ X(r) &= \frac{1}{r^2}(a^2+r^2)(b^2+r^2) - 2m + (a^2+r^2+q)(b^2+r^2+q)/\ell^2\,, \\ C &= f_1\,f_2(X\,+\,2m\,-q^2/\rho^2), \\ Z &= -b^2\,C\,+\,\frac{f_2\,f_3}{r^2}[f_3\,-\frac{r^2}{\ell^2}\,(a^2\,-b^2)(a^2+r^2+q)\cos^2\theta], \\ W &= -a^2\,C\,+\,\frac{f_1\,f_3}{r^2}[f_3\,+\frac{r^2}{\ell^2}\,(a^2\,-b^2)(b^2+r^2+q)\sin^2\theta]\,, \\ \Xi_a &= 1 - \frac{a^2}{\ell^2}\,, \qquad \Xi_b = 1 - \frac{b^2}{\ell^2},, \qquad P_1 = \frac{\sqrt{q^2+2mq}}{\tilde{\rho}^2}\,, \qquad P_3 = \frac{q}{\rho^2}. \end{aligned} \tag{4.5}$$

This family of solutions is specified by four parameters (a, b, q, m). The metric (4.3) is written in an asymptotically *rotating* frame (ARF). The coordinate transformation

$$\phi^S = \phi + \frac{a}{\ell^2}\,t\,, \qquad \psi^S = \psi + \frac{b}{\ell^2}\,t \tag{4.6}$$

brings it to the asymptotically *static* frame (ASF), where it is manifestly the AdS_5 metric with radius ℓ in the standard global coordinate system.

Charges and thermodynamics: Whenever the equation $X(r) = 0$ allows real positive solutions, the configurations (4.3) describe a family of black holes. This is discussed in detail in Appendix 4.A in the regime of charges we are interested in this chapter. In the following, we review their charges and thermodynamics.

The angular momenta and electric charges of the family of black hole solutions can be evaluated using Komar and Gauss integrals respectively [38],

$$J_a = \frac{\pi a\,(2m + q\,\Xi_b)}{4G_5\Xi_b\,\Xi_a^2}\,, \qquad J_b = \frac{\pi b\,(2m + q\,\Xi_a)}{4G_5\Xi_a\,\Xi_b^2}\,, \tag{4.7}$$

$$Q_1 = Q_2 = \frac{\pi\sqrt{q^2+2mq}}{4G_5\Xi_a\,\Xi_b}\,, \quad Q_3 = -\frac{\pi abq}{4G_5\ell^2\Xi_a\,\Xi_b}\,. \tag{4.8}$$

[1]The most general six-parameter solution to this theory was constructed in [89].

The minus sign of Q_3 may seem strange, but we highlight here that it is *not* an independent conserved charge, as it is proportional to both J_a and J_b. An explicit computation of Q_3 may be found in Appendix 4.B. Note that $J_a = J_\phi$ and $J_b = J_\psi$ are the standard angular momentum associated with rotations along the ϕ and ψ angles in the 3-sphere. We saw in section 2.1 that the horizon structure determines the thermodynamic properties of the black hole. Its temperature can be computed through the horizon surface gravity, leading to

$$T_{\rm H} = \frac{2r_+^6 + r_+^4(\ell^2 + a^2 + b^2 + 2q) - a^2b^2\ell^2}{2\pi r_+ \ell^2[(r_+^2 + a^2)(r_+^2 + b^2) + qr_+^2]}\,, \tag{4.9}$$

while the Bekenstein–Hawking entropy is proportional to the area of the black hole horizon,

$$S_{\rm BH} = \frac{\pi^2[(r_+^2 + a^2)(r_+^2 + b^2) + qr_+^2]}{2G_5\Xi_a\Xi_b r_+}\,. \tag{4.10}$$

The outer horizon ($r = r_+$) is the Killing horizon generated by the Killing vector field

$$\xi_\Omega = \partial_t + \Omega_a^S \partial_{\phi^S} + \Omega_b^S \partial_{\psi^S}, \tag{4.11}$$

where Ω_a^S and Ω_b^S stand for the angular velocities on the horizon in the ASF [88]

$$\Omega_a^S = \frac{a(r_+^4 + r_+^2 b^2 + r_+^2 q + \ell^2 b^2 + \ell^2 r_+^2)}{\ell^2(a^2 + r_+^2)(b^2 + r_+^2) + \ell^2 q r_+^2}, \quad \Omega_b^S = \frac{b(r_+^4 + r_+^2 a^2 + r_+^2 q + \ell^2 a^2 + \ell^2 r_+^2)}{\ell^2(a^2 + r_+^2)(b^2 + r_+^2) + \ell^2 q r_+^2}. \tag{4.12}$$

The same angular velocities in the ARF equal $\Omega_a^R = \Omega_a^S - \frac{a}{\ell^2}$ and $\Omega_b^R = \Omega_b^S - \frac{b}{\ell^2}$, calculated by demanding that the Killing vector field (4.11) is invariant under diffeomorphisms:

$$\xi_\Omega = \partial_t + \Omega_a^R \partial_\phi + \Omega_b^R \partial_\psi. \tag{4.13}$$

The electrostatic potentials Φ_i associated to the electric charges can be computed through the definition $\Phi_i = \xi_\Omega^\mu \mathcal{A}_\mu^i|_{r=r_+}$. One finds

$$\Phi_1 = \Phi_2 = \frac{\sqrt{q^2 + 2mq}\, r_+^2}{(a^2 + r_+^2)(b^2 + r_+^2) + qr_+^2}, \qquad \Phi_3 = \frac{qab}{(a^2 + r_+^2)(b^2 + r_+^2) + qr_+^2}\,. \tag{4.14}$$

These values are invariant under the change of frame (4.6), as the effect of this shift in the gauge fields (4.4) is compensated by the redefinition of the Killing vector (4.11).

The mass of these black holes can be determined by integrating the first law of thermodynamics

$$T_{\rm H}\, dS_{\rm BH} = dE - \Omega_a\, dJ_a - \Omega_b\, dJ_b - \sum_{i=1}^{3} \Phi_i\, dQ_i, \tag{4.15}$$

giving rise to

$$E = \frac{\pi[2m(2\Xi_a + 2\Xi_b - \Xi_a\,\Xi_b) + q(2\Xi_a^2 + 2\Xi_b^2 + 2\Xi_a\,\Xi_b - \Xi_a^2\,\Xi_b - \Xi_b^2\,\Xi_a)\,]}{8G_5\Xi_a^2\,\Xi_b^2}\,. \tag{4.16}$$

The BPS black holes among the family (4.3), with energy E a linear combination of the electric charges and angular momenta, [38, 88, 96] parametrically satisfy the condition

$$m = \frac{q(a + b)(a + b + 2\ell)}{2\ell^2}, \tag{4.17}$$

and the generic BPS solutions in this class preserve 1/4 of the supersymmetries of the original theory, i.e. two (out of eight) real supercharges [38, 71].

Embedding in type IIB supergravity: All solutions to (4.1) can be uplifted to on-shell 10 dimensional type IIB supergravity solutions using the ansatz [70]

$$ds_{10}^2 = \sqrt{\widetilde{\Delta}}\, ds_5^2 + \frac{\ell^2}{\sqrt{\widetilde{\Delta}}} \sum_{i=1}^{3} X_i^{-1} (d\mu_1^2 + \mu_i^2 (d\psi_i + \mathcal{A}^i/\ell)^2), \tag{4.18}$$

with X_i as in (4.5), μ_i are functions parameterising a unit 2-sphere

$$\mu_3 = \cos\alpha\,, \qquad \mu_2 = \sin\alpha \sin\beta\,, \qquad \mu_1 = \sin\alpha\cos\beta\,, \quad \alpha, \beta \in [0, \frac{\pi}{2}] \tag{4.19}$$

and

$$\widetilde{\Delta} = \sum_{i=1}^{3} X_i \mu_i^2 = H^{-\frac{1}{3}}(\mu_1^2 + \mu_2^2) + H^{\frac{2}{3}} \mu_3^2\,. \tag{4.20}$$

The 10d metric (4.18) is a solution of IIB supergravity with constant dilaton ϕ, where $e^{\phi} = g_s$, and selfdual RR-fiveform field [70].

Recalling that $G_{10} = 8\pi^6 g_s^2 \ell_s^8$ and performing a standard compactification over the 5-sphere, we learn that the 5d Newton's constant equals

$$G_5 = G_{10} \frac{1}{\pi^3 \ell^5} = \frac{\pi}{2} \frac{\ell^3}{N^2}\,, \tag{4.21}$$

where N is the 5-sphere RR five-form flux and ℓ its radius $\left(\ell^4 = 4\pi g_s \ell_s^4\, N\right)$. Thus, all black hole charges scale like N^2.

The 10d perspective allows to reinterpret the 5d electrostatic potentials Φ_i and electric charges Q_i as angular velocities Ω_i and angular momenta J_i on the transverse S^5. Due to the conventions in (4.18), their relation is

$$\Omega_i = -\frac{\Phi_i}{\ell}\,, \qquad J_i = -\ell Q_i\,. \tag{4.22}$$

As in 5d, all 10d angular velocities can be computed by requiring the vanishing of the norm of the Killing vector field $\xi_\Omega = \partial_t + \Omega_a^S \partial_{\phi^S} + \Omega_b^S \partial_{\psi^S} + \Omega_i \partial_{\psi_i}$ at the outer horizon.

Four dimensional $\mathcal{N} = 4$ super Yang-Mills theory description: Like the black holes analysed in Chapter 3, the black holes (4.3) correspond to thermal states in the dual $\mathcal{N} = 4$ super Yang-Mills theory defined on $\mathbb{R}\times S^3$ carrying charges :

$$\begin{aligned} \Delta_{\rm UV} = \ell E\,, \qquad \mathcal{J}_1 = \mathcal{J}_2 = Q_1 = \frac{\sqrt{q^2 + 2mq}}{2\ell^2 \Xi_a \Xi_b} N^2\,, \\ \mathcal{S}_a = J_a = \frac{a(2m + q\Xi_b)}{2\ell^3 \Xi_a^2 \Xi_b} N^2\,, \qquad \mathcal{S}_b = J_b = \frac{b(2m + q\Xi_a)}{2\ell^3 \Xi_b^2 \Xi_a} N^2\,. \end{aligned} \tag{4.23}$$

As usual, energy E becomes conformal dimension $\Delta_{\rm UV}$, angular momenta J_a, J_b SO(4) spins $\mathcal{S}_a$, $\mathcal{S}_b$ and the electric charges Q_i, R-charges $\mathcal{J}_i$. By construction, these are functions of the four parameters (a, b, q, m) and scale like N^2.

Intersecting giant description: The black holes in this class have an analogous giant graviton description to those introduced in Chapter 3. Their world-volumes reside on two three cycles on the S^5, intersecting on a circle parameterised by ψ_3 in our coordinates. These giant gravitons are rotating on the ψ_1 and ψ_2 directions which are transverse to their world-volume; the electric charges correspond to the angular momenta of the giants in each stack. The number of giants in each stack is then given [72] by the $q_2 = q_3 = q$ case of (3.11),

$$N_1 = N_2 = \frac{2\mathcal{J}_1}{N}\,. \tag{4.24}$$

As we see for generic values of the a, b, q parameters the number of giants in each stack grows as N, and hence we are dealing with a system of order N^2 giants.

We should comment that the intersecting giant graviton picture is a good one if we are close to a BPS point, where moving slightly away from that would correspond to turning on excitations (deformations) on the giant graviton world-volume. In this picture the spins $J_a,\ J_b$ would correspond to rotating the giant on the $S^3 \subset AdS_5$. (Recall that each giant is already rotating on a circle in S^5.)

4.2 The Set of EVH and Near-EVH Black Holes

4.2.1 EVH black holes

Consider the four dimensional black hole parameter space, either in terms of (a, b, q, m) or (a, b, q, r_+). We are physically defining the subset of EVH configurations as a limit of near-extremal black holes in which $A_{\rm H}\,, T_{\rm H} \sim \epsilon \to 0$, keeping $A_{\rm H}/T_{\rm H}$ *finite* as discussed in section 1.8. Inspection of (4.9) and (4.10) reveals

$$A_{\rm H}, T_{\rm H} \sim \epsilon \to 0 \quad \Rightarrow \quad r_+ \sim \epsilon\,, \quad a \sim \epsilon^\alpha\,, \quad b \sim \epsilon^\beta,\ \beta \geq \alpha \geq 0,\ \alpha + \beta \geq 2\,. \tag{4.25}$$

where we used the $a \leftrightarrow b$ exchange symmetry to assume $b \leq a$. This is the most general configuration for $r_+ = \mathcal{O}(\epsilon)$ when $q = \mathcal{O}(1)$.. Thus, EVH black holes require

$$\boxed{r_+ = 0 \quad \text{and} \quad ab = 0\,.} \tag{4.26}$$

These describe a *bifurcate hypersurface*, corresponding to the $a = 0$ or $b = 0$ branches. Since $b \leq a$, we shall focus on the $b = 0$ branch. Requiring $X(r_+ = b = 0)$ to vanish, ensuring the presence of a horizon, gives rise to the further constraint

$$m = \frac{q^2 + a^2(\ell^2 + q)}{2\ell^2}\,. \tag{4.27}$$

In the following, we shall distinguish between two types of EVH configurations:

$$\textbf{Static}: \quad a = b = r_+ = 0 \qquad \text{and} \qquad \textbf{Rotating}: \quad b = r_+ = 0,\ \ a \neq 0\,. \tag{4.28}$$

The static *EVH configuration* corresponds to the $(q_1, q_2, q_3; \mu) = (0, q, q, \mu)$ configuration of Chapter 3 as the subspace spanned here by (m, q) is related to the subspace spanned in Chapter 3 by (μ, q) by the map $(m, q) = (\mu/2, q)$. We will see though that as the full parameter space of the rotating black holes is manifestly different to that of the three-charged black holes Chapter 3, its *near-EVH deformation* describes a different set of black holes. In figure 4.1, we illustrate the space of EVH configurations, where we already took into account that $q \geq 0$ and $|a|, |b| \leq \ell$. Static configurations correspond to the q-axis at $a = 0$ with $2m = q^2/\ell^2$, whereas rotating ones correspond to generic $a \neq 0$ points with m given by (4.27). Among the rotating BPS EVH black holes we have quarter-BPS configurations specified by $q = a\ell,\ b = 0$, or $q = b\ell,\ a = 0$.

4.2.2 Near-EVH black holes

To explore the physics of near-EVH black holes, we describe regions in parameter space close to the EVH hypersurface. Equivalently to the static case study in Chapter 3, given a generic $b = 0$ EVH point parameterised by (4.27), one can decompose the space of deformations into *tangential* and *orthogonal*. The first correspond to

$$m + \delta m = \frac{(q + \delta q)^2 + (a + \delta a)^2(\ell^2 + q + \delta q)}{2\ell^2}\,. \tag{4.29}$$

These tangential deformations take us from one EVH black hole to a different one on the EVH hyperplane. Orthogonal deformations correspond to excitations of an EVH black hole, giving rise to near-EVH black holes. We will study the two cases separately.

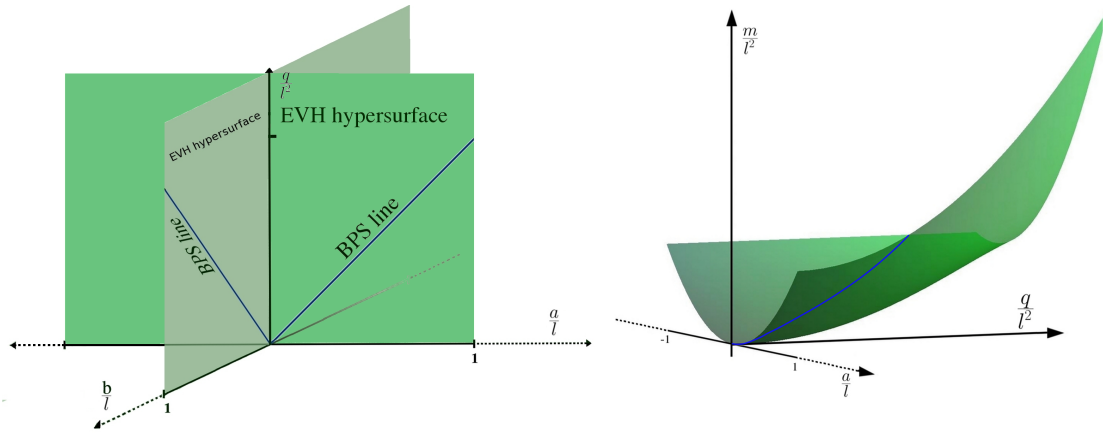

Figure 4.1: *Bifurcate EVH hyperplane.* The left figure shows the EVH hyperplane in (a, b, q) space. The $a = b = 0$ q axis stands for static EVH black holes, while $b = 0$, $a \neq 0$ points correspond to rotating EVH black holes. The subset of EVH BPS configurations, which occur for $q = \ell a$, $b = 0$ or $q = b\ell, a = 0$, are indicated by 45° lines. The right figure shows the $b = 0$ branch of the EVH hyperplane in $(a, q; m)$ space.

Near-EVH nearly-static black holes: Static EVH configurations are described by $(a, b, q; m) = (0, 0, q; q^2/2\ell^2)$ and hence the most general orthogonal deformation is

$$\left(0, 0, q; \frac{q^2}{2\ell^2}\right) \qquad \longrightarrow \qquad \left(\delta a, \delta b, q - \frac{q}{\ell^2}\delta m; \frac{q^2}{2\ell^2} + \delta m\right) . \tag{4.30}$$

Recalling (4.25), one can choose $\delta m \sim \epsilon^2$, $\delta a \sim \epsilon^\alpha, \delta b \sim \epsilon^\beta$ where $\beta \geq \alpha > 0$, $\alpha + \beta \geq 2$. Demanding to have a black hole, i.e. $X(r) = 0$ to have real positive solutions, implies $\alpha \geq 1$. One may hence choose,

$$\delta m = M\epsilon^2 , \quad \delta a = \hat{a}\epsilon , \quad \delta b = \hat{b}\epsilon , \tag{4.31}$$

where $\hat{a}$, $\hat{b}$ are either finite or may go to zero in some positive power of ϵ. Thus, the most general physical excitations of static EVH black holes are described by the three parameters $M, \hat{a}, \hat{b}$, corresponding to nearly-static black holes. This is consistent with the co-dimension three of the EVH surface describing the static case (4.28), as depicted in figure 4.1.

Once these deformations are turned on, the equation determining the horizon location $X(r_\pm) = 0$ becomes

$$\mathbf{V}_s \left(\frac{r}{\epsilon}\right)^4 - \left[2\mathbf{W}_s M - \mathbf{Y}_s(\hat{a}^2 + \hat{b}^2)\right] \left(\frac{r}{\epsilon}\right)^2 + \hat{a}^2\hat{b}^2 = 0 , \tag{4.32}$$

with

$$\mathbf{V}_s = 1 + \frac{2q}{\ell^2} , \qquad \mathbf{W}_s = 1 + \frac{q^2}{\ell^4} , \qquad \mathbf{Y}_s = 1 + \frac{q}{\ell^2} . \tag{4.33}$$

This ensures both $r_\pm \sim \epsilon$ as required in (4.25). In this limit one can work out the temperature (4.9) and entropy (4.10)

$$S_{\rm BH} = \pi N^2 \frac{q}{\ell^2}\frac{r_+}{\ell} , \qquad T_{\rm H} = \frac{(1 + \frac{2q}{\ell^2}) - \frac{\hat{a}^2\hat{b}^2}{r_+^4}}{2\pi q} r_+ = \frac{\mathbf{V}_s}{2\pi q}\frac{r_+^2 - r_-^2}{r_+} , \tag{4.34}$$

where we used $r_+^2 r_-^2 = \mathbf{V}_s^{-1} a^2 b^2$, which follows from (4.32). By construction, as advocated in section 1.8, $A_{\rm H} \sim T_{\rm H} \sim r_\pm \sim \epsilon$.

Near-EVH rotating black holes: Using $m(a,q)$ in (4.27), rotating EVH configurations are described by $(a,0,q;m(a,q))$. Their most general orthogonal deformation is hence

$$(a,0,q;m) \quad \longrightarrow \quad \left(a - a\left(1+\frac{q}{\ell^2}\right)\frac{\delta m}{\ell^2}, \delta b, q - \left(q+\frac{1}{2}a^2\right)\frac{\delta m}{\ell^2}; m+\delta m\right) . \tag{4.35}$$

For finite a, q, the scaling (4.25) requires

$$\delta b = \hat{b}\epsilon^2 \ , \quad \delta m = M\epsilon^2 \, . \tag{4.36}$$

Unlike the static EVH case, the most general excitations of a rotating EVH black hole are described by two parameters, $M, \hat{b}$. This is consistent with the co-dimension two surfaces defining them in (4.28), as shown in figure 4.1.

These deformation parameters determine the location of the horizons

$$\mathbf{V}\left(\frac{r}{\epsilon}\right)^4 - 2\mathbf{W}M\left(\frac{r}{\epsilon}\right)^2 + a^2\hat{b}^2 = 0 \tag{4.37}$$

with

$$\mathbf{V} = 1 + \frac{2q}{\ell^2} + \frac{a^2}{\ell^2}, \qquad \mathbf{W} = 1 + \left(\frac{q}{\ell^2} + \frac{a^2}{2\ell^2}\right)^2 + \frac{a^2}{\ell^2}\left(1+\frac{q}{\ell^2}\right)^2 . \tag{4.38}$$

Notice its $a \to 0$ limit does *not* reproduce the nearly-static equation (4.32). This is because the near-EVH scaling of b with ϵ is different from the nearly-static case in (4.31) and, more importantly, because there exists a non-commuting order of limits between taking a near horizon limit and considering the $a \to 0$ limit, as we shall explicitly see in section 4.3.4. For these reasons, we will study the (nearly-)static and rotating cases separately in the following, noting when the former can be obtained as a limit of the latter.

It is reassuring that whenever the parameters $\{a, q; \hat{b}, M\}$ allow real roots $r_\pm$[2], the entropy and temperature of these near-EVH black holes equal

$$S_{\rm BH} = \pi N^2 \frac{q+a^2}{\ell^2 \Xi_a}\frac{r_+}{\ell} \, , \qquad T_{\rm H} = \frac{(1+\frac{2q+a^2}{\ell^2}) - \frac{a^2\hat{b}^2}{r_+^4}}{2\pi(q+a^2)} r_+ = \frac{\mathbf{V}}{2\pi(q+a^2)}\frac{r_+^2 - r_-^2}{r_+} \, . \tag{4.39}$$

By construction, the ratio $S_{\rm BH}/T_{\rm H}$ is finite. Notice these equations reproduce (4.34) when written as a function of $r_\pm$ at $a = 0$.

We stress expressions (4.39) resemble the analogue quantities for BTZ black holes, i.e. $S_{\rm BTZ} = \frac{\pi r_+}{2G_3}$ and $T_{\rm BTZ} = \frac{r_+^2 - r_-^2}{2\pi\ell_3^2 r_+}$. In fact, we will see in the coming sections that the near horizon of these configurations develops a locally AdS_3 throat. The corresponding 3d Newton's constant G_3 and AdS_3 radius ℓ_3 will be such that this analogy will become an equality.

4.3 Near Horizon Geometry Analysis: Rotating Two Charged Black Holes

In this section we study the near horizon geometries corresponding to the static and rotating EVH black holes identified in (4.28) together with their near-extremal versions (4.30)-(4.35).

[2]For a thorough analysis on when this occurs, see Appendix 4.A.

4.3.1 The static EVH near horizon geometry

Let us consider a static EVH black hole ($a = b = 0$) and study its deep interior geometry by expanding in small ϵ for $r = \epsilon\rho$. The metric expansion is

$$\begin{aligned} ds^2 = \frac{q\ell^2\mu_3}{\ell^2+2q}\bigg[-\frac{\mathbf{V}_s^2\epsilon^2}{q^2}\rho^2 dt^2 + \frac{d\rho^2}{\rho^2} + \frac{\ell^2\mathbf{V}_s^2\epsilon^2}{q^2}\rho^2 d\psi_3^2\bigg] \\ + q\mu_3\bigg(d\theta^2 + \sin^2\theta d\phi^2 + \cos^2\theta d\psi^2\bigg) + \frac{\ell^2(d\mu_1^2+d\mu_2^2)}{\mu_3} \\ + \frac{\ell^2\mu_1^2}{\mu_3}\left(d\psi_1 - \Omega_1^{(0)}dt\right)^2 + \frac{\ell^2\mu_2^2}{\mu_3}\left(d\psi_2 - \Omega_2^{(0)}dt\right)^2 . \end{aligned} \tag{4.40}$$

As we have seen in Chapter 3, extremality determines the scaling $-\epsilon^2\rho^2\ dt^2$ together with $d\rho^2/\rho^2$ giving rise to an AdS_2 throat responsible for the $SO(2,1)$ isometry enhancement of the near horizon geometry [37]. Again, the vanishing one-cycle along ψ_3 is the isometry direction in the 5-sphere with vanishing R-charge ($J_3 = 0$), and the standard AdS_2 throat is transformed into a local AdS_3 throat. We note that, even though $J_a = J_b = 0$, the cycles along ∂_ϕ and ∂_ψ remain of *finite* size.

The near horizon geometry is obtained by considering the limit

$$\psi_i = \hat{\psi}_i + \Omega_i^{(0)}\ t,\ (i=1,2) \quad t = \frac{\ell}{\sqrt{q}}\frac{\tau}{\epsilon}, \quad \psi_3 = -\frac{\hat{\chi}}{\epsilon}, \quad r = \epsilon\frac{\sqrt{q}}{\ell}x\,, \tag{4.41}$$

on the original black hole metric (4.18), with

$$\Omega_1^{(0)} = \Omega_2^{(0)} = -\frac{1}{\ell}\sqrt{1+\frac{q}{\ell^2}} = -\frac{\sqrt{\mathbf{Y}_s}}{\ell}\,, \tag{4.42}$$

being the horizon angular velocity at the EVH point. The resulting metric is

$$\begin{aligned} ds^2 = \mu_3\bigg[-\frac{x^2 d\tau^2}{\ell_3^2} + \frac{\ell_3^2 dx^2}{x^2} + x^2 d\hat{\chi}^2\bigg] + q\mu_3\bigg(d\theta^2 + \sin^2\theta d\phi^2 + \cos^2\theta d\psi^2\bigg) \\ + \frac{\ell^2}{\mu_3}(d\mu_1^2 + d\mu_2^2 + \mu_1^2 d\hat{\psi}_1^2 + \mu_2^2 d\hat{\psi}_2^2)\,. \end{aligned} \tag{4.43}$$

Due to the $2\pi\epsilon$ periodicity in $\hat{\chi}$, this geometry describes a warped locally $AdS_3\times S^3$ geometry, with radii given by

$$R_{AdS_3}^2 = \ell_3^2 = \frac{q}{\mathbf{V}_s}\,, \qquad R_{S^3}^2 = q\,. \tag{4.44}$$

More precisely, the local AdS_3 throat is the *pinching* AdS_3 orbifold introduced in section 1.7, corresponding to the near horizon of a massless BTZ black hole[3]. Once more, notice how the circle in AdS_3 comes from the direction in the 5-sphere where there is no R-charge at the EVH point. Besides the pinching, which does not introduce a curvature singularity, the geometry (4.41) is otherwise everywhere smooth except at $\mu_3 = 0$.

As the EVH configuration coincides with the $q_1 = 0$, $q_2 = q_3 = q$ subset of the non-BPS case in section 3.2, it is not surprising that (4.43) coincides with the $q_2 = q_3 = q$ limit of (3.33).

4.3.2 The nearly-static near-EVH near horizon geometry

Near-EVH nearly-static black holes are described in parameter space by (4.30). These are excitations of the static EVH vacua. Hence, one expects them to be encoded in the near-horizon geometry as *pinching* BTZ black holes [44], that is, BTZ black holes built on the pinching AdS_3 orbifolds of section 1.7. Indeed, as discussed in more detail in section 4.6.1, these excitations are described by the mass and angular momentum of the pinching BTZ with the possible addition of constant electric and magnetic fields on the transverse 3-sphere, describing the J_a and J_b

[3]Massless BTZ black holes allow for a second near horizon limit giving rise to the *null self-dual* orbifold. This near horizon limit is oulined in Appendix 4.C.

rotations.

These expectations are verified when we combine the near horizon limit (4.41) with the angular coordinate redefinitions

$$\hat{\phi} = \phi - \frac{\hat{a}}{q}\frac{\ell}{\sqrt{q}}\tau - \frac{\hat{b}\ell}{q}\hat{\chi} = \phi^S - \frac{\hat{a}\ell}{q\sqrt{q}}\mathbf{Y}_s\tau - \frac{\hat{b}\ell}{q}\hat{\chi}\,, \tag{4.45}$$

$$\hat{\psi} = \psi - \frac{\hat{b}}{q}\frac{\ell}{\sqrt{q}}\tau \; - \frac{\hat{a}\ell}{q}\hat{\chi} \; = \psi^S - \frac{\hat{b}\ell}{q\sqrt{q}}\mathbf{Y}_s\tau - \frac{\hat{a}\ell}{q}\hat{\chi}, \tag{4.46}$$

where we have used (4.6). These shifts are the ones defined (2.63) in Chapter 2, where the following identifications have been made:

$$\varphi_1 = \hat{\phi}^S, \qquad \phi_1 = \phi^S, \qquad A_a = \frac{\hat{a}\ell}{q\sqrt{q}}\mathbf{Y}_s\epsilon, \qquad B_a = \frac{\hat{b}\ell}{q}\epsilon, \tag{4.47}$$

and

$$\varphi_2 = \hat{\psi}^S, \qquad \phi_2 = \psi^S, \qquad A_b = \frac{\hat{b}\ell}{q\sqrt{q}}\mathbf{Y}_s\epsilon, \qquad B_b = \frac{\hat{a}\ell}{q}\epsilon. \tag{4.48}$$

The resulting near horizon metric is

$$\begin{aligned} ds^2 = \mu_3\Big[&- \frac{(x^2-x_+^2)(x^2-x_-^2)}{\ell_3^2 x^2}d\tau^2 + \frac{\ell_3^2 x^2 dx^2}{(x^2-x_+^2)(x^2-x_-^2)} + x^2(d\hat{\psi}_3 - \frac{x_+x_-}{\ell_3 x^2}d\tau)^2\Big] \\ &+ q\mu_3(d\theta^2 + \sin^2\theta d\hat{\phi}^2 + \cos^2\theta d\hat{\psi}^2) + \frac{\ell^2}{\mu_3}(d\mu_1^2 + d\mu_2^2 + \mu_1^2 d\hat{\psi}_1^2 + \mu_2^2 d\hat{\psi}_2^2) \end{aligned} \tag{4.49}$$

where $x_\pm$ are given in terms of (4.33) as

$$x_\pm^2 = \frac{\ell^2}{2q\mathbf{V}_s}\left(2\mathbf{W}_s M - \mathbf{Y}_s(\hat{a}^2+\hat{b}^2) \pm \sqrt{\Big(2\mathbf{W}_s M - \mathbf{Y}_s(\hat{a}^2+\hat{b}^2)\Big)^2 - 4\mathbf{V}_s\hat{a}^2\hat{b}^2)}\right). \tag{4.50}$$

Notice how the original pinching AdS_3 turned into a pinching BTZ metric[4]. The constant shifts in the AdS_3 boundary coordinates $\{\tau, \hat{\chi}\}$ in (4.45) corroborate the existence of constant electric and magnetic fields responsible for the UV spins $\mathcal{S}_a$ and $\mathcal{S}_b$.

We note here again that there is an order of limits between taking a near horizon limit and a near-BPS limit. Analogously to the static case (section 3.3.2), taking the near-BPS limit $q \sim \epsilon$ after the near horizon limit would result in a vanishing AdS_3 radius and divergent BTZ horizon radii.

Temperature & entropy: To use the standard thermodynamic relations satisfied by BTZ black holes, we must compactify (4.49) to three dimensions. Consider the ansatz

$$ds^2 = \mu_3\, g^{(3)}_{\mu\nu}dx^\mu dx^\nu + q\mu_3(d\theta^2 + \sin^2\theta d\hat{\phi}^2 + \cos^2\theta d\hat{\psi}^2) + \frac{\ell^2}{\mu_3}(d\mu_1^2 + d\mu_2^2 + \mu_1^2 d\hat{\psi}_1^2 + \mu_2^2 d\hat{\psi}_2^2),$$

and plug it into the 10d type IIB supergravity action. Focussing on its Einstein-Hilbert term

$$\frac{1}{16\pi G_{10}}\int\sqrt{-g_{(10)}}\left({}^{(10)}\mathcal{R} + \cdots\right) = \frac{1}{16\pi G_3}\int\sqrt{-g_{(3)}}\left({}^{(3)}\mathcal{R} + \cdots\right),$$

we can identify the 3d Newton's constant to be

$$\frac{1}{G_3} = \frac{q^{3/2}\ell^4}{16G_{10}}(2\pi)^4 = \frac{2q^{\frac{3}{2}}N^2}{\ell^4}\,. \tag{4.51}$$

[4]For the subset of excitations that preserve extremality, i.e. $x_+ = x_-$, there exists a second near horizon limit again giving rise to the null self-dual orbifold, discussed in Appendix 4.C.

Thus, the temperature and entropy of the pinching BTZ black holes (4.49) equal

$$\begin{aligned} T_{\rm BTZ} &\equiv \frac{x_+^2 - x_-^2}{2\pi x_+ \ell_3^2} = \frac{\ell}{\epsilon\sqrt{q}}\, T_{\rm H}\,, \\ S_{\rm BTZ} &\equiv \frac{2\pi\epsilon\cdot x_+}{4G_3} = S_{\rm BH}\,, \end{aligned} \tag{4.52}$$

where for $T_{\rm H}$ and $S_{\rm BH}$ we have used (4.34). As expected, the second matches the original 10d black hole entropy whereas the first agrees with the scaling of time in (4.41). This confirms the expectations raised in section 4.2, when interpreting the near-EVH temperature and entropy (4.34) as BTZ thermodynamical quantities.

4.3.3 The rotating EVH near horizon geometry

Consider a rotating EVH black hole ($b = 0$) and study its deep interior geometry by expanding in small ϵ for $r = \epsilon\rho$. The metric expansion is

$$\begin{aligned} ds^2 = {} & h_1 h_2 \left[-\frac{\mathbf{V}}{a^2+q}\epsilon^2\rho^2 dt^2 + \frac{a^2+q}{\mathbf{V}}\frac{d\rho^2}{\rho^2} + \frac{a^2+q}{a^2}\rho^2\epsilon^2 d\psi^2 \right] \\ & + \frac{(a^2+q)h_1h_2}{1-\frac{a^2}{\ell^2}\cos^2\theta}d\theta^2 + \frac{\ell^2 h_1}{h_2}(d\mu_1^2 + d\mu_2^2) + \frac{a^2\ell^2\cos^2\theta}{(a^2+q)h_1h_2}d\mu_3^2 + \frac{a^2\ell^2\cos^2\theta\mu_3^2}{h_1h_2}\left(\frac{q}{a\ell}d\psi + d\psi_3\right)^2 \\ & + \frac{\sin^2\theta\left[a^2\mathbf{Y}_s - \frac{a^2}{\ell^2}(a^2+q)\cos^2\theta + q\Xi_a\mu_3^2\right]}{\Xi_a^2 h_1 h_2}\left(d\phi - \Omega_a^{0R}dt\right)^2 \\ & - \frac{2a\ell\sqrt{q\mathbf{Y}_s}\,\sin^2\theta}{\Xi_a h_1 h_2\sqrt{a^2+q}}\left(d\phi - \Omega_a^{0R}dt\right)\left[\mu_1^2\left(d\psi_1 - \Omega_1^{(0)}dt\right) + \mu_2^2\left(d\psi_2 - \Omega_2^{(0)}dt\right)\right] \\ & + \ell^2\frac{h_1\mu_1^2}{h_2}\left(d\psi_1 - \Omega_1^{(0)}dt\right)^2 + \ell^2\frac{h_1\mu_2^2}{h_2}\left(d\psi_2 - \Omega_2^{(0)}dt\right)^2, \end{aligned} \tag{4.53}$$

where

$$\Omega_1^{(0)} = \Omega_2^{(0)} = -\frac{1}{\ell}\sqrt{\frac{q\mathbf{Y}_s}{a^2+q}}, \qquad \Omega_a^{(0)R} = \frac{a\Xi_a}{a^2+q} \tag{4.54}$$

are the horizon angular velocities at the EVH point, $\mathbf{V}$ is as in (4.38) and

$$h_1^2 = \frac{a^2\cos^2\theta + q}{a^2+q}\,, \qquad h_2^2 = \frac{a^2\cos^2\theta + q\mu_3^2}{a^2+q}\,. \tag{4.55}$$

As before, there is a single vanishing cycle responsible for the vanishing entropy and the emergence of a local AdS_3 throat. This corresponds to the isometry direction ∂_ψ along the 3-sphere in the asymptotic AdS_5. Notice that despite having vanishing J_b, J_3, rotating EVH black holes still have a single vanishing cycle, keeping the $\frac{q}{a\ell}d\psi + d\psi_3$ cycle finite. The relevance of this combination is physically understood noticing that

$$\Omega_b + \frac{a\ell}{q}\Omega_3 = 0 \tag{4.56}$$

(up to $\mathcal{O}(\epsilon^2)$) in the near-EVH limit (4.36), where (4.12), (4.22) and (4.14) have been used. Thus, there is *no* angular velocity along the U(1) defined by $\frac{q}{a\ell}d\psi + d\psi_3$. This point also brings up the question on the uniqueness of the near horizon U(1) describing the AdS_3 angular momentum. We briefly discuss this matter below.

Choice of IR U(1) **:** The previous discussion suggests to work with

$$\xi = C_1\left(\frac{q}{a\ell}\psi + \psi_3\right) \qquad \chi = C_2\psi + C_3\psi_3 \tag{4.57}$$

so that

$$\psi = C_1\chi - C_3\xi, \qquad \psi_3 = -C_1\frac{q}{al}\chi + C_2\xi. \tag{4.58}$$

We *fix*

$$C_1 = \frac{al}{\sqrt{a^2l^2+q^2}}, \tag{4.59}$$

and will comment on this choice later in the subsection. Ensuring that the volume spanned by the two angles is invariant requires

$$C_1\left(C_2 - C_3\frac{q}{al}\right) = 1 \Rightarrow C_2 = \frac{1}{C_1} + \frac{q}{a\ell}C_3. \tag{4.60}$$

After this digression, let us return to the near horizon geometry which is obtained by considering the limit[5]

$$\begin{aligned} &\psi_1 = \hat{\psi}_1 + \Omega_1^{(0)}\, t, \qquad \psi_2 = \hat{\psi}_2 + \Omega_2^{(0)}\, t, \qquad \phi = \hat{\phi} + \Omega_a^{(0)R}\, t\,, \\ &t = \frac{\lambda}{\epsilon}\tau\,, \qquad \chi = \frac{\hat{\chi}}{\epsilon}, \qquad r = \epsilon\frac{x}{\lambda}\,, \quad \left(\lambda = \sqrt{\frac{\ell^2(a^2+q)}{a^2\ell^2+q^2}}\right) \end{aligned} \tag{4.61}$$

on the original black hole metric resulting in

$$\begin{aligned} ds^2 = {} & h_1h_2\left[-\frac{x^2}{\ell_3^2}d\tau^2 + \frac{\ell_3^2dx^2}{x^2} + x^2d\hat{\chi}^2\right] \\ & + \frac{(a^2+q)h_1h_2}{\Delta_\theta}d\theta^2 + \frac{\ell^2\cos^2\alpha\cos^2\theta}{\lambda^2h_1h_2}d\xi^2 + \frac{a^2+q}{\Xi_a^2}\frac{h_2}{h_1^3}\Delta_\theta\sin^2\theta d\hat{\phi}^2 \\ & + \ell^2\frac{h_2}{h_1}d\alpha^2 + \ell^2\frac{h_1}{h_2}\sin^2\alpha d\beta^2 + \ell^2\frac{h_1}{h_2}\left[\mu_1^2(d\hat{\psi}_1 - Ad\hat{\phi})^2 + \mu_2^2(d\hat{\psi}_2 - Ad\hat{\phi})^2\right], \end{aligned} \tag{4.62}$$

where $\alpha,\beta,\theta \in [0,\pi/2]$, $\phi \in [0,2\pi]$, $\mu_1 = \sin\alpha\cos\beta$, $\mu_2 = \sin\alpha\sin\beta$ and

$$\Delta_\theta = 1 - \frac{a^2}{\ell^2}\cos^2\theta, \quad A = \frac{a\sqrt{q\mathbf{Y}_s}}{\ell\ell_3\Xi_a\sqrt{\mathbf{V}}}\frac{\sin^2\theta}{h_1^2}. \tag{4.63}$$

The first line in (4.62) is again conformal to a pinching AdS_3 orbifold with radius

$$\ell_3^2 = \frac{a^2+q}{\mathbf{V}} = \frac{a^2+q}{1+\frac{2q}{\ell^2}+\frac{a^2}{\ell^2}}, \tag{4.64}$$

which reduces to (4.44) in the static limit ($a = 0$). This metric solves the type IIB supergravity equations of motion with a constant dilaton and a RR 5-form. The analysis is very similar to that in [28].

Due to the ϵ scaling in χ, all dependence on C_3 is subleading. In fact, not only the near horizon metric (4.53), but also all physical observables are expected to be independent of C_3. We will see this explicitly in our analysis in the rest of this chapter.

Although the choice (4.59) was the natural candidate in our search for an AdS_3 throat, its value can in principle be arbitrary. An investigation into the impact of this choice is in Appendix 4.D.

Contrary to the static EVH case, which always requires a 10d uplift to have a well defined near horizon geometry, the rotating EVH one does allow a purely 5d description for the particular choice $\chi = \psi$. In this case, the entire pinching AdS_3 lies inside AdS_5. Its near horizon

[5]It is important to note that switching between the two frames does not affect the near horizon prescription $\phi^R = \hat{\phi}^R + \Omega^{R(0)}t$, as this translates to

$$\begin{aligned} \phi^S - \frac{a}{\ell^2}t &= \hat{\phi}^S + (\Omega^{S(0)} - \frac{a}{\ell^2})t \\ \phi^S &= \hat{\phi}^S + \Omega^{S(0)}t; \end{aligned}$$

and similarly for ψ^R.

geometry is presented in Appendix 4.E.

There are special values in parameter space that deserve special mention. For $q = 0$, one recovers Kerr AdS_5, $\xi = \psi_3$ and χ may be chosen entirely inside AdS_5. The BPS surface defined by $q = al$ has no special features compared to the generic case (4.62). Finally, the $a \to \ell$ limit (the edge of the EVH plane in figure 4.1) must be handled with care. Recent work [90] confirms the existence of a 2d chiral spectrum also in this case.

4.3.4 The rotating near-EVH near horizon geometry

Near-EVH rotating black holes are described by (4.36) in parameter space. Their near horizon geometry is obtained through the same limit (4.61) and gives rise to

$$\begin{aligned} ds^2 = h_1 h_2 \Bigg[& -\frac{(x^2-x_+^2)(x^2-x_-^2)}{\ell_3^2 x^2} d\tau^2 + \frac{\ell_3^2 x^2 dx^2}{(x^2-x_+^2)(x^2-x_-^2)} + x^2 \left(d\hat{\chi} - \frac{x_+ x_-}{\ell_3 x^2} d\tau \right)^2 \Bigg] \\ & + \frac{(a^2+q)h_1 h_2}{\Delta_\theta} d\theta^2 + \frac{\ell^2 \cos^2\alpha \cos^2\theta}{\lambda^2 h_1 h_2} d\xi^2 + \frac{a^2+q}{\Xi_a^2} \frac{h_2}{h_1^3} \Delta_\theta \sin^2\theta d\hat{\phi}^2 \\ & + \frac{\ell^2 h_2}{h_1} d\alpha^2 + \frac{\ell^2 h_1}{h_2} \sin^2\alpha d\beta^2 + \frac{\ell^2 h_1}{h_2} \left[\mu_1^2 (d\hat{\psi}_1 - A d\hat{\phi})^2 + \mu_2^2 (d\hat{\psi}_2 - A d\hat{\phi})^2 \right], \end{aligned} \tag{4.65}$$

where $\mu_1,\ \mu_2,\ h_1,\ h_2,\ \Delta_\theta,\ A$ in (4.19), (4.55) and (4.63), and $\alpha, \beta, \theta \in [0, \pi/2]$, $\phi \in [0, 2\pi]$.

The first line is conformal to pinching BTZ black holes in the region of the deformation parameter space where the outer and inner horizons $x_\pm$

$$x_\pm^2 = \lambda^2 \frac{r_\pm^2}{\epsilon^2} = \frac{\ell^2(a^2+q)}{q^2+a^2\ell^2} \left[\frac{\mathbf{W} M \pm \sqrt{\mathbf{W}^2 M^2 - \mathbf{V} a^2 \hat{b}^2}}{\mathbf{V}} \right], \tag{4.66}$$

exist. This holds for[6]

$$\mathbf{W}^2 M \geq \mathbf{V} a^2 \hat{b}^2.$$

Notice $\hat{b} = 0$ corresponds to a vanishing inner horizon, whereas $M = 0$ forces $\hat{b} = 0$, in this region of parameters. Thus M controls the size of the outer horizon. Notice how the outer and inner horizons of the near-EVH static black hole in (4.50) cannot be obtained as a limit of the ones for the rotating case in (4.66). As stressed in section 4.2.2, this is due to the fact that the near horizon and the near-EVH limits in the two cases do not commute.

Temperature & entropy: To use the standard thermodynamic relations satisfied by BTZ black holes, we must compactify (4.65) to three dimensions. This is achieved by considering the ansatz

$$\begin{aligned} ds^2 = & h_1 h_2 g^{(3)}_{\mu\nu} dx^\mu dx^\nu + \frac{(a^2+q)h_1 h_2}{\Delta_\theta} d\theta^2 + \frac{\ell^2 \cos^2\alpha \cos^2\theta}{\lambda^2 h_1 h_2} d\xi^2 + \frac{a^2+q}{\Xi_a^2} \frac{h_2}{h_1^3} \Delta_\theta \sin^2\theta d\hat{\phi}^2 \\ & + \frac{\ell^2 h_2}{h_1} d\alpha^2 + \frac{\ell^2 h_1}{h_2} \sin^2\alpha d\beta^2 + \frac{\ell^2 h_1}{h_2} \left[\mu_1^2 (d\hat{\psi}_1 - A d\hat{\phi})^2 + \mu_2^2 (d\hat{\psi}_2 - A d\hat{\phi})^2 \right]. \end{aligned}$$

Proceeding as in subsection 4.3.2, the 3d Newton's constant is

$$\frac{1}{G_3} = \frac{2N^2 \sqrt{(a^2\ell^2+q^2)(a^2+q)}}{\Xi_a \ell^4}. \tag{4.67}$$

Note that in the $a = 0$ case we recover the static EVH expression (4.51).

[6] For $\mathbf{W}^2 M < \mathbf{V} a^2 \hat{b}^2$ we get a space with a conical defect, in line with the regimes of parameters highlighted in section 1.4.

The temperature and entropy of the pinching BTZ black holes equal

$$\begin{aligned} T_{\rm BTZ} &\equiv \frac{x_+^2 - x_-^2}{2\pi x_+ \ell_3^2} = \frac{\lambda}{\epsilon} T_{\rm H}\,, \\ S_{\rm BTZ} &\equiv \frac{2\pi\epsilon \cdot x_+}{4G_3} = S_{\rm BH}\,. \end{aligned} \tag{4.68}$$

Once more the 3d entropy matches the original 10d black hole one (4.39), while the proportionality of temperatures is consistent with the temporal scaling in (4.61).

4.4 IR 2d Description

We calculate in this section the central charge of the emergent dual conformal field theory, and the quantum numbers associated to states in this theory.

We employ the technique of section 3.4.1 to compute the central charge c and quantum numbers $(L_0,\, \bar{L}_0)$ of the IR 2d CFT dual to the pinching BTZ black hole appearing in the near horizon geometry of the near-EVH black holes. Again, the effective central charge c is related to the pinching central charge c_p by $c = \epsilon c_p$, and the mass and angular momentum of the BTZ built on a pinching AdS_3 orbifold have an extra ϵ in their expressions:

$$c = \frac{3\ell_3}{2G_3}\epsilon = \frac{3(a^2+q)}{\ell^4 \Xi_a}\sqrt{\frac{a^2\ell^2+q^2}{\mathbf{V}}}\; N^2\epsilon \tag{4.69}$$

$$\ell_3 M_{\rm BTZ} = L_0 + \bar{L}_0 - \frac{c}{12} = \frac{x_+^2 + x_-^2}{8\ell_3 G_3}\epsilon \sim N^2\epsilon, \tag{4.70}$$

$$J_{\rm BTZ} = L_0 - \bar{L}_0 = \frac{x_+ x_-}{4\ell_3 G_3}\epsilon \sim N^2\epsilon. \tag{4.71}$$

Requiring a *finite* central charge to have a *finite* gap in this IR 2d CFT is achieved by the *large* N limit:

$$\boxed{N^2\epsilon = \text{fixed.}} \tag{4.72}$$

It is manifest the entropy $S_{\rm BH}$ in (4.39) remains finite in this limit. It is shown below that the same holds for the excitations $M_{\rm BTZ},\ J_{\rm BTZ}$ which will be related with precise combinations of the UV quantum numbers.

4.4.1 Nearly-static near-EVH

The central charge may be obtained from (4.69) at $a = 0$

$$c_{\rm static} = \frac{3q^2}{\ell^4\sqrt{1+\frac{2q}{\ell^2}}}\; N^2\epsilon\,. \tag{4.73}$$

whereas excitations equal

$$\ell_3 M_{\rm BTZ} = \frac{2M\mathbf{W}_s - \mathbf{Y}_s(\hat{a}^2+\hat{b}^2)}{4\ell^2\sqrt{\mathbf{V}_s}}\; N^2\epsilon\,, \qquad J_{\rm BTZ} = \frac{\hat{a}\hat{b}}{2\ell^2}N^2\epsilon\,. \tag{4.74}$$

Notice how the static EVH point $(0,0,q;m(q))$ determines the IR 2d CFT by fixing its central charge, whereas its orthogonal deformations (4.30)-(4.31) encode their *finite* excitations. Any tangential deformation (4.29) would have simply changed the value of q, which would correspond to a different CFT. Note also that the BTZ mass has contributions from all three parameters describing the transverse deviations from the EVH surface.

4.4.2 Rotating near-EVH

The central charge is given by (4.69) with excitations

$$\ell_3 M_{\rm BTZ} = \frac{\ell_3 \lambda}{2\ell^3 \Xi_a}\, M\mathbf{W}\, N^2 \epsilon\,, \qquad J_{\rm BTZ} = \frac{\ell_3 \lambda}{2\ell^3 \Xi_a}\, a\hat{b}\sqrt{\mathbf{V}}\, N^2 \epsilon. \tag{4.75}$$

As before, the rotating EVH point $(a, 0, q; m(a, q))$ determines the IR 2d CFT central charge and vacuum structure, whereas its orthogonal deformations (4.35)-(4.36) encode its excitations.

As we have noted all physical quantities *at* the static EVH point can be recovered from the corresponding expressions *at* the rotating EVH evaluated at $a = 0$ point. This is not true, however, for the excitations above these EVH points. For example, the nearly-static values for $M_{\rm BTZ}$, $J_{\rm BTZ}$ and $T_{\rm H}$ cannot be recovered by simply setting $a = 0$ (or taking $a \to 0$ limit) of the rotating EVH ones. This is due to the fact that in the nearly-static case both a, b scale as ϵ, while in the rotating case, a is finite and $b \sim \epsilon^2$.

Using Cardy's formula [5]

$$S_{\rm CFT} = 2\pi\sqrt{\frac{c}{6}\left(L_0 - \frac{c}{24}\right)} + 2\pi\sqrt{\frac{\bar{c}}{6}\left(\bar{L}_0 - \frac{\bar{c}}{24}\right)}\,, \tag{4.76}$$

one can immediately check the bulk entropy (4.39) is reproduced for both near-EVH black holes.

4.5 First Law of Thermodynamics: Rotating Charged near-EVH Black Holes

Now we explicitly demonstrate how the IR first law of thermodynamics follows from the UV one (4.15) as described in section 2.3, which we may view as further supporting evidence of the EVH/CFT correspondence [51] reviewed in section 1.8. Physical variations appearing in the first law are generically defined as one-forms on the black hole parameter space. In our examples, the UV $\{dE, dJ_a, dJ_b, dJ_i, dJ_3\}$ forms are defined on a four dimensional space spanned by (a, b, q, m), while in the IR, physical variations belong to the subspace of orthogonal deformations to the EVH hyperplane, leaving the EVH point fixed. Below, we consider nearly-static and rotating near-EVH cases separately.

4.5.1 Nearly-static first law

As advocated in section 2.3, we distinguish three categories of 10d black holes charges in the near-EVH nearly-static regime (4.31):

- $Y = \{E, J_1, J_2\}$ with an ϵ expansion of the form $Y = Y^{(0)} + \epsilon^2 Y^{(2)}$.
- $X = \{J_a, J_b\}$ with an ϵ expansion of the form $X = \epsilon X^{(1)}$.
- J_3 with expansion $J_3 = \epsilon^2 J_3^{(2)}$.

Since all charges scale like N^2, charges X have a finite value due to (4.72).

Using (4.52), the left hand side of the UV first law scales like

$$T_{\rm H} dS_{\rm BH} = \epsilon \frac{\sqrt{q}}{\ell} T_{\rm BTZ} dS_{\rm BTZ}, \tag{4.77}$$

noting the difference in time scaling between here, $\epsilon\frac{\sqrt{q}}{\ell}$, and in (2.58), ϵ. When analysing the right hand side, we first identify the angular momenta categorised in (2.61) with the near-EVH

values in the near-static regime:

$$\Omega_i^{(0)} = \Omega_1 \tag{4.78}$$

$$\Omega_{BTZ} \equiv \frac{x_- x_+}{\ell_3 x_+^2} = \frac{\hat{a}\hat{b}}{\sqrt{\mathbf{V}_s}} \frac{1}{\ell_3 \hat{r}_+^2} = -\frac{\ell}{\sqrt{q}}\Omega_3 + \mathcal{O}(\epsilon^2) = \Omega_{\hat{\chi}}$$

$$\Omega_a = \frac{a(b^2 + r_+^2 \mathbf{Y}_s)}{q r_+^2} = \left(A_a^{(1)} + B_a^{(1)}\Omega_{\rm BTZ}\right)\frac{\ell}{\sqrt{q}}\epsilon + \mathcal{O}(\epsilon^3)\,, \tag{4.79}$$

$$\Omega_b = \frac{b(a^2 + r_+^2 \mathbf{Y}_s)}{q r_+^2} = \left(A_b^{(1)} + B_b^{(1)}\Omega_{\rm BTZ}\right)\frac{\ell}{\sqrt{q}}\epsilon + \mathcal{O}(\epsilon^3)\,,$$

where A_α, B_α are defined in (4.47-4.48). Then on the RHS we have

$$E - 2\Omega_1 J_1 - A_a J_a - A_b J_b = \epsilon \frac{\sqrt{q}}{\ell} M_{\rm BTZ}. \tag{4.80}$$

We define

$$(-J_3 + B_a J_a + B_b J_b) = \epsilon J_{\rm BTZ}, \tag{4.81}$$

where the minus sign multiplying J_3 reflects the χ-scaling, so that

$$\Omega_3 J_3 + B_a J_a + B_b J_b = \epsilon \frac{\sqrt{q}}{\ell}\Omega_{\rm BTZ} J_{\rm BTZ}. \tag{4.82}$$

Adding all terms, modulo the overall $\epsilon\sqrt{q}/\ell$ factor, the first order contribution to the UV first law is the first law for a BTZ black hole,

$$\boxed{\begin{array}{c} T_{\rm H} dS_{\rm BH} = dE - 2\Omega_1 dJ_1 - \Omega_a dJ_a - \Omega_b dJ_b - \Omega_3 dJ_3 \\ \Downarrow \\ T_{\rm BTZ} dS_{\rm BTZ} = dM_{\rm BTZ} - \Omega_{\rm BTZ} dJ_{\rm BTZ} \end{array}}\,, \tag{4.83}$$

where we already dropped all vanishing subleading contributions in the $\epsilon \to 0$ limit.

4.5.2 Rotating first law

Given the original 10d black hole charges (4.7), (4.8) and (4.16) and the near-EVH expansion of parameters (4.36), charges fall into two categories in the rotating near-EVH regime:

- $Y = \{E, J_1, J_a\}$ with an ϵ expansion of the form $Y = Y^{(0)} + \epsilon^2 Y^{(2)}$.
- $Z = \{J_b, J_3\}$ with expansion $Z = \epsilon^2 Z^{(2)}$.

$Y^{(0)}$ is the value of charges *at the EVH point*, whereas $Y^{(2)}, Z^{(2)}$ are the *near-EVH excitations*. Ω_1 and Ω_a have analogous expansions to J_1 and J_a, with finite $\Omega_1^{(0)}$ and $\Omega_a^{(0)}$ values at the EVH point (4.54) and with ϵ^2 corrections.

Consider the UV first law (4.15). Using (4.68), its left hand side equals

$$T_{\rm H} dS_{\rm BH} = \frac{\epsilon}{\lambda} T_{\rm BTZ} dS_{\rm BTZ}\,. \tag{4.84}$$

To discuss its right-hand-side, we first note that there are no non-trivial fibrations in the near horizon geometry (4.65), so that $A_\alpha = B_\alpha = 0$. In this case, we identify from (2.61) $\Omega^{(0)} = (\Omega_1^{(0)}, \Omega_a^{(0)})$. Then

$$E - 2\Omega_1 J_1 - \Omega_a J_a = \frac{\epsilon}{\lambda} M_{\rm BTZ}. \tag{4.85}$$

To find the analogous expression for $J_{\rm BTZ}$, we first note that

$$\Omega_b^{(0)} = \frac{a}{q + a^2}\frac{ab}{r_+^2}\,, \qquad \Omega_3^{(0)} = -\frac{q}{\ell(q+a^2)}\frac{ab}{r_+^2}\,, \qquad \Omega_b^{(0)} + \frac{a\ell}{q}\Omega_3^{(0)} = 0\,, \tag{4.86}$$

and[7]

$$\Omega_{\rm BTZ} \equiv \Omega_{\hat{\chi}} = \frac{x_+ x_-}{x_+^2 \ell_3} = \frac{1}{C_1}\Omega_b. \tag{4.88}$$

We use these relations to define

$$\Omega_b J_b + \Omega_3 J_3 = \Omega_{\rm BTZ} C_1 \left(J_b - \frac{q}{a\ell} J_3\right) = \Omega_{\rm BTZ}\frac{\epsilon}{\lambda} J_{\rm BTZ}. \tag{4.89}$$

Note that as expected, the dependence on C_3 drops out of all of the expressions above.

Adding all contributions and dropping the overall ϵ/λ constant factor, the exact IR first law is derived

$$\boxed{\begin{aligned} T_{\rm H} dS_{\rm BH} &= dE - 2\Omega_1 dJ_1 - \Omega_a dJ_a - \Omega_b dJ_b - \Omega_3 dJ_3 \\ &\Downarrow \\ T_{\rm BTZ} dS_{\rm BTZ} &= dM_{\rm BTZ} - \Omega_{\rm BTZ} dJ_{\rm BTZ} \end{aligned}} \tag{4.90}$$

where we already dropped all vanishing subleading contributions in the $\epsilon \to 0$ limit. Notice the ξ direction does not contribute above because the $\Omega_\xi dJ_\xi$ term is an order ϵ^2 smaller than the leading term.

It can be straighforwardly checked using the transformations in Appendix 4.D that the BTZ first law is invariant under the choice of C_1 (4.59).

4.6 EVH/CFT$_2$ vs. AdS$_5$/CFT$_4$

The ten dimensional black holes (4.18) interpolate between asymptotically AdS$_5$ and locally AdS$_3$ geometries. The former has a dual (UV) description in terms of $\mathcal{N} = 4$ super Yang-Mills theory , whereas the latter must have a dual (IR) description as advocated in section 4.4. In this section we provide an explicit map between the IR quantum numbers and those of the 4d UV dual to the original black hole.

We repeat the analysis of section 3.6 by studying how the quantum numbers of a bulk scalar field probe transform along the RG flow. The UV quantum numbers of this scalar field (in the static AdS$_5$ frame) will be associated with the eigenvalues of the operators

$$\Delta_{\rm UV} = \ell E = i\ell\partial_t, \qquad \mathcal{J}_{a,b} = -i\partial_{\phi^s,\psi^s} \qquad \mathcal{J}_{i,3} = -\ell Q_{i,3} = -i\partial_{\psi_{i,3}}. \tag{4.91}$$

Similarly, the IR quantum numbers are mapped to

$$\Delta_{\rm IR} = i\ell_3\partial_\tau, \qquad \mathcal{J}_{\rm IR} = -i\partial_{\hat{\chi}} \qquad \mathcal{J}_\xi = -i\partial_\xi\,. \tag{4.92}$$

From now on, as the notation above suggests, we will identify these eigenvalues with the gravity conserved charges. Though this need not hold generically, it will turn out to provide us with the right intuition.

4.6.1 EVH/CFT$_2$ vs AdS$_5$/CFT$_4$: nearly-static

Given the large gauge transformations (4.41) and (4.45) implemented in the near-EVH static regime, we learn the angular momentum along the AdS$_3$ pinching circle equals

$$\begin{aligned} \mathcal{J}_{\rm IR} = -i\partial_{\hat{\chi}} &= -i\left(-\frac{1}{\epsilon}\partial_{\psi_3} + \frac{\hat{b}\ell}{q}\partial_\phi + \frac{\hat{a}\ell}{q}\partial_\psi\right) = -\frac{1}{\epsilon}\mathcal{J}_3 + \frac{\ell}{q}(\hat{a}\mathcal{J}_b + \hat{b}\mathcal{J}_a) \\ &= J_{\rm BTZ} + \frac{\ell}{2q}(\hat{a}\mathcal{J}_b + \hat{b}\mathcal{J}_a), \end{aligned} \tag{4.93}$$

[7] This is consistent with our expectations, as

$$\Omega_{\rm BTZ} \equiv \Omega_{\hat{\chi}} = \frac{x_+ x_-}{x_+^2 \ell_3} = \lambda\left(C_2\frac{\partial\psi}{\partial t} + C_3\frac{\partial\psi_3}{\partial t}\right) = \frac{1}{C_1}\Omega_b + C_3\left(\frac{q}{a\ell}\Omega_b + \Omega_3\right). \tag{4.87}$$

where we used (4.74). Furthermore, from (4.7) and (4.31)

$$\frac{\ell}{2q}(\hat{a}\mathcal{J}_b + \hat{b}\mathcal{J}_a) = \frac{\hat{a}\hat{b}\mathbf{Y}_s}{2\ell^2}\ N^2\epsilon.$$

The IR conformal dimension equals

$$\begin{aligned}\Delta_{\rm IR} &= i\ell_3\partial_\tau = \frac{\ell_3}{\sqrt{q}\epsilon}\left[\Delta_{\rm UV} - 2\ell\ \Omega_1^{(0)}\mathcal{J}_1 - \frac{\ell\mathbf{Y}_s}{q}(b\mathcal{J}_b + a\mathcal{J}_a)\right] \\ &= \Delta^0_{\rm IR} + \frac{\ell_3\epsilon}{\sqrt{q}}\left(\Delta^{(2)}_{\rm UV} - 2\ell\ \Omega_1^{(0)}\mathcal{J}_1^{(2)} - \frac{\ell\mathbf{Y}_s}{q}(\hat{a}\mathcal{J}_a^{(1)} + \hat{b}\mathcal{J}_b^{(1)})\right),\end{aligned} \tag{4.94}$$

where the "zero point energy" $\Delta^0_{\rm IR}$ is defined as

$$\Delta^0_{\rm IR} = \frac{\ell_3}{\sqrt{q}\epsilon}(\Delta^{(0)}_{\rm UV} - 2\ell\ \Omega_1^{(0)}\mathcal{J}_1^{(0)}) = -\frac{\ell_3}{\sqrt{q}\epsilon}\frac{N^2q^2}{4\ell^4}\,. \tag{4.95}$$

In the BPS case where $q \sim \epsilon$ [28] $\Delta^0_{\rm IR}$ remains finite[8]. It is evident that the zero point energy is the $q_2 = q_3 = q$ case of (3.102) as expected, as the ground states coincide. Using the expressions for mass and angular momenta (4.7), (4.8) and (4.16) and the near-EVH scalings (4.31) we find

$$\begin{aligned}\Delta^{(2)}_{\rm UV} - 2\ell\ \Omega_1^{(0)}\mathcal{J}_1^{(2)} &= \frac{N^2}{2\ell^2}\left[M\mathbf{W}_s + \frac{q\mathbf{Y}_s}{2\ell^2}(\frac{\hat{a}^2+\hat{b}^2}{\ell^2})\right], \\ \frac{\ell}{q}(\hat{a}\mathcal{J}_a + \hat{b}\mathcal{J}_b) &= \frac{(\hat{a}^2+\hat{b}^2)\mathbf{Y}_s}{2\ell^2}N^2\epsilon\,,\end{aligned} \tag{4.96}$$

and hence

$$\Delta_{\rm IR} = \Delta^0_{\rm IR} + \ell_3 M_{\rm BTZ} - \frac{\ell_3}{\sqrt{q}}\frac{\ell}{2q}(\hat{a}\mathcal{J}_a + \hat{b}\mathcal{J}_b)\,, \tag{4.97}$$

where $M_{\rm BTZ}$ is given in (4.74).

Thus, even after removing the "zero point energy", both $\mathcal{J}_{\rm IR}$ and $\Delta_{\rm IR}$ contain extra terms compared with the expected BTZ mass $M_{\rm BTZ}$ and angular momentum $J_{\rm BTZ}$[9]. Similar extra terms appeared in charges associated with the null orbifold that appeared in the near horizon geometry of the non-BPS static charged case in section 3.3.2. These terms are related to the rotation in the S^3 transverse to the local near horizon AdS_3 and should be associated with some notion of spectral flow in the dual CFT. Notice, in particular, how the extra dependence on $\mathcal{J}_a$ and $\mathcal{J}_b$ in (4.97) and (4.93) drops from the IR first law (4.83). This highlights the invariance of the first law under large gauge transformations generating constant electric and magnetic terms on the transverse 3-sphere.

4.6.2 EVH/CFT$_2$ vs AdS$_5$/CFT$_4$: rotating

As discussed in section 4.3.3, the $\mathcal{J}_b$ and $\mathcal{J}_3$ charges

$$\mathcal{J}_b = \frac{\hat{b}(q^2 + a^2\ell^2 + q\ell^2)N^2}{2\ell^5\Xi_a}\epsilon^2, \qquad \mathcal{J}_3 = \frac{a\hat{b}qN^2}{2\ell^4\Xi_a}\epsilon^2\,, \tag{4.98}$$

[8] We comment that the negative value of $\Delta^0_{\rm IR}$ from the dual 2d CFT viewpoint may be attributed to the $-c/12$ Casimir energy of the theory on the cylinder.

[9] We note that it is possible to define new $\hat{\phi}$ and $\hat{\psi}$ coordinates such that (4.93) and (4.97) respectively reduce to simply $\Delta_{\rm IR} = \Delta^0_{\rm IR} + \ell_3 M_{\rm BTZ}$ and $\mathcal{J}_{\rm IR} = J_{\rm BTZ}$. The new $\hat{\phi}$ and $\hat{\psi}$ which do this are

$$\hat{\psi} = \psi - \frac{\hat{b}}{2q}\frac{\ell}{\sqrt{q}}\tau\ - \frac{\hat{a}\ell}{2q}\hat{\chi}\,, \quad \hat{\phi} = \phi - \frac{\hat{a}}{2q}\frac{\ell}{\sqrt{q}}\tau - \frac{\hat{b}\ell}{2q}\hat{\chi}\,.$$

The resulting near horizon geometry would then contain a rotating S^3 transverse to the BTZ black hole. The role of this transformation in terms of spectral flow is yet to be understood.

are naturally encoded in the IR geometry in terms of

$$\mathcal{J}_{\rm IR} = \mathcal{J}_{\hat{\chi}} = \frac{C_1}{\epsilon}\left(\mathcal{J}_b - \frac{q}{al}\mathcal{J}_3\right) = \frac{(a^2+q)}{2\ell^2\Xi_a\sqrt{a^2\ell^2+q^2}}a\hat{b}\ N^2\epsilon = J_{\rm BTZ}\,, \tag{4.99}$$

$$\mathcal{J}_\xi = (-C_3\mathcal{J}_b + C_2\mathcal{J}_3) \sim N^2\epsilon^2\,, \tag{4.100}$$

where we used (4.58-4.60).

The AdS_3 pinching is responsible for the $1/\epsilon$ factor in the first equality of (4.99). This allows $\mathcal{J}_{\rm IR}$ to remain finite, matching the BTZ angular momentum, whereas $\mathcal{J}_\xi \sim \epsilon$ is subleading, in the limit (4.72). This prevents any unphysical dependence on C_3 to survive our limit, as expected on physical grounds.

Let us consider the IR conformal dimension $\Delta_{\rm IR}$. If we proceed analogously to the other charges, we learn

$$\begin{aligned}\Delta_{\rm IR} \equiv i\ell_3\frac{\partial}{\partial\tau} &= \frac{\ell_3}{\ell}\frac{\lambda}{\epsilon}\left(i\ell\frac{\partial}{\partial t} + i\ell\Omega_a^{0S}\frac{\partial}{\partial\phi} + \sum_{i=1,2} i\ell\Omega_i^0\frac{\partial}{\partial\psi_i}\right)\\ &= \frac{\ell_3}{\ell}\frac{\lambda}{\epsilon}\left(\Delta_{\rm UV} - \ell\Omega_a^{0S}\mathcal{J}_a - 2\ell\Omega_1^{(0)}\mathcal{J}_1\right).\end{aligned} \tag{4.101}$$

Using the 5d charges (4.8), (4.7) and (4.16) in the near-EVH regime (4.36), we find

$$\begin{aligned}\Delta_{\rm IR} &= \frac{\lambda\ell_3}{\ell\epsilon}(\Delta_{\rm UV}^{(0)} - \ell\ \Omega_a^{0S}\mathcal{J}_a^{(0)} - 2\ell\ \Omega_1^{(0)}\mathcal{J}_1^{(0)}) + \frac{\lambda\ell_3}{\ell}\epsilon\left(\Delta_{\rm UV}^{(2)} - \ell\ \Omega_a^{0S}\mathcal{J}_a^{(2)} - 2\ell\ \Omega_1^{(0)}\mathcal{J}_1^{(2)}\right)\\ &= \Delta_{\rm IR}^0 + \ell_3 M_{\rm BTZ}\,,\end{aligned} \tag{4.102}$$

where we used (4.75), the identity $\ell M_{\rm BTZ} = \lambda(\Delta_{\rm UV}^{(2)} - \ell\Omega_a^{(0)}\mathcal{J}_a^{(2)} - 2\ell\Omega_1^{(0)}\mathcal{J}_1^{(2)})\epsilon$ and $\Delta_{\rm IR}^0$ is defined as

$$\Delta_{\rm IR}^0 = \frac{\ell_3}{\ell}\frac{\lambda}{\epsilon}\frac{N^2(a^2\ell^2-q^2)}{4\ell^4\Xi_a}\,. \tag{4.103}$$

Note the zero point energy of the nearly-static near-EVH case (4.95) can be obtained as the $a=0$ limit of the rotating EVH case (4.103). Notice $\Delta_{\rm IR}^0$ only depends on the rotating EVH point (and not the excitations) and could consequently be interpreted as a "zero point energy" from the IR 2d CFT perspective. This contribution is generically divergent, but vanishes when supersymmetry is preserved, i.e. $q = a\ell$. This would reproduce the expected $\Delta_{\rm IR} = L_0 + \bar{L}_0 - c/12$ bound in this case, due to the protection of supersymmetry along the RG flow. Near the BPS point, i.e. $q = a\ell - \epsilon^2\delta_s^2/(2a\ell)$, the "zero point energy" still remains finite

$$\Delta_{\rm IR}^0 = \frac{\ell_3}{\ell}\frac{\lambda N^2\epsilon}{4\ell^4\Xi_a}\delta_s^2 + \ell_3 M_{\rm BTZ}. \tag{4.104}$$

Once more, we learn that when the near-EVH near horizon limit does not admit the geometric manifestation of gauge fields in the 3d theory, the quantum numbers $\Delta_{\rm IR}$, $\mathcal{J}_{\rm IR}$ of low-lying excitations in the dual $\mathcal{N}=4$ super Yang-Mills theory are given by the quantum numbers $\Delta_{\rm 2d} = \ell_3 M_{\rm BTZ}$, $\mathcal{J}_{\rm 2d} = J_{\rm BTZ}$ of the emergent two dimensional CFT. This is again evidence that the near-EVH sector in the UV dual 4d CFT is a decoupled sector described by this IR 2d CFT.

4.7 A Check: Comparison with Kerr/CFT

In this section we seek a connection between the 2d CFTs appearing in the EVH/CFT correspondence discussed in previous sections and the 2d chiral CFTs emerging in the Kerr/CFT correspondence described in section 1.5. Our perspective is that a 2d chiral CFT is nothing but the Discrete Light-Cone Quantization (DLCQ) of a standard 2d CFT [40], as was already discussed in section 3.7 for static charged AdS_5 EVH black holes. To explore this perspective, we first review the Kerr/CFT formalism in the context of the family of black holes (4.3) and

their 10d embeddings (4.18). In the region of parameters where Kerr/CFT and EVH/CFT overlap, we can always derive one of the Kerr/CFT descriptions from the EVH/CFT.

Review of Kerr/CFT for AdS$_5$ black holes [38]: The Kerr/CFT correspondence applies to any extremal black hole of finite horizon size. In our notation, one considers the near horizon limit

$$r = r_0(1+\epsilon y)\,, \qquad t = \frac{\tau}{2\pi {T_{\rm H'}}^0 r_0 \epsilon}\,, \qquad \hat{\phi} = \phi + {\Omega_a}^0 t\,, \qquad \hat{\psi} = \psi + {\Omega_b}^0 t\,, \tag{4.105}$$

where r_0 stands for the extremal horizon, $T'_{\rm H}$ is the derivative of Hawking temperature w.r.t. the horizon size r_0 and all 0 indices refer to the thermodynamical quantities being evaluated at it. Using the Taylor expansion for the function X in (4.3) controlling the horizon size,

$$X = (r-r_0)^2\frac{X''(r_0)}{2}+\mathcal{O}(\epsilon^3) \equiv V_f (r-r_0)^2, \text{ with } V_f = 1+\frac{3a^2b^2}{r_0^4}+\frac{6r_0^2+a^2+b^2+2q}{\ell^2}\,, \tag{4.106}$$

the resulting metric describes an S^3 bundle over AdS$_2$ [38]

$$ds_5^2 = A(\theta)\left(-y^2 d\tau^2 + \frac{dy^2}{y^2}\right) + F(\theta)d\theta^2 + B_1(\theta)e_1^2 + B_2(\theta)\left(e_2 + C(\theta)e_1\right)^2\,,$$

where the scalar functions are given by

$$A(\theta) = \frac{X_1^0(\rho_0^2+q)}{V_f}\,, \qquad F(\theta) = \frac{X_1^0(\rho_0^2+q)}{\Delta},$$
$$B_1(\theta) = X_1^0\left(g^0_{\phi\phi} - \frac{{g^0_{\phi\psi}}^2}{g^0_{\psi\psi}}\right), \quad B_2(\theta) = X_1^0 g^0_{\psi\psi}\,, \quad C(\theta) = \frac{g^0_{\phi\psi}}{g^0_{\psi\psi}}\,,$$

$$g^0_{\phi\phi} = \frac{(Z+b^2C\sin^2\theta)\sin^2\theta}{(\rho_0^2+q)f_2^2\Xi_a^2}\bigg|_{\epsilon\to 0}\,, \; g^0_{\psi\psi} = \frac{(W+a^2C\cos^2\theta)\cos^2\theta}{(\rho_0^2+q)f_1^2\Xi_b^2}\bigg|_{\epsilon\to 0}\,, \; g^0_{\phi\psi} = \frac{abC\sin^2\theta\cos^2\theta}{(\rho_0^2+q)f_1 f_2\Xi_a^2\Xi_b^2}\bigg|_{\epsilon\to 0}\,,$$

and the set of one-forms $e_a = d\phi_a + k_{\phi_a} y d\tau$ for $a = 1,2$ (in terms of our earlier notation $\phi_1 = \phi$ and $\phi_2 = \psi$) is determined by the constants

$$k_\phi = \frac{2a\Xi_a({f_2^0}^2+b^2q)}{f_3^0 r_0 V_f}\,, \qquad k_\psi = \frac{2b\Xi_b({f_1^0}^2+a^2q)}{f_3^0 r_0 V_f}\,. \tag{4.107}$$

According to the Kerr/CFT dictionary [91] reviewed in section 1.5, these fix the dual CFT Frolov-Thorne temperatures

$$T_{\phi_a} = \frac{1}{2\pi k_{\phi_a}}\,. \tag{4.108}$$

These expressions agree with the expressions

$$T_i = -\frac{\partial T_{\rm H}/\partial r_+}{\partial\Omega_i/\partial r_+}\bigg|_{r_+=r_0} \tag{4.109}$$

obtained in section 2.2 from the expansion of the first law of thermodynamics around extemality. The central charges of the chiral Virasoro algebra obtained from the asymptotic symmetry group analysis equal [38]

$$c_\phi = \frac{6\pi a[(r_0^2+b^2)^2+qb^2]}{G_5 V_f \Xi_b r_0^2}\,, \qquad c_\psi = \frac{6\pi b[(r_0^2+a^2)^2+qa^2]}{G_5 V_f \Xi_a r_0^2}. \tag{4.110}$$

Embedding to 10 dimensions: As originally discussed in [79], when the 5d geometry is embedded in higher dimensions, as in (4.18), the number of geometrical U(1) isometries that

can get enhanced to a full Virasoro is enlarged. Proceeding as before, we write the 10d near horizon geometry as

$$ds_{10}^2 = \tilde{A}(\theta_n)\left(-y^2 d\tau^2 + \frac{dy^2}{y^2}\right) + \tilde{B}_1(\theta_n) {e_\phi}^2 + \tilde{B}_2(\theta_n)\left(e_\psi + C(\theta_0)^2 e_\phi\right)^2 + \sum_{n,m=0}^{2} F_{\theta_n\theta_m}(\theta_n,\theta_m)\; d\theta_n d\theta_n + \sum_{i=1}^{3} D_i(\theta_n)\left(e_{\psi_i} + P_i(\theta_0)(e_\phi + e_\psi)\right)^2,$$

with θ_0 being the latitudinal coordinate in AdS_5 and θ_1, θ_2 those of the transverse S^5 (the same as α, β angles defined in (4.19)), and

$$\tilde{A}(\theta_n) = \sqrt{\tilde{\Delta}} A(\theta_0)\,, \qquad \tilde{B}_{1,2}(\theta_n) = \sqrt{\tilde{\Delta}} B_{1,2}(\theta_0)\,, \qquad D_i(\theta_n) = \frac{\mu_i^2}{X_i^0}.$$

where $\tilde{\Delta}$ is defined in (4.20). The non-zero $F_{\theta_m\theta_n}$ are

$$F_{\theta_0\theta_0} = \sqrt{\tilde{\Delta}} F(\theta)\,, \qquad F_{\theta_1\theta_1} = H_0(\cos^2\theta_1 + \sin^2\theta_1 \sin^2\theta_2) + \sin^2\theta_1 \cos^2\theta_2\,,$$
$$F_{\theta_2\theta_2} = H_0(\cos^2\theta_1 \cos^2\theta_2) + \cos^2\theta_1 \sin^2\theta_2\,, \quad F_{\theta_1\theta_2} = \sin\theta_1 \sin\theta_2 \cos\theta_1 \cos\theta_2 (1 - H_0).$$

This metric can be viewed as a warped $S^3 \times S^5$ bundle over AdS_2. The corresponding Frolov-Thorne temperatures are fixed by

$$k_{\psi_1} = k_{\psi_2} = \frac{2 r_0^3 q \sqrt{1 + 2m/q}}{\ell^3 f_3^0 V}(2r_0^2 + a^2 + b^2 + 2q),$$
$$k_{\psi_3} = -\frac{2abq}{\ell r_0 f_3^0 V_f}(2r_0^2 + a^2 + b^2 + q)\,, \tag{4.111}$$

corresponding to the three U(1)s in the 5-sphere, whereas the central charges of the corresponding CFTs are[10]

$$c_{\psi_1} = c_{\psi_2} = \frac{6\pi r_0^2 q \sqrt{1 + 2m/q}(2r_0^2 + a^2 + b^2 + 2q)}{\ell^3 G_5 \Xi_a \Xi_b V_f}\,, \qquad c_{\psi_3} = -\frac{6\pi abq(2r_0^2 + a^2 + b^2 + q)}{\ell G_5 \Xi_a \Xi_b V_f r_0^2}\,.$$

Kerr/CFT thus suggests the existence of five apparently inequivalent chiral CFTs reproducing the entropy of the extremal black holes upon using Cardy formula[11]

$$S = \frac{\pi^2}{3} c_i T_i. \tag{4.112}$$

Taking the near-EVH limit: To compare the central charges arising from the Kerr/CFT prescription with the Brown Henneaux central charge of the CFT_2 emerging from the EVH/CFT correspondence, we follow the same procedure as in section (3.7). We take the near-EVH limit of the Kerr/CFT charges, and impose extremality on the near-EVH BTZ black holes, so that there is an overlap in the regions of parameters of the respective correspondences.

We expect that the near-EVH limit will induce a vanishing (in the large N limit) of all Kerr/CFT charges other than the one associated to rotations in the near horizon region. Focussing on extremal near-EVH excitations corresponds to restricting to the chiral sector of the dual CFT, so we anticipate that the Brown Henneaux central charge in this regime of parameters will coincide with the central charge associated to the DLCQ of the theory.

[10] Negative central charge c_{ψ_3} may sound alarming. However, we note that in a 2d CFT the sign which has physical significance is cL_0 or $\frac{1}{c}L_0$ and that the charge corresponding to rotations on ψ_3, Q_3 is negative in our conventions (4.8); had we chosen the opposite orientation for ψ_3, both c_{ψ_3} and Q_3 would have changed sign.

[11] For ψ_3 direction which the central charge was negative, one may directly show that the Frolov-Thorne temperature is also negative, *cf.* discussion in footnote 10.

4.7.1 Nearly-static near-EVH regime

The leading terms in the Kerr/CFT central charges in the nearly-static near-EVH limit (4.31) take the form

$$c_\phi = \frac{3q}{\ell^2\sqrt{\mathbf{V}_s}}\frac{\hat{b}}{\ell}N^2\epsilon\,, \qquad c_\psi = \frac{3q}{\ell^2\sqrt{\mathbf{V}_s}}\frac{\hat{a}}{\ell}N^2\epsilon \tag{4.113}$$

$$c_{\psi_1} = c_{\psi_2} = \frac{6\sqrt{q}\ell_3^3}{\ell^4}\frac{\hat{a}\hat{b}}{\ell^2}\sqrt{\mathbf{Y}_s}N^2\epsilon^2\,, \qquad c_{\psi_3} = -\frac{3q^2}{\ell^4\sqrt{\mathbf{V}_s}}N^2\,, \tag{4.114}$$

where we used the identities $V_f = 4\mathbf{V}_s$ and $r_0^2 = ab/\sqrt{\mathbf{V}_s}$. We are interested in identifying the central charges for the relevant IR U(1)s. Following [81], (4.41) implies

$$c_{\hat{\chi}} = -\epsilon c_{\psi_3} = c_{\text{static}}\,. \tag{4.115}$$

Thus, $c_{\hat{\chi}}$ exactly matches c_{static} (4.73).

This matching supports the claim that the chiral CFT appearing in Kerr/CFT is the DLCQ of the one appearing in the EVH/CFT as outlined in section 1.7. Moreover, the Kerr-CFT T_3 agrees up to the scaling of $\hat{\chi}$ with the temperature of the left-sector T_L of the 2d CFT in EVH/CFT satisfying $T_3 = -\frac{1}{\epsilon}T_L$. (Note that in the extremal case the temperature of the right-moving sector of the 2d CFT appearing in EVH/CFT vanishes.) One may then use Cardy's formula

$$S = \frac{\pi^2}{3}c(\ell_3 T_L) = \frac{\pi}{3}\cdot\frac{3q^2}{\ell^4\sqrt{\mathbf{V}_s}}N^2\epsilon\cdot\frac{x_0}{\ell_3} = \pi\frac{q}{\ell^2}\frac{\hat{r}_0}{\ell}N^2\epsilon = S_{\text{BH}}\,,$$

where in the last equality we used (4.34).

Unlike the rotating case, c_ϕ and c_ψ also remain finite in the near-EVH static limit. They satisfy the relations $c_\phi = c_{\hat{\chi}}\cdot\ell\hat{b}/q$, $c_\psi = c_{\hat{\chi}}\cdot\ell\hat{a}/q$. Notice the proportionality coefficients agree with those appearing in the coordinate transformation (4.45) removing the mixing between the angles on S^3 and the AdS_3 coordinates τ, $\hat{\chi}$. Within the Kerr/CFT mentality, one may then propose that in the near horizon, near-EVH static case we have three chiral CFT descriptions, one associated with the EVH/CFT via the DLCQ description and the other two (related to c_ϕ and c_ψ) with rotations on the S^3. This latter, if true, may not be argued for through the standard Kerr/CFT prescription for computing the central charges, which involves imposing certain boundary conditions for metric fluctuations [79, 91]. To see this we note that the extremal black hole geometry we discuss here is extremal-BTZ$\times S^3$, the near horizon limit of which is AdS_3-selfdual-orbifold$\times S^3$ given in Appendix 4.C. This suggests that one should be able to extend the standard Kerr/CFT prescription to compute the central charge to the cases like extremal-BH$\times X$, where X is a compact geometry. This of course cries for a thorough study and better understanding.

4.7.2 Rotating near-EVH regime

The leading terms in the Kerr/CFT central charges in the near-EVH limit (4.36) take the form

$$c_\phi = \frac{3\hat{b}}{\ell}\frac{q + a^2\mathbf{V}^{-1}}{\ell^2\sqrt{\mathbf{V}}}N^2\epsilon^2\,, \qquad c_{\psi_1} = c_{\psi_2} = \frac{3\sqrt{q}}{\ell}\frac{a\hat{b}}{\ell^2\mathbf{V}}\frac{\ell_3}{\ell}\sqrt{\mathbf{Y}_s}N^2\epsilon^2\,, \tag{4.116}$$

$$c_\psi = \frac{3a\sqrt{\mathbf{V}}}{\ell\Xi_a}\frac{\ell_3^2}{\ell^2}N^2\,, \qquad c_{\psi_3} = -\frac{3q\sqrt{\mathbf{V}}}{\ell^2\Xi_a}\frac{\ell_3^2}{\ell^2}N^2\,, \tag{4.117}$$

where we used the identities $V_f = 4\mathbf{V}$ and $r_0^2 = ab/\sqrt{\mathbf{V}}$. In the infinite N limit (4.72), $c_\phi,\ c_{\psi_1},\ c_{\psi_2} \sim \epsilon \to 0$. Thus, the corresponding CFTs break down. Conversely, c_ψ and c_{ψ_3} diverge. Nonetheless, we already discussed in section 4.3.3 that the relevant IR U(1)s are given

by (4.57). Following [81], the central charges transform like

$$c_\xi = C_1 \left(\frac{q}{al} c_\psi + c_{\psi_3} \right) , \qquad c_{\hat{\chi}} = \epsilon \left(C_2 c\psi + C_3 c_{\psi_3} \right) = \frac{\epsilon}{C_1} c_\psi , \tag{4.118}$$

where we have used (4.60). These equal

$$c_\xi = 0 , \qquad c_{\hat{\chi}} = \frac{3\sqrt{\mathbf{V}}}{\ell^2 \Xi_a} \frac{\ell_3^2}{\ell^2} \frac{\sqrt{q^2 + a^2 \ell^2}}{\ell^2} \, N^2 \epsilon , \tag{4.119}$$

where we used (4.59). The vanishing of c_ξ agrees with the absence of angular velocity and momentum. More importantly, $c_{\hat{\chi}}$ exactly equals the Brown-Henneaux central charge in (4.69). This latter is in accord with our proposal/vision for connecting Kerr/CFT and EVH/CFT: the chiral 2d CFT appearing in Kerr/CFT is the DLCQ of the one appearing in the EVH/CFT.

4.8 Discussion

In this Chapter, we extended the analysis of Chapter 3 to stationary black holes as a case study of the first law analysis of Chapter 2 and the EVH/CFT correspondence (section 1.8). The black holes we studied are in the class of asymptotic AdS_5 black holes with two equal electric charges and two independent spins. We classified all EVH black holes in this class and argued that generically the EVH hypersurface is a bifurcate co-dimension two surface. The bifurcation line, which corresponds to the case with vanishing spin, the static EVH black hole, is then a co-dimension three surface. We studied excitations around any given EVH point and showed that all these excitations can be captured by the near-horizon geometry, which has a locally AdS_3 throat, a pinching AdS_3 [44].

We showed EVH black holes interpolate between AdS_5 at the boundary and a (locally) AdS_3 throat at the horizon and discussed the connection between the UV $\mathcal{N} = 4$ super Yang-Mills theory and the two dimensional conformal field theory appearing in the EVH/CFT proposal. Based on the arguments and proposal made in [44] and discussed in section 1.7, we argued that to resolve the pinching orbifold we should take a large N limit in the dual gauge theory such that its entropy, measured in 5d (or 10d) Planck units, remains finite, and its temperature scales like some small parameter. It is still desirable to have a better understanding of the pinching resolution proposal made in [44].

As a specific example of the first law result described in section 2.3, and as pieces of evidence for the EVH/CFT proposal introduced in section 1.8, we showed that the first law of thermodynamics for the original 5d (or 10d) EVH black hole, in the near-EVH limit reduces to the first law of thermodynamics of the BTZ black hole appearing in the near horizon. This result is remarkable, as it holds quite generically regardless of the details of the EVH black hole geometry.

Although we did not fully specify the IR CFT_2, we mentioned that it can be understood as a sector in the UV CFT_4 in the specific large N limit (4.72). This proposal, in agreement with the large N regime of Chapter 3 and in [28] for different sectors, should still be established through explicit computations.

We also discussed a connection between the EVH/CFT proposal and Kerr/CFT for extremal excitations of EVH black holes, i.e. extremal near-EVH black holes. We showed explicitly that the chiral CFT appearing in the Kerr/CFT proposal for extremal near-EVH black holes can be understood as the DLCQ of the CFT_2 appearing in the EVH/CFT correspondence, realising the proposal made in [40] and discussed in section 1.6. There are several questions and points which asks for further analysis. One closely related idea, providing a "microscopic description" for Kerr/CFT through locally AdS_3 throats, has also appeared in [91, 49].

There are two further points arising from this Chapter that require further study: the identification of IR charges for the near-static near-EVH black holes and its connection with Kerr/CFT.

Regarding the identification of IR charges, it is known that the appearance of constant electric and magnetic fields shift the values for the stress tensor and U(1) R-symmetry currents under spectral flow in the dual CFT [92]. We suspect the same, if not more general set of spectral

flows, should occur here accounting for the extra energy and angular momentum contributions in (4.93) and (4.97). To understand this point, one must study the reduction of our 10d near horizon geometries to three dimensions, extending the reduction to six dimensions done in [28]. As we discussed in section 2.3, the geometric realisation of spectral flow in terms of non-trivial fibrations over the BTZ black hole geometry renders a precise contribution to the BTZ mass and angular momentum that leaves the BTZ first law invariant.

The rotations that induce an apparent spectral flow in the emergent CFT_2 are associated to "extra" chiral CFT descriptions in the Kerr/CFT picture. It would be desirable, given the satisfactory agreement between the EVH/CFT result and that of Kerr/CFT in all other near-EVH regimes, to establish a connection between the suspected spectral flow picture and these central charges.

4.A Horizon Structure

Whenever the equation $X(r) = 0$ allows real positive solutions, the configurations (4.3) describe a family of black holes. When this is not the case, it describes a naked singularity. In this Appendix, we study the constraints in parameter space for black holes to exist. To do so, define

$$\begin{aligned} \ell^2 X &\equiv r^4 + Ar^2 + B + \frac{C}{r^2} \qquad (4.120) \\ &= r^4 + \left[\ell^2 + a^2 + b^2 + 2q\right] r^2 + \left[(a^2+b^2)(\ell^2+q) + a^2b^2 + q^2 - 2m\ell^2\right] + \frac{a^2b^2\ell^2}{r^2} \end{aligned}$$

Note $A, C \in \mathbb{R}^+$, because $a, b \in \mathbb{R}$ and $q \in \mathbb{R}^+$, whereas B can be negative for large m.

We shall denote the outer and inner horizons by $r_\pm$. These correspond to the largest and smallest positive roots of the equation $X(r) = 0$. When $r_+ = r_-$, (4.3) corresponds to extremal black holes. Figure 4.2 shows the root structure for the equation $X(r) = 0$. The existence of a horizon requires $X_c \leq 0$, where X_c is the extremum of X. This constraints the parameters a, b, q and m.

Charges carried by the EVH black holes studied in this work are such that $C \ll |B| \ll A$. When these hold, $r_\pm$ can be expanded as follows

$$r_\pm^2 = -\frac{B}{2A} \pm \sqrt{\left(\frac{B}{2A}\right)^2 - \frac{C}{A}} + \cdots . \qquad (4.121)$$

Existence of horizons requires $B^2 \geq 4AC$.

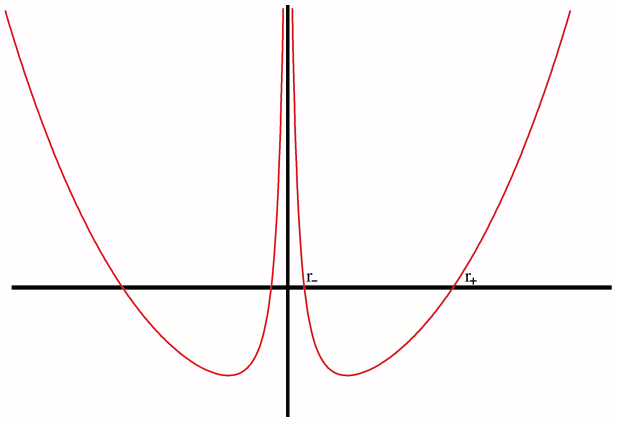

Figure 4.2: X as a function r for a general non-extremal black hole solution.

Near-EVH solutions occur when $r_\pm \sim \epsilon \to 0$. This can happen if (note that A is finite)

$$\text{Rotating EVH}: \quad a = \text{finite}, \;\; b = \hat{b}\epsilon^{2\alpha}, \;\; B = -\hat{B}\epsilon^2\,, \qquad \alpha \geq 1 \tag{4.122}$$

$$\text{Static EVH}: \quad a = \hat{a}\epsilon^{\beta}, \;\; b = \hat{b}\epsilon^{\alpha}, \;\; B = -\hat{B}\epsilon^2\,, \qquad \alpha \geq \beta \geq 1, \tag{4.123}$$

where $\hat{B} \geq 0$ and $C = \hat{C}\epsilon^{4+\gamma}$, $\gamma \geq 0$. These are of course the two cases discussed in (4.28) and (4.27).

Rotating EVH: To study this case let us assume $\alpha = 1$, $\gamma = 0$. Indeed it is not difficult to show that $\alpha > 1$ cases can be recovered from $\alpha = 1$, by sending $\hat{b} \to 0$ and we get back to the solution (4.62). From (4.120) we can read the parameter m

$$m = \frac{1}{2\ell^2}(\ell^2 a^2 + q a^2 + q^2) + \frac{\hat{B}}{2\ell^2}\epsilon^2 + \frac{\hat{b}^2(\ell^2 + a^2 + q)}{2l^2}\epsilon^4. \tag{4.124}$$

For the above parameters, condition $B^2 \geq 4AC$ is given by

$$\hat{B}^2 \geq 4a^2\hat{b}^2\ell^2(\ell^2 + 2q + a^2) + \mathcal{O}(\epsilon^2) \tag{4.125}$$

Static EVH: For this case, without loss of generality we can assume $\alpha = \beta = 1$, $\gamma = 0$ (larger values of α, β and γ may be obtained from this case in the $\hat{a}, \hat{b}$, $\hat{C} \to 0$ limit). In this case the $B^2 \geq 4AC$ condition reduces to

$$\hat{B}^2 \geq (\ell^2 + 2q)\hat{a}^2\hat{b}^2\ell^2\,, \tag{4.126}$$

and the negative $\hat{B}$ condition implies,

$$2m\ell^2 - q^2 \geq (\ell^2 + q)(\hat{a}^2 + \hat{b}^2)\epsilon^2\,. \tag{4.127}$$

Finally, we note that for generic values of the parameters, the black hole horizon topology is S^3 or $S^3 \times S^5$, depending on whether one takes the 5d or 10d perspective. For the specific values discussed in section 4.2, they degenerate to $S^2 \times S^1$. Furthermore, our black hole configurations (4.3) have closed time-like curves. For more discussions on these black holes and their singularity and causal structure, see [38, 88, 96].

4.B Calculation of Q_1 and Q_3

We calculate Q_3 using the expression given in [96]:

$$Q_i = \frac{1}{16\pi}\int_{S^3} X_i^{-2} \star \mathcal{F}^i + \frac{1}{2}|\varepsilon_{ijk}|\mathcal{A}^j \wedge \mathcal{F}^k. \tag{4.128}$$

First we note that

$$\frac{1}{2}|\varepsilon_{3jk}|\mathcal{A}^j \wedge \mathcal{F}^k = \mathcal{A}^1 \wedge \mathcal{F}^1 \tag{4.129}$$

$$= \frac{1}{3!}\mathcal{A}_a\mathcal{F}_{bc}dx^a \wedge dx^b \wedge dx^c \tag{4.130}$$

and over the sphere at infinity this is

$$\frac{1}{16\pi}\int_{S^3}\frac{2}{3!}(\mathcal{A}_\phi\mathcal{F}_{\theta\psi} + \mathcal{A}_\psi\mathcal{F}_{\theta\phi}) \sim \frac{1}{16\pi}\int_{S^3}\mathcal{O}(1/r^4). \tag{4.131}$$

We have

$$\star\mathcal{F}^3 = \frac{1}{3!}(\star\mathcal{F})_{\theta\phi\psi}d\theta\wedge d\phi\wedge d\psi \tag{4.132}$$
$$= \frac{1}{2!}\varepsilon_{\theta\phi\psi}{}^{ab}\mathcal{F}_{ab}d\theta d\phi d\psi \tag{4.133}$$
$$= g_{\theta\theta}[g_{\phi\phi}g_{\psi\psi}\varepsilon^{\theta\phi\psi rt}\mathcal{F}_{rt} + g_{\phi\psi}^2\varepsilon^{\theta\psi\phi rt} + g_{\phi t}g_{\psi\psi}\varepsilon^{\theta t\psi r\phi}\mathcal{F}_{r\phi} \tag{4.134}$$
$$+ g_{\phi t}g_{\psi\phi}\varepsilon^{\theta t\phi r\psi}\mathcal{F}_{r\psi} + g_{\psi t}g_{\psi\psi}\varepsilon^{\theta t\psi r\phi}\mathcal{F}_{r\phi} + g_{\psi t}g_{\psi\phi}\varepsilon^{\theta t\phi r\psi}\mathcal{F}_{r\psi}]d\theta d\phi d\psi. \tag{4.135}$$

The asymptotic metric is

$$\det g = \frac{\sin^2\theta\cos^2\theta}{\Xi_a\Xi_b}r^6, \tag{4.136}$$

and the r-dependence of the metric and the relevant components of the gauge field strength F are

$$\mathcal{F}_{rt}\sim\frac{1}{r^3}\qquad \mathcal{F}_{r\phi}\sim\frac{1}{r^3}\qquad \mathcal{F}_{r\psi}\sim\frac{1}{r^3},\qquad g_{t\phi}\sim g_{t\psi}\sim g_{\phi\psi}\sim\frac{1}{r^2}, \tag{4.137}$$

$$g_{\theta\theta} = \frac{1}{\Delta_\theta}r^2+\mathcal{O}(1)\qquad g_{\phi\phi} = \frac{\sin^2\theta}{\Xi_a}r^2+\mathcal{O}(1)\qquad g_{\psi\psi} = \frac{\cos^2\theta}{\Xi_b}r^2+\mathcal{O}(1). \tag{4.138}$$

Also $X_3^{-2}\sim 1$ so for $\varepsilon^{tr\theta\phi\psi}=1$ we have

$$Q_3 = -\frac{1}{16\pi}\int_{S^3} g_{\theta\theta}g_{\phi\phi}g_{\psi\psi}\frac{\mathcal{F}_{rt}}{\sqrt{\det g}}d\theta d\phi d\psi \tag{4.139}$$
$$= -\frac{1}{16\pi}\frac{2abqg^2}{\Xi_a\Xi_b}\int_{S^3}\sin\theta\cos\theta d\theta d\phi d\psi \tag{4.140}$$
$$= -\frac{abms^2\pi g^2}{2\Xi_a\Xi_b}, \tag{4.141}$$

where we have used

$$\mathcal{F}_{rt} = \frac{2abq\Delta_\theta g^2}{\Xi_a^2\Xi_b^2r^3}+\mathcal{O}(r^{-5}). \tag{4.142}$$

We now calculate Q_1:

$$Q_1 = \frac{1}{16\pi}\int_{S^3} X_1^{-2}\star\mathcal{F}^1 + \frac{1}{2}|\varepsilon_{1jk}|\mathcal{A}^j\wedge\mathcal{F}^k \tag{4.143}$$
$$= \frac{1}{16\pi}\int_{S^3} X_1^{-2}\star\mathcal{F}^1 + \frac{2}{3!}[\mathcal{A}_\phi^1\mathcal{F}_{\theta\psi}^3 + \mathcal{A}_\psi^1\theta\phi^3 + \mathcal{A}_\phi^3\mathcal{F}_{\theta\psi}^1 + \mathcal{A}_\psi^3\theta\phi^1]d\theta d\phi d\psi \tag{4.144}$$
$$= \frac{1}{16\pi}\int_{S^3} X_1^{-2}\star\mathcal{F}^1 + \mathcal{O}(1/r^4). \tag{4.145}$$

We apply the same procedure as above to find

$$Q_1 = -\frac{1}{16\pi}\int_{S^3} g_{\theta\theta}g_{\phi\phi}g_{\psi\psi}\frac{\mathcal{F}_{rt}^1}{\sqrt{\det g}}d\theta d\phi d\psi \tag{4.146}$$
$$= -\frac{1}{16\pi}\int_{S^3}\left(-\frac{2\sqrt{q(q+2m)}}{\Xi_a\Xi_b}\sin\theta\cos\theta\right)d\theta d\phi d\psi \tag{4.147}$$
$$= \frac{msc\pi}{2\Xi_a\Xi_b} \tag{4.148}$$

in agreement with the literature.

4.C Null self dual orbifold: static (near-)EVH

Here, we outline the appearance of the null orbifold for the static EVH (4.28) and near-EVH (4.30) configurations.

In the static EVH case, we define

$$\sigma^+ = \frac{t}{\ell_3} + \frac{\ell}{\sqrt{q}}\psi_3 = \frac{\tilde{x}^+}{\epsilon^2}, \qquad \sigma^- = -\frac{t}{\ell_3} + \frac{\ell}{\sqrt{q}}\psi_3. \tag{4.149}$$

Taking the $\epsilon \to 0$ limit gives a product of the null selfdual orbifold (1.183) and a transverse manifold,

$$ds^2 = \mu_3\left[\rho^2 d\tilde{x}^+ d\sigma^- + \frac{\ell_3^2 d\rho^2}{\rho^2}\right] + q\mu_3\left(d\theta^2 + \sin^2\theta d\phi^2 + \cos^2\theta d\psi^2\right) \tag{4.150}$$

$$+ \frac{\ell^2}{\mu_3}(d\mu_1^2 + d\mu_2^2 + \mu_1^2\left(d\psi_1^2 - \Omega_1^{(0)}t\right)^2 + \mu_2^2\left(d\psi_2^2 - \Omega_1^{(0)}t\right)^2), \tag{4.151}$$

where $\tilde{x}^+$ decompatifies and σ^- remains compact. This is the near horizon limit of a massless BTZ black hole.

In the near-EVH case, we first we take the extremal limit so that $x_+ = x- = x_0$. We make the following coordinate redefinitions

$$\sigma \equiv x^2 - x_0^2, \qquad t = \frac{\ell}{\sqrt{q}}\frac{\tau}{\epsilon^2}, \qquad \psi_3 = -\hat{\psi}_3 - \frac{\tau}{\ell_3\epsilon^2}, \qquad \psi_i = \hat{\psi}_i + \Omega_i^{(0)}\frac{\ell}{\sqrt{q}}\frac{\tau}{\epsilon^2} \tag{4.152}$$

and

$$\phi^S = \hat{\phi}^S + \frac{\tau}{\epsilon}\left(\frac{\hat{a}\ell\mathbf{Y}_s}{q\sqrt{q}} + \frac{\hat{b}\ell}{q\ell_3}\right), \qquad \psi^S = \hat{\psi}^S + \frac{\tau}{\epsilon}\left(\frac{\hat{b}\ell\mathbf{Y}_s}{q\sqrt{q}} + \frac{\hat{a}\ell}{q\ell_3}\right) \tag{4.153}$$

to get a geometry containing the null orbifold introduced in section 1.7:

$$ds^2 = \mu_3\left[\ell_3^2\frac{d\sigma^2}{4\sigma^2} + \frac{2\sigma}{\ell_3}d\hat{\psi}_3 d\tau\right]$$

$$+ q\mu_3(d\theta^2 + \sin^2\theta d\hat{\phi}^2 + \cos^2\theta d\hat{\psi}^2) + \frac{\ell^2}{\mu_3}(d\mu_1^2 + d\mu_2^2 + \mu_1^2 d\hat{\psi}_1^2 + \mu_2^2 d\hat{\psi}_2^2). \tag{4.154}$$

As in the null orbifold discussion in Chapter 3, the second order contribution from expansion of the coefficients of the τ direction in the S^3 may give rise to non-trivial gauge fields.

4.D Choice of U(1)

We can impose constraints on the coefficients of χ, ξ (4.57) to ensure that they have a $2\pi n$ periodicity:

$$C_1 = \frac{1}{n(\frac{q}{al}+1)}, \qquad C_3 = \frac{1}{n(\frac{q}{al}+1)} - n, \qquad n \in \mathbb{Z}. \tag{4.155}$$

For generic C_1 and pinching $\chi = \frac{\hat{\chi}}{\epsilon}$, the 3d part of the metric (4.62) looks like

$$\left[-x^2\frac{d\tau^2}{\ell_3^2} + \ell_3^2\frac{dx^2}{x^2} + \tilde{Q}^2 C_1^2 x^2 d\hat{\chi}^2\right], \tag{4.156}$$

where $\tilde{Q}^2 = \frac{a^2+q}{a^2}$. We can rewrite it as

$$\tilde{Q}^2 C_1^2\left[-x^2\frac{dT^2}{L_3^2} + L_3^2\frac{dx^2}{x^2} + x^2 d\hat{\chi}^2\right], \tag{4.157}$$

with

$$L_3^2 = \frac{\ell_3^2}{\tilde{Q}^2 C_1^2}, \qquad T = \frac{\tau}{\tilde{Q}^2 C_1^2}. \tag{4.158}$$

The 3d Newton's constant transforms as

$$\frac{1}{G_3} = \frac{1}{G_{10}} \int \left(\tilde{Q}^2 C_1^2\right)^{3/2} \sqrt{\ldots} \tag{4.159}$$

so under the redefinition (4.157) the Newton's constant is

$$\frac{1}{G_3'} = \frac{\tilde{Q}^3 C_1^3}{G_3}, \tag{4.160}$$

and the central charge scales like

$$c' = \frac{3L_3}{2G_3'} = \tilde{Q}^2 C_1^2 c. \tag{4.161}$$

The BTZ temperature and angular momentum transform as

$$T'_{\rm BTZ} = \frac{x_+^2 - x_-^2}{2\pi x_+ L_3^2} = \tilde{Q}^2 C_1^2 T_{\rm BTZ}, \qquad \Omega'_{BTZ} = \frac{x_- x_+}{L_3 x_+^2} = \tilde{Q} C_1 \Omega_{BTZ}. \tag{4.162}$$

The BTZ entropy, mass and angular momentum will be

$$S'_{\rm BTZ} = \frac{2\pi \cdot x_+}{4G_3'} = \tilde{Q}^3 C_1^3 S_{\rm BTZ}, \tag{4.163}$$

$$M'_{\rm BTZ} = \frac{x_+^2 + x_-^2}{8L_3^2 G_3'} = \tilde{Q}^5 C_1^5 M_{\rm BTZ}, \qquad J'_{\rm BTZ} = \frac{x_+ x_-}{4L_3 G_3'} = \tilde{Q}^4 C_1^4 J_{\rm BTZ}. \tag{4.164}$$

It is straighforward to check that the first law of thermodynamics for a BTZ black hole is invariant under the choice of U(1).

To sum up, the choice of C_1 alters the AdS_3 radius, time coordinate scaling, and consequently G_3 and c. As a result the BTZ thermodynamic quantities in the first law will have individual scaling dictated by C_1 such that the BTZ first law is invariant.

4.E Near Horizon Geometries as 5 Dimensional Geometries

As discussed in section 4.3.3, for the rotating EVH case there is a freedom in choosing the χ angle. In particular, one may choose it to be proportional to ψ, corresponding to $C_3 = 0$. With this choice, the near horizon geometry may be taken over the 5d black hole solution (4.3) without considering the 10d uplift. To this end, consider the following scalings

$$r = \frac{a}{\sqrt{a^2+q}}\epsilon x, \quad t = \frac{\sqrt{a^2+q}}{a}\frac{\tau}{\epsilon}, \quad \psi = \frac{\tilde{\psi}}{\epsilon}, \quad \phi = \tilde{\phi} + \frac{l^2 - a^2}{l^2 a\sqrt{a^2+q}}\frac{\tau}{\epsilon} \tag{4.165}$$

Taking $\epsilon \to 0$, we get following geometry

$$\begin{aligned} ds^2 = {} & \frac{a^{\frac{2}{3}}\cos^{\frac{2}{3}}\theta}{(q+a^2)^{\frac{1}{3}}} h_1^{\frac{4}{3}} \Bigg[-\frac{(x^2 - x_+^2)(x^2 - x_-^2)}{\ell_3^2 x^2} d\tau^2 + \frac{\ell_3^2 x^2 dx^2}{(x^2 - x_+^2)(x^2 - x_-^2)} + x^2 (d\tilde{\psi} - \frac{x_+ x_-}{\ell_3 x^2} d\tau)^2 \Bigg] \\ & \frac{a^{\frac{2}{3}}\cos^{\frac{2}{3}}\theta}{\Delta_\theta} (a^2+q)^{\frac{2}{3}} h_1^{\frac{4}{3}} \left(d\theta^2 + \frac{\Delta_\theta^2 \sin^2\theta}{\Sigma_a^2 h_1^4} d\tilde{\phi}^2 \right). \end{aligned} \tag{4.166}$$

Scalar fields and non-zero components of gauge fields in this limit are given by

$$X_1 = X_2 = \frac{a^{\frac{2}{3}} \cos^{\frac{2}{3}} \theta}{(a^2+q)^{\frac{1}{3}} h_1^{\frac{2}{3}}}, \quad X_3 = \frac{(a^2+q)^{\frac{2}{3}} h_1^{\frac{3}{3}}}{a^{\frac{4}{3}} \cos^{\frac{4}{3}} \theta} \tag{4.167}$$

$$F^{(1)}_{\theta\tilde{\phi}} = F^{(2)}_{\theta\tilde{\phi}} = -\frac{2a\sqrt{q(1+\frac{q}{l^2})}\sin\theta\cos\theta}{\Sigma_a h_1^4 \sqrt{q+a^2}}. \tag{4.168}$$

Chapter 5

Summary and Outlook

We conclude the thesis by summarising our results and pointing to open questions.

In section 1.8 we introduced the set of extremal vanishing horizon (EVH) black holes (1.196), which by definition have zero temperature and area. The area vanishes because a one-cycle in the EVH black hole geometry shrinks to zero size, resulting in the near horizon region of these black holes containing a local AdS_3 factor (1.194), with a pinched angular direction. The emergence of this near horizon factor gives an indication, via the AdS_3/CFT_2 correspondence (section 1.4), of the existence of a dual 2d CFT description for the EVH black holes. EVH black holes can be excited to near-EVH black holes, with arbitrarily small temperature, area and Newton's constant such that their entropy remains finite. The near horizon AdS_3 factor is excited to a BTZ geometry for these black holes. This asymptotically AdS_3 geometry in the near horizon throat of near-EVH black holes motivated the EVH/CFT correspondence (1.195), which states that gravity near the horizon of an EVH black hole has a dual description in terms of a two dimensional conformal field theory. While in four dimensions it has been proved [51] that the appearance of an AdS_3 throat is generic, and that the near horizon limit is a decoupling limit, in five dimensions these are open questions. The EVH/CFT correspondence in five dimensions has been studied case by case in [28, 34].

Chapter 2 was an investigation into the low temperature expansion of the first law of thermodynamics (2.21) for black holes in generic dimension and background. Associated to black holes are $n+1$ conserved charges, parameterised by a set of variables that span the $n+1$-dimensional black hole parameter space. A generic black hole is represented by a point in this space. An extremal black hole obeys the constraint $T_{\rm H}=0$ so that it is represented by a point on the n-dimensional extremal surface. Infinitesimal movement, measured by a small number ϵ, in parameter space off this extremal surface corresponds to shifting the temperature of the black hole to some value that is proportional to ϵ. We Taylor expanded the components of the first law in ϵ and found that the leading order contribution to the first law is an expression for the entropy (2.37) that is compatible with the Cardy formula for the entropy of a chiral 2d CFT. Our result can be viewed as a thermodynamic derivation of the Frolov-Thorne temperatures (1.150) and, for black holes with one conserved charge, the central charge discussed in the Kerr/CFT correspondence (section 1.5). Our expression also agrees with Sen's entropy function result (2.41), and is reinforced by an analysis of the density matrix of a scalar probe in the relevant black hole background (2.54).

We then applied this first law analysis to the subset of near-EVH black holes. EVH black holes are represented by points on the $(n+1-k)$-dimensional EVH surface, where k is the number of parameters we set to zero to achieve both $T_{\rm H}=0$ and a zero horizon size. Again, orthogonal movement off the EVH surface corresponds to injecting some small temperature of order ϵ into the black hole configuration. It will also increase the horizon size so that the black hole area is $\mathcal{O}(\epsilon)$.

We took into account the fact that in the near horizon region of EVH black holes, the geometry contains a pinching AdS_3 orbifold. The near horizon limit (2.58) provided us with clues as to how to categorise the black hole potentials and charges in the near-EVH regime, and rotations in the directions transverse to the near horizon AdS_3 led us to identities (2.64) satisfied by the associated potentials.

The charges and potentials of near-EVH black holes can be distributed into specific arrangements according to their ϵ expansions, which we defined to be BTZ mass and angular momentum (2.67). We deduced that the angular velocity in the pinching direction is the BTZ angular velocity, and established that these quantities obey the first law of thermodynamics for BTZ black holes (2.66). This result is remarkable, as it does not require details of a BTZ geometry; although we assumed the existence of a single vanishing horizon cycle (and smoothness of the $r \to 0$ geometry), we did not specify the geometric excitations, and the *thermodynamic* excitations allude to the existence of a BTZ black hole in the near horizon geometry.

Our result is again fortified by a scalar probe analysis, from which we deduced that a scalar probe in the background of a near-EVH black hole (2.72) is the same as one in a BTZ background.

As the black holes we studied (2.27) are quite generic, our result suggests that any near-EVH black hole should contain a near horizon BTZ factor. This suggestion remains to be proved.

Chapters 3 and 4 were case studies of the EVH/CFT correspondence and our first law analysis in five dimensions. We chose asymptotically AdS_5 black holes with the intention of comparing the dual $\mathcal{N} = 4$ super Yang-Mills theory descriptions with the two dimensional dual descriptions of the AdS_3 factor in the near horizon geometries.

The near-EVH limit of static three charged non-BPS black holes was obtained by sending one charge parameter to zero, which geometrically corresponds to a vanishing one-cycle in the transverse S^5. The near horizon geometry contains a BTZ black hole built on a pinching AdS_3 geometry, as advocated by the EVH/CFT correspondence. The entropy of this near horizon BTZ black hole entirely captures the entropy of the UV black hole in the near-EVH limit. We demonstrated explicitly how the black hole charges in the near-EVH regime arrange themselves into the BTZ mass and angular momentum (3.82-3.83) that obey the first law for a BTZ black hole (3.84). We stress once again how this result is at the level of the near-EVH limit of the conserved charges in the UV theory, and is independent of, while complementary to, the BTZ geometry.

On the CFT side, we calculated the central charge of the CFT_2 using Brown and Henneaux's expression (1.32) and taking the pinching into account (section 1.7). The near horizon BTZ mass and angular momentum were used as per section 1.4 to compute the quantum numbers $\Delta_{2d}, \mathcal{J}_{2d}$ of the dual two dimensional conformal field theory. We discussed the large N limit (3.67) for which all AdS and CFT quantities are finite. The $\mathcal{N} = 4$ super Yang-Mills theory charges in the near-EVH near horizon limit describe a sector of the full UV theory. We demonstrated how, in a similar fashion to the first law analysis, the IR charges arrange into quantities $\Delta_{IR}, \mathcal{J}_{IR}$ that agree, up to a "ground state" contribution, with the CFT_2 quantum numbers $\mathcal{J}_{2d}, \Delta_{2d}$ (3.97-3.101). This result, which indicates that the near-EVH near horizon limit of the $\mathcal{N} = 4$ super Yang-Mills theory can be described in terms of a two dimensional field theory, is further evidence in favour of the EVH/CFT correspondence.

The Kerr/CFT correspondence (section 1.5) can also be applied to the static charged black holes, indicating the existence of three inequivalent chiral dual CFT descriptions. We compared the Kerr/CFT result in the near-EVH regime with the strictly extremal limit of our EVH/CFT results. In the overlap of parameters, in the large N limit, one Kerr/CFT central charge is kept finite, and the EVH CFT_2 is constrained to its chiral sector. The Kerr/CFT central charge corresponding to the vanishing U(1) matches the Brown Henneaux result (3.121) in the overlap of parameters, and we concluded that the relevant Kerr/CFT description is the DLCQ of the non-chiral CFT that emerges in our EVH/CFT picture.

We also examined the near-EVH regime when the black holes are near-BPS. As ten dimensional supergravity solutions, the BPS black holes are interpreted as distributions of spherical three dimensional giant gravitons rotating in the transverse S^5. Exciting the system slightly away from BPS-ness corresponds to exciting degrees of freedom associated to open strings that stretch between giants [34]. These giants are the source of electric charge in the 5d theory and the number of giants of each type is proportional to each electric charge of the AdS_5 black hole. Since each giant type involves a different $S^3 \subset S^5$, pairs of giants of different species intersect on circles.

The near-EVH near-BPS limit does not obviously fit in with the EVH/CFT correspondence prescription, as the temperature is kept finite in this limit, and there is no "pinching" in the near horizon limit. The near horizon limit does, however, contain a BTZ factor, signalling the

existence of a dual 2d CFT description. In this limit, the number of giants of one species is very small, as its corresponding charge. Pairs of giants of the other two species in this "dilute giant approximation" intersect on the circle associated to the vanishing charge. This S^1 is the angular direction of the (*not pinching*) BTZ black hole.

Ensuring the near horizon geometry remains on shell [75] requires that when we zoom in on the horizon, we focus on a strip of the S^5. For this reason, the thermodynamic quantities $S_{\rm BTZ}$, $M_{\rm BTZ}$, $J_{\rm BTZ}$ are multiplied by a "volume factor" and can be understood as the quantities calculated "per strip". As we lose information of the integration measure of the S^5 when we focussed on the strip, we do not know how to properly integrate these quantities over all strips. However, the identity (3.62) suggests that a suitable integration would result in the BTZ entropy exactly matching the UV entropy in the near-EVH regime, as for the non-BPS case.

The central charge of the dual CFT (3.70) gives, up to the "volume factor", the number of giant graviton intersections. The giants are intersecting on the angular direction of the near horizon BTZ, and the near-BPS excitations can be viewed as stringy excitations. This is evidence that the dual two dimensional CFT describes strings stretched between these giants.

We discussed in some detail the appropriate N scaling to take in the near-BPS regime. In the large N limit (3.80), the number of giants and all BTZ and CFT quantities are finite. We found again that the $\mathcal{N} = 4$ super Yang-Mills theory charges in the near-EVH near horizon limit $\Delta_{\rm IR}, \mathcal{J}_{\rm IR}$ match, up to the "volume factor", those of our emergent 2d CFT.

Connecting with the Kerr/CFT correspondence was analogous (up to the "volume factor") to the non-BPS case, with the extra result that the relevant Kerr/CFT central charge (3.124) is exactly equal to the number of giant graviton intersections, which can be viewed as more evidence in favour of the "strings between giants" interpretation.

We emphasise again that near-EVH near-BPS black holes do not satisfy the conditions, namely a pinching angle and vanishing temperature, shared by the EVH/CFT correpondence and the first law analysis. Nevertheless, the first law obeyed by these black holes is the BTZ first law (3.94), independently of the "volume factor" and scaling of N. It is encouranging that our first law result applies to these near-BPS black holes, and it is a natural future project to derive the IR first law result in a more generic near-EVH regime that includes non-zero temperature and regular AdS_3 angle.

In Chapter 4 we extended our analysis of asymptotically AdS_5 black holes to the set of rotating charged black holes. These black holes have one independent electric charge and rotate in two planes in the AdS_5. They also have associated to them an additional electric charge Q_3 (4.8) that is dependent on this rotation. The near-EVH limit can be taken by sending one (rotating) or both (nearly-static) angular momenta to zero, resulting in a vanishing Q_3.

The nearly-static near-EVH black hole has a near horizon geometry containing a pinching BTZ black hole and a rotating S^3. The diffeomorphisms (4.45) shift the BTZ to a co-rotating frame. In the rotating case, the near horizon BTZ is trivially fibred by a compact seven dimensional manifold, while its angular variable is a linear combination of the angles associated to the vanishing momentum and Q_3. We noted that there is some freedom in choosing this combination.

While the appearance of a near horizon BTZ requires a ten dimensional uplift for all static and nearly-static near-EVH black holes, this is not required in the rotating case.

The calculation of the BTZ entropy, mass and angular momentum, and the Brown Henneaux central charge was analogous for the nearly-static and rotating regimes. We took into consideration the pinching of the BTZ angle to find that the entropy of the BTZ black hole is in exact agreement with the near-EVH limit of the UV black hole. Our expressions for the BTZ thermodynamic quantities and dual CFT_2 central charge indicated that our near-EVH near horizon limit should be accompanied by a large N limit (4.72), in which all quantities are kept finite.

In our first law analysis for the nearly-static black hole, the coefficients of the "co-rotating" diffeomorphism contributed to the mass and angular momentum terms in the BTZ first law (4.83) as expected. For the rotating near-EVH black hole, the appropriate UV conserved charges arranged themselves into the BTZ mass (4.85), and the angular momenta corresponding to the angles that combined to give the BTZ angle summed to give the BTZ angular momentum (4.89), so that the first law again reduced to the BTZ first law (4.90). The invariant nature of the first law result was underlined by its independence of the angular combination (4.57).

The UV quantum numbers of the $\mathcal{N} = 4$ super Yang-Mills theory dual to the rotating near-EVH black holes organise themselves into $\Delta_{\rm IR}, \mathcal{J}_{\rm IR}$ that exactly agree, modulo the ground state term (4.103), with $\Delta_{\rm 2d}, \mathcal{J}_{\rm 2d}$. While this is yet more evidence that near-EVH AdS_5 black holes are described by dual 2d CFTs, the nearly-static case requires more study. Here, the rotations in the S^3 in the near-EVH limit correspond to gauge fields from a three dimensional point of view. Moving to a co-rotating frame is associated to a spectral flow in the dual CFT_2, resulting in residual terms in the comparison between the IR and 2d quantum numbers (4.97). These terms require further understanding, which is postponed to future work.

Comparing the Kerr/CFT central charges to the Brown Henneaux value in the rotating near-EVH regime returned the expected result. Following [81], the effective Kerr/CFT central charge associated to the pinching angle agrees with the Brown Henneaux result (4.119), while all other central charges are subleading. We can again surmise that the CFT_2 charge associated to this charge is the DLCQ of the non-chiral CFT that emerges in the EVH/CFT correspondence.

The contribution of the rotating S^3 arose again in the comparison of our CFT_2 description with the Kerr/CFT result. In the region of parameters where the two proposals overlap, the Kerr/CFT central charge (4.119) associated to the angle we pinched exactly matches our Brown Henneaux computation. There are also two further Kerr/CFT central charges that remain finite in the large N limit, associated with the rotations transverse to the BTZ in the near horizon geometry. The finiteness of these charges in the near-EVH limit deserves further investigation.

One avenue we did not go down is the near-BPS limit of the rotating charged black holes. The ten dimensional picture of these black holes is of giant gravitons rotating in both the S^5 and in the azimuthal planes of AdS_5. It would be interesting to investigate the near-EVH limit in terms of excitations of these giants. Related to this limit, it is clear that although we have provided both thermodynamic and case study evidence in favour of the EVH/CFT correspondence, a more generic prescription of the correspondence, where the temperature is not necessarily zero and the AdS_3 angle does not have to be pinched, would be desirable. We also have yet to prove the five, and higher, dimensional EVH/CFT statement: that a generic EVH black hole has a dual description in terms of a two dimensional conformal field theory. A natural step in this direction is to prove that generic near-EVH black holes have near horizon BTZ factors, and that the near horizon limit is a decoupling limit.

Appendix A

Frolov-Thorne Temperatures

In this Appendix, we calculate the Frolov-Thorne temperatures [93] associated to the near horizon region of a near-extremal black hole. We follow [94] by considering a quantum field in a black hole background at finite temperature, i.e. one assumes the black hole is not extremal. Its quantum state is mixed and described by a density matrix whose eigenvalues equal the standard Boltzmann factors

$$\exp\left[-\beta\left(\omega-\sum_{i=1}^{n} n_i\Omega_i\right)\right], \tag{A.1}$$

where Ω_i denote angular momenta for $i=1,\ldots,m$, and chemical potentials for $i=m+1,\ldots,n$. Notice the "chemical" potentials are fully determined by the black hole geometry, while the quantum numbers $\{\omega, n_i\}$ label the quantum state.

Whenever an extremal limit in the black hole geometry is taken, we can study the behaviour of the above eigenvalues by parameterising the limit. Since all chemical potentials are a *function* of the horizon radius, and the extremal limit can be described as the limit $r_+ = r_0 + \epsilon\rho$ with $\epsilon \to 0$, we expand (A.1) in ϵ, while using the fact that $T_{\rm H} = T_{\rm H}(r_0) + \epsilon\rho T'_{\rm H}(r_0) = \epsilon\rho T'_{\rm H}(r_0)$. We expect two terms, one divergent and one finite. Indeed, by direct calculation, we obtain

$$\exp\left[-\frac{1}{T'_H(r_0)\epsilon\rho}\left(\omega-\sum_{i=1}^{n} n_i\Omega_i^0\right)+\frac{1}{T'_H(r_0)}\sum_{i=1}^{n} n_i\Omega'_i(r_0)\right]. \tag{A.2}$$

In order to avoid a vanishing probability in the extremal $\epsilon \to 0$ limit, we require the divergent piece to vanish, i.e. $\omega = \sum_i \Omega_i^0 n_i + \mathcal{O}(\epsilon^\alpha)$. Notice this constrains the energy quantum of the scalar fields in terms of the remaining modes. The remaining diagonal density matrix becomes

$$\exp\left[\frac{1}{T'_H(r_0)}\sum_{i=1}^{n} n_i\Omega'_i(r_0)\right] = \exp\left[-\sum_{i=1}^{n}\frac{n_i}{T_i}\right] = \hat{\varrho}, \tag{A.3}$$

allowing us to identify the Frolov-Thorne temperatures as

$$T_i = -\frac{T'_H(r_0)}{\Omega'_i(r_0)}. \tag{A.4}$$

Bibliography

[1] S. W. Hawking, "Particle Creation by Black Holes," Commun. Math. Phys. **43** (1975) 199 .

[2] J. D. Bekenstein, "Black holes and entropy," Phys. Rev. D **7**, 2333 (1973).

[3] J. M. Bardeen, B. Carter and S. W. Hawking, "The Four laws of black hole mechanics," Commun. Math. Phys. **31**, 161 (1973).

[4] A. Strominger and C. Vafa, "Microscopic origin of the Bekenstein-Hawking entropy," Phys. Lett. B **379** (1996) 99 [hep-th/9601029].

[5] J. R. David, G. Mandal and S. R. Wadia, "Microscopic formulation of black holes in string theory," Phys. Rept. **369**, 549 (2002) [hep-th/0203048].

[6] J. Polchinski, "Dirichlet Branes and Ramond-Ramond charges," Phys. Rev. Lett. **75** (1995) 4724 [hep-th/9510017].

[7] J. C. Breckenridge, D. A. Lowe, R. C. Myers, A. W. Peet, A. Strominger and C. Vafa, "Macroscopic and microscopic entropy of near extremal spinning black holes," Phys. Lett. B **381** (1996) 423 [hep-th/9603078].

[8] Horowitz, Gary T.; Roberts, Matthew M.; "Counting the Microstates of a Kerr Black Hole in M Theory"; Phys. Rev. Lett. 99 (2007) 221601.

[9] R. Emparan and G. T. Horowitz, "Microstates of a Neutral Black Hole in M Theory," Phys. Rev. Lett. **97** (2006) 141601 [hep-th/0607023].

[10] G. T. Horowitz, J. M. Maldacena and A. Strominger, "Nonextremal black hole microstates and U duality," Phys. Lett. B **383** (1996) 151 [hep-th/9603109].

[11] Jeffrey E. McClintock, Rebecca Shafee, Ramesh Narayan, Ronald A. Remillard, Shane W. Davis, Li-Xin Li, "The Spin of the Near-Extreme Kerr Black Hole GRS 1915+105", Astrophys.J.652:518-539,2006, arXiv:astro-ph/0606076.

[12] C.R. Stephens, G. 't Hooft, B.F. Whiting, "Black Hole Evaporation without Information Loss", Class.Quant.Grav.11:621-648,1994, arXiv:gr-qc/9310006.

L. Susskind, "The World as a Hologram", J.Math.Phys.36:6377-6396,1995, arXiv:hep-th/9409089.

[13] A. Castro, A. Maloney and A. Strominger, "Hidden Conformal Symmetry of the Kerr Black Hole," Phys. Rev. D **82** (2010) 024008 [arXiv:1004.0996 [hep-th]].

[14] S. Carlip, "Black hole entropy from conformal field theory in any dimension," Phys. Rev. Lett. **82** (1999) 2828 [hep-th/9812013].

[15] S. N. Solodukhin, "Conformal description of horizon's states," Phys. Lett. B **454** (1999) 213 [hep-th/9812056].

[16] J. D. Brown and M. Henneaux, "Central Charges in the Canonical Realization of Asymptotic Symmetries: An Example from Three-Dimensional Gravity," Commun. Math. Phys. **104** (1986) 207.

[17] Dirac, P. A. M., "The theory of gravitation in Hamiltonian form", Proc. Roy. Soc. A246, 333 (1958).

[18] Piero Giovanni Luca Mana, "Asymptotic symmetries of anti-de Sitter space in two and three dimensions", PhD Thesis, The University of Cagliari

[19] P. Di Francesco, P. Mathieu, and D. Snchal, "Conformal Field Theory", Springer-Verlag, New York, 1997. ISBN 0-387-94785-X.

[20] David Tong, "Lectures on String Theory", arXiv:0908.0333v2 [hep-th].

[21] J. M. Maldacena, "The Large N limit of superconformal field theories and supergravity," Adv. Theor. Math. Phys. **2** (1998) 231 [hep-th/9711200].

[22] L. Susskind and E. Witten, "The Holographic bound in anti-de Sitter space," hep-th/9805114.

[23] A. W. Peet and J. Polchinski, "UV / IR relations in AdS dynamics," Phys. Rev. D **59** (1999) 065011 [hep-th/9809022].

[24] E. Witten, Anti-de Sitter space and holography, Adv. Theor. Math. Phys. 2 (1998) 253 [arXiv:hep- th/9802150].

[25] E. Witten, "Anti-de Sitter space, thermal phase transition, and confinement in gauge theories," Adv. Theor. Math. Phys. **2** (1998) 505 [hep-th/9803131].

[26] S. Carlip, "Conformal Field Theory, (2+1)-Dimensional Gravity, and the BTZ Black Hole", Class.Quant.Grav.22:R85-R124,2005, arXiv:gr-qc/0503022.

[27] Per Kraus, "Lectures on black holes and the AdS_3 / CFT_2 correspondence", Lect.NotesPhys.755:193-247,2008, arXiv:hep-th/0609074.

[28] R. Fareghbal, C. N. Gowdigere, A. E. Mosaffa, M. M. Sheikh-Jabbari, "Nearing Extremal Intersecting Giants and New Decoupled Sectors in N = 4 SYM," JHEP **0808** (2008) 070. [arXiv:0801.4457 [hep-th]].

[29] J. L. Cardy, "Operator Content of Two-Dimensional Conformally Invariant Theories," Nucl. Phys. B **270** (1986) 186.

[30] R. M. Wald, "Black hole entropy is the Noether charge," Phys. Rev. D **48**, 3427 (1993) [gr-qc/9307038].
V. Iyer and R. M. Wald, "Some properties of Noether charge and a proposal for dynamical black hole entropy," Phys. Rev. D **50**, 846 (1994) [gr-qc/9403028].

[31] M. Guica, T. Hartman, W. Song, A. Strominger, "The Kerr/CFT Correspondence," Phys. Rev. **D80** (2009) 124008. [arXiv:0809.4266 [hep-th]].

[32] G. Barnich, F. Brandt, "Covariant theory of asymptotic symmetries, conservation laws and central charges," Nucl. Phys. **B633** (2002) 3-82. [arXiv:hep-th/0111246 [hep-th]].

[33] R. P. Kerr, Phys. Rev. Lett. 11 (1963) 237.
Gravitational field of: Matt Visser, "The Kerr spacetime: A brief introduction", arXiv:0706.0622 [gr-qc].

[34] V. Balasubramanian, J. de Boer, V. Jejjala, J. Simon, "Entropy of near-extremal black holes in AdS(5)," JHEP **0805** (2008) 067. [arXiv:0707.3601 [hep-th]].

[35] R. Fareghbal, C. N. Gowdigere, A. E. Mosaffa *et al.*, "Nearing 11d Extremal Intersecting Giants and New Decoupled Sectors in D = 3,6 SCFT's," Phys. Rev. **D81**, 046005 (2010), [arXiv:0805.0203 [hep-th]].

[36] H. Lu, J. Mei and C. N. Pope, Kerr/CFT Correspondence in Diverse Dimensions,JHEP 0904:054,2009, arXiv:0811.2225 [hep-th].
D. D. K. Chow, M. Cvetic, H. Lu and C. N. Pope, Extremal Black Hole/CFT Correspondence in (Gauged) Supergravities, Phys.Rev.D79:084018,2009, arXiv:0812.2918 [hep-th].
T. Azeyanagi, N. Ogawa and S. Terashima, Holographic Duals of Kaluza-Klein Black Holes, JHEP 0904:061,2009, arXiv:0811.4177 [hep-th].
H. Isono, T. S. Tai and W. Y. Wen, Kerr/CFT correspondence and ve-dimensional BMPV black holes, Int.J.Mod.Phys.A24:5659-5668,2009, arXiv:0812.4440 [hep-th].
C. M. Chen and J. E. Wang, Holographic Duals of Black Holes in Five-dimensional Minimal Supergravity, arXiv:0901.0538 [hep-th].
F. Loran and H. Soltanpanahi, Near the horizon of 5D black rings, JHEP 0903, 035 (2009) [arXiv:0810.2620 [hep-th]]; 5D Extremal Rotating Black Holes and CFT duals, Class.Quant.Grav.26:155019,2009, arXiv:0901.1595 [hep-th].
H. Lu, J. w. Mei, C. N. Pope and J. F. Vazquez-Poritz, Extremal Static AdS Black Hole/CFT Correspondence in Gauged Supergravities, Phys. Lett. B 673, 77 (2009) [arXiv:0901.1677 [hep-th]].
19G. Compere, K. Murata and T. Nishioka, Central Charges in Extreme Black Hole/CFT Correspondence, JHEP 0905:077,2009, arXiv:0902.1001 [hep-th].
T. Azeyanagi, N. Ogawa and S. Terashima, The Kerr/CFT Correspondence and String Theory, Phys.Rev.D79:106009,2009, arXiv:0812.4883 [hep-th].

[37] H. K. Kunduri, J. Lucietti and H. S. Reall, "Near-horizon symmetries of extremal black holes," Class. Quant. Grav. **24** (2007) 4169 [arXiv:0705.4214 [hep-th]].

[38] D. D. K. Chow, M. Cvetic, H. Lu and C. N. Pope, "Extremal Black Hole/CFT Correspondence in (Gauged) Supergravities," Phys. Rev. D **79**, 084018 (2009) [arXiv:0812.2918 [hep-th]].

[39] T. Hartman, K. Murata, T. Nishioka, A. Strominger, "CFT Duals for Extreme Black Holes," JHEP **0904** (2009) 019. [arXiv:0811.4393 [hep-th]].

[40] V. Balasubramanian, J. de Boer, M. M. Sheikh-Jabbari, J. Simon, "What is a chiral 2d CFT? And what does it have to do with extremal black holes?," JHEP **1002** (2010) 017. [arXiv:0906.3272 [hep-th]].

[41] J. M. Maldacena, J. Michelson and A. Strominger, "Anti-de Sitter fragmentation," JHEP **9902**, 011 (1999), [arXiv:hep-th/9812073].

[42] A. Strominger, "AdS(2) quantum gravity and string theory," JHEP **9901**, 007 (1999) [hep-th/9809027].
A. Sen, "Quantum Entropy Function from AdS(2)/CFT(1) Correspondence," Int. J. Mod. Phys. **A24**, 4225-4244 (2009), [arXiv:0809.3304 [hep-th]]; "State Operator Correspondence and Entanglement in AdS_2/CFT_1," [arXiv:1101.4254 [hep-th]].
R. K. Gupta and A. Sen, "Ads(3)/CFT(2) to Ads(2)/CFT(1)," JHEP **0904**, 034 (2009) [arXiv:0806.0053 [hep-th]].

[43] V. Balasubramanian, A. Naqvi, J. Simon, "A Multiboundary AdS orbifold and DLCQ holography: A Universal holographic description of extremal black hole horizons," JHEP **0408** (2004) 023. [hep-th/0311237].

[44] J. de Boer, M. M. Sheikh-Jabbari, J. Simon, "Near Horizon Limits of Massless BTZ and Their CFT Duals," Class. Quant. Grav. **28** (2011) 175012. [arXiv:1011.1897 [hep-th]].

[45] V. Balasubramanian, J. Parsons and S. F. Ross, "States of a chiral 2d CFT," Class. Quant. Grav. **28**, 045004 (2011) [arXiv:1011.1803 [hep-th]].

[46] G. Compere, W. Song, A. Virmani, "Microscopics of Extremal Kerr from Spinning M5 Branes," [arXiv:1010.0685 [hep-th]].

[47] J. M. Bardeen and G. T. Horowitz, "The extreme Kerr throat geometry: A vacuum analog of AdS(2) x S(2)," Phys. Rev. D **60** (1999) 104030, [arXiv:hep-th/9905099].

[48] R. Fareghbal, C. N. Gowdigere, A. E. Mosaffa, M. M. Sheikh-Jabbari, "Nearing 11d Extremal Intersecting Giants and New Decoupled Sectors in D = 3,6 SCFT's," Phys. Rev. **D81** (2010) 046005. [arXiv:0805.0203 [hep-th]].
T. Azeyanagi, N. Ogawa and S. Terashima, "Emergent AdS3 in the Zero Entropy Extremal Black Holes," JHEP **1103**, 004 (2011) [arXiv:1010.4291 [hep-th]].
H. Yavartanoo, "On EVH black hole solution in heterotic string theory," Nucl. Phys. B **863**, 410 (2012), arXiv:1212.3742 [hep-th].
H. Yavartanoo, "EVH black hole solutions with higher derivative corrections," Eur. Phys. J. C **72**, 1911 (2012), arXiv:1301.4174 [hep-th].
H. Yavartanoo, "Five-dimensional heterotic black holes and its dual IR-CFT," Eur. Phys. J. C **72**, 2197 (2012), arXiv:1301.3706 [hep-th]
H. Yavartanoo, "On heterotic black holes and EVH/CFT correspondence," Eur. Phys. J. C **72**, 2256 (2012)

[49] M. Guica, A. Strominger, "Microscopic Realization of the Kerr/CFT Correspondence," JHEP **1102** (2011) 010. [arXiv:1009.5039 [hep-th]].

[50] Y. Matsuo, T. Nishioka, "New Near Horizon Limit in Kerr/CFT," JHEP **1012**, 073 (2010), [arXiv:1010.4549 [hep-th]].

[51] M. M. Sheikh-Jabbari and H. Yavartanoo, "EVH Black Holes, AdS3 Throats and EVH/CFT Proposal," JHEP **1110** (2011) 013 [arXiv:1107.5705 [hep-th]].

[52] J. Simon, "Extremal black holes, holography and coarse graining," Int. J. Mod. Phys. **A26** (2011) 1903-1971. [arXiv:1106.0116 [hep-th]].

[53] T. Hartman, A. Strominger, "Central Charge for AdS(2) Quantum Gravity," JHEP **0904** (2009) 026. [arXiv:0803.3621 [hep-th]].

[54] Maria Johnstone, M.M. Sheikh-Jabbari, Joan Simon, Hossein Yavartanoo, "Extremal Black Holes and First Law of Thermodynamics", arXiv:1305.3157 [hep-th]

[55] H. S. Reall, "Black Holes", http://www.aei.mpg.de/ gielen/black.pdf

[56] Hawking, S.W., Gravitational Radiation from Colliding Black Holes, Phys. Rev. Lett., 26, 13441346, (1971)

[57] S. W. Hawking and J. B. Hartle, "Energy and angular momentum flow into a black hole," Commun. Math. Phys. **27** (1972) 283.

[58] "Black Holes and Relativistic Stars" Edited by Robert M. Wald University of Chicago Press

[59] G.W. Gibbons, M.J. Perry, C.N. Pope, "The First Law of Thermodynamics for Kerr-Anti-de Sitter Black Holes", Class.Quant.Grav.22:1503-1526,2005, arXiv:hep-th/0408217.

[60] Bekenstein, J.D., Generalized Second Law of Thermodynamics in Black- Hole Physics, Phys. Rev. D, 9, 32923300, (1974).

[61] Roberto Emparan, Harvey S. Reall, "Black Holes in Higher Dimensions", Living Rev.Rel.11:6,2008, arXiv:0801.3471 [hep-th].

[62] Jianwei Mei, C.N. Pope, "New Rotating Non-Extremal Black Holes in D = 5 Maximal Gauged Supergravity", Phys.Lett.B658:64-70,2007, arXiv:0709.0559 [hep-th].

[63] T. Azeyanagi, G. Compere, N. Ogawa, Y. Tachikawa, S. Terashima, "Higher-Derivative Corrections to the Asymptotic Virasoro Symmetry of 4d Extremal Black Holes," Prog. Theor. Phys. **122** (2009) 355; [arXiv:0903.4176 [hep-th]].

[64] A. Castro and F. Larsen, "near-extremal Kerr Entropy from AdS(2) Quantum Gravity," JHEP **0912** (2009) 037. [arXiv:0908.1121 [hep-th]].

[65] A. Sen, "Black Hole Entropy Function, Attractors and Precision Counting of Microstates," Gen. Rel. Grav. **40** (2008) 2249. [arXiv:0708.1270 [hep-th]].

[66] M. Johnstone, M. M. Sheikh-Jabbari, J. Simon, H. Yavartanoo, "Charged-Rotating AdS_5 EVH Black Holes and Their Dual 2d IR CFTs," JHEP **1304** (2013) 045; arXiv:1301.3387 [hep-th];

[67] M. Banados, M. Henneaux, C. Teitelboim and J. Zanelli, "Geometry of the $(2+1)$ Black Hole," Phys. Rev. D **48**, 1506 (1993), gr-qc/9302012.

[68] J. M. Maldacena, "The Large N limit of superconformal field theories and supergravity," Adv. Theor. Math. Phys. **2** (1998) 231-252. [hep-th/9711200].
O. Aharony, S. S. Gubser, J. M. Maldacena, H. Ooguri, Y. Oz, "Large N field theories, string theory and gravity," Phys. Rept. **323** (2000) 183-386. [hep-th/9905111].

[69] J. de Boer, M. Johnstone, M. M. Sheikh-Jabbari and J. Simon, "Emergent IR Dual 2d CFTs in Charged AdS5 Black Holes," Phys. Rev. D **85** (2012) 084039; [arXiv:1112.4664 [hep-th]].

[70] M. Cvetic *et al.*, "Embedding AdS black holes in ten and eleven dimensions," Nucl. Phys. B **558** (1999) 96, [arXiv:hep-th/9903214].
For a review see, M. J. Duff, "Lectures on branes, black holes and anti-de Sitter space," arXiv:hep-th/9912164.

[71] H. K. Kunduri, J. Lucietti and H. S. Reall, "Supersymmetric multi-charge AdS(5) black holes," JHEP **0604**, 036 (2006) [hep-th/0601156].
S. Kim and K. M. Lee, "1/16-BPS black holes and giant gravitons in the AdS(5) x S**5 space," JHEP **0612**, 077 (2006) [arXiv:hep-th/0607085].

[72] R. C. Myers, O. Tafjord, "Superstars and giant gravitons," JHEP **0111** (2001) 009. [hep-th/0109127].

[73] J. McGreevy, L. Susskind, N. Toumbas, "Invasion of the giant gravitons from Anti-de Sitter space," JHEP **0006** (2000) 008. [hep-th/0003075].

[74] S. S. Gubser, J. J. Heckman, "Thermodynamics of R-charged black holes in AdS(5) from effective strings," JHEP **0411** (2004) 052. [hep-th/0411001].

[75] R. P. Geroch, "Limits of spacetimes," Commun. Math. Phys. **13** (1969) 180.

[76] A. Castro, A. Maloney and A. Strominger, "Hidden Conformal Symmetry of the Kerr Black Hole," Phys. Rev. D **82**, 024008 (2010), [arXiv:1004.0996 [hep-th]].

[77] M. Cvetic, F. Larsen, "Conformal Symmetry for General Black Holes," [arXiv:1106.3341 [hep-th]].

[78] T. Hartman, K. Murata, T. Nishioka, A. Strominger, "CFT Duals for Extreme Black Holes," JHEP **0904** (2009) 019. [arXiv:0811.4393 [hep-th]].

[79] M. Guica, T. Hartman, W. Song, A. Strominger, "The Kerr/CFT Correspondence," Phys. Rev. **D80** (2009) 124008. [arXiv:0809.4266 [hep-th]].

[80] H. Lu, J. -w. Mei, C. N. Pope, J. F. Vazquez-Poritz, "Extremal Static AdS Black Hole/CFT Correspondence in Gauged Supergravities," Phys. Lett. **B673** (2009) 77-82. [arXiv:0901.1677 [hep-th]].

[81] F. Loran and H. Soltanpanahi, "5D Extremal Rotating Black Holes and CFT duals," Class. Quant. Grav. **26** (2009) 155019 [arXiv:0901.1595 [hep-th]].

[82] S. El-Showk, M. Guica, "Kerr/CFT, dipole theories and nonrelativistic CFTs," [arXiv:1108.6091 [hep-th]].

[83] R. d. M. Koch, N. Ives and M. Stephanou, "Correlators in Nontrivial Backgrounds," Phys. Rev. D **79**, 026004 (2009), [arXiv:0810.4041 [hep-th]].

R. de Mello Koch, T. K. Dey, N. Ives and M. Stephanou, "Correlators Of Operators with a Large R-charge," JHEP **0908** (2009) 083, [arXiv:0905.2273 [hep-th]].

W. Carlson, R. d. M. Koch, H. Lin, "Nonplanar Integrability," JHEP **1103**, 105 (2011). [arXiv:1101.5404 [hep-th]].

[84] T. Azeyanagi, N. Ogawa, S. Terashima, "Emergent AdS_3 in the Zero Entropy Extremal Black Holes," JHEP **1103** (2011) 004. [arXiv:1010.4291 [hep-th]].

[85] T. Azeyanagi, N. Ogawa, S. Terashima, "On Non-Chiral Extension of Kerr/CFT," JHEP **1106** (2011) 081. [arXiv:1102.3423 [hep-th]].

[86] M. Gunaydin, G. Sierra and P. K. Townsend, "Gauging the d = 5 Maxwell-Einstein Supergravity Theories: More on Jordan Algebras," Nucl. Phys. B **253**, 573 (1985).

[87] K. Behrndt, A. H. Chamseddine and W. A. Sabra, "BPS black holes in N=2 five-dimensional AdS supergravity," Phys. Lett. B **442**, 97 (1998) [hep-th/9807187].
K. Behrndt, M. Cvetic and W. A. Sabra, "Nonextreme black holes of five-dimensional N=2 AdS supergravity," Nucl. Phys. B **553**, 317 (1999) [hep-th/9810227].

[88] Z. W. Chong, M. Cvetic, H. Lu and C. N. Pope, "Five-dimensional gauged supergravity black holes with independent rotation parameters," Phys. Rev. D **72** (2005) 041901 [arXiv:hep-th/0505112].

[89] S. -Q. Wu, "General Nonextremal Rotating Charged AdS Black Holes in Five-dimensional $U(1)^3$ Gauged Supergravity: A Simple Construction Method," Phys. Lett. B **707**, 286 (2012) [arXiv:1108.4159 [hep-th]].

[90] M. Berkooz, A. Frishman and A. Zait, "Degenerate Rotating Black Holes, Chiral CFTs and Fermi Surfaces I - Analytic Results for Quasinormal Modes," JHEP **1208** (2012) 109. [arXiv:1206.3735 [hep-th]]

[91] G. Compere, "The Kerr/CFT correspondence and its extensions: a comprehensive review," Living Rev. Rel. **15**, 11 (2012) [arXiv:1203.3561 [hep-th]].

[92] V. Balasubramanian, J. de Boer, E. Keski-Vakkuri and S. F. Ross, "Supersymmetric conical defects: Towards a string theoretic description of black hole formation," Phys. Rev. D **64** (2001) 064011 [hep-th/0011217].
J. M. Maldacena and L. Maoz, "Desingularization by rotation," JHEP **0212** (2002) 055 [hep-th/0012025].
J. Hansen, P. Kraus, "Generating charge from diffeomorphisms," JHEP **0612** (2006) 009. [hep-th/0606230].

[93] V.P. Frolov and K.S. Thorne, "Renormalized stress-energy tensor near the horizon of a slowly evolving, rotating black hole", Phys. Rev. D39 (1989) 2125.

[94] H. Lu, J. Mei and C. N. Pope, Kerr/CFT Correspondence in Diverse Dimensions,JHEP 0904:054,2009; arXiv:0811.2225 [hep-th].

[95] A. Strominger, "Black hole entropy from near horizon microstates," JHEP **9802** (1998) 009 [hep-th/9712251].

[96] Z. -W. Chong, M. Cvetic, H. Lu and C. N. Pope, "General non-extremal rotating black holes in minimal five-dimensional gauged supergravity," Phys. Rev. Lett. **95**, 161301 (2005) [hep-th/0506029]; "Non-extremal rotating black holes in five-dimensional gauged supergravity," Phys. Lett. B **644**, 192 (2007) [hep-th/0606213].
J. Mei and C. N. Pope, "New Rotating Non-Extremal Black Holes in D=5 Maximal Gauged Supergravity," Phys. Lett. B **658**, 64 (2007) [arXiv:0709.0559 [hep-th]].

[97] S. Carlip, "Extremal and nonextremal Kerr/CFT correspondences," JHEP **1104** (2011) 076. [arXiv:1101.5136 [gr-qc]].

[98] H. K. Kunduri, J. Lucietti and H. S. Reall, "near-horizon symmetries of extremal black holes," Class. Quant. Grav. **24**, 4169 (2007), [arXiv:0705.4214 [hep-th]].
H. K. Kunduri, J. Lucietti, "A Classification of near-horizon geometries of extremal vacuum black holes," J. Math. Phys. **50**, 082502 (2009), [arXiv:0806.2051 [hep-th]].

[99] A. Sen, "Black Hole Entropy Function and the Attractor Mechanism in Higher Derivative Gravity," JHEP **0509**, 038 (2005), [arXiv:hep-th/0506177].
A. Sen, "Black Hole Entropy Function, Attractors and Precision Counting of Microstates," Gen. Rel. Grav. **40**, 2249 (2008), [arXiv:0708.1270 [hep-th]].

[100] E. Witten, "Anti-de Sitter space, thermal phase transition, and confinement in gauge theories," Adv. Theor. Math. Phys. **2** (1998) 505-532. [hep-th/9803131].

[101] D. E. Berenstein, J. M. Maldacena and H. S. Nastase, "Strings in flat space and pp waves from N = 4 super Yang Mills," JHEP **0204**, 013 (2002), [arXiv:hep-th/0202021].

D. Sadri and M. M. Sheikh-Jabbari, "The plane-wave / super Yang-Mills duality," Rev. Mod. Phys. **76**, 853 (2004), [arXiv:hep-th/0310119].

[102] R. C. Myers and M. J. Perry, "Black Holes In Higher Dimensional Space-Times," Annals Phys. **172**, 304 (1986).

[103] A. J. Amsel, G. T. Horowitz, D. Marolf and M. M. Roberts, "No Dynamics in the Extremal Kerr Throat," JHEP **0909**, 044 (2009), [arXiv:0906.2376 [hep-th]].
O. J. C. Dias, H. S. Reall and J. E. Santos, "Kerr-CFT and gravitational perturbations," JHEP **0908**, 101 (2009), [arXiv:0906.2380 [hep-th]].

[104] S. A. Hartnoll, "Lectures on holographic methods for condensed matter physics," Class. Quant. Grav. **26** (2009) 224002. [arXiv:0903.3246 [hep-th]].
C. P. Herzog, "Lectures on Holographic Superfluidity and Superconductivity," J. Phys. A **A42** (2009) 343001. [arXiv:0904.1975 [hep-th]].
J. McGreevy, "Holographic duality with a view toward many-body physics," Adv. High Energy Phys. **2010** (2010) 723105. [arXiv:0909.0518 [hep-th]].
S. A. Hartnoll, "Quantum Critical Dynamics from Black Holes," [arXiv:0909.3553 [cond-mat.str-el]].
S. A. Hartnoll, "Horizons, holography and condensed matter," [arXiv:1106.4324 [hep-th]].

[105] T. Faulkner, H. Liu, J. McGreevy, D. Vegh, "Emergent quantum criticality, Fermi surfaces, and AdS(2)," Phys. Rev. **D83** (2011) 125002. [arXiv:0907.2694 [hep-th]].

[106] J. de Boer, S. El-Showk, I. Messamah and D. Van den Bleeken, "A Bound on the entropy of supergravity?," JHEP **1002** (2010) 062 [arXiv:0906.0011 [hep-th]].

[107] V. Balasubramanian, D. Marolf and M. Rozali, "Information Recovery From Black Holes," Gen. Rel. Grav. **38** (2006) 1529 [Int. J. Mod. Phys. D **15** (2006) 2285] [hep-th/0604045].

[108] V. Balasubramanian, P. Kraus, "Space-time and the holographic renormalization group," Phys. Rev. Lett. **83** (1999) 3605-3608. [hep-th/9903190].
J. de Boer, E. P. Verlinde, H. L. Verlinde, "On the holographic renormalization group," JHEP **0008** (2000) 003. [hep-th/9912012].
T. Faulkner, H. Liu, M. Rangamani, "Integrating out geometry: Holographic Wilsonian RG and the membrane paradigm," JHEP **1108** (2011) 051. [arXiv:1010.4036 [hep-th]].

[109] R Penrose, "Any space-time has a plane wave as a limit", Differential geometry and relativity, Reidel, Dordrecht, 1976, pp. 271–275.

[110] O. Coussaert, M. Henneaux, "Selfdual solutions of (2+1) Einstein gravity with a negative cosmological constant," [hep-th/9407181].

[111] E. J. Martinec, W. McElgin, "String theory on AdS orbifolds," JHEP **0204** (2002) 029. [hep-th/0106171].

[112] A. Chamblin, R. Emparan, C. V. Johnson and R. C. Myers, "Holography, thermodynamics and fluctuations of charged AdS black holes," Phys. Rev. D **60**, 104026 (1999), [arXiv:hep-th/9904197].

S. Bhattacharyya, S. Minwalla, K. Papadodimas, "Small Hairy Black Holes in $AdS_5 \times S^5$," [arXiv:1005.1287 [hep-th]].

[113] R. M. Wald, "The thermodynamics of black holes," Living Rev. Rel. **4** (2001) 6, [gr-qc/9912119].

[114] M. Berkooz, A. Frishman and A. Zait, "Stability of rapidly-rotating charged black holes in $AdS_5 \times S^5$," arXiv:1301.6524 [hep-th].

[115] A. J. Amsel, G. T. Horowitz, D. Marolf and M. M. Roberts, "No Dynamics in the Extremal Kerr Throat," JHEP **0909** (2009) 044. [arXiv:0906.2376 [hep-th]].

[116] R. M. Wald, "Ńernst theorem and black hole thermodynamics", Phys. Rev. D 56, 1997, 6467-74.

[117] J. Rasmussen, "On the CFT duals for near-extremal black holes", Mod.Phys.Lett.A26:1601-1611,2011, arXiv:1005.2255.

[118] Jan de Boer, "Introduction to the AdS/CFT Correspondence",www-library.desy.de

[119] Angel Uranga, "Introduction to String Theory", http://gesalerico.ft.uam.es/paginaspersonales/angeluranga/firstpage.html.

[120] R. J. Szabo, "BUSSTEPP lectures on string theory: An Introduction to string theory and D-brane dynamics," hep-th/0207142.

[121] M. Cvetic and F. Larsen,"Conformal Symmetry for Black Holes in Four Dimensions," JHEP **1209** (2012) 076 [arXiv:1112.4846 [hep-th]].
M. Cvetic and G. W. Gibbons, "Conformal Symmetry of a Black Hole as a Scaling Limit: A Black Hole in an Asymptotically Conical Box," JHEP **1207** (2012) 014 [arXiv:1201.0601 [hep-th]].
A. Virmani, "Subtracted Geometry From Harrison Transformations," JHEP **1207** (2012) 086 [arXiv:1203.5088 [hep-th]].
A. Chakraborty and C. Krishnan, "Subttractors," arXiv:1212.1875 [hep-th].